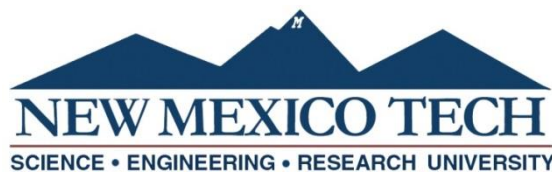


**AN INVENTORY AND MINERALOGICAL
CHARACTERIZATION OF MINES AND PROSPECTS IN
THE NORTH MAGDALENA MINING DISTRICT,
SOCORRO COUNTY, NEW MEXICO**

by

Marcus E. Silva

Submitted in Partial Fulfillment
of the Requirements for the Degree of
Master of Science in Mineral Engineering
with a Specialization in Mineral Exploration



New Mexico Institute of Mining and Technology
Socorro, New Mexico
December, 2019

This thesis is dedicated to Megan Dill—a dear friend and fellow geology student who, as much as any of us, deserved a bright future doing what she loved.

Marcus E Silva
New Mexico Institute of Mining and Technology
December, 2019

ABSTRACT

The North Magdalena mining district is located approximately one mile north of the town of Magdalena in Socorro County, New Mexico. It is a historic district with recorded past production of silver, copper, lead, and gold; zinc, vanadium, and barium were explored for, but never produced. The district is a volcanic-epithermal precious- and base-metal vein deposit and most of the mines are located along subparallel N-S trending veins that crosscut the rolling hills and grasslands of the district. Situated at the northern edge of the Mogollon-Datil Volcanic field, vein systems are associated with regional extension along the western margin of the Rio Grande Rift and late-stage caldera-related magmatism. Some mine features pose physical and potential environmental hazards to residents of the area, but most of the mine features are not hazardous. This study will serve as a guide for prioritizing mine features for reclamation and catalog the district's mineralogy with implications for future work in the area. After examining more than 170 mine features, it was determined that physical hazards should be the focus of future reclamation projects. Field and laboratory results indicate no potential for acid generation from mine waste, thereby minimizing environmental concerns. Furthermore, the arid climate and lack of flowing water in the region means that leaching of heavy metals from mine waste is limited, but illegal disposal of household waste in mine features may present some risk to groundwater. Many waste rock piles have elevated concentrations of copper, lead, zinc, silver and potentially gold that could be considered for reprocessing, rather than backfill. Minerals observed through various analytical methods and in hand sample include, but are not limited to barite, bornite, chalcocite, chalcopyrite, covellite, descloizite, galena, oxidized copper minerals, sphalerite, and vanadinite. Relationships between these and other minerals were then used to propose a paragenetic history of ore deposit formation in the district.

Keywords: *Mineralogy; Reclamation; Abandoned Mine Lands; Ore Deposits; Volcanic-Epithermal Systems; Economic Geology*

ACKNOWLEDGMENTS

First and foremost, I wish to thank my parents Lydia DeLaRocha, Thomas Silva, and Renee Bliss for their encouragement to pursue science early in life and both moral and financial support along my journey through higher education. Next, it must be said that I could not possibly have done this without the network of close friends I have made in Socorro. There is nothing easy about living here and the strong sense of community and camaraderie among us is something that could only have developed in the most bleak and dire of situations (grad school). You have all made a remarkable impact on my life and will always be welcome to crash on my couch. I'd also wish to extend many thanks to my advisor Dr. Virginia McLemore and committee members Dr. William Chavéz and Dr. Navid Mojtabai for getting me out here in the first place and putting me on a project I truly enjoyed and cared about. Additional appreciation goes to Joseph Shackelford, Bon and John Durica, and all who helped with the AML project. Special thanks to Alexandra Pearce, Dante Padilla Romero, Dr. Kierran Maher, and others who helped with fieldwork and geochemical interpretations. Finally, I would like to thank NMBGMR staff members Connie Apache, Kelsey McNamara, Lynn Heizler, Dr. Virgil Lueth, Brian Wheeler, and Phil Miller for help with contracts, analytical methods, vehicle procurement, and GIS. I couldn't have done this without all of you.

TABLE OF CONTENTS

ABSTRACT.....	i
ACKNOWLEDGMENTS	ii
LIST OF FIGURES	vi
LIST OF TABLES.....	viii
LIST OF ABBREVIATIONS AND SYMBOLS	ix
LIST OF MINERALS, ABBREVIATIONS, AND CHEMICAL FORMULAE	xi
Chapter 1: Introduction.....	1
1.1 Introduction.....	1
1.2 Geographic Setting.....	7
1.2.1 Central Socorro County	7
1.2.2 Quadrangles and Nearby Districts	7
1.2.3 Flora and Fauna.....	7
1.2.4 Precipitation and Hydrogeology	9
1.3 Abandoned Mine Lands Project.....	9
1.4 Problem Being Addressed.....	10
1.5 Previous Studies.....	10
Chapter 2: Geologic and Historical Background	12
2.1 Geology.....	12
2.1.1 Regional Geology	12
2.1.2 District Geology.....	13
2.1.3 Pre-Tertiary Lithologies.....	14
2.1.4 Tertiary Lithologies	14
2.1.5 Tertiary-Quaternary Deposits:	16
2.2 Structural Influences	17
2.3 Economic Geology.....	18
2.3.1 General Deposit Type Characteristics.....	18
2.3.2 Deposit Characteristics at North Magdalena.....	20
2.4 Historic Mining, Production, and Exploration.....	21
2.5 Patented and Unpatented Mining Claims.....	24
2.6 Mining Methods.....	25
2.7 Land Ownership.....	28
2.7.1 Federal Lands.....	29

2.7.2 State Lands.....	29
2.7.3 Private Lands	29
Chapter 3: Methods.....	30
3.1 Field Methods	30
3.1.1 Mine Inventory and Nomenclature	30
3.1.2 Improved Location Data	33
3.1.3 Sampling Methods	33
3.1.4 Photography	34
3.2 Laboratory Methods.....	35
3.2.1 Geochemistry	35
3.2.2 Mine Soil Petrography	36
3.2.3 Acid-Base Accounting	37
3.2.4 Reflected Light Petrography (RLP).....	38
3.2.5 X-Ray Diffraction (XRD).....	39
3.2.6 Electron Microprobe (EMP)	40
Chapter 4: Results.....	41
4.1 Field Results	41
4.1.1 Mine Inventory.....	41
4.1.2 Mine Mineralogy	44
4.2 Laboratory Results	46
4.2.1 Geochemistry	46
4.2.2 Mine Soil Petrography	49
4.2.3 Acid-Base Accounting	51
4.2.4 Reflected Light Petrography (RLP).....	52
4.2.5 X-Ray Diffraction (XRD).....	56
4.2.6 Electron Microprobe (EMP)	58
Chapter 5: Discussion	62
5.1 Field Inventory.....	62
5.2 Geochemistry and Environmental Implications.....	64
5.3 Mineralogical Interpretations	66
5.4 New Minerals, Ore Formation, and Paragenesis.....	77
5.4.1 New Minerals.....	77
5.4.2 Precipitation Mechanisms and Ore Formation.....	78

5.4.3 Mineralization Events and Paragenesis.....	79
Chapter 6: Conclusions	82
REFERENCES	85
APPENDIX A: Forms.....	92
A.1 Mine Inventory Form	92
A.2 AML Sample Form	94
A.3 Thesis Mineralogy Sample Form	95
APPENDIX B: Mine Feature Information.....	96
B.1 Mine IDs, Database Mine Names, and Corresponding Field Mine Names/Aliases.....	96
B.2 Mines Features and Associated Samples.....	98
B.3 Mine IDs, Database & Field Names, and Location Information from AML and Thesis Inventory	99
B.4 Mine Feature Mineralogy	103
B.5 Mine Feature Hazard Rankings.....	107
B.6 Mine Features with Trash.....	110
B.7 Patented Claims Information.....	111
B.8 Mine Feature Photographs: Labeled by Field Mine Name (Mine ID)	113
APPENDIX C: Supplementary Analytical Data.....	189
C.1 Geochemical Data	189
C.1.A Geochemical Data (Samples)	189
C.1.B Geochemical Data (Standards)	194
C.2 Electron Microprobe Data.....	196
C.2.A Galena.....	196
C.2.B Chalcopyrite.....	197
C.2.C Sphalerite	197
C.2.D Cerussite	198
C.2.E Fe-Oxide	199
C.2.F Au-Ag Standards.....	199
C.3 Electron Microprobe BSE Imagery	200
C.4 Electron Microprobe Spectra	202
C.5 X-ray Diffractograms	204
C.6 Reflected Light Photomicrographs.....	214
APPENDIX D: Permissions	218

LIST OF FIGURES

Figure 1. New Mexico mining districts (after McLemore (2017)).	3
Figure 2. Map of the North Magdalena mining district.	4
Figure 3. Silver Hill area and mine features.	5
Figure 4. Granite Mountain area and mine features.	6
Figure 5. Map of historic metals districts near Socorro and Magdalena (after McLemore (2017)).	8
Figure 6. Cropped section of geologic map from Osburn (1984).	13
Figure 7. SC-D1 (NMSO0866); massive hydrothermal breccia with carbonate cement.	19
Figure 8. Mag23-S1 (NMSO0921); drusy quartz coating fractures and cavities in andesite.	19
Figure 9. NM169-P2 (NMSO0835); looking south towards Magdalena Mountains.	26
Figure 10. SH-T2 (NMSO0897); massive trench located on south slope of Silver Hill.	26
Figure 11. SH-C1; View south towards Ace of Spades on north slope of Silver Hill.	27
Figure 12. Mag4-S1 (NMSO0377); main shaft on the Chief vein sank ca. 1919 (Lasky, 1932). Headframe collapsing into collar of shaft (¼ mi from NM-169).	27
Figure 13. Mag4-S1 (NMSO0377); interior of shaft. Note the broken rungs on ladder and other indicators of instability. This shaft is >300 ft deep.	28
Figure 14. NM354-A1 (NMSO0879); an untimbered adit in extremely altered rock.	42
Figure 15. SH-S2 (NMSO0898); deep shaft plugged with trash. Circled area is opening to shaft below. Note proximity to road above.	43
Figure 16. SH-S3i; phyllic (sericite-carbonate) alteration of calcic plagioclase.	45
Figure 17. ARD diagram of acid generating potential of mine soils in North Magdalena.	51
Figure 18. Cuprite replacing native copper.	53
Figure 19. Assemblage of Cu-sulfides with an unclear paragenesis.	54
Figure 20. Complex replacement assemblage within galena.	55
Figure 21. SH-4; Phenocrysts of Fe-Ox after ankerite and a yellow phase suspected to be bromargyrite.	58
Figure 22. NMA-1B-1; spectral profile of CuS phase (covellite).	59
Figure 23. NMA-1B-2; BSE image of Ag-rich inclusions in chalcopyrite, etc.	60
Figure 24. VL-WS; combined plot of spectra collected from points on oxidation fronts.	61
Figure 25. VL-WS; oxidation fronts on galena surround pore spaces.	61
Figure 26. ARD comparison of Rosedale, Jicarilla, and North Magdalena districts.	66
Figure 27. Supergene jalpaite (?), “chalcocite”, digenite, and covellite.	69

Figure 28. Bright blue-white anisotropy of jalpaite (?).	69
Figure 29. Mag20-S1 (NMSO0180); vein of oxidized copper minerals representing the surface exposure of supergene enrichment mined by the shaft.	71
Figure 30. Grain of “chalcocite” and oxidation phases.	71
Figure 31. Anisotropy of paramelaconite is very distinct.	72
Figure 32. Noisy chrysocolla diffractogram with “amorphous hump”.....	74
Figure 33. Paragenetic relationships of selected minerals in North Magdalena.....	81
Figure 34. SH-S1 (NMSO0230); barn owl taking flight.	82
Figure 35. SH-P15 (NMSO0830); a prospect pit south of Silver Hill filled with trash. ..	83

LIST OF TABLES

Table 1. Production from epithermal districts in New Mexico; after McLemore (1996).	21
Table 2. Abbreviations for location component of mine name.	31
Table 3. Abbreviations for feature type component of mine name.	31
Table 4. BLM hazard ranking system (Bureau of Land Management, 2014)	32
Table 5. NOAMI hazard ranking system (“NOAMI”, 2019)	32
Table 6. Grinding procedures for creating polished sections.	39
Table 7. Polishing procedure for creating EMP billet.	40
Table 8. Feature types and counts.	41
Table 9. Geochemistry samples and types according to Mine ID and feature type.....	47
Table 10. Selected element concentrations from samples described in Table 9.....	48
Table 11. Concentrations of potentially hazardous elements and sulfur in samples described in Table 9.	49
Table 12. Characteristics of unwashed mine soil petrographic samples.	50
Table 13. Characteristics of washed mine soil petrographic samples.	50
Table 14. Lithology and mineralogy of samples used in ABA.....	51
Table 15. Paste pH data used to predict acid-generating potential of selected composite samples.....	51
Table 16. Polished sections and primary mineralogy.	52
Table 17. Results of XRD analysis on selected minerals.	57
Table 18. CuS phases (covellite) with elevated Ag-values.....	59
Table 19. Number of features associated with NOAMI hazard rankings.	63
Table 20. Abundances of selected elements in mine waste from North Magdalena.	64
Table 21. Abundances of potentially hazardous elements in waste rock at North Magdalena.	64
Table 22. Abundances of selected elements in the Earth’s crust and intermediate rocks (after Yaroshevsky (2006)).	64
Table 23. Abundances of potentially hazardous elements in the Earth’s crust and intermediate rocks (after Yaroshevsky (2006)).	64
Table 26. Minerals previously unreported in the North Magdalena district; (?) indicates species remains unconfirmed by EMP or XRD.	77

LIST OF ABBREVIATIONS AND SYMBOLS

ABA	Acid Base Accounting
AMD	Acid Mine Drainage
AML	Abandoned Mine Lands
AMS	Abandoned Mines Survey (1986)
Ang	Angular
AP	Acid Potential (%S \times 31.25)
ARD	Acid Rock Drainage
BLM	Bureau of Land Management
BSE	Backscattered electron
DI	De-ionized [water]
DIS	District (in NM Mines Database)
DIS223	North Magdalena District ID
E	East
EMP	Electron microprobe
Eq.	Equivalent
Fm.	Formation
ft	Feet
g	Gram
Gal	Gallon
GARD	Global Acid Rock Drainage
GLO	Government Land Office (BLM)
GPM	Gallons Per Minute
GPS	Global Positioning System
GSD	Grain Size Distribution
HCl	Hydrochloric Acid
hr	Hour
I-25	U.S. Interstate 25
ICP-AES	Inductively Coupled Atomic Emission Spectrometry
ICP-MS	Inductively Coupled Plasma Mass Spectrometry
in	Inch
kV	Kilovolt
LCC	Lambert Conformal Conic
LCC27	NM_Contiguous_Lambert_Conformal_Conic_NAD27
LiF	Lithium Fluoride (EMP spectrometer crystal)
LOI	Lost On Ignition
M	Molar
mA	Milliamperere
Ma	Mega-annum
MDVF	Mogollon-Datil Volcanic Field
mi	Mile
mi ²	Square Mile
min	Minute
ml	Milliliter
mm	Millimeter
MMD	Mining and Minerals Division

MVT	Mississippi Valley Type
N	North
NAD27	North American Datum 1927
NAG	Net Acid Generation
NE	Northeast
NM-107	New Mexico State Road 107
NM-169	New Mexico State Road 169
NM-354	New Mexico Forest Road 354
NMBGMR	New Mexico Bureau of Geology and Mineral Resources
NMEMNRD	(NM) Energy, Minerals, and Natural Resources Department
NMSO	New Mexico Socorro [County] (Mine ID Prefix)
NMT	New Mexico Tech
NNP	Net Neutralization Potential (NP-AP)
NNW	North-Northwest
No.	Number
NP	Neutralization Potential (%C × 83.3)
NPR	Net Potential Ratio (NP/AP)
NW	Northwest
Oz	Ounce
PET	Pentaerythritol (EMP spectrometer crystal)
PPL	Plane-Polarized Light
ppm	Parts per million
QA/QC	Quality Assurance/Quality Control
r	Pearson Correlation Coefficient
REE	Rare Earth Element
RGR	Rio Grande Rift
RLP	Reflected Light Petrography
Rnd	Round
S	South
SE	Southeast
SE	Secondary Electron
SOP	Standard Operating Procedure
SubAng	Subangular
SubRnd	Subround
SW	Southwest
TAP	Thallium Acid Phthalate (EMP spectrometer crystal)
μm	Micrometer (micron)
US-60	U.S. Highway 60
USBM	United States Bureau of Mines
USFS	United States Forest Service
UTM	Universal Transverse Mercator
W	West
Wt%	Weight Percent
XPL	Cross-Polarized Light (crossed-nicols)
XRD	X-ray diffraction
XRF	X-ray fluorescence

LIST OF MINERALS, ABBREVIATIONS, AND CHEMICAL FORMULAE

“Carbonates”	CO _{3-s}	----
“Chalcocite”	“Cc.”	Cu _{2-x} S
“Iron Oxides”	Fe-Ox	----
“Mn Oxides”	Mn-Ox	----
“Oxidized copper minerals”	Cu-Ox	----
Acanthite	Ac.	Ag ₂ S (monoclinic)
Adelite	----	CaMg(AsO ₄)(OH)
Adularia	----	KAlSi ₃ O ₈
Aluminoceladonite	----	K(Mg,Fe ²⁺)Al(Si ₄ O ₁₀)(OH) ₂
Alunite	----	KAl ₃ (SO ₄) ₂ (OH) ₆
Amethyst	----	SiO ₂
Anglesite	Ang.	PbSO ₄
Anilite	----	Cu ₇ S ₅
Ankerite	----	Ca(Fe ²⁺ ,Mg)(CO ₃) ₂
Aragonite	----	CaCO ₃
Argentite	Arg.	Ag ₂ S (cubic)
Argentotennantite	----	Ag ₆ Cu ₄ (Fe ²⁺ ,Zn) ₂ As ₄ S ₁₂ S
Arsenopyrite	----	FeAsS
Baileychlore	----	(Zn,Fe ²⁺ ,Al,Mg) ₆ (Si,Al) ₄ O ₁₀ (OH) ₈
Barite	Ba.	BaSO ₄
Blaubleibender	Bb.	Cu _{1+x} S
Bornite	Bn.	Cu ₅ FeS ₄
Brochantite	----	Cu ₄ (SO ₄)(OH) ₆
Bromargyrite	Brm.	AgBr
Calcite	Cal.	CaCO ₃
Celadonite	----	K(Mg,Fe ²⁺)Fe ³⁺ (Si ₄ O ₁₀)(OH) ₂
Celestine	----	SrSO ₄
Cerussite	Cer.	PbCO ₃
Chalcedony	----	SiO ₂
Chalcocite	Cc.	Cu ₂ S
Chalcopyrite	Cpy.	CuFeS ₂
Chlorite (clinocllore)	Chl.	Mg ₅ Al(AlSi ₃ O ₁₀)(OH) ₈
Chlorite (chamosite)	Chl.	(Fe ²⁺ ,Mg,Al,Fe ³⁺) ₆ (Si,Al) ₄ O ₁₀ (OH,O) ₈
Chrysocolla	Chr.	Cu _{2-x} Al _x (H _{2-x} Si ₂ O ₅)(OH) ₄ · nH ₂ O (X<1)
Cinnabar	----	HgS
Conichalcite	----	CaCu(AsO ₄)(OH)
Cornetite	----	Cu ₃ (PO ₄)(OH) ₃
Coronadite	----	Pb(Mn ⁴⁺ ₆ Mn ³⁺ ₂)O ₁₆
Corundum	----	Al ₂ O ₃
Covellite	Cv.	CuS
Cuprian Descloizite	----	Pb(Zn,Cu)(VO ₄)OH
Delafossite	Del.	CuFeO ₂
Descloizite	Des.	PbZn(VO ₄)OH
Diaspore	----	AlO(OH)
Djurleite	Dj.	Cu _{1.97} S

Dickite	----	$\text{Al}_2(\text{Si}_2\text{O}_5)(\text{OH})_4$
Digenite	Dig.	Cu_9S_5
Diopside	Dio.	$\text{CuSiO}_3 \cdot \text{H}_2\text{O}$
Duftite	Duf.	$\text{PbCu}(\text{AsO}_4)(\text{OH})$
Electrum	----	(Au,Ag)
Emplectite	Em.	CuBiS_2
Enargite	----	Cu_3AsS_4
Epidote	----	$\{\text{Ca}_2\}\{\text{Al}_2\text{Fe}^{3+}\}(\text{Si}_2\text{O}_7)(\text{SiO}_4)\text{O}(\text{OH})$
Fluorite	----	CaF_2
Fornacite	For.	$\text{Pb}_2\text{Cu}(\text{CrO}_4)(\text{AsO}_4)(\text{OH})$
Freibergite	----	$(\text{Ag,Cu})_{10}\text{Fe}^{2+}_2\text{Sb}_4\text{S}_{12}$
Galena	Gal.	PbS
Geerite	----	$\text{Cu}_{1.6}\text{S}$
Goethite	Gt.	$\text{FeO}(\text{OH})$
Gypsum	Gyp.	$\text{CaSO}_4 \cdot 2\text{H}_2\text{O}$
Hematite	Hem.	Fe_2O_3
Hollandite	----	$\text{Ba}(\text{Mn}^{4+}_6\text{Mn}^{3+}_2)\text{O}_{16}$
Hydroxylapatite	Hap.	$\text{Ca}_5(\text{PO}_4)_3(\text{OH})$
Idaite	Id.	Cu_5FeS_6
Illite	----	$\text{K}_{0.65}\text{Al}_{2.0}[\text{Al}_{0.65}\text{Si}_{3.35}\text{O}_{10}](\text{OH})_2$
Iranite	----	$\text{Pb}_{10}\text{Cu}(\text{CrO}_4)_6(\text{SiO}_4)_2(\text{OH})_2$
Jalpaite	Jal.	Ag_3CuS_2
Jarosite	----	$\text{KFe}^{3+}_3(\text{SO}_4)_2(\text{OH})_6$
Kaolinite	Kao.	$\text{Al}_2\text{Si}_2\text{O}_5(\text{OH})_4$
Magnetite	Mt.	Fe_3O_4
Malachite	Mal.	$\text{Cu}_2(\text{CO}_3)(\text{OH})_2$
Melanterite	----	$\text{FeSO}_4 \cdot 7\text{H}_2\text{O}$
Molybdoformacite	----	$\text{Pb}_2\text{Cu}(\text{MoO}_4, \text{CrO}_4)(\text{AsO}_4, \text{PO}_4)(\text{OH})$
Mottramite	Mot.	$\text{PbCu}(\text{VO}_4)(\text{OH})$
Native Copper	Cu°	Cu
Native Gold	Au°	Au
Native Silver	Ag°	Ag
Paramelaconite	Pm.	Cu_4O_3
Plagioclase (feldspars)	Plag.	$\text{NaAlSi}_3\text{O}_8\text{-CaAl}_2\text{Si}_2\text{O}_8$
Pyrite	Py.	FeS_2
Pyrophyllite	----	$\text{Al}_2\text{Si}_4\text{O}_{10}(\text{OH})_2$
Quartz	Qtz.	SiO_2
Rosasite	Ros.	$(\text{Cu,Zn})_2(\text{CO}_3)(\text{OH})_2$
Sanidine	----	KAlSi_3O_8
Siderite	Sid.	FeCO_3
Smithsonite	----	ZnCO_3
Specularite	Spc.	Fe_2O_3
Sphalerite	Spl.	ZnS
Spionkopite	----	$\text{Cu}_{39}\text{S}_{28}$
Stromeyerite	Str.	AgCuS
Tangeite	Tan.	$\text{CaCu}(\text{VO}_4)(\text{OH})$

Tennantite	Tnn.	$\text{Cu}_6\text{Cu}_4(\text{Fe}^{2+}, \text{Zn})_2\text{As}_4\text{S}_{12}\text{S}$
Tenorite	Ten.	CuO
Tetrahedrite	Tet.	$\text{Cu}_6\text{Cu}_4(\text{Fe}^{2+}, \text{Zn})_2\text{Sb}_4\text{S}_{12}\text{S}$
Todorokite	Tod.	$(\text{Na}, \text{Ca}, \text{K}, \text{Ba}, \text{Sr})_{1-x}(\text{Mn}, \text{Mg}, \text{Al})_6\text{O}_{12} \cdot 3-4\text{H}_2\text{O}$
Vanadinite	Van.	$\text{Pb}_5(\text{VO}_4)_3\text{Cl}$
Vermiculite	Ver.	$(\text{Mg}, \text{Fe}, \text{Al})_3(\text{Al}, \text{Si})_4\text{O}_{10}(\text{OH})_2 \cdot 4(\text{H}_2\text{O})$
Willemite	Wil.	Zn_2SiO_4
Yarrowite	-----	Cu_9S_8
Zincian muscovite	-----	$\text{K}(\text{Al}, \text{Zn})_2(\text{AlSi}_3\text{O}_{10})(\text{OH})_2$
Zincite	-----	ZnO

Note: Not all of these minerals are found in North Magdalena; many are simply mentioned in the text.

The thesis is accepted on behalf of the faculty Institute by the following committee:

Dr. Navid Mojtabai

Academic Advisor

Dr. Virginia T. McLemore

Research Advisor

Dr. William X. Chavéz

Committee Member

I release this document to the New Mexico Institute of Mining and Technology.

Marcus E Silva

December, 2019

CHAPTER 1

Introduction

1.1 Introduction

The North Magdalena district sits on the western margin of the Rio Grande Rift (RGR) and the northern boundary of the Mogollon-Datil Volcanic Field (MDVF). The Magdalena area has been mined since the mid-1800s and hosts the famous Kelly mine, which is known for its exemplary smithsonite and other rare minerals. While substantial research has been conducted on the mining districts immediately south of Highway 60, there has been far less published work focused on the North Magdalena district. Since 1904, there have been few reports examining the economic geology of the area. This is one of three historic districts that were included in an abandoned mine lands (AML) contract between New Mexico Tech (NMT) and the New Mexico State AML program. The other districts—Rosedale and Jicarilla—historically produced gold with minor other commodities including silver and iron, respectively. The Rosedale mine is located in the Withington Wilderness in the San Mateo Mountains about 30 mi south of Magdalena (Zutah, 2017; McLemore et al., 2019), while Jicarilla is in Lincoln County, approximately 15 mi north of the village of White Oaks. These are only 3 of 274 mining districts in the state of New Mexico that together comprise more than 15,000 abandoned or inactive mine features (Fig. 1) (“Abandoned Mine Lands”, 2019). See McLemore (2017) for names and summaries of all mining districts.

North Magdalena is a volcanic-hosted epithermal deposit (Lindgren, 1933; McLemore, 1996; John et al., 2018) and the primary commodities are silver, copper, lead, and minor gold. Orientations measured in the field indicate that veins in this district strike roughly N-S at $355\text{-}357^\circ$ with minor NW-SE trending systems. The district (Fig. 2) can be broken into two major areas that feature the most extensive mining: the Silver Hill area, located on the western side of the district, and the Granite Mountain area on the eastern side. The Silver Hill area, a roughly 3 mi^2 section of the district, has at least 140 mine features (Fig. 3), while the Granite Mountain area (Fig. 4) has 30-50 features, though not all features have been inventoried in this project. This district was chosen by the NMT AML team because of its proximity to the town of Magdalena and the potential hazards it poses to residents.

Sampling and inventory of mines in this district during the AML project focused mostly on characterizing waste rock for potential backfill-material and evaluating features for environmental hazards. However, the goals of this thesis were to examine waste rock material to characterize mineralogy on a mine-by-mine basis to better understand occurrence, distribution, and availability of commodities. Additional inventory and environmental evaluation were performed throughout this project. The main product of this thesis is a dataset that contains accurate GPS location data combined with mineralogy that will assist in mine remediation and waste reprocessing projects as well as future academic studies in the area.

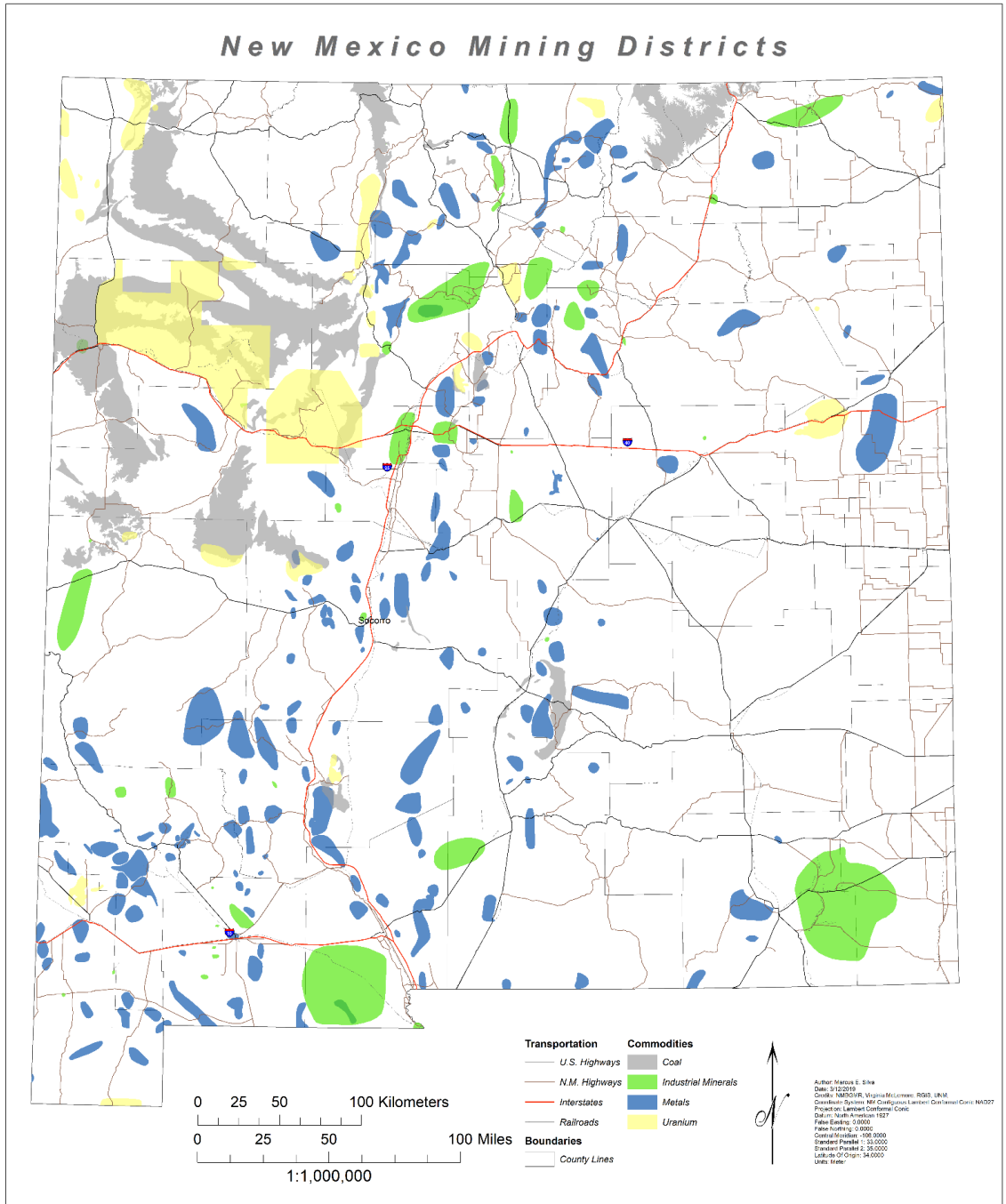


Figure 1. New Mexico mining districts; after McLemore (2017).

North Magdalena District

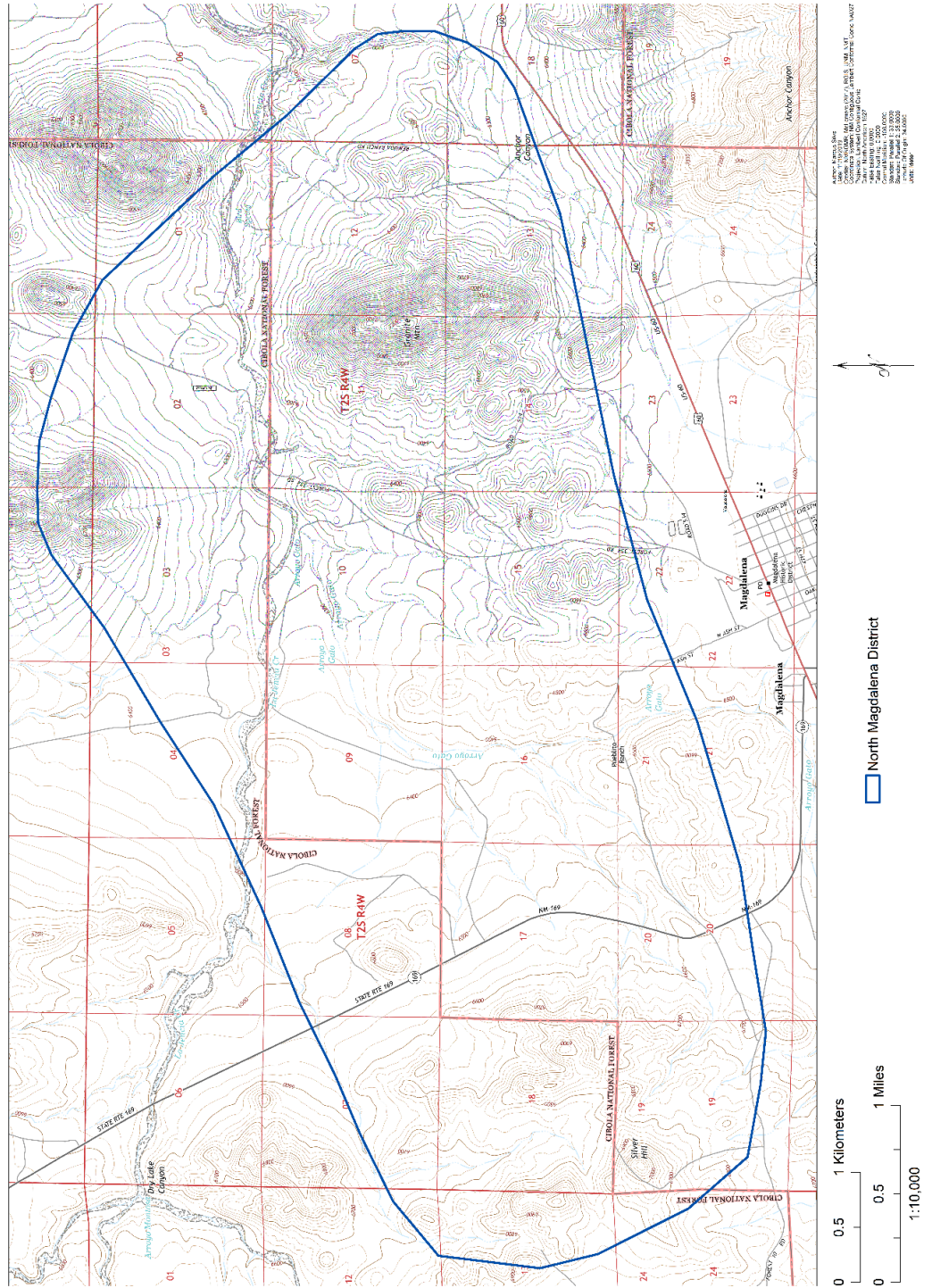


Figure 2. Map of the North Magdalena mining district.

North Magdalena: Silver Hill Area

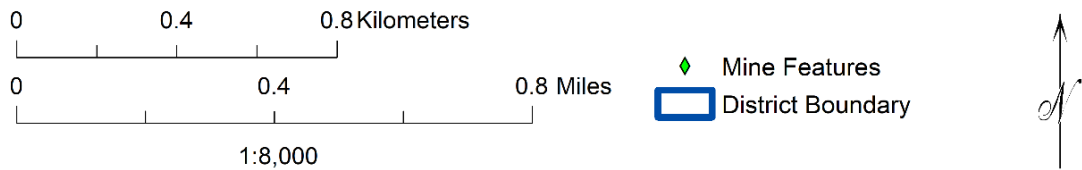
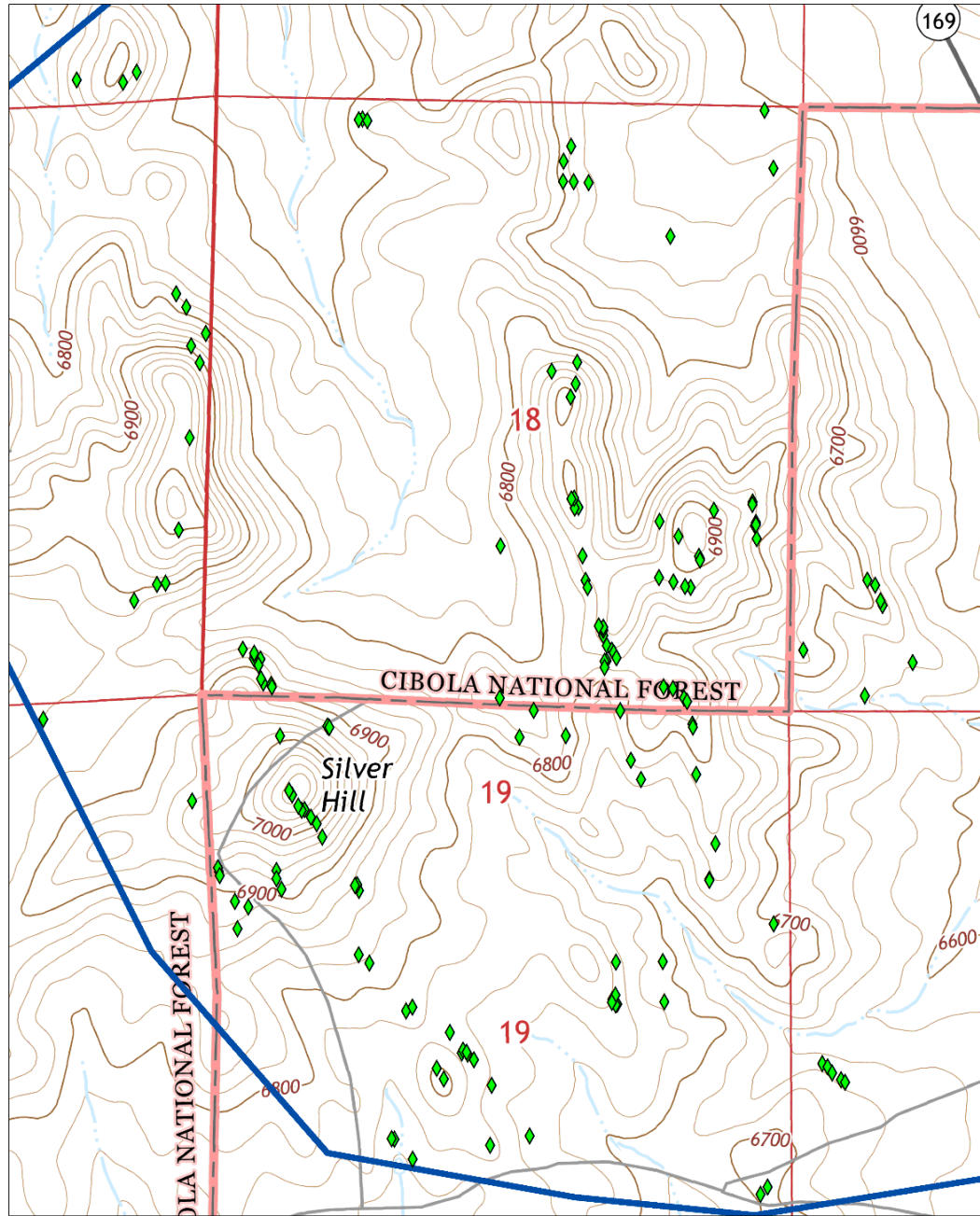


Figure 3. Silver Hill area and mine features.

North Magdalena: Granite Mountain Area

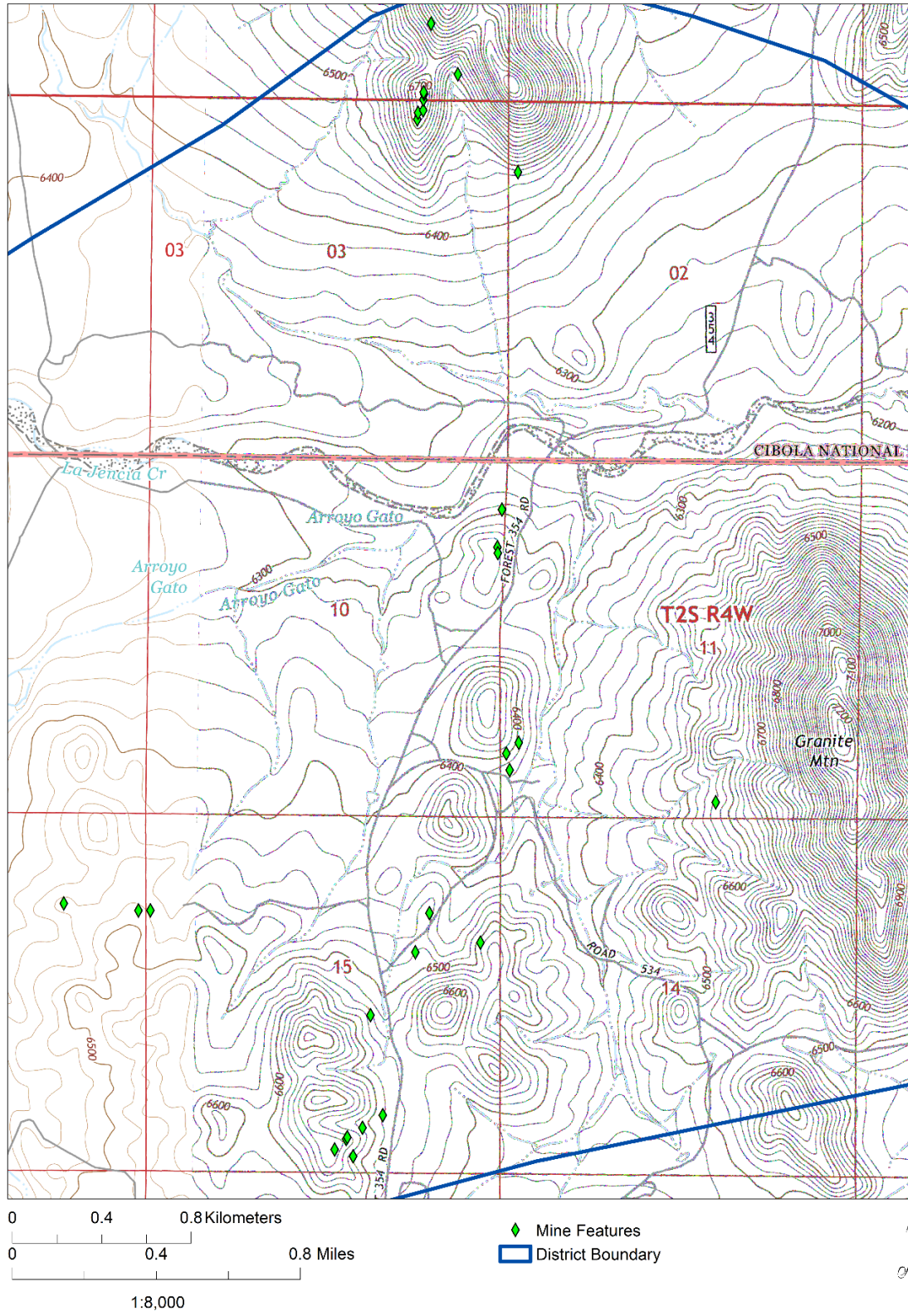


Figure 4. Granite Mountain area and mine features.

1.2 Geographic Setting

1.2.1 Central Socorro County

The North Magdalena mining district, located in central Socorro County, New Mexico, lies immediately (<1 mi) north of the town of Magdalena. Approximately 35 mi to the west, the nearest settlement is Datil and to the east lies Socorro, roughly 27 mi away. Situated between these two communities and located along U.S. Highway 60 (US-60), Magdalena is a hub for access to remote areas of west-central New Mexico. Other notable intersections in the area include New Mexico State Road 107 (NM-107), which runs south past the Rosedale district, intersecting Interstate 25 (I-25) near Fort Craig, and Forest Road 354 (NM-354), which becomes County Road 12 and reemerges on I-25 just north of the Sevilleta National Wildlife Refuge. New Mexico State Road 169 (NM-169) runs north through the district to the Alamo Navajo Reservation providing vehicle access to many mines and prospects along the way.

1.2.2 Quadrangles and Nearby Districts

Three 7.5-minute quadrangle maps cover the area that makes up the North Magdalena district. The Silver Hill quadrangle covers the westernmost extent, the Arroyo Landavaso quadrangle covers the southwestern tip of the district, and the Granite Mountain quadrangle encompasses the eastern and northernmost portions of the district. McLemore (2017) defined shapefiles for the district boundary in ArcGIS based on prior studies by Mardirosian (1971) and geological features, which have been used for the AML project and this thesis. There are several nearby mining districts including the Bear Mountains district to the north and the Magdalena, Hop Canyon, and Water Canyon districts to the south. A map showing metals districts and major roads relative to Socorro and Magdalena can be seen in Figure 5.

1.2.3 Flora and Fauna

Vegetation in the district is dominated by grasses, shrubs, and low-trees characteristic of high plateaus above the Chihuahuan Desert Ecoregion. Oneseed (*Juniperus monosperma*) and alligator (*Juniperus deppeana*) juniper are common and can be found alongside piñon pine (*Pinus edulis*) depending on relative elevations. The rolling hills and plains of the district are used by ranchers for grazing cattle. Wild animals in the area include rodents (woodrats, jackrabbits, cottontails, etc.), badgers, coyotes, foxes, deer, elk, and possibly mountain lions. Barn owls (*Tyto alba*) have been observed in mine shafts and bats probably dwell in some of the adits, though none were observed during this study.

Metals Districts Near Socorro

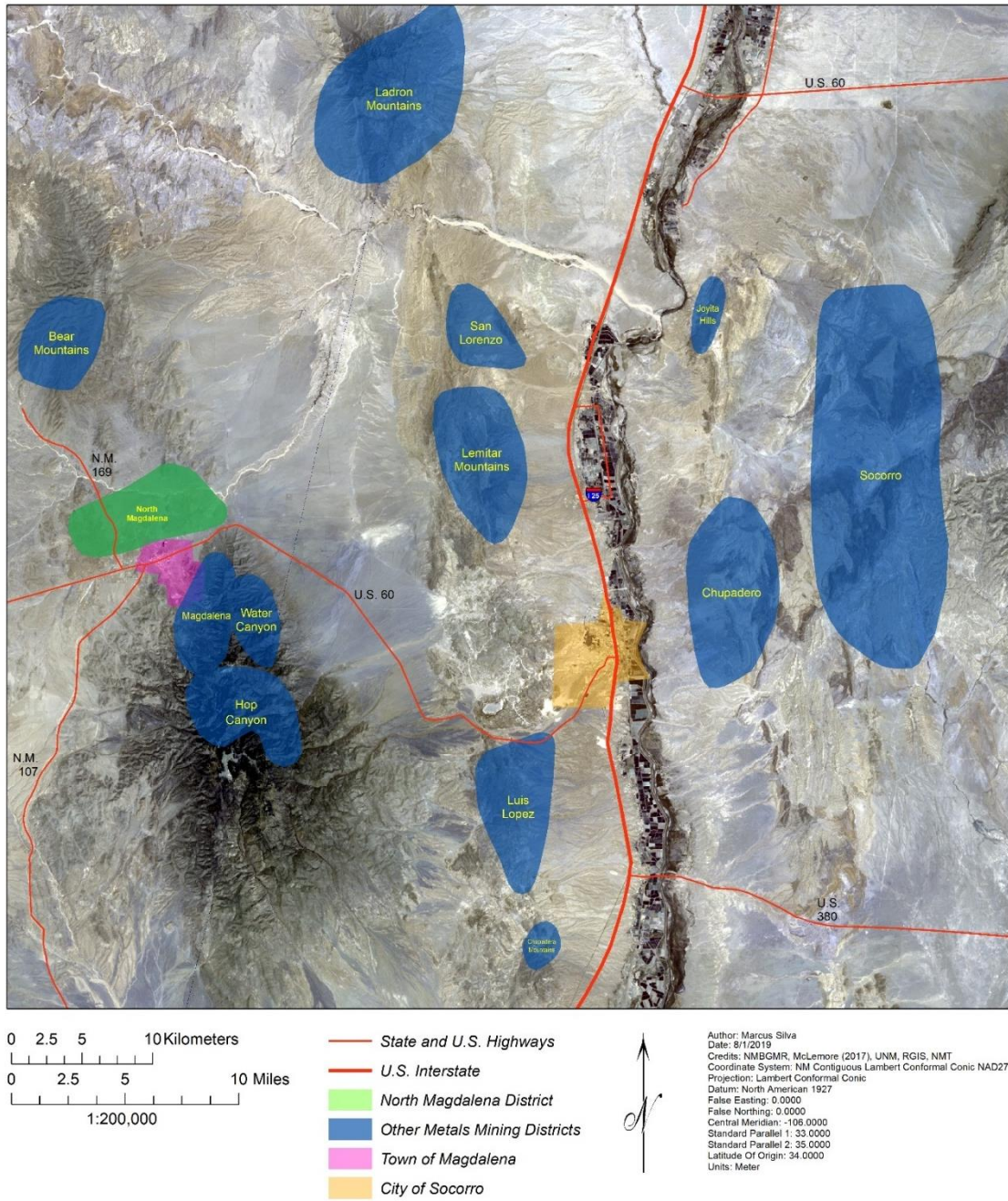


Figure 5. Map of historic metals districts near Socorro and Magdalena; after McLemore (2017).

1.2.4 Precipitation and Hydrogeology

Precipitation in the Magdalena area is higher than at lower elevations such as Socorro but is still typical of high desert/plateau climates averaging about 13 inches per year. The average annual high temperature is 69°F and the average annual low is 38°F with an overall average temperature of 54°F (“U.S. Climate Data”, 2019). Precipitation from October to May is low to moderate with rain and snowfall in the winter and little during the spring. During the summer months of June to September, the monsoon season that affects much of the southwest delivers the highest rainfall through thunderstorms and cloudbursts most afternoons. Precipitation in the region migrates into fractured bedrock and alluvial aquifers, which store most of the groundwater in the Magdalena area. According to Timmons (2013), water production is highest (~200 GPM) along the Magdalena fault zone which trends NE-SW. Because precipitation is the primary form of recharge for these aquifers, water levels at wells may drop during the dry season.

1.3 Abandoned Mine Lands Project

Two purposes of the AML project were to inventory and prioritize historic mine features for remediation based on physical and environmental hazards. The Mining and Minerals Division (MMD) of the New Mexico Energy, Minerals, and Natural Resources Department (NMEMNRD) oversees state AML work and contracted New Mexico Tech to study three districts near Socorro. The AML contract with New Mexico Tech was focused on the Rosedale, Jicarilla, and North Magdalena districts. Rosedale and North Magdalena are low sulfidation volcanic-epithermal-Au-Ag systems, while Jicarilla (Lincoln County) is a Great Plains margin or alkaline-related Au-Te vein deposit (North & McLemore, 1986; McLemore, 1996).

Analytical methods used throughout the AML project included geochemistry, acid-base accounting (ABA)/paste pH, and mine soil petrography. Implementing these techniques upon waste rock at selected mines allowed the material to be classified as suitable or unsuitable for backfill. Backfill-material, from a reclamation standpoint, must not be potentially acid-generating, as waters from the features have the potential to seep into groundwater or affect adjacent soils. Determination of potential acid formation is described in the Global Acid Rock Drainage (GARD) Guide (“Global acid”, 2012) and based upon earlier work by Price (2009). This provides steps and equations for calculating acid generating potential from mine waste using simple proxies and will be discussed thoroughly in Chapter 3. This thesis will supplement the AML and NMBGMR reports for the district; the environmental hazards sections of these reports will be built-upon using more advanced analytical techniques to examine small-scale mineralogy.

1.4 Problem Being Addressed

The goals of this study are 1) to locate and inventory mines and prioritize them for reclamation and 2) characterize the mineralogy of each mine to provide a strong background for future work in the district. When conducting initial research on the North Magdalena district for the AML project, the first issue that arose was a lack of information regarding locations and site-specific geology of mines and prospects. The NMBGMR records for mines in the area are incomplete; the most recent information comes from the 1986 Abandoned Mines Survey (AMS) of the Magdalena district. This survey did not consider Magdalena and North Magdalena to be distinct districts, so many features in North Magdalena were included in their inventory (Bobrow et al., 1986). However, this earlier survey was conducted without the use of GPS, so mine locations were marked on topographic maps in the field. By performing field inventory of mine features in the North Magdalena district, a comprehensive record of GPS location data (accurate to ± 12 ft) and mineral assemblages will be generated and presented in the appendices and the New Mexico Mines Database (McLemore et al., 2005).

1.5 Previous Studies

Though there were probably newspaper articles from the late 1800s reporting on activity in the district, it was beyond the scope of this project to locate them. The next earliest work on the area is Jones (1904), which describes ore deposits and mining in the state of New Mexico, refers to North Magdalena as the Pueblo district (sometimes used as an alternate name for the Granite Mountain area), and summarizes the early history of some of the mines, including the Ace of Spades (NMSO0811). One local newspaper article and a journal publication from 1907 and 1908, respectively, were found in the NMBGMR archives that report on the discovery and development of vanadium occurrences in the district ("A vein of vanadium", 1907; Heister, 1908). Lindgren et al. (1910) describes ore deposits at a state-wide level and features a section on the Magdalena district, but does not discuss deposits north of US-60. The first county-scale work regarding ore deposits was by Lasky (1932), where the author describes the Nighthawk, Jack Frost, Pleasant View, and Pennsylvania claims, as well as 13 unpatented claims owned by the Copper Belt Silver & Copper Company. The author also briefly describes some ore and vein characteristics. Throughout the early to mid-1900s, sporadic examinations by mining companies have produced reports, which always conclude with a recommendation not to pursue further exploration and mine development because of insufficient grade and deposit size (Frolli, 1943; Holmquist, 1946; Williams, 1963; Vista, 1977).

Three master's theses were produced by New Mexico Tech students who examined and characterized the volcanic lithology and stratigraphy of the district, but only one goes into detail regarding ore mineralization. Johnson (1955) first described the lithology and structure of the area, followed by Brown (1972), who focused on the geology of the southern Bear Mountains, which intersect the northernmost portion of the district. The most comprehensive study of the area was Simon (1973), who did a detailed petrographic and stratigraphic analysis of volcanic units in the Silver Hill area. The author also includes a chapter on economic geology, describing alteration and vein paragenesis. Osburn & Chapin (1983) checked and corrected many of these volcanic units and included them in the nomenclature for Cenozoic rocks of the northeastern MDVF. Osburn (1984) then produced a small-scale geologic map of Socorro County (Fig. 6) and used the volcanic units described by Simon (1973) and other workers in his mapping of the area. The last major work performed in the district was Bobrow et al. (1986). However, in the 33 years since Bobrow et al. (1986) inventoried mines in the area, many features have experienced erosional and structural deterioration. Therefore, an updated inventory of the condition and locations of mine features will be of great use. Other works briefly mentioning the district as a component of larger studies include Metzger (1938), Anderson (1957), Howard (1967), North (1983), North & McLemore (1986, 1988), Ackerly (1997), McLemore (1994, 1996, 2001, 2017).

CHAPTER 2

Geologic and Historical Background

2.1 Geology

2.1.1 Regional Geology

The Mogollon-Datil Volcanic Field extends from southwest New Mexico, near Silver City (with some related volcanism in the Organ Mountains outside Las Cruces), north to the Socorro-Magdalena area, and westward to Datil and the Arizona border. It represents the northern reach of a field that extends south into central Mexico (McIntosh, 1991). Magmatism began with regional extension and normal faulting from the Basin and Range Physiographic Province; in fact, the MDVF straddles the boundary between the Basin and Range Province and Colorado Plateau. Early magmatism was dominated by andesites from approximately 38-30 Ma, while ignimbrites have been dated from 36-24 Ma (McIntosh et al., 1992). This later transitioned to basaltic andesites and more silicic rocks such as quartz latites and rhyolites by 30-18 Ma. After 15 Ma, basalt flows began to erupt across the landscape (Elston & Abitz, 1989). The North Magdalena district lies at the northern boundary of the MDVF and features almost all representative lithologies, the majority of which are calc-alkalic.

Precious metal mineralization in the MDVF has led to a suite of productive mining districts over the years including Mogollon, Chloride, and Kingston (McLemore, 1996, 2017). Generally, less-altered and more silicic rocks like dacites and rhyolites of the MDVF have higher silver concentrations than more-altered, less silicic lithologies such as andesites and basalts though exceptions, including Rosedale and North Magdalena, exist (Bornhorst & Wolfe, 1985). Some caldera magmatism in the MDVF is associated with the Morenci and Santa Rita Lineaments, which also appear to control major copper porphyry systems (Mayo, 1958; Lowell, 1974; McLemore, 1996; Chapin et al., 2004). Three MDVF calderas proximal to the North Magdalena district are the Magdalena, Sawmill Canyon, and Socorro calderas (Chamberlin, 2001).

2.1.2 District Geology

The suite of volcanic lithologies found within the district have been characterized in several studies including Johnson (1955), Brown (1972), Simon (1973), Osburn & Chapin (1983). Osburn (1984) produced a geologic map of Socorro County from which Figure 6 was derived.

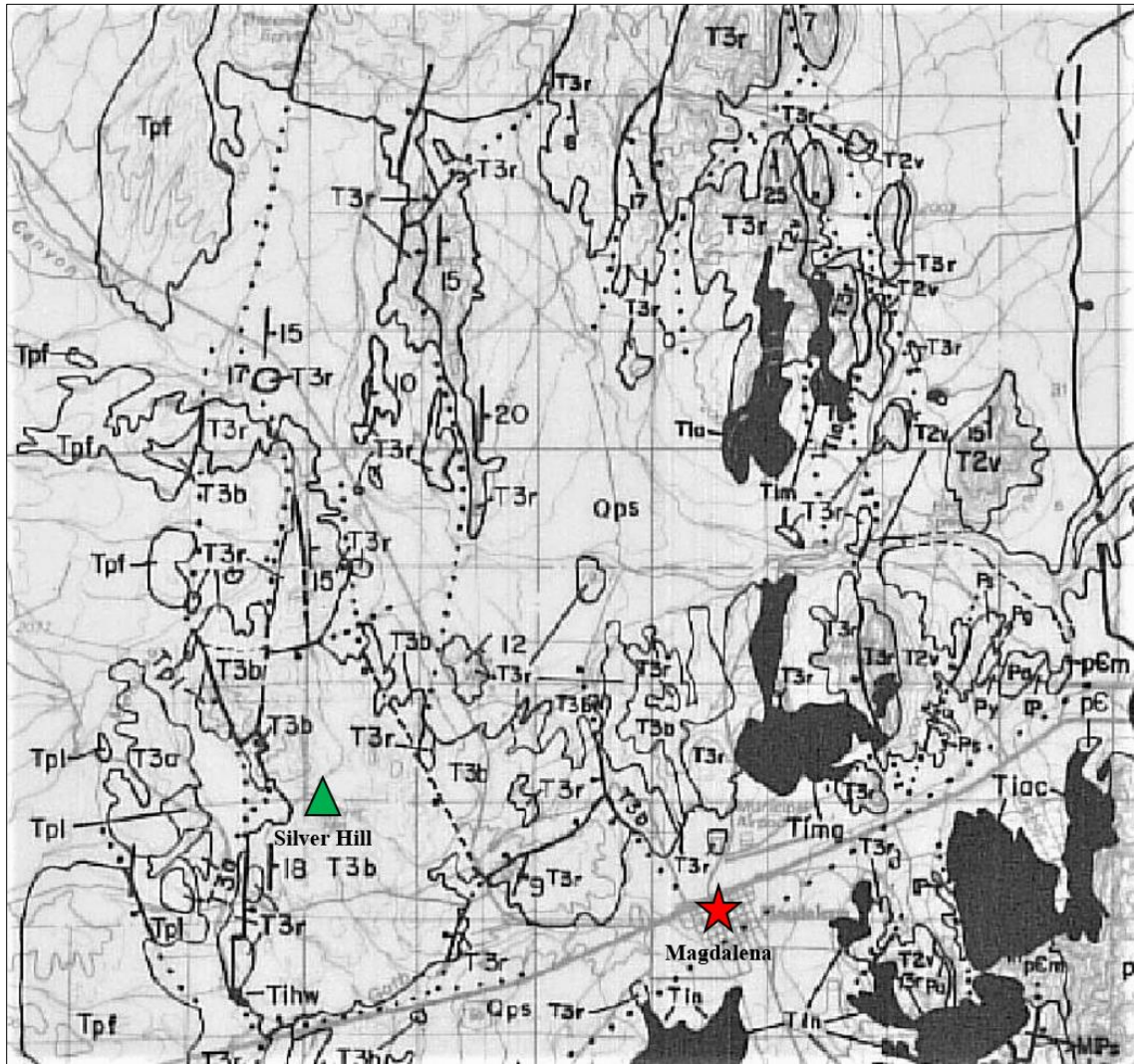


Figure 6. Cropped section of geologic map from Osburn (1984).

Precambrian units: **pCm** (metasedimentary/volcanic rocks). Permian units: **Pg** (Glorieta Sandstone), **Ps** (San Andres Limestone), **Py** (Yeso Formation). Tertiary units: **T2v** (Datil Group), **T3a, b, r** (regional ash-flow tuffs), **T1a** (Anchor Canyon Stock), **T1hw** (Hale Well Pluton), **T1m** (monzonitic intrusive), **T1pf** (fanglomerates), **T1pl** (mudflows). Quaternary units: **Qps**: piedmont-slope alluvium.

2.1.3 Pre-Tertiary Lithologies

Johnson (1955) and Brown (1972) suggest that there are no rocks predating the Tertiary Period outcropping within the district. While this true for much of the district, the current district boundary extends to the east side of Granite Mountain, which does host limited outcrops of Precambrian granite and metamorphic rocks (Simon, 1973).

2.1.4 Tertiary Lithologies

The rocks within the district are predominantly Tertiary (Oligocene-Miocene) in age. The volcano-stratigraphic sequence (from oldest to youngest) representing emplacement during the Oligocene Epoch is the Hells Mesa Tuff, La Jencia Tuff¹, Andesite of Landavaso Reservoir, and Upper Tuffs. These formations are part of the larger Datil Volcanics that were first identified by Winchester (1920) as the “Datil Volcanics Formation” but were later upgraded to the “Datil Volcanics Group” by Weber (1971). There is also an intrusive body known as the Hale Well stock that outcrops to the southwest. It is monzonitic and is likely a small, exposed portion of a much larger body. An erosional unconformity separates the Upper Tuffs from the lower-Miocene strata. This marks the start of the Miocene-aged Arroyo Montosa unit, which is overlain by the La Jara Peak Andesite. The uppermost portion of this sequence is the Popotosa Formation, which is the lower part of the larger Santa Fe Group.

Although the local geology is dominated by volcanic rocks, there are minor sedimentary outcrops within the district. Sandstones outcrop on the west slope of Granite Mountain and conglomerates are found in the far northwestern corner of the district. The attitudes of these exposures could not be determined as the sandstone is encased as float in latite and the conglomerate is buried under pediment and can only be seen in a drainage of La Jencia Creek². The sandstone, which is incorporated into latite outcrops, may be as old as Cretaceous, but no dating or further work has been done, so the age and stratigraphic assignment remains undetermined. The conglomerate is suspected to be associated with the Santa Fe Group and is thus one of the younger units in the area. Finally, some of the volcanic rocks have weathered into minor volcanoclastic sandstone lenses, but are not designated as official members (Johnson, 1955). Because of the limited amount of information regarding sediments in the district and their irrelevance to mineral deposits, the remainder of this section will focus on summarizing lithologic characteristics of volcanic rocks from the available reports.

¹ La Jencia Tuff formerly known as the A-L Peak Formation (Simon, 1973; Osburn & Chapin, 1983).

² Johnson (1955) refers to this as “La Jenze Creek”, which is likely an older name for, or misspelling of, “La Jencia Creek”.

2.1.4.1 Oligocene Lithologies

Hells Mesa Tuff: The oldest rocks in the area outcrop in a very limited region on the hills adjacent to Arroyo Montosa, which lie outside the district boundary. This formation is of mid-Oligocene age, associated with the Socorro Caldera (Chamberlin, 2001), and likely does not outcrop within the current district boundary as it has only been recorded in the northern sections of the Silver Hill quadrangle (Simon, 1973). However, it is likely found at depth within the district and may be intersected by some of the deeper mine shafts in the area. Named by Tonking (1957), described by Simon (1973) and Osburn & Chapin (1983), and mapped by Osburn (1984), the Hells Mesa Formation is composed of regional ash-flow tuffs mostly of rhyolitic and quartz latitic composition ranging from 600-3,850 ft thick in some areas. It is overlain (unconformably) by the La Jencia Tuff.

La Jencia Tuff: Six tuffaceous members that constitute this formation are described by Simon (1973) and distinguished by lithologic characteristics observed in the field and in thin section. However, according to Osburn & Chapin (1983), the second and sixth members (tuffs of La Jencia Creek and Allen Well) are now obsolete as they were miscorrelated and represent sections of Lemitar Tuff. The lowest member, called the gray massive member, conformably overlies the Hells Mesa Tuff and is a very crystal-poor, rhyolitic ash-flow tuff. Overlying a section of Lemitar Tuff, the flow-banded member outcrops at the border of Arroyo Landavaso and is strongly welded with a very low phenocryst concentration. The next member is characterized by pumice autoliths and known as the pumiceous member. The fifth member of the La Jencia Tuff is referred to as the andesite flows. These are thin and have weathered in places to produce minor lenses of volcanoclastic sandstones. Another section of Lemitar Tuff overlies the andesite flows and small andesite dikes cut the flow-banded member and Lemitar Tuffs. Alteration in this formation is weakly argillic and often follows the more permeable sandstones or fractures. (Brown, 1972; Simon, 1973, Osburn & Chapin 1983).

Andesite of Landavaso Reservoir: Originally mapped and described by Loughlin and Koschmann (1942) at an outcrop in the Magdalena District, this porphyritic unit has a maximum thickness of 800 ft and in some locations manifests as a banded vitrophyre. The Andesite of Landavaso Reservoir largely occurs outside the southern boundary of the district.

Upper Tuffs: The most recent Oligocene volcanic rocks in this area are a series of poorly defined and variable tuffs that have a combined thickness of over 600 ft. Textures range from vitrophyric to coarse-grained ash-fall material (Simon, 1973). According to Deal & Rhodes (1976) and Osburn & Chapin (1983), these tuffs may be correlated with a mix of tuffs (South Canyon, La Jencia, Lemitar, Hells Mesa, and Tuff of Caronita Canyon) that occur in the northern San Mateo Mountains. The upper tuffs make up the final section of Oligocene-aged rocks in the area.

2.1.4.2 Miocene Lithologies

Unit of Arroyo Montosa: This unit features volcanic rocks interbedded with conglomerates. The volcanic facies comprise latites to dacites, while the conglomeratic facies consist chiefly of subangular-subround pebble-sized clasts with large plagioclase phenocrysts; within the beds are thin sandstone lenses. Because of stratigraphic ambiguity, it is unclear which facies is older (Simon, 1973). However, the conglomerates clearly predate the overlying formation because La Jara Peak Andesite does not occur as clasts. This unit mostly outcrops outside the western boundary of the district.

La Jara Peak Andesite: Tonking (1957) named this formation and described it as a thick sequence of basaltic andesite flows and volcanoclastic sandstones. It is the final volcanic event that is represented in the Silver Hill area and in outcrop forms rounded hills which are the most common elevated features in the field area. It is generally porphyritic and often contains elongated vesicles of quartz and calcite. Flow direction was determined from the direction of elongation and has been reported as either NW or SE. Many unconformable contacts occur between the La Jara Peak Andesite and older units mentioned above. Because this is the uppermost unit, it has been designated as the host rock for mineralization on all mine inventory forms. This is largely because it is extremely difficult to tell from which of the volcanic sequences mineralized waste rock originated.

Popotosa Formation: The uppermost Miocene strata in the Silver Hill area is represented by this formation and is assigned to the Santa Fe Group. Uplift and basin and range deformation provided the erosional material that composes the playa deposits and conglomerates of this formation. Clasts are predominantly La Jara Peak Andesite and range in size from a few inches to a foot (Simon, 1973).

2.1.5 Tertiary-Quaternary Deposits:

On the land surface there are pediments that contain a caliche zone and poorly sorted clasts of a variety of lithologies from the tertiary volcanics. Quaternary alluvial deposits and eolian sand occur sporadically throughout the rest of the district (Simon, 1973; Osburn, 1984).

2.2 Structural Influences

The general structural regime in the North Magdalena district is extensional, with most faulting occurring during the Oligocene-Miocene along the western margin of the RGR. These faults are responsible for many of the erosional features, unconformities, and mineralized/altered zones found in the field area. Veins at most mines in the district trend very nearly N-S at about 350-0°, with smaller scale NW-SE veins striking at 310-330°. Vein trends become obvious when plotting mine locations in ArcGIS as most features fall along roughly north-south lines. Observations made during this project corroborate earlier claims by Simon (1973) that most faults in the district dip from about 60° to nearly vertical. There is a shallow syncline in the southern portion of the Bear Mountains at the north end of the district, but it is poorly exposed and has not been well-characterized (Simon, 1973).

The Magdalena fault zone and La Jencia Fault are proximal to the district (“Geologic map”, 2003). The Magdalena fault zone runs NE-SW and passes directly through the town, separating the North Magdalena and Magdalena districts. La Jencia Fault, a late Cenozoic structure which delineates the western edge of the RGR, is characterized by an approximately 21 mi scarp from the east side of the Magdalena Mountains to the Bear Mountains (Machette, 1988). Furthermore, the fractured ring structure associated with the Magdalena caldera may have increased rock permeability and allowed for additional hydrothermal fluid flow during the formation of the district’s deposits (Chamberlin et al., 2004).

2.3 Economic Geology

2.3.1 General Deposit Type Characteristics

The North Magdalena district, like many districts in the MDVF, is a low sulfidation volcanic-hosted epithermal deposit (Lindgren, 1933; McLemore, 1996; John et al., 2018). Also known as alkali-chloride or adularia-sericite deposits, these are common in the MDVF because of their close association with caldera- and intrusion-related geothermal systems. Heat from large magmatic bodies causes convection of groundwater and meteoric water, typically mixed with magmatic fluids that rise to the surface (as hot springs) or near surface (<0.5 mi). As heated fluids migrate along faults and other structural conduits created by fracturing and deformation of country rock in part by the associated magmatic body, they scavenge and concentrate metals; additional metals are derived from the magma. Precipitation of ore minerals, in some cases, is initiated by boiling of fluids which destabilizes transport ligands and releases metals from solution. These metallic ions are then free to pair with elements such as sulfur, selenium, tellurium, or others depending on the wall rock and fluid characteristics. Another mechanism for mineralization is the mixing of different fluids. Hydrothermal fluids associated with Ag-Pb-Zn deposits are generally of slightly higher salinity (10-20 wt% NaCl eq.) than Au-dominated systems (<5 wt% NaCl eq.) and range in temperature from 150-300°C. At near-neutral pH (compared to high-sulfidation systems), there is limited cation-leaching, which results in less destruction of host-rock feldspars and produces fewer clays as gangue. Finally, high concentrations of CO₂ in ore-forming fluids will depress the depth of boiling causing deposition of ore minerals deeper in the system (Simmons et al., 2005).

Intrusions or collapsing calderas shatter the country rock, which is subsequently infiltrated by convecting fluids. This creates hydrothermal breccias with predominantly silica or carbonate cementation. These breccias can be 2 in to 2 ft wide (Fig. 7). Common gangue minerals in low-sulfidation epithermal systems include adularia, sericite³, carbonates, fluorite, chlorite, magnetite, epidote, and silica (drusy quartz, chalcedony, and amethyst) (Fig. 8). Economically significant minerals in low sulfidation systems include electrum, native gold, sphalerite, chalcopyrite, galena, sulfosalts, pyrite, and arsenopyrite. The latter two minerals may contain trace gold, and also can result in environmental and metallurgical challenges during production.

³ “Sericitite” is used as a non-specific term for fine-grained, white to pale-green phyllosilicates (Eberl et al., 1987). In this case, it includes muscovite, celadonite, and aluminoceladonite which are members of the “phengite” solid solution series (Rieder et al., 1998). A specific designation was not possible due to the fine-grained nature of the mineral as well as time and analytical constraints.



Figure 7. SC-D1 (NMSO0866); massive hydrothermal breccia with carbonate cement.



Figure 8. Mag23-S1 (NMSO0921); drusy quartz coating fractures and cavities in andesite.

For comparison, high-sulfidation epithermal systems (also referred to as acid-sulfate or quartz-alunite deposits) feature ore minerals with higher oxidation states of sulfur (e.g. pyrite) and more intense alteration and textural destruction of the host rocks. While there are many high sulfidation deposits in New Mexico, Alum Mountain is the only deposit with limited precious metal production (McLemore, 1996, 2017). High-sulfidation deposits are typically associated with low-pH fluids of $>300^{\circ}\text{C}$ and typically <5.5 wt% NaCl eq., though some can be highly saline. Degassing of magmatic vapors or boiling at depth produces acidic vapors rich in SO_4^{2-} , which rise and condense or mix with and acidify groundwater. Often, there is additional contribution of magmatic fluids (John et al., 2018), which, if present, are usually derived from a magmatic system at depth (Cooke et al., 2011). The expression of mineralization and alteration depend on the fluid and buffering capabilities of the wall rock. Alteration is controlled by progressive hydrolysis reactions upon wall rock mineralogy by acidic fluids until the buffering capabilities are overcome. This manifests in early stages as argillic alteration and later stages as advanced argillic alteration, though most conduits exhibit locally zoned alteration with greater textural destruction proximal to the vein center (Henley & Berger, 2010). Alteration and gangue minerals therefore include silica plus kaolinite, dickite, pyrophyllite, alunite, diaspore, and other aluminous feldspar alteration products. Common trace and ore minerals include tellurium and bismuth minerals, cinnabar, enargite, pyrite, covellite, sulfosalts, and precious metals.

Buchanan (1981) noted that there is often strong vertical or on-strike mineralogical zonation in these systems. Gold is typically deposited at shallow levels of 0-200 m and $100\text{-}200^{\circ}\text{C}$, while silver and sulfosalts occur from around 200-350 m and $200\text{-}225^{\circ}\text{C}$. Base metals are usually found at depth in the system from around 350-500 m and at temperatures of $225\text{-}250^{\circ}\text{C}$.

2.3.2 Deposit Characteristics at North Magdalena

North Magdalena is a typical low-sulfidation epithermal system with gangue and ore mineralogy reflective of formative near-neutral, moderate temperature, and low-to moderate-salinity fluids. Gangue mineralogy mostly comprises silica, carbonates, barite, and clays, and the host rocks have undergone little to no textural destruction. Alteration is weak but pervasive and includes argillic, propylitic, and some phyllic. Elevated silver concentrations and widespread base-metal sulfides imply low-moderate salinity fluids were key in the formation of this deposit. Mechanisms of ore formation and paragenesis will be proposed in Chapter 5.

Because of the association between volcanic-epithermal systems and intrusions, there had been some speculation that a buried porphyry may exist in the western portion of the district as alteration increases in intensity to the west (Simon, 1973). Several intrusions in the Magdalena district have produced alteration and contributed to formation of the district's carbonate replacement deposits (Blakestad, 1978), but it is unclear if these had any influence on the North Magdalena deposits. A more likely intrusive association would be with the Magdalena caldera, which is proximal to the southern boundary of the North Magdalena district and may have provided the necessary structures, heat, and fluids to generate an epithermal deposit (Chamberlin et al., 2004).

Mineralization is largely constrained to small shoots within larger veins and fissures (Lasky, 1932; observations in this thesis). Veins pinch and swell both vertically and horizontally, often breaking into smaller stringers (Simon, 1973). Mineralization appears independent of host rock geochemistry and more controlled by hydrothermal fluid compositions. Lasky (1932) reports that strong copper-silver mineralization was observed on veins east of Silver Hill. These veins trend roughly NNW-NW and are often discontinuous along strike, splaying into other veins or being truncated by faults.

The Jack Frost vein is a major vein structure that hosts Ag-Pb-Zn-V mineralization. It strikes NW at about 280° and dips irregularly at 65-80° to the NE. This splits into stringers several inches across, which connect to another major (though less mineralized) vein striking 310° and dipping 70° NE. Basic dikes often form walls of the Jack Frost vein, which in places is about 6-9 ft wide. The Pleasant View vein and group of workings host vanadium and lead as well and are located about one mile south of the Jack Frost vein. Gold was mined from the Pennsylvania group of claims (Lasky, 1932), which are hosted in a shear zone of white rhyolite north of the Jack Frost group.

2.4 Historic Mining, Production, and Exploration

Most productive mining and prospecting occurred during the late 1800s to early 1900s and throughout its history, North Magdalena has produced silver, gold, lead, and copper in limited quantities. Some sporadic exploration ventures in the mid-1900s targeted Zn, V, and Ba, but no production records for these commodities could be found. Some of the earliest recorded production, reported by The Socorro Bullion (1885), stated that 200 sacks of an unspecified ore from the Sophia Lode were sent to the Billing smelter near Socorro (as cited in North, 1983, p. 263); other production prior to 1900 was not well-documented. According to North (1983), the district has produced <500 tons of ore in its history; low compared to some other districts in the MDVF (Table 1). There are currently no active mining operations in the district.

District (production dates)	Ore (short tons)	Au (oz)	Ag (oz)	Cu (lbs)	Pb (lbs)	Zn (lbs)
Mogollon (1902-1969)	--	365,000	>20,000,000	1,500,000	1,200,000	Some
Cochiti (1894-1963)	205,045	42,000	210,000	2,500	22,457	-
Steeple Rock (1880-1991)	365,000	151,000	3,400,000	1,200,000	5,000,000	4,000,000
Rosedale (1882-1981)	<100,000	27,750	10,000	-	-	-
Kimball (1875-1953)	-	1,500	400,000	12,000	125,000	Some
San Jose (1932-1941)	5,000	900	13,000	250	100	-
North Magdalena (1900-1957)	<500	35	<200	At least 1,138	1,400	-

Table 1. Production from epithermal districts in New Mexico; after McLemore (1996).

In 1919, the Copper Belt Silver & Copper Company filed 14 claims (unpatented) east of Silver Hill (North, 1983), which can be seen on a claim map from Lasky (1932). Several workings (known as the Chief Group), including Mag4-S1 (NMSO0377) (Fig.12), encountered Cu-Ag ore on the Chief vein at 300 ft. A short distance to the southeast, the Red Rose vein intersects the Chief vein and produced small amounts of ore. The claims filed by this company also covered the Long Lost, Comanche, and Bartlett veins. Reportedly, mineralization included acanthite⁴, chalcocite, covellite, chrysocolla, and malachite. Approximately 3 short tons of ore were mined from these claims producing 1,138 lbs of copper and 149 oz of silver (Loughlin & Koschmann, 1942). Production records from this company are the only records for copper production in the district and the last records of production for the district, overall. North (1983) states that from 1900-1957, <200 oz of silver, 35 oz of gold, and 1400 lbs of lead were produced, but it is likely the majority of this was produced during and prior to mining activity in 1919. It appears that mining efforts in the district post-1919 did not pass the exploration stage.

There are no records of production for Zn, V, or Ba. Lasky (1932) mentioned that early in the district's history, ore from the Jack Frost, Night Hawk, and Pennsylvania claims (known to host Zn and V) was sent by ox team to the Billing smelter and the Pennsylvania stamp mill in Pueblo Canyon. Based on mid-century exploration reports, however, grades of vanadium and zinc were too low to be of economic importance and no properties produced. This fact, combined with the processing methods, suggests ore from these claims most likely yielded Pb, Cu, Ag, and Au. Sphalerite has been seen in many waste piles, but not in large enough quantities to be produced. It is possible that production records for zinc and other commodities were incorporated into the Magdalena district production records from before they were considered separate districts. From 1963 to the late 1970s, barite was targeted as an industrial commodity, but little, if any, production occurred (Williams, 1963; North, 1983).

⁴ Lasky (1932) and Simon (1973) refer to this as "argentite". However, argentite (cubic) is only stable above 177°C. This habit can be preserved below 177°C but will have undergone a reversible phase transition to acanthite (monoclinic). All room temperature samples are therefore pseudomorphs of acanthite after argentite (Ramsdell, 1943; Taylor, 1969). As such, "acanthite" will be used throughout the rest of this report.

The first exploration efforts following activity by the Copper Belt Silver & Copper Company in 1919 were undertaken in 1925. Neale (1926) mentioned that drilling was conducted in 1925 to depths of 820-1,042 ft in an attempt to intercept the highly mineralized Kelly Limestone, which potentially underlies the volcanic strata (as cited in Simon, 1973, p. 3). This drill data could not be located but it is reported that attempts to reach the Kelly Limestone were unsuccessful, with drill holes bottoming-out in igneous rock. Since then, several exploration ventures have taken place which targeted Ag, Cu, Pb, Zn, V, and Ba.

During the spring of 1943, the American Smelting and Refining Company examined properties owned by Emmett Nutter (Virginia Lee #1-4 Claims) and two men with the surnames Hammond and Johnston (Lucky Dog #1 Claim) (Frolli, 1943). These properties had reported occurrences of vanadium, lead, zinc, and silver, which were needed for the war effort. Located on state land, the claims were originally leased to A. Dugger as 8 claims named the “Jack Frost Group” and P.B. Moore as 4 claims named the “Night Hawk Group”. The company collected nearly 70 samples from accessible drifts in the main shaft (the “Dugger shaft”) and other workings along the Jack Frost vein. Out of 67 samples, only 9 samples featured lead grades of >3% while only 3 samples had >3% zinc. Silver values averaged about 0.1 oz/ton. The low and inconsistent grades at depths of 140 ft were enough evidence that a minable deposit at greater depth was unlikely and the purchase option was declined. At the same time, Mr. Nutter requested a survey of the Dugger Shaft by a U.S. Bureau of Mines (USBM) engineer to determine if it qualified for a Reconstruction Finance Corporation development loan to sink the shaft an additional 100 ft (total 240 ft). However, the shaft was inaccessible due to bad air, poor timbering, and flooding, so sample assays and maps prepared by the American Smelting and Refining Company during their initial survey were examined instead. These data coupled with exploration by shorter shafts and pits along strike of the Jack Frost vein provided a comprehensive assessment of the property. The federal loan for a deeper shaft was not granted to Mr. Nutter for the same reasons the American Smelting and Refining Company declined the purchase option. The American Smelting and Refining Company dropped the purchase option for the Lucky Dog #1 Claim as well, presumably for similar reasons (Holmquist, 1946). With the end of WWII less than two years later, the need for vanadium and base metals dropped-off and the properties saw no further development.

Under new lease by Clarence Barrett of Socorro, the Dugger shaft (part of Jack Frost group) was reexamined in 1963 for potential exploitation of barite and fluorite (Williams, 1963). A USBM engineer visited the property, but the shaft was inaccessible because of further deterioration of the mine feature since the examination in 1943. A grab sample, obtained from the rock pile stacked near the shaft, was later assayed. It was determined to contain 25% BaSO₄, 23.7% SiO₂, 9.9% CaCO₃, 3.6% Fe, and 0.7% CaF₂. The USBM engineer determined that barite and fluorite grade and distribution within the host rock was not economically favorable and the mine has been inactive since.

In 1977, there was interest from ASARCO Incorporated to explore for silver resources in the district. The target for exploration was the Blackbird Mine, an Ag-Cu prospect on one of 12 claims owned by Ellwood Hunt of Magdalena from 1976-1977. Due to the size and grade of the prospect and ore characteristics that were incompatible with the mill in Deming, ASARCO declined to pursue further exploration or development. Though it is unconfirmed, the feature description in the report by Vista (1977) roughly matches SC-D1 (NMSO0866), which is in a field between Silver Hill and Cedar Hill on the far western edge of the district.

Due to its proximity to the town of Magdalena, low grades and heterogeneity of the deposits, and potential permitting difficulties, it is unlikely that the North Magdalena district will host any future large-scale production. However, the abundance of mineralized waste rock, network of dirt roads, and potential need for reclamation could make it an interesting target for waste rock reprocessing companies. One company is currently considering building a plant in Magdalena to produce fertilizers from waste in the Magdalena district and has shown interest in waste rock from North Magdalena. It is unclear whether North Magdalena waste material would be economic to reprocess due to low grades and volume (relative to those in the Magdalena district) and a more dedicated evaluation by the interested company would be necessary.

2.5 Patented and Unpatented Mining Claims

Many mine features are situated on claims, some of which date back to the late 1800s. These are a mix of patented and unpatented claims with patented claims remaining under different ownership today. Patented claims within the district are outnumbered by unpatented claims. Though the district was discovered in 1863, records prior to 1880 are poor. Plats and surveys of patented mining claims from the BLM Government Land Office (GLO) document some of the earliest mining activity in the district. These plats are excellent historical resources, documenting landowners, purchase and survey dates, the name of the surveyor, or the company that owned the claims. A table of patented mining claims and ownership can be reviewed in Appendix **B.7**.

While patented claims have historic, well-documented names, names of unpatented mine features and claims often change with each new owner. After 150 years of name changes it becomes quite difficult to assign accurate historical mine names to features inventoried on unpatented claims. For features situated on unpatented claims, mine names are based on the most recent claim name available or the most accepted name in the literature or U.S. Bureau of Mines records (at the NMBGMR). These are entered in the database along with other mine aliases and former claim names, if possible. Determination of whether an inventoried mine feature falls on an unpatented claim is difficult as most unpatented claims were not mapped or not mapped in detail; one would have to spend a tremendous amount of time in the Socorro County Courthouse records to locate the original mining claims. Distinguishing which feature inventoried in the field corresponds to which feature on the claim map is even more difficult when multiple features are present. When it was not possible to determine a mine name from a claim map or current owner, the mine name was entered as “unknown” in the database.

Some attempt was made to link mine features to unpatented claims when maps were available. This includes some features within the 13 claims filed by the Copper Belt Silver & Copper Company and workings of the Jack Frost Group. Usually, one of the best ways to link features with unpatented claims is to try and match the description of features in old reports with the features inventoried in the field. However, the major issue with this approach is that the features have often deteriorated from erosion and precipitation to a point that they are unrecognizable by their historic description; minor features are often not mentioned at all. As a result, it is usually only the major workings (shafts, declines, and adits) that can still be identified, while pits, cuts, and trenches remain unnamed. Fortunately, good records were kept from mining and exploration ventures on some of these unpatented claims in the 1900s, which greatly aided in identifying these features. For example, the description of the Dugger shaft on the Virginia Lee #1 Claim in Frohli (1943), Holmquist (1946), and Williams (1963) matched what was observed in the field and the main shaft of the Chief Group was well indicated on the claim map in Lasky (1932). These two instances, which had good descriptions and claim maps, are exceptions within the district and most mines features on unpatented claims could not be given historic names. Context clues, outdated feature descriptions, and landmarks are useful to a degree, but they are limited in many ways making positive identification of historic features quite difficult. Those that could not be positively identified were listed as “Unknown” in the NM Mines Database.

2.6 Mining Methods

Mines and prospects in the district comprise both surface and underground workings. Surface features include pits, cuts, and trenches while underground features include shafts, adits, and declines. Underground workings are less common, but far more dangerous. Many still have headframes, timbering, or other relic structures in or around them and these features pose the greatest hazards at which reclamation should be aimed.

Generally, pits range in size from shallow 1 ft deep impressions on the land surface to 15 ft wide, 6 ft deep holes. Pits are often unnamed and occur across the district having historically been used for exploration or staking claims (Fig. 9). Trenches vary in size, the largest of which can be up to 70 ft long and 15 ft deep (Fig. 10). Cuts are generally long, but shallow features which deepen uphill. The majority are small, at about 6 ft wide and 10 ft long, but some can be as large as 15 ft wide and >100 ft long (Fig. 11). Shafts dot the landscape (Figs. 12 & 13) and range in depth from 7 ft to ~300 ft. Adits are less common, but still pose physical hazards as they are much easier to explore than shafts and are far less stable. Declines are the least common but are typically very deep. See Table 7 for the number and types of each feature.



Figure 9. NM169-P2 (NMSO0835); looking south towards Magdalena Mountains. Presumably a very old feature (full-grown juniper on waste rock pile).

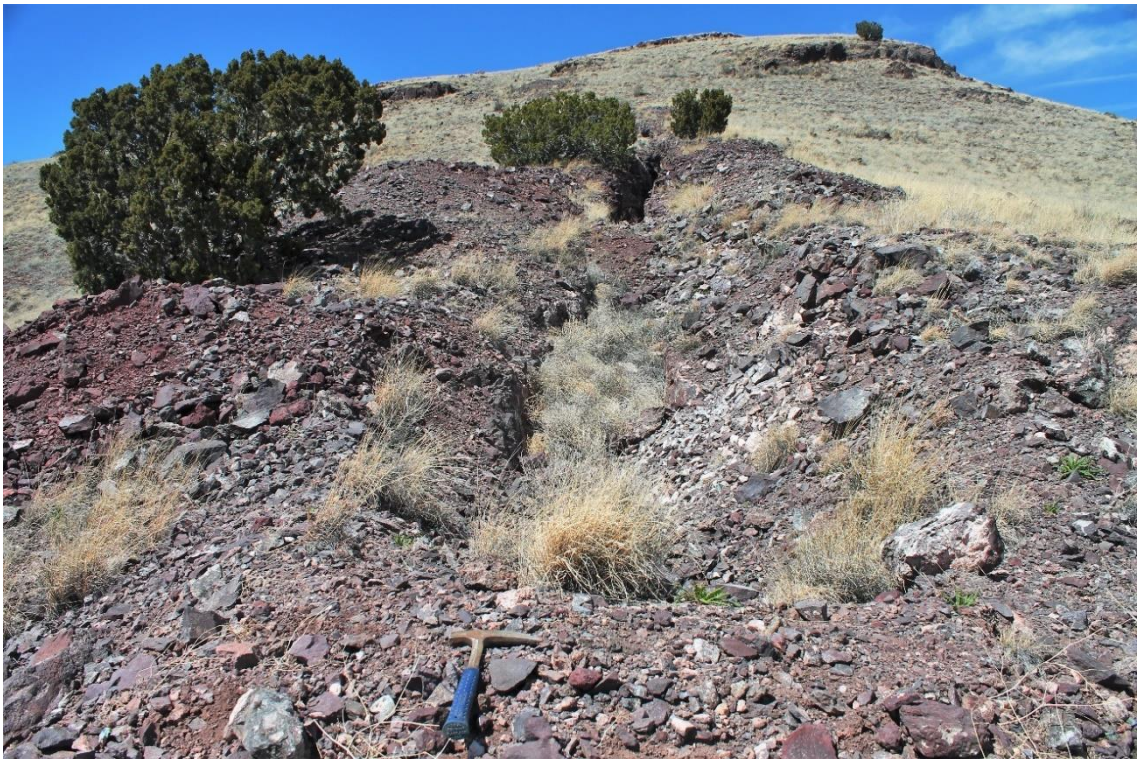


Figure 10. SH-T2 (NMSO0897); massive trench located on south slope of Silver Hill.



Figure 11. SH-C1; View south towards Ace of Spades on north slope of Silver Hill.



Figure 12. Mag4-S1 (NMSO0377); main shaft on the Chief vein sank ca. 1919 (Lasky, 1932). Headframe collapsing into collar of shaft (¼ mi from NM-169).



Figure 13. Mag4-S1 (NMSO0377); interior of shaft. Note the broken rungs on ladder and other indicators of instability. This shaft is >300 ft deep.

2.7 Land Ownership

Lands status in the field area is a mix of federal, state, and private land. Federal lands are open-access and host the greatest number of features, many on unpatented claims. However, these are less often major features or underground workings and are more commonly pits and trenches associated with exploration rather than production. In addition to federally owned land, some sections are owned by the state of New Mexico (state land) and other areas are private property, mostly homesteads. State lands require permission or a mining lease to access, and private lands require landowner permission. Mine features on state and private lands are usually larger workings on patented or unpatented claims that were leased to an individual or entity at some point in the district's history for exploration or mining.

2.7.1 Federal Lands

Federal lands regulated by the Bureau of Land Management (BLM) and United States Forest Service (USFS) offer public access by foot or vehicle on a network of dirt and gravel roads. At the time, a discovery pit or shaft was required to stake a claim on federal land. Furthermore, normal exploratory procedures for the time (late 1800s-early 1900s) involved digging small pits and other surface workings or sinking short shafts. As a result, there are many small features scattered across the hillsides and valleys. Fortunately, most of these features pose limited physical or natural environmental hazards. Unfortunately, however, many have become sites of illegal waste disposal by the public. Refrigerators, mattresses, water heaters, air conditioners, tires, and other refuse commonly fill pits and shafts on federal lands which are a hazard to groundwater and owls or other wildlife that live in the deeper workings.

2.7.2 State Lands

New Mexico state land is also part of the checkerboard of land ownership in the district. Rules for mining or exploration are different than specified in the Mining Act of 1872 that govern mining and exploration on federal land and require the land to be leased to the interested party; this may be an individual or company. The State Land Office controls mining leases on state land.

2.7.3 Private Lands

Private land, including mineral patents, constitutes a portion of the field area, but permission was obtained prior to conducting work in most of these areas. Some landowners allowed the survey to take place, while others did not grant permission or did not respond to the letters requesting permission. In cases where no written response was received, landowners were contacted in person or the mines on their land were not inventoried.

CHAPTER 3

Methods

3.1 Field Methods

3.1.1 Mine Inventory and Nomenclature

Mine inventory was an essential component of the AML project that has been continued through this thesis study. Information such as coordinates, feature dimensions, stability, geology, hydrology, ecology, hazards, commodities, and land ownership are recorded on mine inventory forms (Appendix **A.1**). Only dimensions and trends of features, notable geologic attributes, and other critical information are recorded during field investigations, while other details are entered into the forms later in the office. These forms are entered into the database and stored as hard copies in the Mine Records Office at the NMBGMR for future reference.

During the AML project, arbitrary mine names were assigned to many features. The AML project and database rely on a Mine ID number to distinguish features and historic names are assigned when possible. However, during this thesis project it was easier to keep track of mine features by creating mine names that reflected the general location and type of mine feature. Mines in this thesis are assigned names with a location prefix and an alphanumeric abbreviation that describes the feature type and which one it is relative to multiple features at the same location. For example, the first mine shaft located on Silver Hill would be named SH-S1, where SH=Silver Hill and S1=Shaft 1. If the author did not visit the feature or couldn't confirm the feature type, the feature type was not indicated and only a number was assigned after the location prefix (e.g. GM-1). Later, if possible, the original name(s) were determined based upon historic mine records or the BLM GLO records, and a unique Mine ID was assigned. Appendix **B.1** lists database (historic) mine names along with their associated field names and other mine aliases. All mine features inventoried in the North Magdalena district during the AML project, this thesis, and earlier work can be found in the NM Mines Database.

While all features are marked with a GPS point, if they are within ~30 ft of each other, some may locally fall under the same mine name and Mine ID in the database. In the field, these were assigned two numbers: one after the location abbreviation and one indicating the feature number after a dash. This condition mostly applies to the “Mag” series of mines. Multiple features in proximity required two numbers to distinguish them. As an example, feature Mag5 (NMSO0831) is a cluster of four pits and one shaft, but all are listed under the same Mine ID. The names are therefore Mag5-P1, Mag5-P2, Mag5-P3, Mag5-P4, and Mag5-S1. See Tables 2 & 3 for the full list of abbreviations.

Abbreviation	Location
SH	Silver Hill
SC	South Cedar (Hill)
WC	West Cedar (Hill)
NC	North Cedar (Hill)
NMC	North Magdalena Crest
Mag	Magdalena (between Silver Hill and town)
NM354	New Mexico Forest Road 354
VL	Virginia Lee
BM	Bear Mountains
GM	Granite Mountain
NM169	New Mexico State Road 169

Table 2. Abbreviations for location component of mine name.

Abbreviation	Feature Type
A	Adit
C	Cut
D	Decline
P	Pit
S	Shaft
T	Trench

Table 3. Abbreviations for feature type component of mine name.

Mine ID numbers are used for identifying mines within the database along with a District ID. The District ID (DIS) is a 3-digit number, which, in the case of North Magdalena, is 223. Rosedale, for comparison, is DIS225. Some districts in the database have subdistrict designations, but not in this case. Some reports have broken North Magdalena into the Silver Hill and Pueblo/Granite Mountain subdistricts (McLemore, 1996), but the AML project considered it a single district and it has been treated as such during this study. Mine ID numbers are assigned to all known historic mine features in the state of New Mexico and start with the prefix “NM”. The next component of the Mine ID is the county abbreviation, in this case “SO”, for Socorro. Each Mine ID ends with a 4-digit number that identifies the specific feature. Therefore, a North Magdalena mine feature would be listed in the database as “DIS223, NMSO####”.

Two hazard rankings were used during mine inventory to classify physical and environmental hazards. These were created by the BLM and National Orphaned/Abandoned Mines Initiative (NOAMI) and are number and letter-based systems, respectively. The BLM hazard system allows the worker to assign a number from 0-7 to characterize the hazards of the mine while NOAMI rankings are A-D, O, and R (Bureau of Land Management, 2014; “NOAMI”, 2019). These hazard rankings are recorded on each mine inventory form and in the database. See Tables 4 and 5 for the definitions assigned to each ranking. Hazard rankings for all mines and prospects as they appear in the database are compiled in Appendix B.5. Hazard rankings are later used to prioritize features for reclamation. The NOAMI system better describes physical hazards by the type of feature, so it is more appropriate for this study.

Hazard Level	Name	Description
0	Remediated	Remediated
1	None	No danger level
2	Low	Sites located more than a quarter mile from areas of human activity
3	Medium	Sites near historic mining towns, historic schools, recreation areas, parks, camps, or trails
4	High	Sites near homes or school or within a quarter mile of one or more AML sites
5	Extreme	Extreme danger level
6	Unknown	Unknown danger level or not visited
7	Active Mining	Active mining: reclamation planned or underway

Table 4. BLM hazard ranking system (Bureau of Land Management, 2014)

Hazard Level	Description
A	Highest class: deep unprotected openings to surface, hazardous openings on surface, crown pillars, or waste rock piles with AMD/radioactivity
B	Deep unprotected openings to surface such as shafts, raises, and open stopes
C	Hazardous openings to surface, waste rock piles, and possible dilapidated structures associated with the mine openings; no tailings or tailings are safe
D	Minor surface features only, such as trenches, test pits, and stripping; no tailings
O	No information
R	Remediated

Table 5. NOAMI hazard ranking system (“NOAMI”, 2019)

3.1.2 Improved Location Data

Perhaps the most crucial component of this project as it pertains to future work is the development of location information. In the older literature, mine locations are usually described by township, range, section, and quarter section, resulting in a large area of uncertainty. Other databases can have even larger errors in the locations though; entries for mine features on Mindat.org, for example, have up to 26 miles of error in some of the coordinates. With the high density of mine features in North Magdalena, it is difficult to determine to which individual feature a record or database is referring. Commonly, the location information in the archives is for an entire claim (patented or unpatented) and while the major features might be indicated on a map, this typically does not include all the minor pits, trenches, or short shafts on the property. Claims are usually described by township and range, but specific feature locations are not always provided. Smaller features are almost never indicated and thus remain largely unrecorded. The aim of this project is to ensure as many features are accounted for as possible, no matter how small. Furthermore, most claim maps do not overlie a topographic map, so it is hard to match indicated features with features observed in the field.

For this study, a Garmin Montana 610t GPS unit was used to record each mine's location in North American Datum 1927 (NAD27) with a Clarke 1866 spheroid. Though this is an older coordinate system, it is used on the topographic maps referenced throughout this study and matches many of the historic locations already in the mine records. This GPS unit has an error of ± 12 ft which is sufficiently accurate for recording locations of mine features. The GPS unit is used to record coordinates as latitude, longitude, and Universal Transverse Mercator (UTM). Elevations are documented but may contain significant error. This location information is entered in the database as a component of mine inventory and can be referenced in Appendix **B.3**.

Coordinates obtained in the field are also used to map features in ArcGIS. Seven-and-a-half-minute topographic quadrangles, satellite imagery, road, city, hydrology, county, rail, and other data were downloaded from the University of New Mexico RGIS website ("UNM", 2019) an open source for GIS data relevant to New Mexico. This information was used to produce Figures 1-5.

3.1.3 Sampling Methods

During the AML project, waste material was sampled to characterize environmental hazards and determine its suitability for backfill. As such, the majority of samples collected were "composite" samples. Composite samples (also called "composite dump" samples) were collected from mine feature waste rock piles in a 30-point grid. A stainless-steel trowel was used to scrape a few inches of mine soil off the top and then a scoop or two of soil was taken from underneath. This was repeated a minimum of 30 times along rows horizontally and vertically arranged to cover the whole waste pile. Each time, soils were sieved to remove particles $\geq \frac{1}{2}$ in, and put into a 5-gallon bucket. These samples were mixed thoroughly in the lab and split for geochemistry, paste pH, and mine soil petrography.

While AML sampling mostly focused on composite samples, this study focused more on mineralized waste rock, or “dump select” samples, though some composite samples were collected. In addition to mineralized rock, non-mineralized rock and overburden were collected to obtain a representative sample of the waste rock pile in the field. Two other types of samples collected during this portion of the study were outcrop and vein chip samples. Outcrop chips were only collected when possible and safe. Many mine features do not occur near outcrops and those that do are often deeply mined at the base of the outcrop, so sample collection can be dangerous. In addition, the outcrop is often not representative of what was mined at depth—sometimes a different unit entirely. Mineralized veins comprise a small portion of samples collected over the course of this study but are valuable in terms of the information they provide regarding ore mineralogy. Most veins in the area occur at depth or have been mined down to depth, so only the few that were visible at the surface were sampled. One-gallon, thick plastic bags were used to hold samples and were usually filled, at minimum, halfway with rock. Samples are designated on the bag as dump select (DS), outcrop (OC), or vein samples (VS) and labeled with the name of the mine feature from which they were collected. If applicable, trends of veins and any structures are recorded on sample forms and mine inventory sheets. Not all samples that were collected were subject to further analysis.

The AML project used sampling forms (Appendix **A.2**), but because the goals of this thesis study are unique, a new sampling form (Appendix **A.3**) was created. This form allows the worker to quickly record data using a streamlined check-box system; eliminating the need to hand-write every detail of the rocks found at the mine. Boxes for lithologic characteristics, mineral species, alteration, sample type, and feature/area description allow the worker to quickly check-off relevant information and reduce time spent filling-out paperwork. Samples that are selected for further analysis such as reflected light petrography (RLP), X-ray diffraction (XRD), or electron microprobe (EMP) are labeled with the overall sample name and then lowercase Roman numerals to distinguish them. For example, three samples from the same mine (e.g. SH-S1) would be labeled SH-S1i, SH-S1ii, and SH-S1iii.

3.1.4 Photography

Every mine and prospect encountered in the field is photographed; usually with a rock hammer, backpack, or map board for scale. The most frequently used camera is a Canon Rebel T3 and photographs are downloaded from the memory card onto a laptop. On several occasions a whiteboard with the mine name was included in the photo next to the feature, but because the boards were so reflective in bright sunlight, the writing was often unreadable; this practice was therefore discontinued. In early 2018, a memory card with photographs of around a dozen mines was lost along with the inventory forms. Fortunately, the forms had already been entered into the database, so the mine information was retained, but the photographs remain missing. Labeled photographs of almost all inventoried mine features can be seen in Appendix **B.8**.

3.2 Laboratory Methods

From the AML project to this thesis study, multiple laboratory analytical methods have been employed in order to better understand the geochemistry and mineralogy of these mines and prospects. AML funding was directed towards geochemistry and acid-base accounting, while New Mexico Geological Society grants funded electron microprobe, X-ray diffraction, and additional geochemical analyses. Sample names and corresponding analyses can be found in Appendix **B.2**.

Geochemistry of AML samples provided information necessary to perform and optimize other analytical methods. Acid-base accounting is used to determine potential for acid mine drainage (AMD) and this method relies on % total sulfur and carbon from geochemistry. Results of paste-pH analysis are supplemented and reinforced by performing mine soil petrography, which is used to characterize soil textures and components, such as acid-forming and neutralizing minerals (e.g. pyrite and calcite).

Geochemistry, RLP, XRD, and EMP were the primary analytical methods used for this study. Geochemistry of mineralized rock samples provided a full elemental analysis including metals and rare earth elements (REEs). Reflected light petrography was essential for identifying ore minerals and their paragenesis in addition to confirming observations from EMP. X-ray diffraction was performed throughout the duration of this project to identify mineral phases that occur in vugs or as encrustations. EMP was useful for examining extremely small-scale features such as weathering textures and mineral inclusions.

3.2.1 Geochemistry

Geochemical analyses of samples from the AML project to this study have been performed by ALS USA Inc. At least 100g of representative sample material is sent for full analysis. An internal standard, powdered waste rock from the Molycorp Project in the early 2000s, is sent along with each batch. At least one duplicate sample (often the standard) is sent to check consistency of analyses being performed. Geochemical data for all samples as well as the Molycorp standard used can be found in Appendices **C.1.A** and **C.1.B**, respectively.

A suite of analyses is performed to fully characterize the elemental contents of the waste rock. Oxides of major rock-forming elements are determined by fused-disk X-ray fluorescence (XRF). Lost on ignition (LOI) can be determined by preparing the sample in a furnace or thermogravimetric analyzer. REEs, uranium, vanadium, tungsten, and zirconium are analyzed with a lithium borate fused bead, acid digestion, and inductively coupled plasma mass-spectrometry (ICP-MS). Most transition metals and base metals can be detected with a four-acid digestion and inductively coupled plasma atomic emission spectrometry (ICP-AES). Total sulfur and carbon are measured using a LECO induction furnace. Finally, gold content is obtained by ICP-AES (“ALS”, 2019).

Results are returned from the lab as a Microsoft Excel spreadsheet and pulps are mailed back as requested. Data included in analyses are oxide weight percentages, total sulfur and carbon percentages, and ppm values for all other analyzed elements including REEs, precious metals, and uranium. Sulfur and carbon content are used in acid-base accounting and by understanding what elements are found in these samples it helps optimize costly studies like EMP.

3.2.2 Mine Soil Petrography

Every composite waste sample collected during the AML project for geochemistry was also subject to soil petrographic analysis. Usually, this was done while awaiting results from the geochemistry lab. The primary purpose of this method is to characterize the sample and determine if acid-generating or neutralizing minerals are present in mine soils, both of which have important environmental implications. A small portion (enough to fill a watch glass) representative of the larger composite sample was separated with a plastic cup and examined under Bausch & Lomb StereoZoom 4 binocular microscope. The unwashed sample is examined first to determine the percent fines (<1 mm) relative to the whole sample along with cohesion, effervescence and intensity, and grain shape. The sample is lightly dampened, and the color is described according to “Globe” (2005).

The unwashed sample is scraped into an Erlenmeyer flask and decanted with deionized (DI) water. Swirling and rinsing the sample several times removes organic matter and fines and wastewater is poured into a designated bucket. If gypsum is observed prior to washing, it is important to record this or to take care during rinsing so as not to dissolve it by exposing it to too much water. Once the water from the rinse is clear, the sample has been sufficiently cleaned. The last rinse along with the sample are poured into a funnel fitted with filter paper that drains into another flask. The filter paper containing the sample is labeled with the sample name and placed in a fume hood to dry at room temperature.

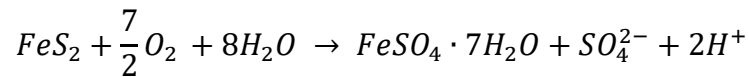
Once the sample is dry, further analyses can be performed. The sample is returned to a clean watch glass and examined under the microscope. After clays and other fines have been removed, rock fragments and lithology can be identified. Each rock type is recorded along with what percentage of the total sample it comprises. Clast shapes and effervescence are reevaluated and alteration, weathering features, and overall mineralogy are recorded. Notable or economic minerals are described in greater detail in terms of their habit, color, texture, and their occurrence relative to other grains. Final comments regarding the presence of organic matter or other noteworthy content are added to the spreadsheet and the sample is placed in a small plastic bag with a paper label inside to indicate it has been fully examined. Data from this analysis was included in the AML report for the district.

3.2.3 Acid-Base Accounting

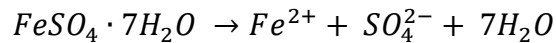
The first step in ABA is determining the paste pH. Paste pH analysis is a quick and relatively accurate method that provides an estimate of the pH of a composite mine soil sample exposed to water. First, 25 g are split from the bulk composite sample are run through a No.10 stainless-steel sieve to eliminate particles greater than or equal to 2.00 mm. These fines are then soaked for 10 min in 25 ml of DI water to form a paste; the pH of the water is then measured using an electronic pH probe.⁵ This is recorded and used in further calculations to determine the acid generating potential of the waste rock.

To predict acid generating potential, % total sulfur and carbon from geochemistry are plugged into equations from Price (2009) and the GARD Guide (“Global acid”, 2012) and used to calculate the net potential ratio (NPR). NPR is a function of the neutralization potential (NP) divided by the acid potential (AP). A factor of 31.25 is multiplied by the % total sulfur. This factor assumes one mole of sulfur from pyrite oxidation and one mole of sulfur from melanterite dissolution (with oxidation) produces two moles of H⁺ each time. It also assumes one mole of CaCO₃ neutralizes these two moles of H⁺. The outcome is a conversion from total sulfur (% pyrite S + % melanterite S) to kg CaCO₃ equivalent/ton. Now this can be compared to the NP, which is equal to the % total carbon multiplied by 83.3—another factor that results in a conversion to kg CaCO₃ equivalent/ton. This assumes all carbon in the waste rock is in the form of calcite. Reactions 1-3 are after Frau (2000) and equations 4-6 are after Price (2009).

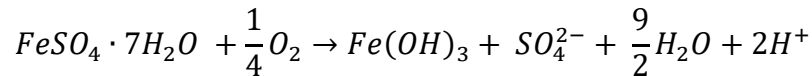
- (1) Pyrite Oxidation and formation of melanterite:



- (2) Melanterite dissolution (no oxidation):



- (3) Melanterite dissolution (with oxidation):



⁵ Conductivity of the water was measured to approximate total dissolved solids, which typically include metalliferous salts and sulfates that are often the products of sulfide mineral oxidation and thus, AMD. However, the author was unable to get the conductivity probe to stabilize and results were equivocal.

The AP and NP are calculated according to Equations 4 and 5, respectively, and the NPR is determined using Equation 6:

$$(4) \quad AP = \%S \times 31.25$$

$$(5) \quad NP = \%C \times 83.3$$

$$(6) \quad NPR = \frac{NP}{AP}$$

Next, NPR is plotted against net acid generation (NAG) pH, which is the measured paste pH, and the resulting acid rock drainage (ARD) diagram predicts acid generating potential of the mine waste. Points fall into three potential categories: **non-acid forming**, **potentially acid forming**, and **uncertain**. Mine waste that plots in the potentially acid forming field or uncertain fields should not be used as backfill-material. Non-acid forming waste can be considered for backfill and the associated feature will be evaluated for physical hazards and remediated accordingly. If mine waste plots in the uncertain field, it is treated as potentially acid forming. AMD can dissolve and mobilize metals into the surrounding environment which can have damaging impacts on nearby ecology and hydrology. Predicting acid generating potential of mine waste for a particular feature helps determine the priority with which that feature should be remediated.

3.2.4 Reflected Light Petrography (RLP)

Polished sections have provided a wealth of information for this project. Unlike with EMP, there are fewer size restrictions for the polished sections, which often makes larger scale features such as veining or zonation more obvious. It is also more useful for identifying actual mineral species, whereas EMP only allows for a chemical approximation of minerals. Plus, it is essentially a free analysis requiring only a sample, rock saw, lapidary wheel, microscope, and time to perform.

First, samples are cut in a way that best represents the ore mineralogy as it occurs in the rock. The sample is then mounted in epoxy with a label and allowed to dry. Next, a coarse grit is applied to expose the surface of the sample for polishing. The next several polishing levels, with thorough rinsing between each stage, bring the sample to a highly reflective surface and, once completed, allow for effective petrographic analysis. These steps, for reproducibility, can be reviewed in Table 6. The microscope used for all RLP in this study was a Nikon Optiphot-Pol. It has three objectives: a 5x, 10x, and 40x, plus an oil lens of 50x, which was used to identify certain phases like blaubleibender, covellite and violet micro-inclusions. The oculars have a magnification of 10x, so total magnification with the objectives is 50x, 100x, 400x, and 500x. The crosshairs in the ocular have tick marks that were used to measure grains and provide scale in photos. The space between two tick marks at 50x, 100x, 400x, and 500x represents 20 μm , 10 μm , 2.5 μm , and 2 μm , respectively.

Grit	Micron	Duration
80	200	Until surface exposed
240	50	6 minutes
400	30	6 minutes
800	15	6 minutes
1000	12	6 minutes
1400	6	8 minutes
-	0.05	1-4 minutes

Table 6. Grinding procedures for creating polished sections.

By studying samples in reflected light, it becomes much easier to identify and characterize ore minerals and interpret their paragenesis. Due to the nature of mineralization in the North Magdalena district, minerals can be very small, which makes hand sample identification difficult. Moreover, species are typically oxidized or weathered beyond recognition from centuries of atmospheric exposure. Cutting and polishing the sample exposes fresh mineralization and removes these oxide coatings for easier study. Understanding the paragenesis of the minerals, including trace minerals, provides insight to the stages of mineralization and nature of fluids that created this economically significant area.

3.2.5 X-Ray Diffraction (XRD)

Because this study is primarily aimed at mineralogical characterization of mines and prospects, XRD remains one of the most practical analytical methods. It can be very difficult to identify thin mineral crusts coating rocks waste rock pile as many mine waste oxidation products have similar properties. Many occur as light green, blue, or yellow microcrystalline coatings and usually cannot be identified in hand sample. Therefore, XRD remains one of the only means of identification. XRD has worked well to identify most of the more enigmatic minerals collected in the field. However, some occur in such small quantities or are spread so thinly on the rock that a good sample could not be obtained for powder diffraction. The NMBGMR XRD lab utilizes a Panalytical X'Pert Pro diffractometer that analyzes samples on a rotating stage with monochromatic X-rays produced by a copper X-ray tube. Machine power is typically set to 40 mA and 45 kV.

Samples were crushed to a fine powder with a quartz or corundum mortar and pestle and placed into silicon-backed sample trays of an appropriate size. The machine can analyze up to 15 samples in sequence before needing to be reloaded. A 5-minute scan was usually enough to identify mineral species if ample material was available, but a 40-minute scan was often necessary to characterize some of the cryptic species that occur in very small quantities. Forty-minute scans became the standard for all samples after the first batch because the higher resolution data was worth the time and cost. Diffraction patterns are plotted and examined with HighScore Plus, a crystallographic analysis program by Malvern Panalytical. Adjusting the data by removing background peaks, noise, and other interference allows the worker to use the “search and match” feature to match the recorded spectra with a standard from a diffractogram database. Once finished, powders are removed from the silicon holding trays and placed into baggies or vials. These are labeled and stored together with the other samples from that batch, allowing for quick re-analysis, should data be lost or of poor quality.

3.2.6 Electron Microprobe (EMP)

EMP analysis can be done at the NMBGMR, but it is costly (about \$33/hr), so its use was limited during this project. The instrument at the NMBGMR is a Cameca SX-100 microprobe featuring 3 wavelength-dispersive spectrometers, as well as secondary electron (SE) and high-speed backscattered electron (BSE) detectors. Each detector houses two crystals which include large and small LiFs, two normal TAPs, and large and small PETs (“Electron”, 2019). EMP analysis is very useful for examining micro-inclusions and weathering textures on mineral surfaces.

Samples from two mines that represented the major mineralization styles in the district were selected for EMP analysis: The Ace of Spades (Cu-Ag) and Virginia Lee (Pb-Zn-V) Mines (NMSO0811 and NMSO0878, respectively). Rocks from the mines were cut to produce two chips each that isolated interesting mineralization. An epoxy billet containing the 4 chips was then polished to a highly reflective surface with increasingly fine grits on magnetic lapidary wheels. Fine polishing was performed using glass plates and polishing cloths with diamond grit. Between the rough polishing and each subsequent diamond polish, the sample was placed in an ultrasonic bath for 40 seconds and then rinsed with DI water to remove remaining coarse grit and prevent scratch contamination on the glass plates. After the final polish, the sample was rinsed as before and then cleaned with petroleum ether. These steps, for reproducibility, can be seen in Table 7. Polishing quality was checked using a petrographic microscope with reflected light capability and final steps were repeated if necessary. Finally, a carbon coating was applied to the billet to enhance penetration of the electron beam into the sample.

Grit	Micron	Duration	Cleaning
100	163	Until surface exposed	Rinse
220	68	3-minutes	Rinse
600	60	3-minutes	Ultrasonify 40-seconds, rinse
Diamond I	15	4-minutes	Ultrasonify 40-seconds, rinse
Diamond II	6	6-minutes (3-6 extra if needed)	Ultrasonify 40-seconds, rinse
Diamond III	1	1-minute	Ultrasonify 40-seconds, rinse, petroleum ether

Table 7. Polishing procedure for creating EMP billet.

Mineral grains were qualitatively analyzed by detecting key elements such as transition metals, sulfur, or large cations like barium. Once a rough identification had been made, select minerals were probed with a point beam (essentially 0 μm) to produce spectra and determine major and trace element content. A beam size of 5-10 μm was used to characterize less distinct phases such as oxidation rinds on galena. In doing so, it was possible to gather more data from less homogenous materials and use this “average” to assign species names. Standards that were chemically similar to the species under investigation were used for longer scans.

CHAPTER 4

Results

4.1 Field Results

4.1.1 Mine Inventory

During the AML project, mine inventory was completed with the help of undergraduate assistants and was continued by the author following expiration of the contract. There are 203 total mine features recorded for North Magdalena in the New Mexico Mines Database, however, this study only focuses on 186 features that were examined by the author and other AML team members from 2016-2019. There may be additional workings that were missed or inaccessible due to time constraints and land ownership restrictions. Some of these can be seen in satellite imagery and are mostly on the eastern side (Granite Mountain area) of the district. Many of these were surveyed during and reclaimed following the 1986 AMS (Bobrow et al., 1986). Additional features from previous studies and topographic estimations are listed in the database, but they were not inventoried during these projects, so their type and current condition is unknown. The types and numbers of each feature can be reviewed in Table 8. Pits outnumber all other feature types. Shafts are the next most common, followed by trenches, cuts, adits, and declines. Appendix B.3 lists all the location data for mine features in the district by Mine ID, database name, and field name.

Feature Type	Number Inventoried
Adits	5
Cuts	7
Declines	2
Pits	86
Shafts	40
Trenches	11
In database (remediated/unidentified)	52
Total:	203

Table 8. Feature types and counts.

Many deep mine workings are located close to roads or on public lands, which provides easy access to these dangerous features (Fig. 14). Some shafts, including Mag4-S1 (NMSO0377) can reach depths of ~300ft and are open, posing a serious risk to individuals and livestock. Many dirt roads pass directly next to open shafts including SH-S1 (NMSO0230), SH-S2 (NMSO0898), SH-S5 (NMSO0910), and others. The town of Magdalena and US-60 are only about a mile from the district's southern boundary and there is clear evidence of recent human use at many of the more accessible sites. This includes fire pits, tire tracks, footprints, beer cans, cigarette butts, and other trash. Trash is always recorded when first performing mine inventory and can present an environmental hazard of its own depending on the nature of the refuse. Implications of waste disposal in some of the deeper mine features will be covered in the next chapter. Some mine features with trash and the severity of the pollution are listed in Appendix B.6.

Ecosystem health surrounding mine features does not appear to be significantly impacted. Vegetation is healthy and natural, i.e. unstressed from acidic mine soils and not clearly invasive. Many of the waste rock piles even feature full-grown juniper trees or coatings of grasses and shrubs. None of the mine features contained water at a level that was visible to the author, though some major shafts reportedly struck water at depths of greater than 60 ft (Lasky, 1932; Holmquist, 1946). Many pits and surface workings contained woodrat nests which sometimes made it challenging to determine true depths of features. Several shafts were occupied by barn owls, but no bats were observed. Rattlesnakes, garter snakes, mice, and lizards were seen occupying crevices in waste rock. Waste piles on hillsides did not appear to be affecting the health of plants in drainages below and there is no flowing water in the district, so transport of any leached metals would be minimal and restricted to prolonged, high precipitation events.



Figure 14. NM354-A1 (NMSO0879); an untimbered adit in extremely altered rock.

At the time of this study, none of the mine features in the Silver Hill area have been officially safeguarded, but many in the Granite Mountain area were closed in 1995 (“AML construction”, 2019). Some appear to be backfilled or collapsed, but these “false-bottoms” are just mats of tumbleweeds or other vegetal detritus accumulated on old timbering and may conceal many more feet of depth; these are particularly hazardous. Other openings are blocked with trash; a prime example of which would be SH-S2 (NMSO0898). This feature has a very large waste rock pile suggesting great depth, but the opening is plugged with tires and an old refrigerator. There is a small space leading to an open shaft below the refrigerator and the stability of this opening is highly questionable (Fig. 15). Many of the shafts in the district are home to roosting barn owls, often hosting 3-5 at a time. Bats were not encountered during this study, but it is highly likely that they too inhabit many of these old workings. There are no grates or structures that both prevent human access and allow for ingress or egress of bats and owls on the western side of the district. Therefore, closure either by backfill or engineering methods should be pursued by the New Mexico AML program and federal agencies. Backfilling these features will render much of the mineralized waste rock inaccessible, however, making any future mine waste reprocessing or research difficult.



Figure 15. SH-S2 (NMSO0898); deep shaft plugged with trash. Circled area is opening to shaft below. Note proximity to road above.

4.1.2 Mine Mineralogy

Mineralogy recorded from field observations, hand samples, and analytical methods described in the previous chapter have been documented for each mine and are listed in Appendix **B.4**. Gangue mineralogy is listed for each feature in one column and usually includes the typical assemblage of barite, calcite, and quartz. Barite was historically explored for (Williams, 1963) and appeared to be the only commodity at certain mine features, so it is listed in the ore mineralogy column in these cases. Barite occurs in massive veins and lenses which is characteristic of epithermal deposits in which fluid mixing occurred. Where multiple or finely disseminated carbonate phases were observed, but not readily discernable, the appendix entry is abbreviated “CO₃-s”.

The next column in Appendix **B.4** lists ore mineralogy. Most mine features were mineralized to some degree with oxidized copper minerals (Cu-Ox) which in this case usually means some mix of chrysocolla, malachite, or other phases like tenorite or possibly brochantite. Often, these phases were hard to distinguish in hand sample where they were finely disseminated or mixed, hence the shortened “Cu-Ox” designation. Where possible, these are differentiated in the appendix entry for the feature. Due to time and funding constraints, not all features could be thoroughly analyzed, so many only have a field-level description of mineralogy. The larger shafts that probably produced are assumed to have sulfide minerals present and this is mentioned in their appendix entry, even if the author did not observe any during field examination.

General alteration and lithological assignments follow in the next two columns of Appendix **B.4**. It was beyond the scope of this project to do a detailed examination of alteration, but previous studies, including Simon (1973), had already characterized it to some extent. Prior work combined with field and hand sample observations provided an adequate level of detail to meet the goals of this study. Silicification, weak propylitic, and moderate argillic alteration were observed. An interesting style of phyllic alteration (Fig. 16) was observed at SH-S3 (NMSO0809). In this case, calcic feldspars have undergone phyllic alteration in the presence of water and CO₂. This produced ankerite, sericite, and acid. Ankerite, which is unstable under oxidizing conditions, was further altered to a mix of Fe-oxides (hematite and goethite) giving the grains a distinct reddish color. While at least one alteration style was recorded for each mine and prospect, it is likely that there are multiple alteration types at each, especially within deep features that intersect multiple units. A common issue in epithermal vein deposits is overprinting by multiple hydrothermal events, which can make it difficult to assign a specific alteration type to the area. Unlike copper porphyries, which often have distinct alteration halos surrounding the deposits, volcanic-epithermal systems can have mixed alteration patterns both vertically and laterally with replacements of one alteration style by another (Heald et al., 1987). Bleaching is also common in many of the mineralized host rocks, suggesting proximity to a fluid source.

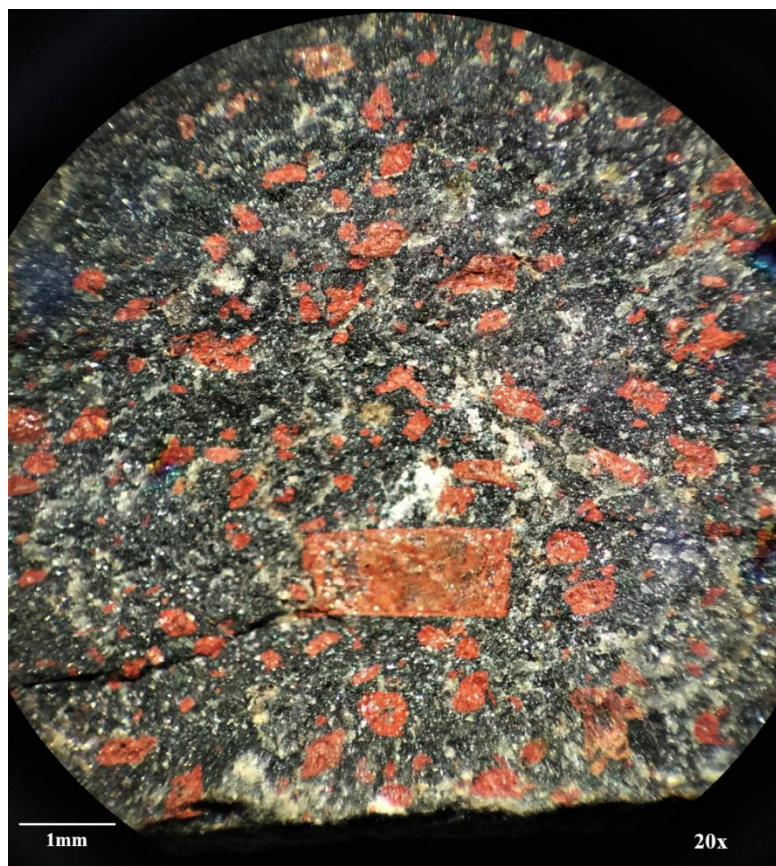


Figure 16. SH-S3i; phyllic (sericite-carbonate) alteration of calcic plagioclase.

The La Jara Peak Andesite was described in section **2.1.4.2** and is the predominant host for mineralization because it is the uppermost unit in the district and forms much of the local topography. While most mineralization in deep shafts likely occurs in other units, it is difficult to identify the altered, mineralized host rock unit or formation. Determination of the host rock is further complicated because many of the volcanic units are distinguished only by very minor characteristics like flow-banding, crystal content, phenocryst orientation, and other textures (Simon, 1973). Thus, in the interest of simplicity, the La Jara Peak Andesite has been designated as the host rock for many mine features. Of course, some exceptions exist where the rocks were clearly rhyolitic or tuffaceous. Feldspars are argillically altered or have been replaced by iron carbonates in the aforementioned style of phyllic alteration. Weak propylitic alteration featuring chlorite, epidote, and magnetite were observed elsewhere in the field by the author and described in Simon (1973).

Environmental hazards associated with mineralogy appear to be minimal, particularly acid-generating potential. Pyrite was not observed in any of the mine waste encountered in the field. Simon (1973) remarked that oxidizing pyrite was seen in association with argillic alteration on the western side of the field area, though this is interpreted to be beyond the current district boundary. Sulfides of copper such as chalcopyrite, “chalcocite”⁶, and covellite were common, but apart from chalcopyrite, did not appear to be strongly weathered. Chalcopyrite in many cases is observed with rims of Fe-oxides and hydroxides like hematite and goethite but it typically appears intact when fresh surfaces are exposed. These less-weathered chalcopyrite grains were studied further and will be covered in the reflected light section of this chapter. In addition to a lack of acid-forming sulfides, the gangue mineralization is extremely neutralizing and would likely buffer any acid formed from sulfide oxidation. Finally, leaching of lead is limited as oxidation of galena results in the formation of many secondary lead phases. Sphalerite observed in the district was usually light yellow to yellow-green (Fe-poor) and appears to contain very low levels of cadmium.

4.2 Laboratory Results

4.2.1 Geochemistry

In total, 18 samples from the North Magdalena District were selected for geochemical analyses (Table 9). Samples were selected either for size of the feature from which they came or location within the district (or both) with the goal of creating a dataset that would represent major geochemical trends of the district. “(Dup.)” indicates duplicate samples sent for QA/QC of geochemical analysis.

⁶ “Chalcocite” is used in this paper to refer to any mineral with an intermediate (non-stoichiometric) composition between CuS and Cu₂S where a distinct species could not be determined (V. Lueth, personal communication, October 22, 2019). This includes the minerals chalcocite, djurleite (Morimoto, 1962; Roseboom, 1962), digenite, anilite (Morimoto et al., 1969), geerite (Goble & Robinson, 1980), and spionkopite and yarrowite (Goble, 1980). In this case, it does not include covellite or blaubleibender because even though they fall within this range, they are easy to identify and will be specified where applicable.

Mine ID	Sample Name	Sample Type	Feature Type
NMSO0809	SH-S3	Dump Select	Double Shaft
NMSO0897	SH-T2	Dump Select	Trench
NMSO0909	SH-P14	Dump Select	Pit
NMSO0180	Mag20-S1	Dump Select	Shaft
NMSO0928	Mag29-D1	Dump Select	Decline
NMSO0229	Mag38-S1	Dump Select	Shaft
NMSO0811	NMA1A	Composite	Cut
NMSO0811	NMA1B	Dump Select	Cut
NMSO0810	NMA15	Dump Select	Trench
NMSO0866	SC-28	Vein Chip	Decline
NMSO0866	SC-5A	Composite	Decline
NMSO0866	SC-5B	Composite (Dup.)	Decline
NMSO0865	SCP-4v	Vein Chip	Pit
NMSO0865	SCP-4ds	Dump Select	Pit
NMSO0872	Mcu-ds	Dump Select	Pit
NMSO0876	VL-1	Composite	Shaft
NMSO0876	VL-1_B	Composite (Dup.)	Shaft
NMSO0823	NM-24	Dump Select	Shaft
NMSO0208	NM-36	Dump Select	Shaft (?)
NMSO0608	NM-354B	Composite	Pit or collapsed shaft
NMSO0608	NM-354B_2	Composite (Dup.)	Pit or collapsed shaft

Table 9. Geochemistry samples and types according to Mine ID and feature type.

Geochemistry results confirm the district's commodities as Ag, Cu, Pb, and minor Au, Zn and V. Table 10 shows the chemical concentrations of these elements from waste rock and vein samples. Ba has been included as well since historic exploration efforts have targeted it as an industrial mineral. Table 11 displays chemical analyses of potentially hazardous elements and sulfur content. Lead is not included because it is listed in Table 10. All geochemical data is in Appendix **C.1.A.**

Sample Name	Ag	Cu	Zn	Pb	V	Au	Ba
	ppm	ppm	ppm	ppm	ppm	ppm	ppm
SH-S3	<0.5	57	97	10	232	0.004	1190
SH-T2	37.9	9130	1140	666	143	0.061	>10000
SH-P14	131	1920	147500	9790	1430	0.429	>10000
Mag20-S1	851	23400	999	1720	361	0.301	>10000
Mag29-D1	481	17750	666	1310	311	0.638	>10000
Mag38-S1	154	15050	428	378	214	0.098	>10000
NMA1A	42	949	361	391	273	0.269	7500
NMA1B	530	50400	4940	1705	566	9.03	>10000
NMA15	206	23200	896	323	132	0.101	>10000
SC-28	538	29000	63	25	216	0.459	1820
SC-5A	3.7	1270	136	40	151	0.01	2550
SC-5B (Dup.)	4.2	1390	141	39	146	0.005	2660
SCP-4v	35.1	20300	69	35	167	0.012	1345
SCP-4ds	5.7	3090	70	17	95	0.002	1730
Mcu-ds	<0.5	41	131	17	224	<0.001	930
VL-1	6.4	784	7270	26400	729	0.111	>10000
VL-1_B (Dup.)	8	872	7570	35300	779	0.09	>10000
NM 24	91.5	62400	11650	2270	338	1.39	>10000
NM 36	3.5	545	220	7380	71	0.16	>10000
NM-354B	3	326	2170	1320	231	0.142	4530
NM-354B_2 (Dup.)	7	232	1485	12750	143	0.091	>10000

Table 10. Selected element concentrations from samples described in Table 9.

Sample Name	As	Cd	Sb	Hg	Ni	Cr	U	S
	ppm	ppm	ppm	ppm	ppm	ppm	ppm	%
SH-S3	0.8	0.6	2.06	0.011	210	440	1.82	0.01
SH-T2	46	9.9	8.75	0.079	41	100	3.34	0.24
SH-P14	>250	25.6	11.15	2.06	6	100	12.4	6.93
Mag20-S1	>250	4.9	>250	3.22	153	50	7.01	1.28
Mag29-D1	>250	17.8	20.5	0.262	32	40	3.22	2.3
Mag38-S1	91.8	1.6	56.5	0.076	32	50	3.27	1.54
NMA1A	24.6	1.6	4.07	0.099	139	340	2.73	0.13
NMA1B	248	14.7	108.5	2.83	89	370	19.5	1.27
NMA15	24.9	4.3	7.81	0.157	96	230	3.93	0.88
SC-28	6.9	<0.5	6.58	0.115	45	150	3.97	0.14
SC-5A	7	0.6	3.25	0.051	86	130	1.76	0.04
SC-5B (Dup.)	6.5	0.6	3.13	0.054	89	130	1.68	0.04
SCP-4v	5.5	<0.5	5.48	0.458	162	90	3.3	0.03
SCP-4ds	8.8	<0.5	2.68	0.231	54	90	2.61	0.03
Mcu-ds	1.1	<0.5	0.99	0.042	110	110	1.25	<0.01
VL-1	36.9	82.4	1.79	0.668	58	130	4.36	2.57
VL-1_B (Dup.)	37.5	99.8	2.17	0.656	61	130	4.67	2.51
NM 24	>250	42.2	43.9	0.208	16	10	20.3	0.52
NM 36	5	1.4	0.88	0.04	12	80	1.68	1.57
NM-354B	58	19.9	2.35	0.18	92	480	5	0.14
NM-354B_2 (Dup.)	109	45.6	16.25	0.379	59	350	3.23	0.81

Table 11. Concentrations of potentially environmentally hazardous elements and sulfur in samples described in Table 9.

4.2.2 Mine Soil Petrography

Upon examination of five different composite dump samples (Table 12), it was clear that all mine soils contain abundant carbonates. As mentioned previously, carbonate minerals (primarily calcite) are ubiquitous across the district. When dilute (0.1 M) HCl was dropped on the unwashed samples, moderate to vigorous effervescence of both fines and clasts occurred in all cases. Soil colors were typically a dark red or brown, which reflects the oxidation that is commonly associated with atmospheric exposure. Because this is mine waste that was removed quickly (often with explosives) and no transport of grains has occurred, they are generally angular to subrounded. Mine soils have all exhibited loose cohesion and no cementation and organic material has been found in all samples.

Sample #	Abundance of Fines	Color	Cohesion/cementation	Grain Shape	Effervescence + intensity	Comments
VL-1	50%	10YR 3/3	Loose/uncemented	SubAng-SubRnd	Yes, vigorous on soil and clasts	Some mud clasts, organic material
SC-5	70%	7.5YR 2.5/3	Loose/uncemented	Ang-SubRnd	Yes, vigorous on soil and clasts	Secondary copper minerals
NMA1A	70%	5YR 2.5/2	Loose/uncemented	Ang-SubRnd	Yes, vigorous on soil and clasts	Some organic matter
NM354B	60%	10YR 3/6	Loose/uncemented	Ang-SubRnd	Yes, vigorous on soil and clasts	Some organic matter
SH-S2	40%	10R 2.5/2	Loose/uncemented	Ang-SubRnd	Yes, moderate on soil and clasts	Formerly SH-1B

Table 12. Characteristics of unwashed mine soil petrographic samples.

After washing and drying the samples (Table 13), the abundance of fines was greatly reduced. Prior to washing, fines made up 40-70% of each sample, but were reduced to 20-40% after this step. NM354B was an exception because the rock fragments comprise clays and other phyllosilicates and disaggregated when mixed with water, yielding more fines than were initially observed. Samples continued to react vigorously to HCl after washing and lithologies could be determined now that adsorbed fines were no longer covering the clasts. Lithologies are varied due to the volcanostratigraphy of the area, but were very generally andesite, tuff, rhyolite, or a combination of these. The clasts in NM354B are so altered that a protolith could not be accurately determined. It is possible that this sample represents a shear zone and/or large-scale fault gouge in rhyolite, but its true nature is unknown. Oxidation products were common in most of the samples either as spots on surfaces of clasts or as grains within clasts. Grains of calcite, quartz, and barite were common and reflect the dominant gangue mineralogy of most of the mines. No sulfides were observed in these samples, and only minor gypsum occurred as a weathering product in sample NMA1A (Ace of Spades). Secondary copper minerals like chrysocolla were seen coating clasts while others, like malachite, occurred as individual clusters of bladed green crystals. A green phyllosilicate and vermiculite were observed in sample NM354B, which add to the unusual nature of this sample compared to others from across the district.

Sample	Rock Fragment %s	Clast Shape	Effervescence + location	Type of HT Alt.	Intensity of HT Alt.	Weathering	Overall Mineralogy	Quartz
VL-1	60%, mostly andesite	SubAng-SubRnd	Vigorous, throughout	Silicification	Moderate	Vanadinite, desclorite	Barite, calcite, quartz	Prismatic in vugs
SC-5	40%, mostly andesite	Ang-SubRnd	Vigorous on fines>clasts	Silicification	Moderate	Oxidized spots on clasts	Calcite, chrysocolla, quartz	Milky
NMA1A	60% mostly andesite	SubAng-SubRnd	Vigorous, throughout	Silicification	Moderate	Oxidized spots on clasts	Calcite, malachite, quartz	Clear, prismatic
NM354B	25% too altered to identify	SubAng-SubRnd	Moderate, throughout	Argillie?	Strong	Goethite throughout	Calcite, chlorite quartz, vermiculite	Clear, prismatic
SH-S2	80% total; 60% andesite, 20% tuff	Ang-SubRnd	Vigorous, throughout	Silicification	Moderate	Clasts red with oxidation	Barite, calcite, hematite, quartz	Clear, prismatic

Sample	Feldspar	Oxides	Jarosite	Pyrite	Calcite	Gypsum	Copper Min.	"Micas"	Comments
VL-1	None	On clasts	None	None	Fine-medium grained rhombs	None	None	None	None; secondary vanadates in hand sample only
SC-5	None	On clasts	None	None	In soil and on clasts	None	Chrysocolla	None	None
NMA1A	Replaced in clasts	Replacing plagioclase in clasts	None	None	Grains and in clasts	Flakes	Malachite	None	None
NM354B	None	Goethite, hematite	None	None	Disseminated	None	None	Vermiculite: loose clasts	Small pink grain, but too tiny to ID.
SH-S2	Replaced in clasts	Sample is red-brown	None	None	Grains and in clasts	None	Small amount	None	Formerly SH-1B

Table 13. Characteristics of washed mine soil petrographic samples.

4.2.3 Acid-Base Accounting

Four composite samples were analyzed from mines spread across the district that featured different lithologies and mineralization (Table 14). Additional samples were not collected because pyrite was not observed in this district, indicating a low potential for acid generation, which the following results confirmed. Carbon and sulfur content were used with Equations 4-6 described in the previous chapter to calculate AP, NP, and NPR (Table 15). Results were plotted against NAG pH on the ARD graph to predict acid generating potential (Fig. 17). All samples plotted high in the non-acid forming section of the chart, which suggests that waste rock can be used as backfill material and has little or no potential to generate acid, which is needed to dissolve metals into surface and groundwater. Based on these results, it is unlikely that any mines or prospects in the district are acid forming or metal-leaching.

Sample	Lithology	Mineralogy
NMA1A	Porphyritic andesite	Bn., "cc", CO ₃ -s, cpy., cv., spl.
NM354B	Highly altered (shear zone?)	Green phyllosilicate, kao., ver.,
SC-5	Aphanitic andesite	Ba., CO ₃ -s, Cu-Ox
VL-1	Andesite and rhyolite	Ba., CO ₃ -s, <Cu-Ox, des., gal., van.

Table 14. Lithology and mineralogy of samples used in ABA.

Sample	% S	% C	AP	NP	NNP	NPR	NAGpH
NMA1A	0.13	2.51	4.06	209.08	205.02	51.47	8.55
NM354B	0.14	0.82	4.38	68.31	63.93	15.61	8.37
SC-5	0.04	3.06	1.25	254.90	253.65	203.92	8.71
VL-1	2.57	3.42	80.31	284.89	204.57	3.55	8.79

Table 15. Paste pH data used to predict acid-generating potential of selected composite samples.

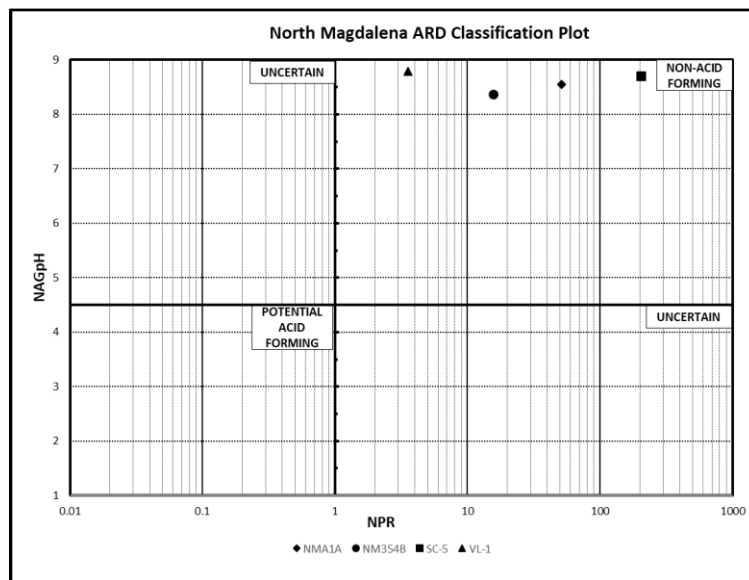


Figure 17. ARD diagram of acid generating potential of mine soils in North Magdalena. Template from "Global acid" (2012).

4.2.4 Reflected Light Petrography (RLP)

A selection of samples representing varied mineralization styles and mine types that also covered a large portion of the district were analyzed using RLP. The aim in this phase of analysis was to determine any small-scale ore mineralization not visible in hand sample, and where possible, interpret paragenetic relationships. Samples and their primary mineralogy can be seen in Table 16. Gangue mineralogy observed in most of the samples included goethite, hematite, barite, calcite, and quartz, but only reflective/opaque minerals are listed in this table.

Sample	Ore Mineralogy	Gangue Mineralogy
SH-S5i	Chr., Cu ^o , cup., mal., ten.	Gt.
SH-C1i	Bb., bn., cpy., cv., dig.,	Mt.(?)
SH-S4ii	Bb., "cc.", cv., dig., jal. (?), mal.	
SH-P14i	Cv., dig., gal., spl., tnn.	
Mag20-S1 (vs)	"Cc.", cv., cup., del., pm.	
Mag22-T1ii	"Cc.", cv., del., pm.	
VL-P1i	"Cc.", cpy., cv., gal., spl. (?)	
VL-S1i	Gal.	Gt.
NMA-1B-2	Ac.(?), bn., cc., cpy., cv., em. (?), id. (?), spl.	Gt., hem.

Table 16. Polished sections and primary and trace mineralogy.

Native copper occurs with cuprite and other oxidized copper minerals such as tenorite and chrysocolla in sample SH-S5i (Fig. 18). The author noted bornite associated with chalcopyrite in digenite with octahedral cleavage in SH-C1i (Fig. 19). SH-S4ii (Figs. 27 & 28) contained both normal and blaubleibender covellite, plus what appears to be jalpaite, a silver-copper sulfide. The most commonly observed sulfides across all samples were chalcocite varieties, covellite, chalcopyrite, sphalerite, and galena. The next sample, SH-P14i, was selected for analysis because in hand sample the author noticed that what appeared to be galena with typical isometric cleavage, was translucent and yellow, having been almost completely replaced by sphalerite. A polished section was prepared and determined to have a more complex mineral assemblage than initially thought, which included galena, sphalerite, "chalcocite", covellite, and tennantite. (Fig. 20).

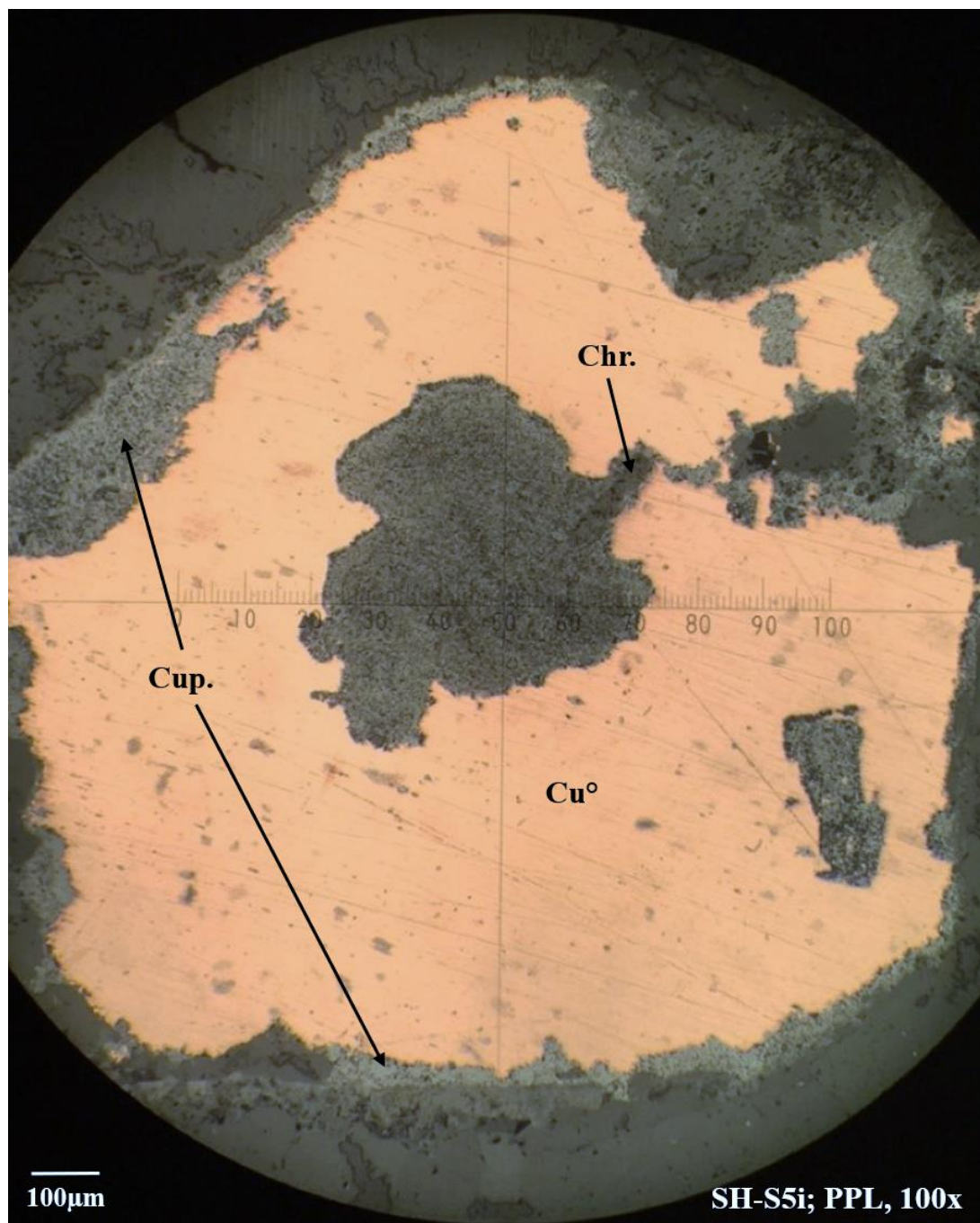


Figure 18. Cuprite replacing native copper.

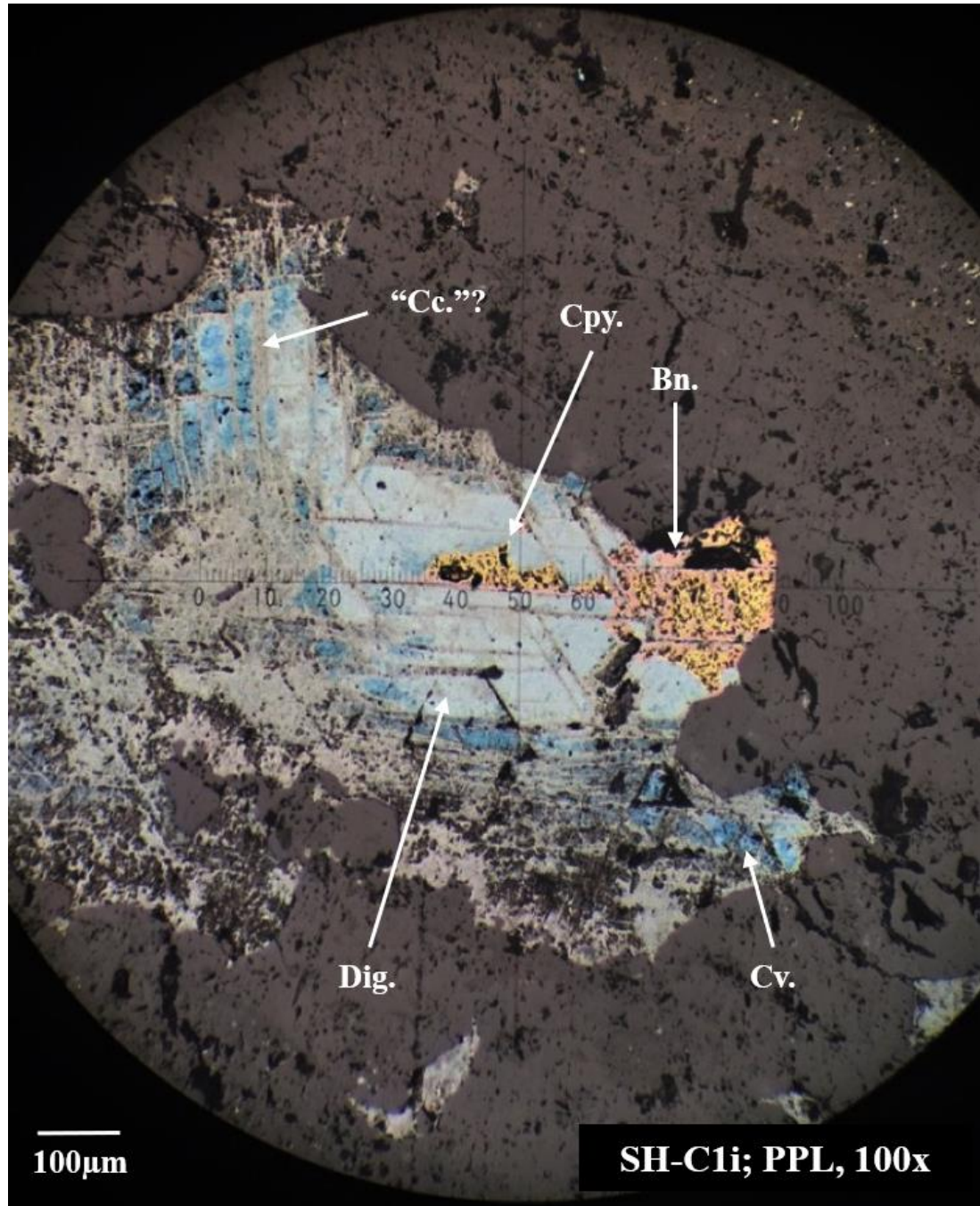


Figure 19. Assemblage of Cu-sulfides with an unclear paragenesis.

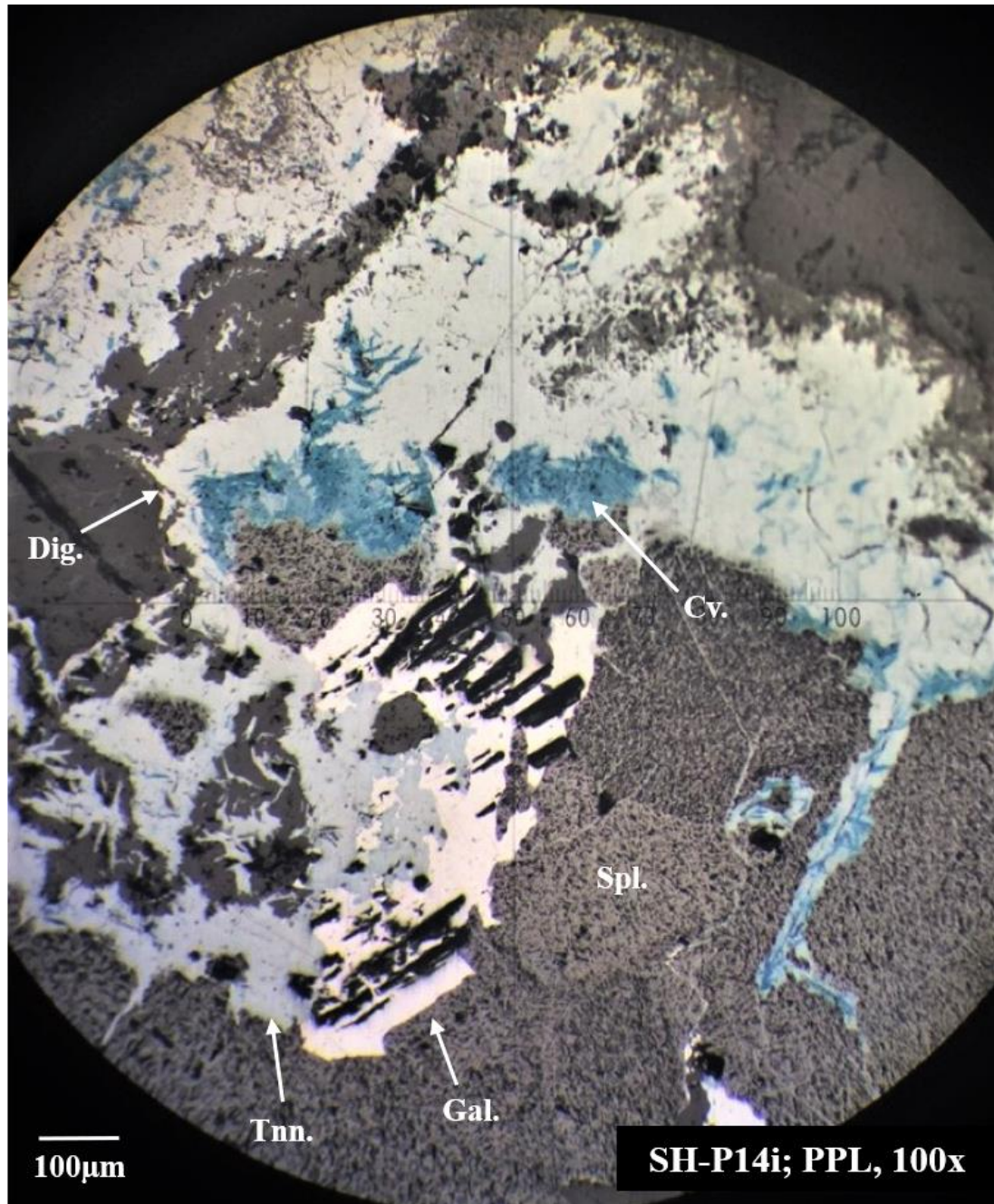


Figure 20. Complex replacement assemblage within galena.

Mag20-S1 (vs) consisted chiefly of malachite and chrysocolla, which were obvious in hand sample, but small amounts of “chalcocite”, covellite, cuprite, and paramelaconite were observed in reflected light (Figs. 30 & 31). Mag22-T1ii was collected in a shallow trench and has very large grains of “chalcocite”, which are all rimmed with covellite. Paramelaconite is intimately intergrown with the “chalcocite” in this section, just like Mag20-S1 (vs) and delafossite may be present in both, though it was not probed for confirmation. Sample VL-P1i contained a significant amount of galena and came from a vanadium prospect pit several hundred feet to the west of the main workings of the Virginia Lee Mine. It also contained minor covellite, chalcopyrite, and “chalcocite”. This accessory copper mineralization was observed along the rims of large grains of galena and in very small, disseminated blebs. VL-S1i was examined as a comparison to lead mineralization in VL-P1i and came from waste rock outside of the Dugger shaft, the main working at the Virginia Lee Mine. It did not appear to contain any copper sulfides. The distinguishing characteristic of this sample is warped triangular pits in galena. Additional photomicrographs of the samples mentioned above can be found in appendix C.6.

4.2.5 X-Ray Diffraction (XRD)

Waste rock collected in the field was examined under the stereomicroscope to see if there were any unusual minerals occurring in vugs or fractures. In doing so, about 20 uncertain mineral species were encountered and selected for further XRD analysis. Several samples were selected to distinguish them from other minerals that look very similar such as platy barite and anglesite. Others, which occur on waste rock piles as thin crusts had to be X-rayed to determine their identity because there are no other distinguishing features or tests that can be performed on such small, poorly formed specimens. The results of XRD analysis can be seen in Table 17. In a few cases, the minerals in question were identified as some form of chrysocolla or cryptocrystalline silica that was an unusual color or habit and formed dusty blue or gray coatings on many of the rocks. Other mineral crusts were identified as duftite, tangeite, and hydroxylapatite. What was suspected to be anglesite after galena was sphalerite nearly completely replacing the lead sulfide; the mechanism for this will be described in the following chapter. At least two samples were inconclusive, and the minerals remain unidentified.

Sample	XRD Result
Mag40-S1i	Chrysocolla
Mcu-d_5	Silica var.
SC-28_9	Barite, plumbian
SCg_6	Unidentified
SCh_7	Silica var.
SCi_8	Barite
SCP-4v_10	Unidentified
VLW-a_1	Descloizite, cuprian
VLW-b_3	Barite, plumbian
VLW-c_4	Vanadinite
NM354Bi	Barite
NM354Bii	Vermiculite
NM354Biii	Muscovite, zincian (?)
SH-1Ai	Tangeite (?)
SH-1Aii	Hydroxylapatite
SH-1Aiv	Duftite
SH-3ii	Chrysocolla
SH-4	Hematite + bromargyrite (?)
SH-P14i	Vanadinite
SH-P14ii	Sphalerite

Table 17. Results of XRD analysis on selected minerals.
(?) indicates uncertainty in the mineral identity.

Vanadinite and descloizite were shown to be the primary vanadium minerals at the Virginia Lee Mine (NMSO0878, NMSO0876). While descloizite is typically black to reddish-brown, it was greener in these samples. XRD matching software identified it specifically as cuprian-descloizite in which $Cu > Zn$, though this is not recognized as a formal species. Galena is common at this mine and has almost always undergone some degree of oxidation, forming coatings of anglesite and cerussite. Most of the lead mineralization is hosted in massive barite. Vanadinite was also observed at SH-P14 (NMSO0909) southwest of Silver Hill, but it was poorly formed and bright yellow-orange as opposed to the well-formed dark red-orange hexagonal crystals at the Virginia Lee Mine. Unlike the Virginia Lee Mine, no descloizite was observed at SH-P14. The zinc and copper silicates willemite and diopside, were seen filling vugs.

Samples from SH-S3 (NMSO0809) exhibited one of the more unusual mineralization styles observed in the field. Here, a porphyritic andesite underwent phyllic alteration and later oxidation. This converted ankerite to a mix of Fe-oxides, which can be seen replacing all feldspar phenocrysts. Interestingly, one out of approximately 20 of the oxidized phenocrysts contained intergrowths of a soft, honey-yellow colored mineral with resinous luster. XRD patterns produced from powdered phenocrysts matched hematite and shared many peaks with bromargyrite, though some uncertainty surrounding the yellow mineral remains due to amount of available material. A closeup of these phenocrysts can be seen in Figure 21.

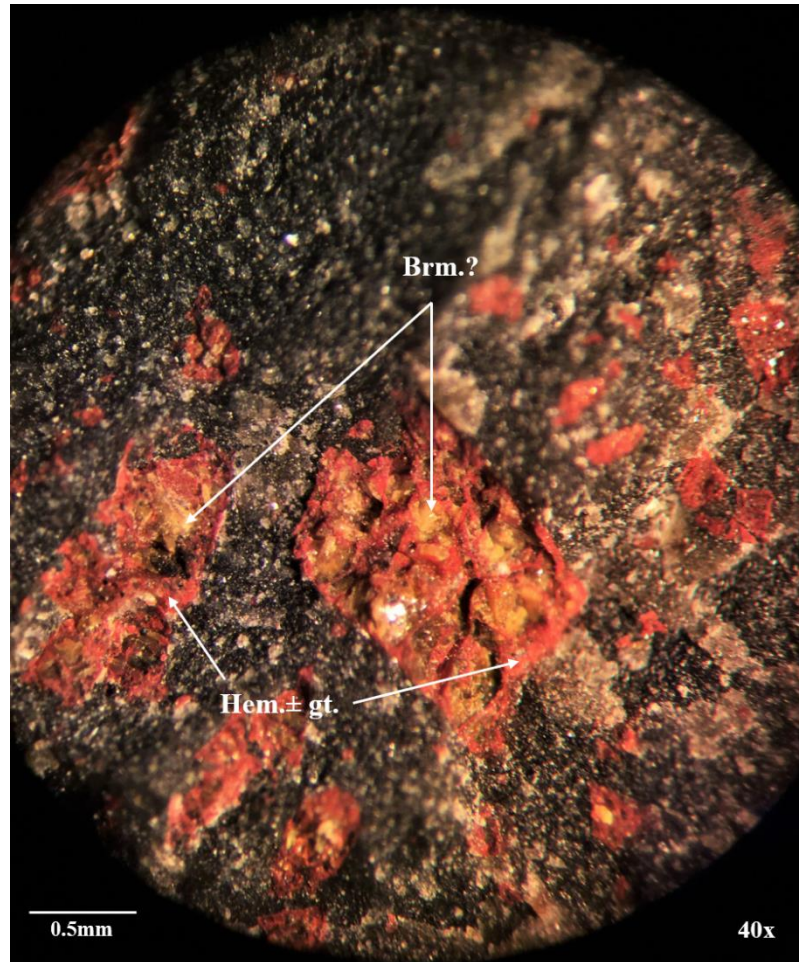


Figure 21. SH-4; Phenocrysts of Fe-Ox after ankerite and a yellow phase suspected to be bromargyrite.

4.2.6 Electron Microprobe (EMP)

Extremely small-scale mineralization styles were observed using electron microprobe. Samples from two locations representative of major mineralization styles in the area, the Ace of Spades (NMSO0811) and Virginia Lee Mines (NMSO0878), were examined with electron probe to study oxidation products of chalcopyrite and galena, respectively. Galena, pyrite, and sphalerite standards were used to identify most mineral phases in these samples, but some could only be identified with RLP. Gold and silver standards were also included for precious metal detection.

Sample NMA1B (Ace of Spades) was cut into two pieces (NMA-1B-1 and NMA-1B-2) and small veinlets of extremely weathered chalcopyrite and other sulfides in the sample were examined. Sample NMA-1B-1 featured sphalerite, galena, and cerussite, which had not been previously described at this mine. Additionally, copper phases were detected in NMA-1B-1 which, based on the weight percentages of copper and sulfur combined with a quick spectral analysis, were determined to be covellite (Table 18, Fig. 22). Covellite in these samples has anomalously high Ag concentrations and these are reflected in the results from geochemical analysis of samples from this mine (530 ppm Ag).

Sample/ Point	Wt%				
	S	Pb	Cu	Ag	Total
NMA-1B-1-07	34.89	0.14	64.94	0.53	100.50
NMA-1B-1-08	21.68	4.02	54.84	1.08	81.61
NMA-1B-1-09	29.04	1.63	62.52	0.72	93.92
NMA-1B-1-10	33.50	0.28	62.44	0.74	96.96
NMA-1B-1-12	23.93	0.10	71.23	1.87	97.13
NMA-1B-1-13	22.74	0.08	70.09	1.72	94.64

Table 18. CuS phases (covellite) with elevated Ag-values.

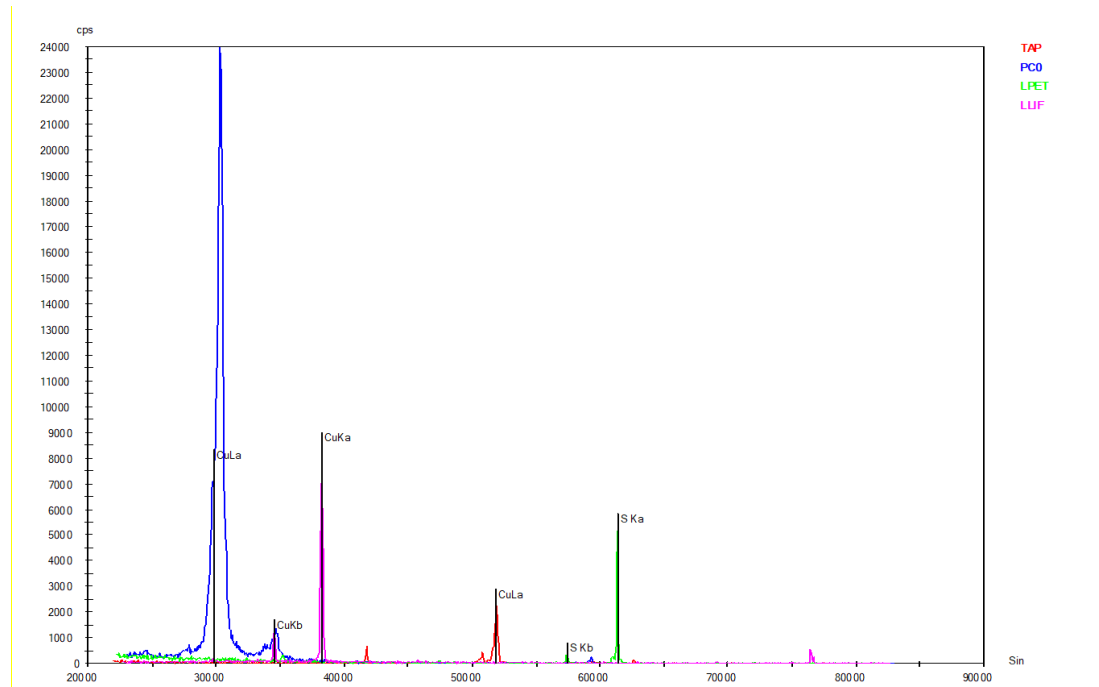


Figure 22. NMA-1B-1; spectral profile of CuS phase (covellite).

In NMA-1B-2, chalcopyrite has not been fully replaced and tetragonal cleavage is still visible despite intense oxidation along rims and cleavage planes. In addition to multiple Cu and Fe phases, BSE imagery and elemental maps showed small, Ag-rich (15.73-24.98 wt%) inclusions within the larger grain (Fig. 23). These inclusions were examined with reflected light, but their identity is unclear. Barite was an extremely common gangue mineral in this sample and formed rinds around some of the sulfides, including the oxidizing chalcopyrite grain.

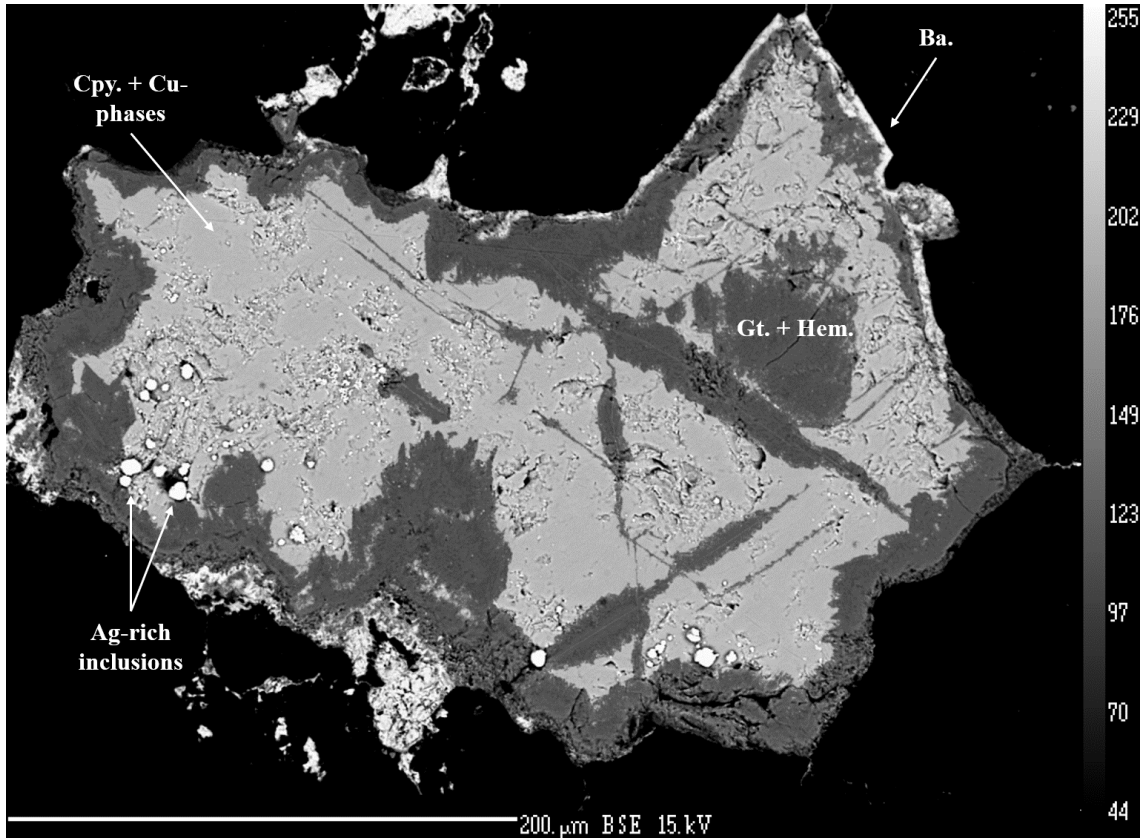


Figure 23. NMA-1B-2; BSE image of Ag-rich inclusions in chalcopyrite, etc.

Sample VL-WS, from waste rock at the Dugger shaft of the Virginia Lee Mine (VL-S1, NMSO0878), was cut and polished to expose galena with a pronounced oxidation rind. With BSE imagery, two mineral phases can be seen forming distinct “fronts” around edges of the galena and proximal to pore spaces. This rind comprised anglesite and cerussite which were determined using a galena standard (Fig. 24). Cerussite forms on the outside, progressing inwards to anglesite, and finally, unaltered galena (Fig. 25). Again, barite was the primary accessory mineral in this sample and plays an important role in the development of these oxidation fronts; this will be discussed in the next chapter. Pore spaces formed by relic euhedral quartz grains appear black and facilitate fluid flow for oxidation. All EMP data can be found in Appendix C.2-C.4.

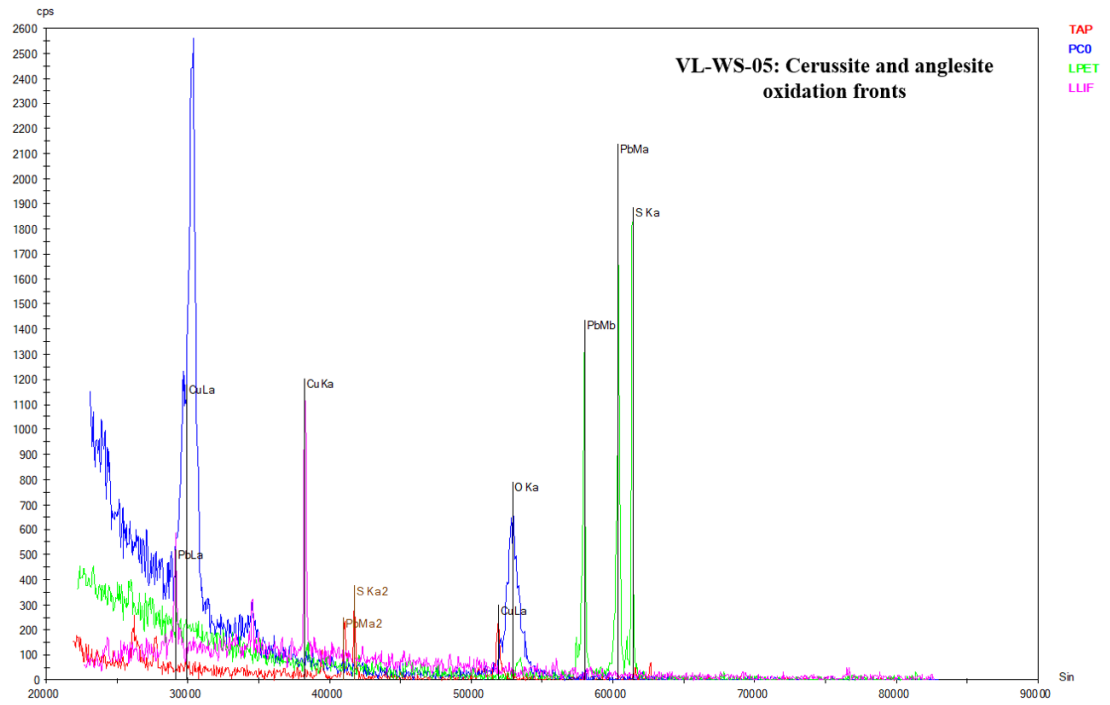


Figure 24. VL-WS; combined plot of spectra collected from points on oxidation fronts.

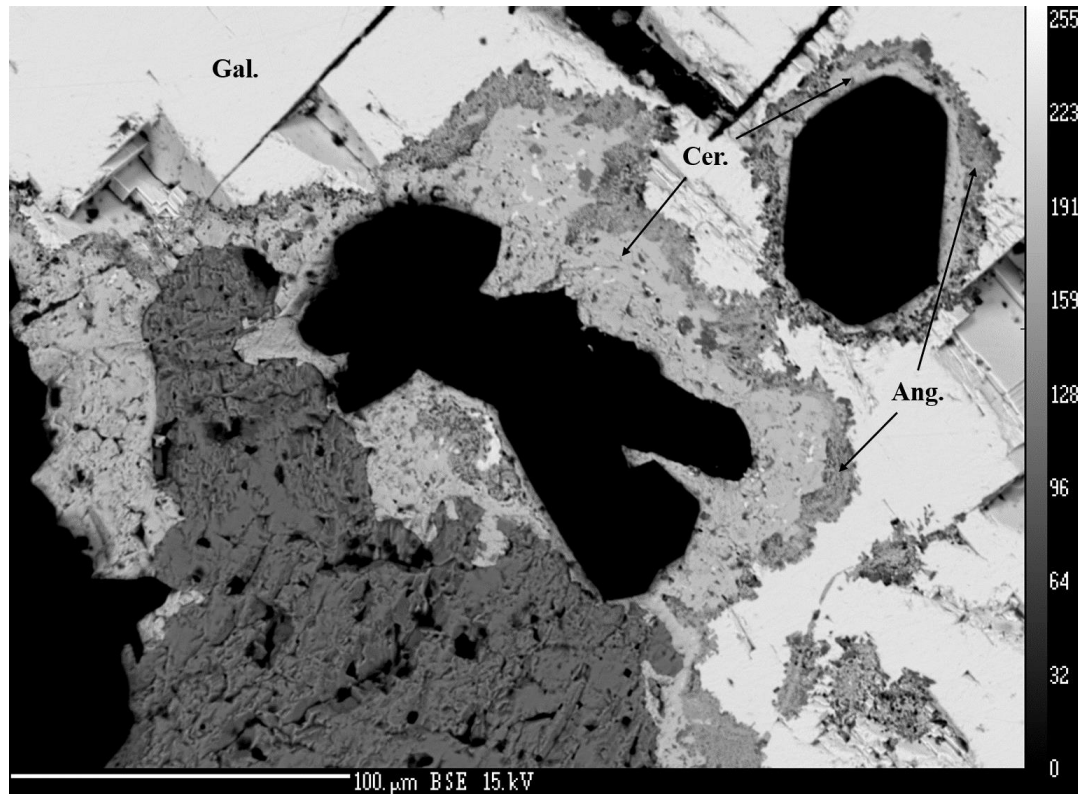


Figure 25. VL-WS; oxidation fronts on galena surround pore spaces.

CHAPTER 5

Discussion

5.1 Field Inventory

Results obtained from field surveys of mine features have highlighted trends in locations, hazards (physical and environmental), and mineralogy. The largest and most dangerous mine features are located along major veins and should be prioritized for safeguarding. Fortunately, environmental impacts of all mines appear to be minimal. Mineralogy is diverse and reflective of most low-sulfidation volcanic-hosted epithermal systems. Epithermal systems are not known for significant hydrothermal vanadium input, but supergene oxidation of lead mineralization in the district has produced notable secondary vanadium occurrences. Yaroshevsky (2006) reports 100 ppm vanadium in intermediate rocks and 90 ppm in the Earth's crust, so the vanadium was probably remobilized from the host rocks during chemical weathering.

Mine locations recorded during field inventory provided a convenient proxy for vein trends and extents in the district. When mine locations are plotted in ArcGIS, the points fall along roughly N-S lines which are consistent with vein strikes observed in the field and RGR extension. This corroborates earlier observations by Lasky (1932) and Simon (1973), which describe similar trends on vein and fault maps. Veins vary slightly in dimensions, style, mineralization, and strike from mine to mine, but patterns can be visualized by examining mine location maps. Based on earlier work and observations made during this study, it appears that the Cu-Ag mineralization is more associated with N-S veining, while the Pb-Zn-V mineralization is associated with NW-SE veins. The mines associated with major veins pose the greatest physical hazards because they tend to be the deepest and largest features with the strongest mineralization, making them attractive to curious members of the public. In New Mexico, between 1960 and 2012, there have been 7 fatalities and 8 injuries reported to have occurred in and around abandoned mines, though more injuries may have gone unreported ("NMEMNRD", 2019). One of these fatalities occurred in 2009 at the Iron Mask Mine in the Magdalena district, when a 53-year-old man fell into the 65 ft shaft and landed in 8-10 ft of water at the bottom. He was found a month later by search and rescue crews from Socorro (Admin, 2009). Table 19 displays the number of features associated with each NOAMI hazard ranking.

NOAMI Ranking	Number of Features
A	0
B	11
C	50
D	90
O	31
R	21

Table 19. Number of features associated with NOAMI hazard rankings.

Most features received a D ranking meaning they are shallow surface features and therefore present little to no physical hazard. Open shafts, declines, and adits received B and C rankings. No A rankings were assigned because none of the features have acid-generating or radioactive mine waste. An R ranking was assigned to 21 features that were remediated in the past. In the database, 31 features did not have a ranking assigned and were therefore given an O ranking. The individual hazard rankings assigned to every mine in the database are listed in Appendix **B.5**. While physical hazards are present in the district, most features are relatively harmless.

A lack of pyrite plus a carbonate-rich gangue mineralogy virtually eliminates the risk of AMD. Pyrite is extremely abundant at the Magdalena district, just a few miles to the south, which is currently oxidizing in waste rock piles and poses major environmental hazards that have yet to be addressed. Heavy metals, such as lead or cadmium, are not a major concern either. Galena, under oxidizing conditions, forms secondary lead minerals like cerussite and anglesite, which sequester lead and sulfur (anglesite) and create a carbonate buffer (cerussite) against acid production in the form of a mineral rind. Lead is also redistributed to other minerals such as vanadinite, descloizite, and duftite in the oxidized zones of the small lead occurrences in the field area. Sphalerite is common in the district but appears to host little trace cadmium as evidenced by geochemical results that will be discussed in the next section. Metal leaching is further restricted by low precipitation and the absence of AMD, which can liberate and mobilize many contaminants into the surrounding area.

Although there do not appear to be any natural environmental hazards, the disposal of household waste in mine features poses a potential risk. Trash fills many of the shafts and pits in the district, especially those easily accessible by road. Refrigerators, air conditioners, car parts, water heaters, televisions, tires, nylon rope, glass, paint and oil cans, and more have all been observed by the author and need to be removed as part of the reclamation process. Precipitation events can cause some of these features to fill with water, leaching metals and other hazardous chemicals from the refuse. Most natural mine waste on the surface poses little environmental risk to groundwater due to generally low precipitation and depth to the water table, but trash sitting at the bottom of shafts that intersect the water table has a much higher chance of leaching toxins into aquifers. Many of the ranches and houses outside of town surrounded by AML sites have wells which could be affected by this type of contamination. Further work in hydrogeochemistry should be considered in this and other districts with abundant anthropogenic pollution.

5.2 Geochemistry and Environmental Implications

Geochemistry is controlled by mineralogy, and waste rock geochemical data (from composite and whole rock samples) were separated into results from analysis of mines with Cu-Ag mineralization and Pb-Zn-V mineralization in order to calculate averages for comparison to natural abundances of selected elements. Averages of potentially economic elements and potentially hazardous elements were determined from 13 samples of Cu-Ag mineralization and 6 samples of Pb-Zn-V mineralization and can be seen in Tables 20 and 21. Elemental concentrations of waste rock can then be compared with natural abundances in the Earth's crust and intermediate rocks (andesites) in Tables 22 and 23. Vein samples were not included in calculations so as not to skew results.

	Ag	Cu	Pb	Zn	V	Au	Ba
	ppm	ppm	ppm	ppm	ppm	ppm	ppm
Cu-Ag mine waste rock averages	185.23	16009.77	683.54	1665.77	245.08	0.92	6658.46
Pb-Zn mine waste rock averages	26.48	779.83	15490	27702.5	563.83	0.17	9088.33

Table 20. Abundances of selected elements in mine waste from North Magdalena.

	As	Cd	Sb	Hg	Ni	Cr	U	S
	ppm	ppm	ppm	ppm	ppm	ppm	ppm	ppm
Cu-Ag mine waste rock averages	93.04	7.68	39.40	0.56	88.23	160.77	5.57	6400
Pb-Zn mine waste rock averages	82.73	45.78	5.8	0.66	48	211.67	5.22	24200

Table 21. Abundances of potentially hazardous elements in waste rock at North Magdalena.

	Ag	Cu	Pb	Zn	V	Au	Ba
	ppm	ppm	ppm	ppm	ppm	ppm	ppm
Earth's crust	0.07	47	16	83	90	0.0043	650
Intermediate rocks	0.07	35	15	73	100	--	650

Table 22. Abundances of selected elements in the Earth's crust and intermediate rocks (after Yaroshevsky (2006)).

	As	Cd	Sb	Hg	Ni	Cr	U	S
	ppm	ppm	ppm	ppm	ppm	ppm	ppm	ppm
Earth's crust	1.7	0.13	0.5	0.08	58	83	2.5	470
Intermediate rocks	2.4	--	0.2	--	55	50	1.8	200

Table 23. Abundances of potentially hazardous elements in the Earth's crust and intermediate rocks (after Yaroshevsky (2006)).

Results show that mine waste is enriched in all selected elements relative to natural abundances in the Earth's crust and intermediate rocks. This is unsurprising but demonstrates the importance of examining mine waste for commodities with respect to future exploration or reprocessing. Waste rock at North Magdalena would likely be uneconomic to reprocess, but other, more historically productive districts may have greater volumes of waste rock with even higher concentrations of economic elements and would be worth investigating in other studies.

AMD in North Magdalena is virtually non-existent due to three factors: 1) a lack of acid-generating sulfides, 2) highly buffering gangue and host-rock mineralogies, and 3) a lack of abundant precipitation. While no pyrite has been observed during this study other sulfides exist in most samples but have not weathered out of the rock in any significant quantity to be seen in soils. Any acid generated from these species during sporadic precipitation events would immediately be buffered by the carbonate gangue mineralogy. All composite samples plotted in the non-acid forming field of the ARD diagram (Fig. 17) and therefore the waste rock can be used as backfill-material or left in-place. Furthermore, without AMD, the mobility of heavy metals is greatly reduced. Work by Saria et al. (2006) has demonstrated that increased transport of heavy metals occurs in the presence of acid mine fluids. Although North Magdalena mine waste contains above average concentrations of several potentially hazardous elements, the lack of AMD and precipitation makes it unlikely that these will leach into surrounding soils or groundwater to any significant degree.

While it could have been beneficial to examine acid generating potential of more mines in the district the samples that were analyzed were representative of the major mineralization styles encountered in the field; they therefore provide a good representation of the acid-generating potential of the rest of the district. In Figure 26, paste pH results for the other two districts evaluated during the AML project are plotted for comparison. Jicarilla featured one potentially acid generating and two uncertain waste rock piles, while Rosedale only plotted one mine in the uncertain category. Recall that industry protocol is to treat any "uncertain" mine waste as potentially acid forming and it should not be used as backfill. Fortunately, this is not a concern in the North Magdalena district.

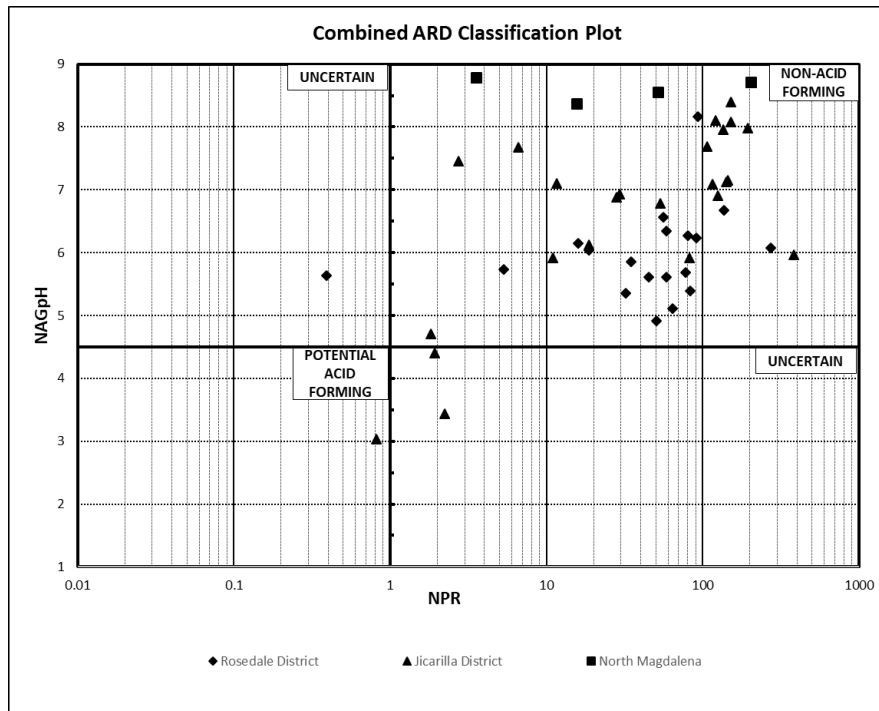


Figure 26. ARD comparison of Rosedale, Jicarilla, and North Magdalena districts.

5.3 Mineralogical Interpretations

In performing RLP, XRD, and EMP on several samples, small scale, but significant economic mineralogy and paragenetic relationships became apparent. Dominant sulfides include “chalcocite”, digenite, covellite, sphalerite, galena, chalcopyrite, and bornite, while oxides comprise cuprite, paramelaconite, tenorite, malachite and chrysocolla. Multiple stages of replacement can be seen in individual grains across several samples, and many follow a similar paragenesis.

Sample SH-S5i (from SH-S5, NMSO0910), which hosted the only native copper found in the district, exhibited a classic replacement of native copper by cuprite. This occurs on the rims of most copper grains and in the interiors where microfracturing allowed for fluid penetration. Finer grained and more, well-formed cuprite is disseminated throughout the rock. In hand sample, the copper is coated with black tenorite, though this is easily removed by abrasion. In addition to tenorite, other oxides of copper (chrysocolla and malachite) were present in samples from this locality. The presence of native copper indicates the bottom of a supergene oxidation zone. As hypogene copper sulfides oxidized at the near surface from interaction with meteoric water, copper ions migrated downwards progressively forming supergene carbonates and later oxides until they encountered the water table. Rapid reduction of these copper ions resulted in the precipitation of native copper, cuprite, and tenorite. No copper sulfides were observed in these samples, and samples with native copper were collected from waste rock closest to the opening of the shaft indicating it was some of the last mined material. This suggests the mine was only targeting oxidized copper minerals and may not have intersected the sulfide zone below the water table. The idea that this working started in a supergene oxidation zone and ended in a reduced zone at or just above the paleo water table is corroborated by the presence of what appears to be a leached cap just uphill of this feature. A short shaft (SH-S6, NMSO0911) was sunk about 8 ft into an extremely oxidized horizon which was probably depleted in Cu. Workers presumably moved downhill and sank shaft SH-S5 encountering a narrow zone of supergene carbonates and oxides before hitting the paleo water table. It is unknown if they intersected a supergene sulfide zone below.

Sample SH-C1 features a mineralogical association explained by four potential parageneses. Figure 19 shows a large grain of digenite and covellite (some blaubleibender), with enclosed chalcopyrite and bornite. The digenite has well-defined octahedral cleavage that could be derived from crystallization processes or mechanical fracturing. The true paragenesis may be some combination of these hypotheses.

1. It is possible that hypogene chalcopyrite is being replaced by digenite and that the bornite is a reaction rim, while covellite has begun replacing the digenite.
2. It could be that the chalcopyrite, bornite, and covellite are exsolution products from formation of digenite above 83°C. The unusual texture, in which octahedral cleavage is obvious, could be an exsolution product as well if the above is true (Uytenbogaardt & Burke, 1971). Bornite appears to form loosely along cleavage planes, corroborating the exsolution theory. However, covellite and chalcopyrite seem more randomly distributed.

3. A cellular structure can be seen in the top-left section of the grain (and many others, not pictured). This might be pseudo-orthorhombic cleavage associated with low chalcocite. Low chalcocite was originally thought to be orthorhombic (Lasky, 1932; Buerger & Buerger, 1944; Ramdohr, 1969), but has since been demonstrated to have a monoclinic crystal system (Evans, 1971). Assuming this is the case, low-chalcocite can only exist between 70-103°C, while large grains of digenite tend to only form above 80°C (Barton & Skinner, 1979; Pinget et al., 2011). Consequently, low-chalcocite and digenite (and chalcopyrite) in the sample are formed between 80-103°C; somewhat low to be considered hypogene. The bornite and covellite, however, are probably supergene based primarily on texture and distribution in the sample.
4. The sample is also magnetic; Ramdohr (1969) mentions a situation where magnetite replaces chalcopyrite and is accompanied by the formation of bornite and chalcocite. While this could be possible, it is more likely due to weak propylitic alteration and associated magnetite.

SH-S4ii, a sample collected from a short shaft (NMSO0122) on the very top of Silver Hill, is a section of copper mineralization with malachite and sulfides. The mine shaft from which this sample was collected appears to intersect a supergene oxidation horizon where fine grained chalcocite has formed and is now undergoing replacement and oxidation to covellite and malachite, respectively. A mineral inclusion can be seen at high magnification within an intermediate phase of chalcocite (Fig. 27). Because it had distinct blue-white anisotropy and was pale yellow compared to the surrounding “chalcocite”, it has been tentatively identified as jalpaite (Fig. 28). Jalpaite commonly occurs with covellite (Grybeck & Finney, 1968) and has a tetragonal crystal system (apparent tetragonal cleavage can be seen in this grain). However, there is some disagreement as to whether jalpaite and chalcocite are stable associates. Literature on this mineralogical association is limited to the mid-1900s and no recent work describing the two species could be found. It was unclear from the literature if the two phases are unstable associates only during hypogene formation, but because this sample represents supergene mineralization it is reasonable that these two species could coexist. Unfortunately, no geochemistry or EMP analyses were performed on samples from this mine as it would have been interesting to quantify the silver content and confirm the mineral’s identity. In addition, two forms of covellite, normal and blaubleibender, can be distinguished by anisotropy. Blaubleibender covellite is an older term, which means that the color remains blue in oil and cross polarized light rather than displaying the deep crimson anisotropy of normal covellite; this was the case when examined with the oil lens on the petrographic microscope. More recently, blaubleibender has been determined to be two intergrown, but distinct minerals: yarrowite and spionkopite (Goble, 1980). It is presumed to form by the action of acidic water upon “orthorhombic” (low) chalcocite or digenite (Uytenbogaardt & Burke, 1971). The term “blaubleibender” has been used throughout this paper because spionkopite and yarrowite were indistinguishable using reflected light and the samples were not probed.

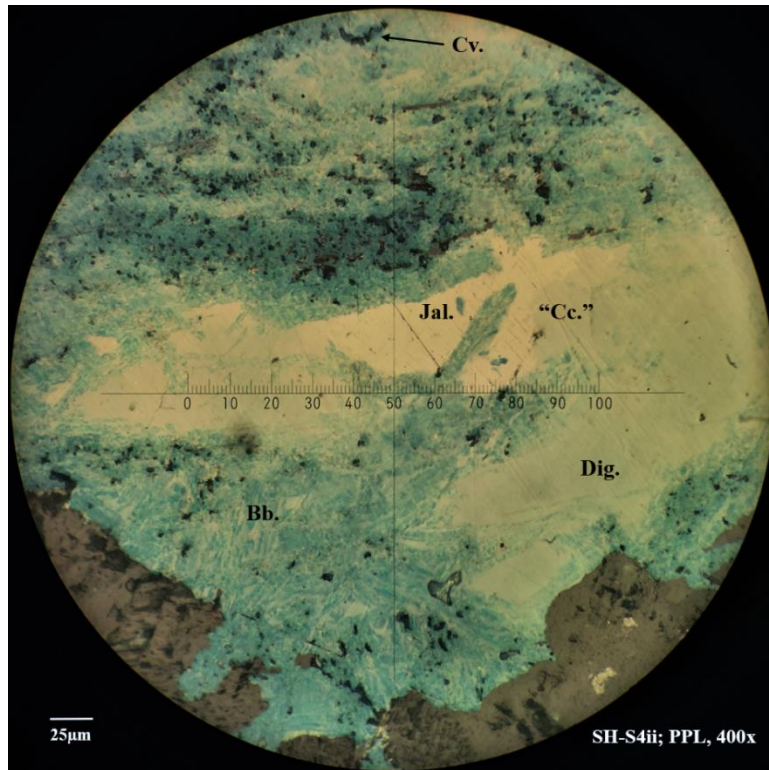


Figure 27. Supergene jalpaite (?), “chalcocite”, digenite, and covellite.

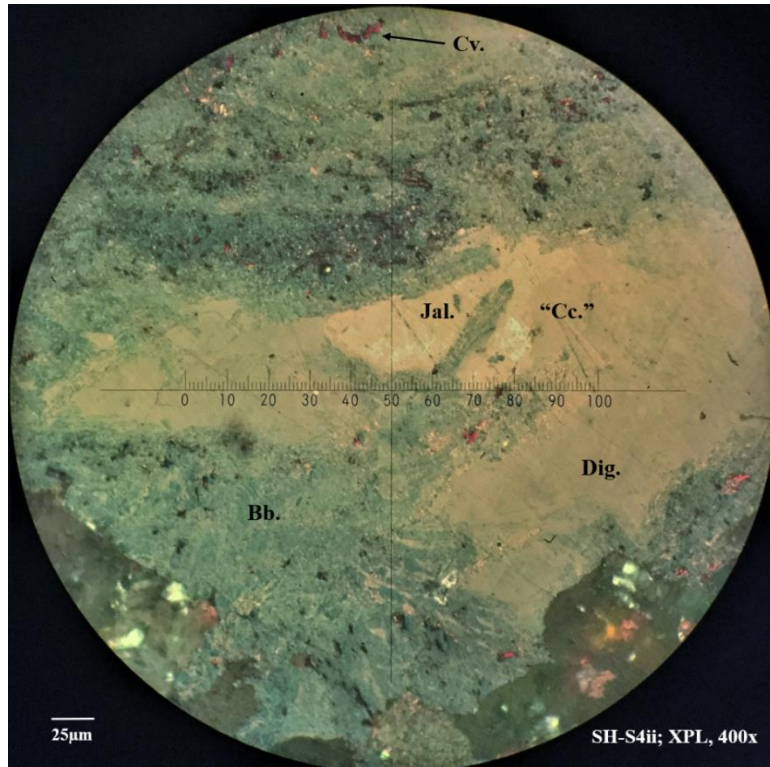
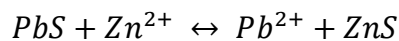


Figure 28. Bright blue-white anisotropy of jalpaite (?).

SH-P14i exhibited multiple phases of replacement. Most, but not all, of the galena had been replaced by sphalerite, which occurs easily by a cation exchange reaction (Reaction 7). Sphalerite has a lower molecular volume (39.37\AA^3) than galena (52.13\AA^3), so one mole of ZnS occupies only 75% of the volume of one mole of PbS. Because of the difference in volumes, as sphalerite forms a replacement rind on galena, a microscopic pore space forms between the two grains. This porosity allows for fluid flow between the two species which facilitates the replacement reaction, allowing sphalerite to grow inwards toward the center of the original galena grain as it dissolves. The isometric cleavage was preserved on the outside edges because the rind of sphalerite replaces the galena at a rate equal to the rate of its dissolution, leaving structures intact (Maurel, 1973). In addition to patches of relic galena and a core of sphalerite, the grain had copper minerals accumulating around the margins. Covellite is replacing digenite, which is replacing sphalerite, while galena is being replaced by both sphalerite and tennantite. The distinction between tennantite and tetrahedrite can be difficult in reflected light, but because the geochemistry results for this sample reported >250 ppm As and only 11.15 ppm Sb, it was clear that the species in the sample was indeed the As-endmember of the tetrahedrite group. Tennantite is also distinctly green when compared to galena which is quite obvious in this sample and can be seen in Figure 20 (Uytenbogaardt & Burke, 1971). Geochemistry showed elevated silver levels at this site so if any trace Ag is contained in sulfosalts, argentotennantite would be a more likely host than freibergite. Finally, shrinkage cracks can be seen in the digenite which indicates a volume reduction from the phase that it replaced.

(7) Sphalerite-galena replacement reaction



After Maurel (1973)

Mag20-S1 (vs) was collected from a vein of oxidized copper minerals (Fig. 29) that was mined by a shaft at least 60 ft deep. Minor copper sulfides and oxides are only visible with reflected light. The largest grain is a composite of “chalcocite”, paramelaconite, cuprite, and what appears to be delafossite (Figs. 30 & 31). Bluish-gray “chalcocite”, which is somewhere between stoichiometric chalcocite and digenite, forms one half of the pictured grain, while paramelaconite, evidenced by a faint pinkish-brown tint in PPL, white to pink bireflectance, and strong anisotropy (Uytenbogaardt & Burke, 1971; W.X. Chavéz, personal communication, August 8, 2019) makes up the other side of the grain. A third phase, intergrown between the “chalcocite” and paramelaconite, has tentatively been designated as delafossite. Sample geochemistry, optical properties, and mineralogical associations support this claim, but the phase was not probed or X-rayed to confirm its identity. A small amount of cuprite can be also seen between the two phases, suggesting a two-stage replacement of cuprite by paramelaconite after cuprite replaced “chalcocite”; small amounts of disseminated cuprite were also observed in the section. Covellite replacing “chalcocite” can be seen at the top left portion of the figure. This assemblage is typical at the base of copper deposits oxidized by fluids of near-neutral to alkaline pH (Dana & Hurlbut, 1948; W.X. Chavéz, personal communication, August 8, 2019).



Figure 29. Mag20-S1 (NMSO0180); vein of oxidized copper minerals representing the surface exposure of supergene enrichment mined by the shaft.

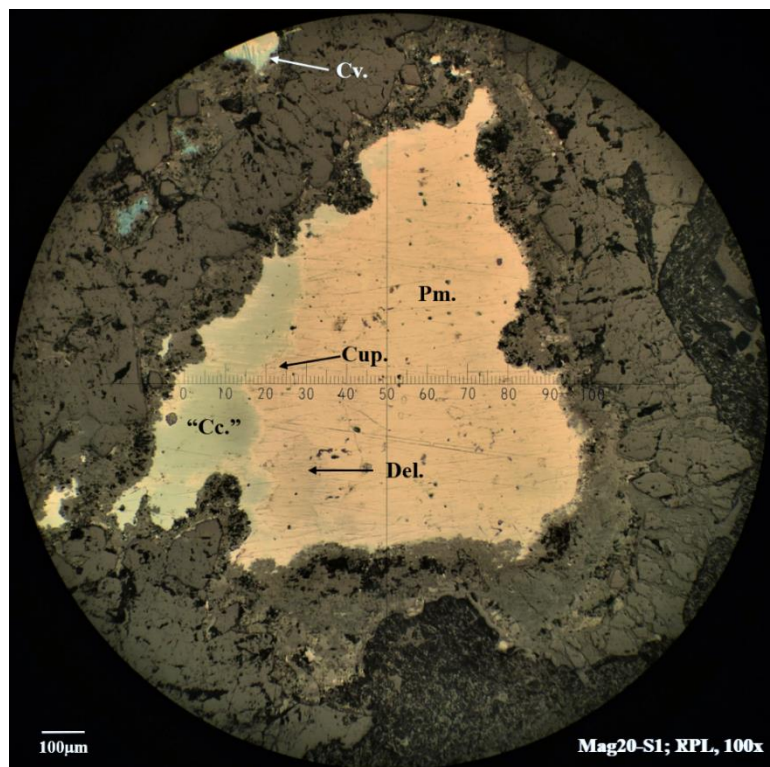


Figure 30. Grain of "chalcocite" and oxidation phases.

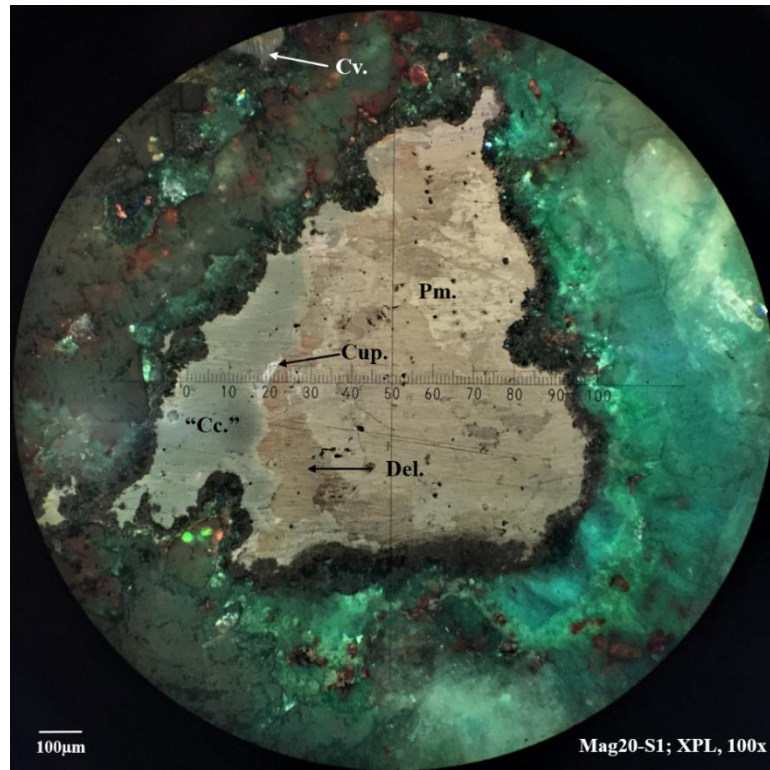


Figure 31. Anisotropy of paramelaconite is very distinct.

A similar assemblage of coarse-grained “chalcocite” with covellite and paramelaconite was observed in Mag22-T1ii, a sample taken from a trench in the Silver Hill area not far from Mag20-S1. It appears intergrown with “chalcocite” in both this sample and in Mag20-S1(vs). The paragenetic relationship remains unclear but generally represents oxidation of supergene sulfides.

Collected from a pit associated with the Virginia Lee Mine (NMSO0877), VL-P1i was selected for its galena content and under closer examination contained additional copper sulfides. At very high magnification, covellite can be seen replacing galena on certain grain boundaries. Chalcopyrite was also observed intergrown with disseminated grains of a silvery-white mineral (either galena or chalcocite), but these were too small to identify. Galena does not appear to have experienced any deformation in its history and has undergone less oxidation than the galena at VL-S1 (NMSO0878) as indicated by intact copper sulfides (not altered to goethite, etc.) and the absence of a cerussite-anglesite rind. However, the presence of vanadinite and descloizite at this locality does suggest some degree of oxidation has taken place, perhaps paragenetically earlier than the emplacement of these copper sulfides.

Sample VL-S1i comprised massive galena and no other ore minerals observable by the author. A notable feature in this sample was warped triangular pits in galena. This suggests some plastic deformation in its history, likely due to post-mineralization reactivation of NW-SE faults that host galena. Galena was found to be associated with goethite that may have come from the oxidation of other copper sulfides. Small amounts of malachite present on the waste rock piles support this theory that copper sulfides accompanied galena at one time but have since been lost via oxidation. Observations made during reflected light analysis will contribute to a proposed paragenesis for mineralization in the district at the end of this chapter.

While XRD results were generally favorable, a few of the minerals that were hard to identify in hand sample were also difficult to match to a single XRD pattern. In addition, a few minerals were unidentifiable after having been lost in the diffractograms of a more dominant mineral, like chrysocolla, in the same powder. Other potential issues were that the powder may have been ground too fine or that the run-time was too short to generate a well-defined pattern.

Minerals of questionable identity even after XRD analysis include tangeite (?), bromargyrite (?), and zincian muscovite (?). Sample SH-1Ai was visually similar to the mineral fornacite, which has been reported in this district (Moats & North, 1982), but had an XRD pattern very similar to several minerals (including tangeite, conicalcrite, and duftite), making it a challenge to distinguish in both hand sample and in the lab. Most of these species are similar in color, chemistry, and conditions of formation and all belong to the adelite-descloizite group. Moats & North (1982) also mentioned that the mineral they described as fornacite would be identical in structure and chemistry to a newly discovered mineral in Tsumeb, Namibia, but that it had not yet been named; this turned out to be molybdofofnacite. In the same abstract, the authors make a mention that iranite has been reported (but not confirmed) in the district and provide no references for this claim. In the end, tangeite was tentatively assigned as the mineral name for this unidentified species based on a greater number of matching peaks than with fornacite. For the purposes of this study, it was sufficient to narrow the mineral down to the group-level as individual solid solution members can be difficult to distinguish even with advanced methods. Fornacite, along with conicalcrite and other adelite-descloizite group minerals surely occur elsewhere in the district.

Bromargyrite (?), as mentioned in the preceding chapter, was a possible component of replacement mineralization in samples from SH-S3 along with hematite, but geochemistry performed on those same samples yielded low Ag values (<0.5 ppm). This is higher than average Ag concentrations in intermediate rocks and the Earth's crust (0.07 ppm), but low compared to other waste rock in the district. Bromargyrite contains 57.45 wt% Ag, so Ag concentrations should have been higher. It is therefore unclear if these values are low because the mineral:rock ratio is low (approximately one out of 20 phenocrysts), or because it is not bromargyrite. Another potential candidate was sphalerite, as there were many matching peaks; however, the hardness was too low and geochemical analysis indicated a concentration of 97 ppm, which is only slightly higher than average Zn concentrations in intermediate rocks and the Earth's crust—73 ppm and 83 ppm, respectively (Yaroshevsky, 2006).

It is unclear whether a pale blue-green, hexagonal, phyllosilicate in sample NM354B is zincian muscovite or baileychlore, the zinc endmember of the chlorite group (Rule & Radke, 1988). XRD patterns for baileychlore are not present in the database referenced by XRD software, but zincian muscovite was a close match. Elevated zinc levels determined with geochemistry in the absence of sphalerite or anglesite were confounding but could be explained by a zinc-rich phyllosilicate. Vermiculite, which is also present in the sample could host additional Pb and potentially Zn in its structure.

Chrysocolla was an issue for analyzing mineralogy by XRD in two ways. First, chrysocolla can exhibit several different colors and habits, which make it appear to be separate minerals. It can be blue, blue-green, green, brown, or even yellow and can have a botryoidal, crusty, dusty, fibrous, or acicular habit. All of these have been observed in the field area and were mistaken on several occasions for unique species, which is why it shows up at least twice in Table 20. The second issue is that because chrysocolla is more technically a mineraloid, it does not have a regular crystal structure and thus does not produce distinct peaks in most instances of XRD (one sample produced a very neat spectrum). A large, “amorphous hump” usually occupies the majority of the diffractogram which can obscure the peaks of other minerals that are the primary target of analysis (Fig. 32). In other words, chrysocolla “contaminates” diffractograms and prevents identification of other mineral species; hence the two “unidentified” minerals in Table 17. These species were closely associated with chrysocolla and despite the author’s best efforts to separate them, chrysocolla still obscured the peaks necessary to identify them. The author suspects one of them may have been cornetite, which had the right physical properties, environment of formation, and mineralogical associations, but it could not be confirmed as it was too intimately intergrown with chrysocolla.

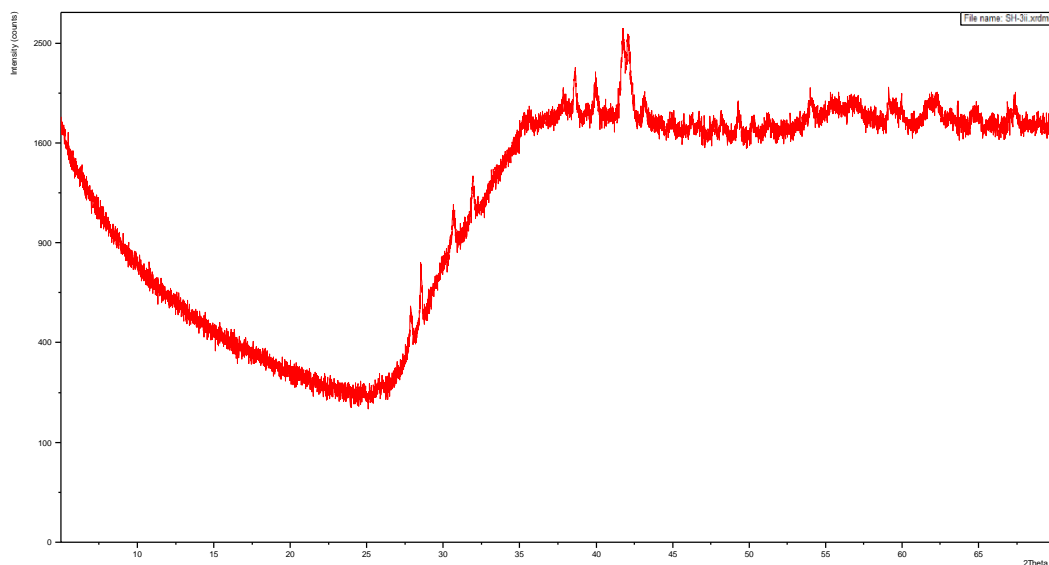


Figure 32. Noisy chrysocolla diffractogram with “amorphous hump”.

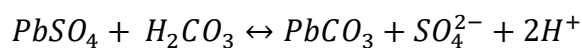
It is possible that a few of the samples analyzed early in the project could have been better characterized by longer scan times and better sample preparation. The first round of XRD analyses were a series of 5-minute scans, but all batches after that were run for 40-minutes, which produced much higher resolution diffractograms. The samples that were X-rayed for only 5 minutes, were not re-analyzed. Raw diffractograms of all samples can be reviewed in **C.5**.

Samples analyzed with the electron microprobe featured notable inclusions and oxidation rinds. Samples from the Ace of Spades Mine contained silver-rich inclusions associated with an oxidizing grain of chalcopyrite and a grain of sphalerite. Sphalerite—along with galena, cerussite, and anglesite—had not previously been recorded at this mine as they are only visible at the microscopic scale. NMA-1B-2 was reexamined with reflected light to characterize the Ag-rich inclusions. The hypogene sulfide was chalcopyrite but has since been oxidized to goethite (\pm hematite) and is actively being replaced by chalcocite which is being replaced by covellite. There may be minor amounts of bornite as well, but the grain is so small it is hard to distinguish from tarnish. The silver-rich grains could be acanthite or jalpaite but are too small to discern by optical properties. Furthermore, these minerals do not have silver or copper compositions that match compositions detected during microprobe analysis. A needle-like microinclusion within a silver-rich grain was observed at 500x using the oil lens on the microscope and could be stromeyerite or emplectite based on its habit and violet anisotropy. Acanthite can replace chalcopyrite, but if this is the case, then the violet microinclusion cannot be stromeyerite, as this is physically impossible based on conditions of formation alone (Uytenbogaardt & Burke, 1971). Therefore, the microinclusion could potentially be emplectite, a copper-bismuth sulfide that, if argentian, could have appropriate Ag and Cu concentrations (W.X. Chavéz, personal communication, July 25, 2019). One sphalerite grain that was examined in EMP featured a similar Ag-rich grain, but it was not observable in reflected light and thus could not be optically compared. In short, the identity of this mineral is unclear, but it is silver-rich, contains copper, and is likely a replacement phase of chalcopyrite and sphalerite; future work would see this inclusion probed for bismuth content. Additionally, there is a small amount of what could be idaite intergrown with chalcocite, hematite, and covellite, but again, the grains are so small, optical properties are difficult to discern. Photomicrographs of the Ag-rich inclusions and violet microinclusion can be seen along with other RLP photomicrographs in Appendix **C.6**.

While these silver-bearing inclusions contribute to the overall silver content of the rocks, covellite at this mine is also enriched in silver (Table 18). Though there is some variation in Cu and S content in the covellite, it is part of a solid solution series with other chalcocite group minerals, so this is to be expected. Stoichiometric covellite usually has 66.46 wt% Cu and 33.54 wt% S, so most of these values fall within a reasonable range. Structural complexities associated with chalcocite group minerals make them favorable hosts for trace elements such as Fe, Ag, and Pb. The additional Ag and Pb content detected with the electron probe could be altering the amount of Cu that the crystal structure can accommodate, causing deviation from stoichiometric covellite. The silver content in supergene covellite is also reasonable given recent EMP studies by Reich et al. (2010), who demonstrated the ability of supergene digenite from porphyry and manto deposits to incorporate up to 1.16 wt% Ag as nanoparticles or in solid solution. It is possible that by supergene enrichment, these Ag nanoparticles could mobilize and form larger inclusions, similar to what was observed in sample NMA-1B-2. Reich et al. (2010) also indicated a preferential partitioning of Ag into chalcocite group minerals (including covellite) over other copper sulfides like bornite. Geochemistry performed on rock from the mine returned 530 ppm Ag, which can therefore be attributed to a mix of microinclusions and trace silver in covellite and probably other chalcocite varieties.

In hand sample, oxidation rinds on galena are blue-gray and surround grains even within the rock away from atmospheric exposure. This suggests that the rinds are not necessarily from atmospheric oxidation, but from meteoric fluids or earlier phases of fluid circulation within the rock. The phases that compose the rinds are nearly impossible to distinguish in hand sample, but their nature becomes quite apparent under inspection with EMP. The two oxidation fronts described in the last chapter were cerussite (outside) and anglesite (inside). In MVT deposits, such as the Silesia deposit in Poland, galena readily oxidizes to anglesite, but only oxidizes to cerussite under higher pH conditions (Sutley et al., 1999). Anglesite is relatively soluble in water, but this decreases with input of SO_4^{2-} ions, which also lower the activity of Pb. Additional SO_4^{2-} ions can come from H_2SO_4 produced by oxidizing sulfides, or, as is the case at the mines in this district: an abundance of sulfate minerals. Massive barite hosts much of the galena in the district, including the galena in this sample. With barite as a source of SO_4^{2-} ions, anglesite can precipitate as a rind on the surface of galena. However, as oxidation takes place, the pH becomes more basic, at which point cerussite becomes a more stable phase. Reaction 8, after Sangameshwar & Barnes (1983), describes the replacement of anglesite by cerussite, which explains the relationship between the two oxidation fronts observed with electron microprobe. With an oxidative rind, the galena becomes armored and is far less reactive, which is an environmentally favorable effect of sulfide oxidation (Reichert, 2007).

(8) Replacement of anglesite, $PbSO_4$, by cerussite, $PbCO_3$:



5.4 New Minerals, Ore Formation, and Paragenesis

5.4.1 New Minerals

Minerals previously unreported in the district have been observed during this study. These were mostly observed with reflected light and comprise several copper species. Though they are very fine-grained, their presence is important, and several will be included in the NM Mines Database and added to Mindat.org. Other new minerals were observed in the field and include amethyst, siderite, and diopside. Table 26 lists all new minerals for the district as observed during this study along with their occurrence and location.

New Minerals	Occurrence and Location
Amethyst	Gangue at SH-S5 (NMSO0910)
Ankerite	Intermediate stage in phyllic alt. at SH-S3 (NMSO0809)
Aragonite	Colloform carbonate component at many mines
Baileychlore (?)	Well-formed green hexagonal crystals at NM354-P1 (NMSO0608)
Bornite	Supergene phase seen in RLP from SH-C1 (NMSO0811)
Bromargyrite (?)	Soft, honey-yellow phase replacing some phenocrysts at SH-S3 (NMSO0809)
Delafossite (?)	Oxidized phase replacing supergene sulfides in vein at Mag20-S1 (NMSO0180) and Mag22-T1 (NMSO0919)
Digenite	Hypogene and supergene phase at multiple locations; observed with RLP.
Diopside	Filling vugs in some waste rock at SH-P14 (NMSO0909); derived from oxidation of Cu-sulfides.
Emplectite (?)	Microinclusions in Ag-rich inclusions in oxidizing hypogene chalcocite grains at SH-C1 (NMSO0811)
Hydroxylapatite	White crusts on waste rock from SH-S1 (NMSO0230); occurs elsewhere
Idaite (?)	Supergene phase seen in RLP from SH-C1 (NMSO0811)
Jalpaite (?)	Supergene Ag-Cu sulfide intergrown within supergene digenite, "chalcocite", & covellite in SH-S4 (NMSO0122)
Native Copper	Visible in hand sample, but coated with tenorite at SH-S5 (NMSO0910)
Paramelaconite	Replacing supergene chalcocite (and possibly cuprite) in Mag20-S1 (NMSO0180) and Mag22-T1 (NMSO0919)
Siderite	Best sample was rhythmically banded with quartz at SC-P8 (NMSO0869); occurs elsewhere
Spionkopite	Component of blaubleibender seen in many RLP samples. Not distinguished in this study, but present, no less.
Tangeite (?)	One of many similar mineral crusts on rocks near Silver Hill. This sample was from SH-S1 (NMSO0230).
Tennantite	Seen in RLP replacing galena and sphalerite in a sample from SH-P14 (NMSO0909).
Tenorite	Coating native copper at SH-S5 (NMSO0910); present wherever supergene oxidation of Cu-sulfides has occurred.
Yarrowite	Component of blaubleibender seen in many RLP samples. Not distinguished in this study, but present, no less.

Table 24. Minerals previously unreported in the North Magdalena district; (?) indicates species remains unconfirmed by EMP or XRD.

5.4.2 Precipitation Mechanisms and Ore Formation

The origin of ore mineralization in North Magdalena is relatively simple, and observations suggest at least two major precipitation mechanisms: fluid mixing and boiling. The most widespread mechanism of precipitation appears to be fluid mixing, which is common in volcanic-epithermal systems and is evidenced by certain mineralogical assemblages observed in the field. The occurrence of barite at mines and prospects across the district, particularly those with Pb-Zn ± Ag mineralization, is indicative of saline and dilute fluid mixing (Savage, 2003). Chloride complexes in low-temperature epithermal systems like North Magdalena are the primary transport ligands for base metals and silver. Dilution destabilizes chloride complexes and results in precipitation of base-metal sulfides when sulfur is available, which is clear given the close association of galena and sphalerite with barite in these systems. Furthermore, Ba²⁺ has a high affinity for oxidizing ions such as SO₄²⁻ and will always combine to form barite when these two ions are present in the same solution. Transport of SO₄²⁻ in fluids along structural conduits is therefore only possible when these fluids are depleted in Ba²⁺. The presence of massive barite intergrown with galena and sphalerite near the surface suggest late mixing of a Ba²⁺-rich, SO₄²⁻-poor solution and an SO₄²⁻-rich, Ba²⁺-poor solution saturated in base-metal chlorides (Savage, 2003). This resulted in rapid precipitation of barite, sphalerite, and galena along fluid conduits; similar to processes seen in Mississippi Valley Type (MVT) deposits (Leach et al., 2006). Hypogene copper sulfides in the district were also precipitated via fluid mixing and they are often accompanied by minor barite.

The other probable precipitation mechanism is boiling. This is evidenced by bladed calcite (often pseudomorphed by quartz) and colloform silica (Hedenquist, et al., 2000). If native gold were mined in the district, as has been reported by Lasky (1932), then boiling would be responsible for precipitation by destabilizing bisulfide complexes. If the fluid temperatures were high enough, silver could be transported and precipitated by bisulfide and boiling as well. However, it appears most of the silver was transported by chloride complexes and precipitated by mixing due to its association with barite and base-metal mineralization. Furthermore, silver-chloride complexes are more common at temperatures below 350°C, which would make sense in a low-sulfidation epithermal system like North Magdalena (Seward et al., 2013). Silver was probably mobilized, concentrated, and re-precipitated during supergene enrichment creating the historically significant occurrences in the district. A separate study focused on fluid inclusion and stable isotope analysis would better clarify the precipitation mechanisms and their relative timing throughout the district's formation.

5.4.3 Mineralization Events and Paragenesis

While it is likely that many fluid events have occurred throughout the formation of the district, three main mineralization episodes have been interpreted from observations made during this study and from prior research. Paragenesis of minerals across these three events have been summarized in Figure 33 and are based on interpretations from field and lab investigations. Gangue mineralization spans the geologic history of the district occurring before, during, and after economic mineralization. Simon (1973) noted cross-cutting relationships that indicate that quartz and calcite veining in many cases predate economic mineralization; recent field observations corroborate these claims. Additional silica in the form of drusy quartz, amethyst, and more well-developed euhedral crystals accompany mid-stage copper mineralization. Calcite veining and breccias seem early and/or concurrent with most mineralization, but it is unclear at what point calcite precipitation ceased; uncertain depositional periods are represented by dashed lines in the paragenetic diagram. Minor platy barite was observed in association with copper mineralization, but its timing is uncertain and may have occurred later. The precipitation of massive barite with Pb-Zn mineralization is linked to a separate fluid pulse that postdates the earlier copper-bearing fluids. This later fluid flux is probably associated with the NW-SE trending vein systems and may be concurrent with tectonic processes that created these structures. Hematite and goethite are late stage (supergene) gangue minerals associated with oxidizing copper sulfides.

Each of the three major mineralization episodes are characterized by distinctive ore mineralogies. The first economic mineralization event deposited hypogene oxidized copper minerals. Simon (1973) suggested that some malachite and chrysocolla was emplaced early in the system before enough sulfur was available to produce sulfide mineralization. This is entirely possible, as is the case at some mines in Nevada (W.X. Chavéz, personal communication, November 21, 2019). Some evidence of this was seen in the field where oxidized copper minerals were present with no obvious association to oxidizing sulfides or supergene processes.

The second mineralization event was characterized by fluids rich in sulfur, copper, and silver. These fluids precipitated well formed, veinlet-controlled hypogene copper sulfides (e.g. chalcopyrite, digenite, chalcocite) along N-S trending structures in the district. Following deposition, these minerals began to undergo supergene enrichment. As seen in RLP analyses, hypogene copper sulfides oxidized producing malachite, hematite, goethite, chrysocolla, tenorite, and paramelaconite (samples NMA-1B-2, Mag20-S1 (vs), and Mag22-T1ii). Supergene copper sulfides formed progressively downwards along the veins and include poorly formed chalcocite, digenite, and bornite; replacement of supergene chalcocite and digenite by covellite occurred shortly after (SH-C1i and many other samples). Jalpaite (?) appears to be associated with supergene chalcocite varieties (SH-S4iii) as do the unknown Ag-rich inclusions observed in EMP and RLP (NMA-1B-2). It is likely that these phases formed by remobilization of solid solution Ag during supergene enrichment. Native copper precipitated low in the supergene enrichment profile and was later replaced by cuprite which was subsequently replaced by tenorite (SH-S5i). Silica, carbonates, and minor barite continued to deposit alongside economic minerals.

Input of hydrothermal fluids with $Pb-Zn > Cu-Ag$ resulted in the third episode of mineralization. At this time, hypogene galena and sphalerite were emplaced along NW-SE structures like the Jack Frost vein. Galena was subsequently oxidized to produce vanadinite and descloizite (VL-P1i, VL-S1i) but is being replaced by sphalerite and tennantite in other settings (SH-P14i). The sphalerite and copper sulfides at SH-P14 (NMSO0909) have undergone further oxidation to form willemite and diopside, respectively. Sphalerite was observed in NMA-1B-1 being replaced by chalcocite, which was being replaced by covellite (C.6). Minor chalcopyrite and possibly chalcocite appeared concurrent with galena in VL-P1i. The galena was observed undergoing replacement by covellite and any chalcocite in the sample was probably doing the same. These minor copper sulfides have undergone further oxidation to produce malachite and goethite, which were seen on the waste rock piles at VL-S1 (NMSO0878). Silica and carbonates are still present, but in lower amounts and continued to deposit after economic mineralization. Barite is the dominant gangue mineral associated with the Pb-Zn-V occurrences in North Magdalena.

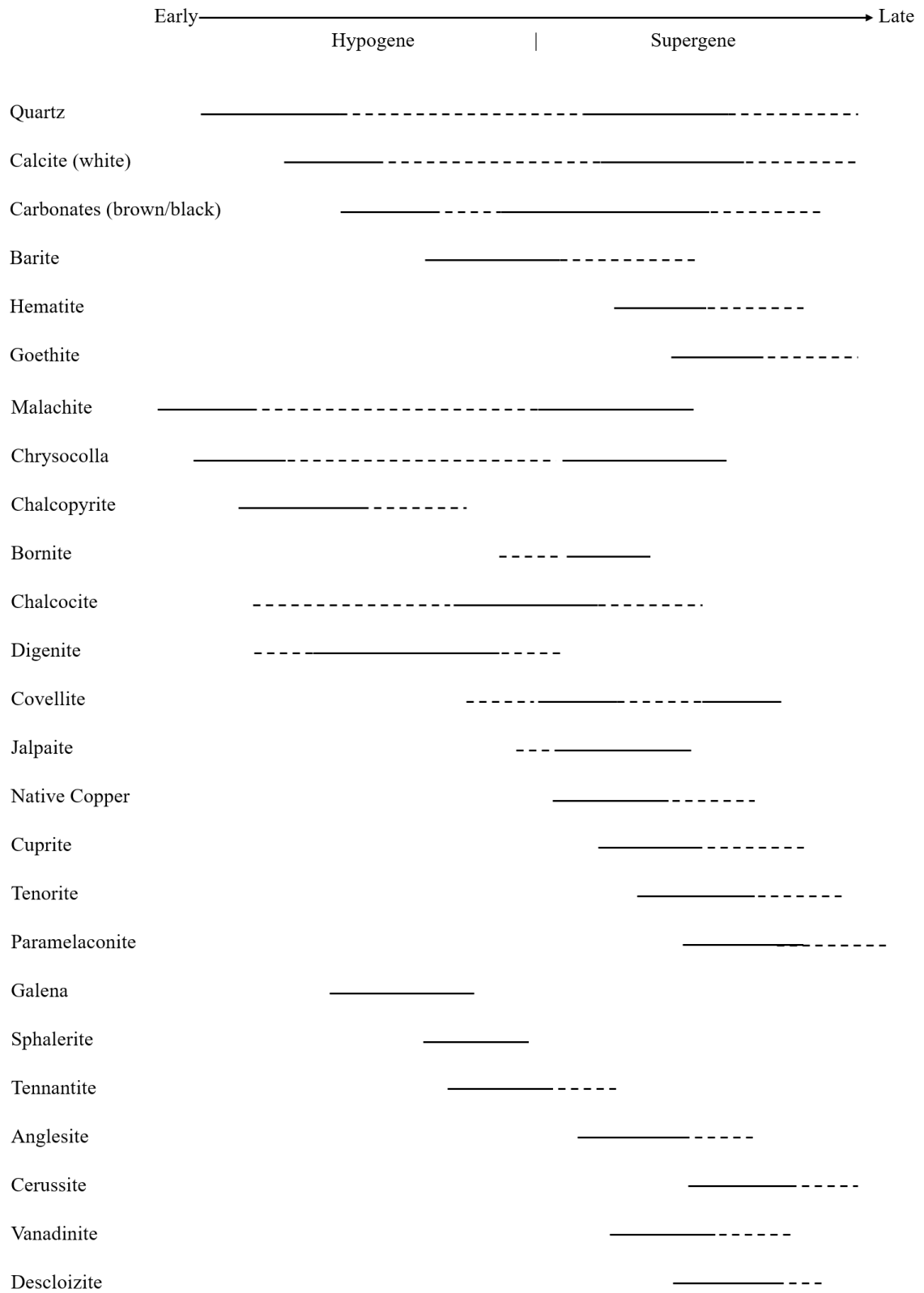


Figure 33. Paragenetic relationships in North Magdalena

CHAPTER 6

Conclusions

By inventorying mine features, it was determined that the primary hazards that should be addressed by reclamation efforts are physical rather than environmental. Open shafts, adits, and declines near roads should be considered a priority, but the methods for reclamation need to take a few things into consideration prior to implementation. Wildlife, particularly owls and bats, need to retain access to these mine features. Many of these abandoned mines serve as excellent refuges for these animals and should not be backfilled and eliminated as artificial habitats (Fig. 34). Instead, closures should be installed appropriate to the type of animal that inhabits the feature that will also serve to keep humans and cattle out. Additionally, trash removal should be a top priority for reclamation in the area as many sites host large volumes of potentially hazardous refuse (Fig. 35).

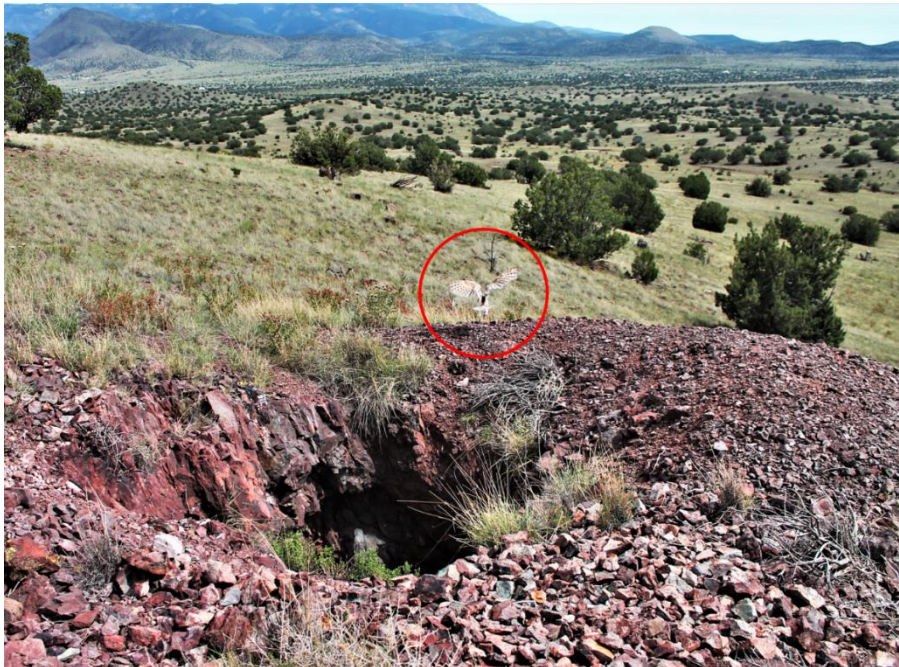


Figure 34. SH-S1 (NMSO0230); barn owl taking flight.



Figure 35. SH-P15 (NMSO0830); a prospect pit south of Silver Hill filled with trash.

Though waste rock in North Magdalena is safe for backfill, the potential value of mine waste for future academic studies, waste-reprocessing, exploration, and mineral collecting should be considered. Mine waste provides valuable insight into historic mining activity, mineralization, paragenesis, and geochemistry of mining districts and should be examined thoroughly before using it as backfill-material. All composite samples were shown to contain moderate amounts of organic matter, which indicates mine waste is suitable—or even favorable—for plant growth. In many cases, grasses, shrubs, and even full-grown juniper trees were seen growing on waste rock piles. High permeability of disturbed mine soils facilitates root access to water and oxygen, while mineralization contributes beneficial micronutrients; a testament to the potential value of producing fertilizers from reprocessed abandoned mine waste. Additionally, mineral collecting is popular in North Magdalena and accounts for most economic activity in the district. Many collectors acquire specimens from the waste rock piles, which could be lost if backfilling is employed as a primary reclamation strategy. Lastly, mine waste is inert and poses no natural hazards; disturbing the waste rock piles could actually expose reactive minerals to the atmosphere, causing unintended problems. Again, grates should be installed to safeguard the more dangerous features instead of backfilling them and rendering waste inaccessible.

Though it is beyond the scope of this project to determine the district's mineral-resource potential, McLemore (2018) has determined the mineral-resource potential for mining districts in New Mexico. Based on resource estimations for similar districts, North Magdalena has a low potential for copper and a moderate potential for gold and silver. There is no economic potential for vanadium, lead, tellurium, uranium, REEs, or zinc, and the economic potential for barite is unknown. See McLemore (2018) for a description of how mineral-resource potential is determined.

A mineralogical characterization of mines and prospects in the district has improved records and created a strong background that can now be used in future studies and projects. Small-scale mineralization styles and textures have provided insight into the large-scale mineralogical trends within the district. By examining mineralogy in the field and lab, a paragenetic history of the district has been proposed and environmental hazards are better understood. Due to a lack of AMD and low precipitation rates, heavy metal leaching is inhibited, and secondary mineral phases sequester potentially hazardous elements. Many of these mineral species form during oxidative processes and have not been previously reported in the district. Some were only observable with a petrographic microscope or more advanced techniques and would easily have been missed by prospectors at the turn of the 20th century. This fact, more than anything, demonstrates the importance of reexamining the mineralogy of historic mine waste for future projects.

REFERENCES

- A vein of vanadium (1907, August 3). *El Defensor Chieftain*, 25, 1.
- Abandoned Mine Lands (AML) Project (2019). Retrieved from <https://geoinfo.nmt.edu/hazards/mines/aml/>
- Ackerly, N.W. (1997). An overview of the historic characteristics of New Mexico's mines: Dos Ríos Consultants, Inc., Silver City, New Mexico, Prepared for the Historic Preservation Division, Santa Fe, New Mexico.
- Admin (2009, September 2). Man found dead in mine shaft near Magdalena. *El Defensor Chieftain*. Retrieved from http://www.dchieftain.com/news/man-found-dead-in-mine-shaft-near-magdalena/article_77aa7fc0-c923-5597-976d-df68e70b3a3d.html#comments
- ALS Global (2019). Retrieved from <https://www.alsglobal.com/en-us/locations/americas/north-america/usa/nevada/reno-geochemistry>
- AML construction projects (2019). Retrieved from <http://www.emnrd.state.nm.us/MMD/AML/AML-ConstructionProjects.html#Projects1995>
- Anderson, E.G. (1957). The metal resources of New Mexico and their economic features through 1954. New Mexico Bureau of Mines and Mineral Resources, Bulletin 39, 183.
- Barton, P.B., & Skinner, B.J. (1979). Sulfide mineral stabilities. In: Barnes, H.L. (1997). *Geochemistry of hydrothermal ore deposits* (3rd ed.). New York, NY: John Wiley & Sons, Inc., 278-403.
- Blakestad, R.B. Jr. (1978). Geology of the Kelly mining district, Socorro County, New Mexico. Master's thesis, University of Colorado, New Mexico Bureau of Geology and Mineral Resources Open-File Report 43, 150.
- Bornhorst, T.J., & Wolfe, S.P. (1985). Abundance of silver in mid-Cenozoic volcanic rocks of the Mogollon-Datil Volcanic Field, southwestern New Mexico. New Mexico Bureau of Mines and Mineral Resources Circular, 199, 41-43
- Brown, D.M. (1972). Geology of the southern Bear Mountains, Socorro County, New Mexico. Unpublished master's thesis, New Mexico Institute of Mining and Technology, 110.
- Bobrow, D.J., Johnpeer, G.D., & Osburn, G.R. (1986). Abandoned mines survey, Magdalena mining district, Socorro County, New Mexico. Abandoned Mine Land Bureau, Energy and Minerals Department, Santa Fe, New Mexico, 1, 379.
- Buchanan, L.J. (1981). Precious metal deposits associated with volcanic environments in the southwest. *Arizona Geological Society Digest*, 14, 237-261.
- Buerger, M.J., & Buerger, N.W. (1944). Low-chalcocite and high-chalcocite; *American Mineralogist*, 29, 55-65.

- Bureau of Land Management (2014). Abandoned Mine Land inventory study for BLM-managed lands in California, Nevada, and Utah: site and feature analysis. Department of the Interior, Bureau of Land Management, National Operations Center, Denver, CO., 24. Retrieved from https://www.blm.gov/sites/blm.gov/files/uploads/AML_PUB_Inventory.pdf
- Chamberlin, R.M. (2001). Waning-stage eruptions of the Oligocene Socorro caldera, central New Mexico. In: Crumpler, L.S., & Lucas, S.G. (2001). *Volcanology in New Mexico*. New Mexico Museum of Natural History and Science Bulletin 18, 69-77.
- Chamberlin, R.M., McIntosh, W.C., & Eggleston, T.R. (2004). $^{40}\text{Ar}/^{39}\text{Ar}$ geochronology and eruptive history of the eastern sector of the Oligocene Socorro caldera, central Rio Grande rift, New Mexico. *New Mexico Bureau of Geology and Mineral Resources Bulletin* 160, 251-279.
- Chapin, C.E., Wilks, M., & McIntosh, W.C. (2004). Space-time patterns of Late Cretaceous to present magmatism in New Mexico—comparison with Andean volcanism and potential for future volcanism. *New Mexico Bureau of Geology and Mineral Resources, Bulletin* 160, 40.
- Cooke, D.R., Deyell, C.L., Waters, P.J., Gonzales, R.I., Zaw, K. (2011). Evidence for magmatic-hydrothermal fluids and ore-forming processes in epithermal and porphyry deposits of the Baguio district, Philippines. *Economic Geology*, 106, 1399-1424.
- Dana, J.D., & Hurlbut, C.S. (1948). *Manual of mineralogy* (15th ed.). New York, NY: John Wiley & Sons.
- Deal, E.G., & Rhodes, R.C. (1976). Volcano-tectonic structures in the San Mateo Mountains, Socorro County, New Mexico. *Cenozoic volcanism in southwestern New Mexico: New Mexico Geological Society Special Publication*, 5, 51-66.
- Eberl, D.D., Środoń, J., Lee, M., Nadeau, P.H., & Northrop, H.R. (1987). Sericite from the Silverton caldera, Colorado: correlation among structure, composition, origin, and particle thickness. *American Mineralogist*, 72, 914-934.
- Electron microprobe (2019). Retrieved from <https://geoinfo.nmt.edu/labs/microprobe/description/instrumentation.html>
- Elston, W.E., & Abitz, R.J. (1989). Regional setting and temporal evolution of the Mogollon-Datil Volcanic Field, southwestern New Mexico. *Continental Magmatism Abstracts, International Association of Volcanology and Chemistry of the Earth's Interior (general assembly)*, Santa Fe, New Mexico.
- Evans, H.T. (1971). Crystal structure of low chalcocite. *Nature Physical Science*, 232, 69-70.
- Frau, F. (2000). The formation-dissolution-precipitation cycle of melanterite at the abandoned pyrite mine of Genna Luas in Sardinia, Italy: environmental implications. *Mineralogical Magazine*; 64, 995-1006.

- Frolli, A.W. (1943). Report on Nutter and Hammond-Johnston prospects. American Smelting and Refining Company, Magdalena Unit, Magdalena, New Mexico, 1-3.
- Geologic map of New Mexico (2003). New Mexico Bureau of Geology and Mineral Resources, scale 1:500,000.
- Global Acid Rock Drainage Guide (2012) Retrieved from http://www.gardguide.com/index.php?title=Chapter_5b#5.4.10_Net_Acid_or_AR_D_Potential
- Globe Program (2005). The Globe soil color book: a pocket guide for the identification of soil colors. Globe Program, 41.
- Goble, R.J. (1980). Copper sulfides from Alberta: yarrowite Cu_9S_8 and spionkopite $\text{Cu}_{39}\text{S}_{28}$. *Canadian Mineralogist*, 18, 511-518.
- Goble, R.J., & Robinson, G. (1980). Geerite, $\text{Cu}_{1.60}\text{S}$, a new copper sulfide from DeKalb Township, New York. *Canadian Mineralogist*, 18, 519-523.
- Grybeck D., & Finney, J.J. (1968). New occurrences and data for jalpaite. *The American Mineralogist*, 53, 1530-1542.
- Heald, P., Foley, N.K., & Hayba, D.O. (1987). Comparative anatomy of volcanic-hosted epithermal deposits: acid-sulfate and adularia-sericite types. *Economic Geology*, 82, 1-26.
- Hedenquist, J.W., Arribas, A., & Gonzalez-Urien, E. (2000). Chapter 7: exploration for epithermal gold deposits. *SEG Reviews*, 13, 245-277.
- Heister, A.L. (1908). Vanadium deposit at Magdalena, New Mexico. *The Engineering and Mining Journal*, 85, 246.
- Henley, R.W., & Berger, B.R. (2010). Magmatic-vapor expansion and the formation of high-sulfidation gold deposits: chemical controls on alteration and mineralization. *Ore Geology Reviews*, 39, 63-74.
- Holmquist, R.J. (1946). Dugger Group, Socorro County, New Mexico. U.S. Bureau of Mines Supplemental Examination Report, 1-5.
- Howard, E.V. (1967). Metalliferous occurrences in New Mexico. Phase 1 state resources development plan, State Planning Office, Santa Fe, 270.
- John, D.A., Vikre, P.G., du Bray, E.A., Blakely, R.J., Fey, D.L., Rockwell, B.W., ... Graybeal, F.T. (2018). Descriptive models for epithermal gold-silver deposits. U.S. Geological Survey Scientific Investigations Report 2010-5070-Q, 247.
- Johnson, J.T. (1955). A northern extension of the Magdalena mining district, Socorro County, New Mexico. Unpublished master's thesis, Geology Department, New Mexico Institute of Mining and Technology, 1-46.

- Jones, F.A. (1904). Mineral deposits of New Mexico, World's Fair edition. The New Mexico Printing Company, Santa Fe, New Mexico, 388.
- Lasky, S.G. (1932). The ore deposits of Socorro County, New Mexico. New Mexico Bureau of Mines and Mineral Resources Bulletin, 8, 139.
- Leach, D., Macquar, J.-C., Lagneau, V., Leventhal, J., Emsbo, P., & Premo, W. (2006). Precipitation of lead-zinc ores in the Mississippi Valley-type deposit at Trèves, Cévennes region of southern France. *Geofluids*, 6, 24-44.
- Lindgren, W. (1933). Mineral deposits: fourth edition revised and reset. New York: McGraw-Hill Book Company.
- Loughlin G.F., & Koschmann, A.H. (1942). Geology and ore deposits of the Magdalena mining district, New Mexico. USGS Professional Paper 200, 168.
- Lowell, J.D. (1974). Regional characteristics of porphyry copper deposits of the southwest. *Economic Geology*, 69, 601-617.
- Machette, M.N. (1988). Quaternary movement along the La Jencia Fault, central New Mexico. USGS Professional Paper 1440, 1-82.
- Mardirosian, C.A. (1971). Mining districts and mineral deposits of New Mexico (exclusive of oil and gas). Mineral Research Company of Albuquerque.
- Maurel, C. (1973). Mechanism of hydrothermal sphalerite-galena replacement at 300°C. *Economic Geology*, 68, 665-670.
- Mayo, E.B. (1958). Lineament tectonics and some ore districts of the southwest. *Mining Engineering*, 11, 1169-1175.
- McIntosh, W.C. (1991). Evaluation of paleomagnetism as a correlation criterion for Mogollon-Datil ignimbrites, southwestern New Mexico. *Journal of Geophysical Research*, 96, B8, 13459-13483.
- McIntosh, W.C., Chapin, C.E., Ratté, J.C., & Sutter, J.F. (1992). Time-stratigraphic framework for the Eocene-Oligocene Mogollon-Datil volcanic field, southwest New Mexico. *Geological Society of America Bulletin*, 104, 20.
- McLemore, V. T. (1994). Volcanic-epithermal deposits in the Mogollon-Datil volcanic field, New Mexico. New Mexico Geological Society, Guidebook 45, 299-309.
- McLemore, V.T. (1996). Volcanic-epithermal, precious metal deposits in New Mexico. Geology and ore deposits of the American Cordillera: Geological Society of Nevada symposium proceedings, Reno/Sparks, Nevada, April 1995, 951-969.
- McLemore, V.T. (2001). Silver and gold resources in New Mexico. New Mexico Bureau of Mines and Mineral Resources, Resource Map 21, 60.
- McLemore, V.T., Krueger, C.B., Johnson, P., Raugust, J.S., Jones, G.E., Hoffman, G.K., & Wilks, M. (2005). New Mexico mines database. *Mining Engineering*, 42-47.

- McLemore, V.T. (2017). Resource map 24: mining districts and prospect areas in New Mexico. <https://geoinfo.nmt.edu/publications/maps/resource/24/>
- McLemore, V.T. (2018). Mineral-resource potential of proposed U.S. Bureau of Land Management exchange of lands with New Mexico State Land Office. New Mexico Bureau of Geology and Mineral Resources Open-File Report 598, 152.
- McLemore, V.T., Zutah, W., Silva, M., Asafo-Akowuah, J., Trivitt-Kracke, A., Shackelford, J.,...Sears, B. (2019). Geology, mineral-resource potential, and potential environmental impacts of the Rosedale mining district, Socorro County, New Mexico. New Mexico Bureau of Geology and Mineral Resources OFR-603.
- Metzger, O.H. (1938). Gold mining in New Mexico. U.S. Bureau of Mines, Information Circular, 6987.
- Moats, W.P., & North, R.M. (1982). Minerals of the Silver Hill subdistrict, Socorro County, New Mexico. Abstract, 3rd Annual New Mexico Mineral Symposium.
- Morimoto, N. (1962). Djurleite, a new copper sulphide mineral. *Mineralogical Journal*, 3, 5 & 6, 338-344.
- Morimoto, N., Koto, K., & Shimazaki, Y. (1969). Anilite, Cu_7S_4 , a new mineral. *The American Mineralogist*, 54, 1256-1268.
- NMEMNRD (2019). Retrieved from <http://www.emnrd.state.nm.us/MMD/AML/AccidentsFatalities.html>
- NOAMI (2019). Retrieved from http://www.noami.org/definitions_e.php
- North, R.M. (1983). History and geology of the precious metal occurrences in Socorro County, New Mexico. New Mexico Geological Society, Guidebook 34, 261-268.
- North, R.M., & McLemore, V.T. (1986). Silver and gold occurrences in New Mexico: New Mexico Bureau of Mines and Mineral Resources, Resource Map 15, 32, scale 1:1,000,000.
- North, R.M., & McLemore, V.T. (1988). A classification of the precious metal deposits of New Mexico. In: Bulk mineable precious metal deposits of the western United States. Geological Society of Nevada, Symposium, April 6-8, 1987, 625-660.
- Osburn, G.R., & Chapin, C.E. (1983). Nomenclature for Cenozoic rocks of northeast Mogollon-Datil volcanic field, New Mexico. New Mexico Bureau of Mines & Mineral Resources, Stratigraphic Chart 1, 7.
- Osburn, G.R. (1984). Explanation: Socorro County Geologic Map. New Mexico Bureau of Mines and Mineral Resources, OFR-238, 1-15.
- Pinget, M.C., Fontboté, L., Dold, B., Ramirez, F., & Vergara, M. (2011). The supergene enrichment at Chuquicamata revisited. Proceedings, 11th SGA Biennial Meeting, Antofagasta, Chile, 823-825.
- Price, W.A. (2009). Prediction manual for drainage chemistry from sulphidic geologic materials. MEND Report 1.20.1, 579.


- Ramdohr, P. (1969). The ore minerals and their intergrowths (3rd ed.). Germany: Pergamon Press, 1174.
- Ramsdell, L.S. (1943). The crystallography of acanthite, Ag₂S. *American Mineralogist*, 28, 401-425.
- Reich, M., Chryssoulis, S.L., Deditius, A., Palacios, C., Zúñiga, A., Weldt, M., & Alvear, M. (2010). “Invisible” silver and gold in supergene digenite (Cu_{1.8}S). *Geochimica et Cosmochimica Acta*, 74, 6157-6153.
- Reichert, J. (2007). A metallogenic model for carbonate-hosted non-sulphide zinc deposits based on observations of Mehdi Abad and Irankuh, central and southwestern Iran. Unpublished dissertation, Martin-Luther-Universität Halle-Wittenberg, 2007.
- Rieder, M., Cavazzini, G., D’Yakonov, Y.S., Frank-Kamenetskii, V.A., Gottardi, G., Guggenheim, S.,... Wones, D.R. (1998). Nomenclature of the micas. *The Canadian Mineralogist*, 36, 905-912.
- Roseboom, E.H., Jr. (1962). Djurleite, Cu_{1.96}S, a new mineral. *The American Mineralogist*, 47, 1181-1184.
- Rule, A.C., & Radke, F. (1988). Baileychlorite, the Zn end member of the trioctahedral chlorite series. *American Mineralogist*, 73, 135-139.
- Sangameshwar, S.R., & Barnes, H.L. (1983). Supergene processes in zinc-lead-silver sulfide ores in carbonates. *Economic Geology*, 78, 1379-97.
- Saria, L., Shimaoka, T., & Miyawaki, K. (2006). Leaching of heavy metals in acid mine drainage. *Waste Management and Research*, 24, 2, 134-140.
- Savage, D. (2003). Barite as an indicator of cross-formational fluid flow. Conference paper, Eleventh International Symposium on Water-Rock Interaction, Saratoga Springs, 1, 4.
- Seward, T.M., Williams-Jones, A.E., & Migdisov, A.A. (2013). The chemistry of metal transport and deposition by ore-forming hydrothermal fluids. *Treatise on Geochemistry 2nd edition*, 13, 29-57.
- Simon, D. B. (1973). Geology of the Silver Hill area, Socorro County, New Mexico. Master’s thesis, New Mexico Institute of Mining and Technology, Department of Geoscience, OFR-41.
- Simmons, S.F., White, N.C., & John, D.A. (2005). Geological characteristics of epithermal precious and base metal deposits. *Economic Geology 100th Anniversary Volume*, 37.
- Sutley, S., Gustkiewicz, M.S., Mayer, W., & Leach, D. (1999). Mineralogy and chemistry of oxidized ores of the Upper Silesia Mississippi Valley-type zinc-lead deposits, Poland. U.S. Geological Survey Open File Report 99-394, 43.

- Taylor, L.A. (1969). The significance of twinning in Ag_2S . *American Mineralogist*, 54, 961-963.
- Timmons, S.S. (2013). An update on the hydrogeology of Magdalena, Socorro County, New Mexico. New Mexico Bureau of Geology and Mineral Resources, OFR-556, 7-8.
- Tonking, W.H. (1957). Geology of the Puertecito quadrangle, Socorro County, New Mexico. New Mexico Bureau of Mines and Mineral Resources Bulletin 41, 67.
- UNM RGIS (2019). Retrieved from <http://rgis.unm.edu/>
- U.S. Climate Data (2019, April 10), Climate—Magdalena, NM. Retrieved from <https://www.usclimatedata.com/climate/magdalena/new-mexico/United-states/usnm0185>
- Uytenbogaardt, W., & Burke, E.A.J. (1971). Tables for microscopic identification of ore minerals (2nd ed.). New York: Dover Publications.
- Vista, A.D. (1977). Prospect examination, Silver Hill District, Socorro County, New Mexico. ASARCO Incorporated file memorandum, 9.
- Weber, R.H. (1971). K/Ar ages of Tertiary igneous rocks in central and western New Mexico. *Isochron/West*, 71-1, 33-45.
- Williams, F.E. (1963). Summary report of minerals examination, Jack Frost mine (Dugger shaft). U.S. Bureau of Mines, form 6-803 (1952), Williams No. 25, 2.
- Winchester, D.E. (1920). Geology of Alamosa Creek Valley, Socorro County, New Mexico, with special reference to the occurrence of oil and gas. U.S. Geological Survey Bulletin 716-A, 1-15.
- Yaroshevsky, A.A. (2006). Abundances of chemical elements in the Earth's crust. *Geochemistry International*, 44, 1, 48-55.
- Zutah, W.T. (2017). Origin and mineral resource potential of the Rosedale district, Socorro County, New Mexico. Independent study, New Mexico Institute of Mining and Technology, Department of Mineral Engineering, 71.

APPENDIX A

Forms

A.1 Mine Inventory Form (front)



Mine Entry

NM Bureau of Geology and Mineral Resources

Mine ID _____ Mine Name _____
District id _____ District _____
 Active Location: _____ Too Dangerous to Approach _____
 Historic/legacy location: _____ Aggregate mine _____
Latest year of information _____

LOCATION
County _____ USGS Quadrangle _____
Location Assurance _____ Location Reference _____
Latitude _____ Longitude _____ Coordinate system _____
Township _____ Range _____ Section _____ Subsection _____
UTM Northing _____ UTM Easting _____ UTM zone _____
Elevation _____ Elev. Source _____
Location Notes _____

GENERAL MINE HISTORY
Commodity Category _____ Production Category _____
Year of Initial Production _____ Year of Last Production _____ Year of Discovery _____
Commodities Produced _____ Commodities Present Not Produced _____

FEATURE DESCRIPTION _____ Volume of waste rock _____
Development _____
Access _____ Visibility _____ Known Multiple Entrances _____
Depth _____ Length/height _____ Width: _____
Disturbed acres _____ Reclaimed acres _____ Mining Methods _____
Condition Mine Feature _____ General Slope _____
Aspect (trending direction)/
slope of feature _____
Surface Land Status _____ Minerals Land Status _____ Ownership _____


CULTURAL SIGNIFICANCE Note UTM for sites in field notes! They get entered into another database.
Cultural resources _____ Description of features _____
Archeology site no.: _____

GEOLOGY
Host Formation: _____
Geology: _____
Stability: _____ Rock type: _____
Mineralogy: _____
Nonore mineralogy: _____
Type of deposit: _____ Size of deposit: _____
Alteration: _____ Soils: _____

TERRAIN
Type of terrain: _____ Land use: _____

Mine _____ District _____ 6/26/2018

A.1 Mine Inventory Form (back)



Mine Entry

NM Bureau of Geology and Mineral Resources

Is water present?
 Is waste rock present?
 Subsidence?
 Maintenance Required?

Recent Human Use: _____

Sensitive environments: _____

Erosion: _____

HYDROLOGY

Hydrology: _____ Receiving Stream: _____

Water drainage: _____ Floodplain: _____ Aquatic Life: _____ Color of Water: _____

Evidence of potential acid drainage: _____

Ecosystem

Vegetation: _____ Vegetation density: _____ Vegetation type: _____

Animals: _____ Animal rating: _____ Are bats present? Are owls present?

ENVIRONMENTAL DATA AND POTENTIAL HAZARDS

Radiation readings: _____

Air quality/condition: _____ Mitigation Status: _____

Reclamation: _____ Trash In Mine?

Circle the number or value that is correct!

BLM Danger Level	0 remediated 1 None 2 Low 3 Medium 4 High 5 Extreme 6 Unknown 7 active mining	remediated no danger level sites located more than a quarter mile sites near historic mining towns, historic schools, recreation areas, parks, camps, or trails sites near homes or school, within a quarter mile of one or more AML sites extreme danger level unknown danger level, not visited active mining, reclamation planned or underway
---------------------------------	--	---

NOAMI	A B C D O R	highest class, deep unprotected openings to surface, Hazardous openings on surface, crown pillars, waste rock piles with ARD and radioactive deep unprotected openings to surface such as shafts, raises and open stops; Hazardous openings on surface, crown pillars, waste rock piles with hazardous openings to surface, waste rock piles and possible dilapidated structures associated with the mine openings, no tailings or tailings are minor surface features only such as trenches, test pits and stripping, no tailings no information remediated
--------------	----------------------------	---

Are lead or sulfide minerals present? Note here also.

Potential hazardous materials: _____

Comments: _____

Recommendations: _____

Remediated? **Data Reliability**
 Data reliability: _____
 Inspected by: _____
 Date inspected: _____

Verified by: _____
 Date last modified: _____

Mine: _____ District: _____ 6/26/2018

A.2 AML Sample Form

AML SAMPLING FORM		
PROJECT NAME:	AREA:	
SAMPLE ID:		
DATE:	WEATHER CONDITIONS:	
MINE ID:	TYPE OF MEDIA SAMPLED:	COLLECTED BY:
ELEVATION:	METHOD OF OBTAINING ELEVATION:	
LATITUDE:	LONGITUDE:	DATUM:
POINT OF SAMPLE LOCATION:		
METHOD OF SAMPLE COLLECTION:		
DECONTAMINATION:		
TYPE OF SAMPLE:		
SAMPLE DESCRIPTION:		
REASON FOR SAMPLING:		
SAMPLE LOCATION:		
LOCATION COMMENTS:		
SOP:	DEVIATION FROM SOP:	
Standard Operating Procedure No. 5: Sampling Outcrops, Rock Piles, and Drill Core (Solid)		
Standard Operating Procedure No. 15: Surface Water and Seep Sampling		
Standard Operating Procedure No. 16: Ground-Water Sampling		
Standard Operating Procedure No. 100: Sampling waste dumps (in preparation)		

A.3 Thesis Mineralogy Sample Form

Thesis Mineralogy Sample Form v3

Collector's Name: _____ **Date Collected:** _____
Sample ID: _____ **District:** _____
Elevation: _____ (ft) **Mine Name:** _____
UTM: _____ E _____ N **Mine ID:** _____
Latitude (DD): _____ **Longitude (DD):** _____
Coordinate System: _____ **Trend of Vein (if applicable):** _____
Feature dimensions: l: _____ ft × w: _____ ft × d: _____ ft **Size of Sample:** _____
Sample Type: Channel Chip Dump Select Dump Composite Outcrop Select Sieved
Analytical Methods: Geochemistry XRD EMP Polished Section Paste pH Soil Petrography

Lithology (check all that apply):

Type: Andesite Basalt Dacite Granitic Limestone Rhyolite Sandstone Schist Skarn

Characteristics: Altered Aphanitic Bleached Brecciated Caliche Fractured Mineralized Non-Mineralized Phaneritic Porphyritic Slickenlines Trachytic Veinlets Vuggy Weathered Xenoliths

Other: _____

Mineralogy:

Native Elements: Copper Gold Silver

Sulfides: Acanthite Arsenopyrite Bornite "Chalcocite" Chalcopyrite Covellite Digenite Emplectite Galena Pyrite Sphalerite Stromeeyerite Tennantite Tetrahedrite

Oxides & Hydroxides: Delafossite Goethite Hematite Magnetite Mn-oxides Tenorite

Halides: Fluorite Bromargyrite

Carbonates: Aragonite Azurite Calcite Cerussite Malachite Rosasite Siderite Smithsonite

Sulfates: Anglesite Barite Gypsum Jarosite

Phosphates, Arsenates, & Vanadates: Descloizite Duftite Fornacite Hydroxylapatite Tangeite Vanadinite

Silicates: Amphiboles Biotite Chlorite Chrysocolla Clays Dioptase Epidote K-Spar Plagioclase Pyroxenes Quartz Willemite

Other: _____

Alteration:

Type: Argillic Chloritic Dolomitization Phyllic Potassic Propylitic Silicification

Degree: Weak Moderate Intense

Other: _____

Description of Area (check all that apply):

Drainage Field Hillside Hilltop Near Road Outcrop Private Property State Land BLM USFS

Other: _____

Mine Feature Description (check all that apply):

Type: Adit Cut Decline Drill Holes Pit Shaft Structures Tailings Trench Waste Rock

Condition: Intact Backfilled Collapsed Exploratory Trash in Mine Fenced off Overgrown Wildlife

Production Likely: Yes No Unknown

Other Notes/Comments:

APPENDIX B

Mine Feature Information

B.1 Mine IDs, Database Mine Names, & Corresponding Field Mine Names/Aliases

Mine ID	Database Mine Name	Field Names/Aliases
NMSO0208	Jack Frost	NM36
NMSO0180	Arroyo Landavaso	Mag 20-S1
NMSO0342	Jack Frost Mine	
NMSO0355	Vanadium Friend	
NMSO0371	Jack Frost	
NMSO0378	Heister	
NMSO0608	Turquoise/Barrett	NM354B
NMSO0795	Arroyo Landavaso	Mag21-A1
NMSO0858	K7	
NMSO0881	Love Bug	
NMSO0916	Arroyo Landavaso	Mag17-P1
NMSO0918	Arroyo Landavaso	Mag 19-S1
NMSO0951	Unknown	SH-S9, SH-T5
NMSO0122	Sophia	NMA12, SH-S4 (SH-6), SH-P2
NMSO0229	Anirhoid	NM22, Mag38-S1
NMSO0230	Silver Hill	NMA18, SH-S10, SH-S1
NMSO0254	Silver Hill	NM30, Mag13-P1, P2, P3, S1, S2
NMSO0263	Gutierrez	NMC-P5
NMSO0373	Anirhoid	NM20, Mag29-p1
NMSO0377	Arroyo Landavaso	Mag4
NMSO0706	Turquoise H	NM52
NMSO0809	Silver Hill	NMA16, SH-S3 (SH-4)
NMSO0810	Sophia	NMA15
NMSO0818	Unknown	Mag31-P1
NMSO0819	Unknown	NM31
NMSO0823	Emerald	NM24, Mag40-S1, S2
NMSO0825	Unknown	NM26, Mag14-S1
NMSO0828	Unknown	NM28, Mag15-S1
NMSO0831	Unknown	Mag5
NMSO0838	Gutierrez	shaft1, NMC-P4,
NMSO0839	Unknown	mag2
NMSO0841	Unknown	NM51
NMSO0844	Carnero	
NMSO0848	Chloride	NMBC2
NMSO0850	NMB1	NMBC5/BM-5
NMSO0851	Unknown	
NMSO0852	NMB3	
NMSO0853	NMB4	
NMSO0854	NMAB1	
NMSO0855	NMAB2	
NMSO0862	Carnero	
NMSO0870	Cedar Hill	SCedarPit6
NMSO0871	Candelaria	SCedarPit7
NMSO0873	Gutierrez	SCedarShaft1, NMSO0275 is a duplicate (deleted)
NMSO0874	Unknown	MagCuShaft
NMSO0876	Lucky Dog	MagCushaft2
NMSO0877	Unknown	NCedarTrench

Mine ID	Database Mine Name	Field Names/Aliases
NMSO0878	Virginia Lee	WC-P1, P2
NMSO0879	Turquoise	NM37
NMSO0897	Sophia	NM354A
NMSO0898	Sophia	from MRDS
NMSO0902	Unknown	SH-P1
NMSO0904	Unknown	SH-P3
NMSO0905	Unknown	SH-P4
NMSO0910	Unknown	SH-P12
NMSO0911	Unknown	SH-P13
NMSO0912	Unknown	SH-P14, NM34, south pit
NMSO0915	Unknown	SH-S7
NMSO0921	Unknown	Mag 21-S1,S2
NMSO0922	Unknown	Mag 22-T1
NMSO0923	Unknown	Mag23-P1
NMSO0924	Unknown	Mag23-S1
NMSO0928	Candelaria	Mag27-P1
NMSO0242	Turquoise/Barrett	NM53
NMSO0243	Turquoise/ Barrett	
NMSO0262	Unknown	NM169-P5, T1
NMSO0698	Turquoise	
NMSO0714	Jack Frost	NM39
NMSO0715	Jack Frost B	NM38, on Lucky Dog claim
NMSO0796	Ace of Spades	NMA2, SH-T4
NMSO0797	Ace of Spades	NMA3, SH-C4
NMSO0798	Ace of Spades	NMA4
NMSO0799	Ace of Spades	NMA5, SH-P19
NMSO0800	Ace of Spades	NMA6, SH-P20
NMSO0801	Ace of Spades	NMA7, SH-P21
NMSO0802	Ace of Spades	NMA8, SH-S8
NMSO0803	Sophia	NMA9,SH-T3
NMSO0804	Sophia	NMA10
NMSO0805	Sophia	NMA11
NMSO0806	Sophia	NMA13, SH-P16
NMSO0807	Sophia	NMA14
NMSO0808	Sophia	NMA17, SH-C5
NMSO0811	Sophia	NMA1, SH-C1
NMSO0820	Anirhoid	NM21, Mag37-P1, P2
NMSO0821	Unknown	NM22, SH-P11
NMSO0822	Unknown	NM23, Mag41-C1
NMSO0824	Unknown	NM25
NMSO0826	Emerald	NM27
NMSO0827	Unknown	NM27
NMSO0829	Unknown	NM33, SH-P10
NMSO0830	Unknown	NM34, SH-P15, north pit
NMSO0832	Unknown	Mag6
NMSO0833	Unknown	pit1
NMSO0834	Unknown	pit2
NMSO0835	Unknown	pit3

Mine ID	Database Mine Name	Field Names/Aliases
NMSO0836	Unknown	pit4
NMSO0837	Unknown	pit5
NMSO0842	Carnero	NMBL1
NMSO0843	Unknown	NMBC1
NMSO0845	Carnero	NMBC2
NMSO0846	Carnero	NMBC2
NMSO0847	Carnero	NMBC3
NMSO0849	Random	
NMSO0857	K6	
NMSO0859	K	
NMSO0860	Unknown	
NMSO0861	Cedar Hill	
NMSO0863	Cedar Hill	
NMSO0864	Cedar Hill	SCedarpit1
NMSO0865	Cedar Hill	
NMSO0866	Cedar Hill	SCedarPit2
NMSO0867	Cedar Hill	SCedarPit3
NMSO0868	Cedar Hill	SCedarPit4
NMSO0869	Cedar Hill	SCedarPit5
NMSO0872	Unknown	SCedarPit8
NMSO0875	Unknown	MagCu
NMSO0896	Sophia	
NMSO0899	Unknown	SH-C3
NMSO0900	Unknown	SH-T2
NMSO0901	Unknown	SH-S2 (sample SH-1B), 50 ft n SH-1A
NMSO0903	Unknown	SH-T1
NMSO0906	Unknown	SH-P6
NMSO0907	Unknown	SH-P7
NMSO0908	Unknown	SH-P8
NMSO0909	Unknown	SH-P9
NMSO0913	Unknown	SH-S5
NMSO0914	Candelaria	SH-S6
NMSO0917	Arroyo Landavaso	Mag18-P1, P2, P3, P4
NMSO0919	Unknown	Mag20-S2
NMSO0920	Unknown	Mag21-C2
NMSO0925	Candelaria	Mag24-S1
NMSO0926	Candelaria	Mag25-S1
NMSO0927	Candelaria	Mag26-S1
NMSO0929	Candelaria	Mag27-P2
NMSO0930	Candelaria	Mag27-T1
NMSO0931	Arroyo Landavaso	Mag29-D1
NMSO0932	Anirhoid	Mag30-P1,P2
NMSO0933	Unknown	Mag30-P3
NMSO0938	Unknown	Unk32, shaft 2, NM169- P6
NMSO0939	Unknown	
NMSO0940	Unknown	
NMSO0941	Unknown	SH-P4
NMSO0942	Unknown	Mag32-P1 was a duplicate, renamed Mag12-P1
NMSO0943	Anirhoid	Mag33-P1
NMSO0944	Emerald	Mag34-P1
NMSO0945	Unknown	Mag35-P1
NMSO0946	Unknown	Mag36-P1
NMSO0947	Unknown	Mag39-P1
NMSO0948	Ace of Spades	Mag42-P1
NMSO0949	Ace of Spades	SH-P17
NMSO0950	Unknown	SH-P18
NMSO0951	Unknown	SH-P22
NMSO0951	Unknown	SH-P22
NMSO0934	Unknown	Mag28-P1
NMSO0936	Pueblo Spring	Mag28-P2
NMSO0937	David	Mag32-P1

Mine ID	Database Mine Name	Field Names/Aliases
NMSO0949	Candelaria	SH-P23, SH-P24
NMSO0950	Unknown	SH-P25
NMSO0952	Unknown	NMC-P2, NMC-P3
NMSO0060	Unknown	
NMSO0179	Unknown	
NMSO0185	Charlie Spear	
NMSO0186	Charlie Spear	
NMSO0209	Jack Frost	
NMSO0227	Unknown	
NMSO0228	Northeast Area	
NMSO0231	Silver Hill	
NMSO0240	Pajaro	
NMSO0241	Turquoise/ Barrett	
NMSO0261	Unknown	
NMSO0606	Unknown	
NMSO0607	Silver Hill area	
NMSO0699	Turquoise/Barrett Shaft (B)	
NMSO0700	Turquoise/Barrett Shaft (C)	
NMSO0701	Turquoise Claims	
NMSO0703	Turquoise/Barrett Shaft (F)	
NMSO0704	Turquoise/Barrett Shaft (G)	
NMSO0705	Turquoise/Barrett Adit	
NMSO0707	Jack Frost Area Shaft (A)	
NMSO0708	Jack Frost Area Shaft (B)	
NMSO0709	Jack Frost Area Shaft (C)	
NMSO0710	Jack Frost Area Shaft (D)	
NMSO0711	Jack Frost Area Shaft (E)	
NMSO0712	Jack Frost Area Shack	
NMSO0713	Jack Frost Area Mine Dump	
NMSO0716	Jack Frost Area Pit and Adit	
NMSO0040	Saint Vicente	AML 1
NMSO0041	Saint Vicente	AML 11
NMSO0042	Saint Vicente	AML 12
NMSO0043	Saint Vicente	AML 13
NMSO0044	Saint Vicente	AML 15
NMSO0045	Saint Vicente	AML 16
NMSO0046	Saint Vicente	AML 17
NMSO0047	Saint Vicente	AML 18
NMSO0048	Saint Vicente	AML 19
NMSO0049	Saint Vicente	AML 2
NMSO0050	Saint Vicente	AML 3
NMSO0051	Saint Vicente	AML 5
NMSO0052	Saint Vicente	AML 6
NMSO0053	Saint Vicente	AML 7
NMSO0054	Saint Vicente	AML 8
NMSO0055	Saint Vicente	AML 9
NMSO0056	Saint Vicente	AML 10
NMSO0605	Saint Vicente	AML 14
NMSO0702	Jack Frost	NM41
NMSO0840	Unknown	Mag16
NMSO0856	K5	

B.2 Mines Features and Associated Samples

Mines			Sample Names Organized by Analytical Methods					
Mine ID	New Field Name	Old Field Name	Geochemistry	ABA	EMP	Soil Petrography	XRD	Polished Sections
NMSO0811	SH-C1	SH-5	NMA1A, NMA1B	NMA1A	NMA-1B-1, NMA-1B-2	NMA1A		SH-C1i (after SH-5viii), NMA-1B-1
NMSO0909	SH-P14	N/A	SH-P14				SH-P14i, SH-P14ii	SH-P14i
NMSO0230	SH-S1	SH-1A					SH-1Ai, SH-1Aii, SH-1Aiv	
NMSO0898	SH-S2	SH-1B				SH-S2		
NMSO0809	SH-S3	SH-4	SH-S3				SH-4	
NMSO0122	SH-S4	SH-6						SH-S4ii (after SH-6ii)
NMSO0910	SH-S5	N/A						SH-S5i
NMSO0900	SH-T1	SH-3					SH-3ii	
NMSO0897	SH-T2	NMA15	SH-T2, NMA15					
NMSO0866	SC-D1	SC-28, SC-5, Nmab2	SC-28, SC-5A, SC-5B	SC-5		SC-5	SC-28_9, SCg_6, SCh_7, SCi_8	
NMSO0865	SC-P4	SCP-4	SCP-4v, SCP-4ds				SCP-4v_10	
NMSO0939	Mag12-P1	Mag12-S1, Mag32-P1						
NMSO0180	Mag20-S1	N/A	Mag20-S1					Mag20-S1(vs)
NMSO0919	Mag22-T1	N/A						Mag22-T1ii
NMSO0928	Mag29-D1	N/A	Mag29-D1					
NMSO0229	Mag38-S1	N/A	Mag38-S1					
NMSO0823	Mag40-S1	NM24	NM24				Mag40-S1i	
NMSO0833	Mag43-P1	UNK-P1						
NMSO0834	NM169-P1	UNK-P2						
NMSO0872	NMC-P1	NMagCu	Mcu-ds				Mcu-d_5	
NMSO0608	NM354-P1	NM354B	NM-354B, NM-354B_2	NM354B		NM354B	NM354Bi, NM354Bii, NM354Biii	
NMSO0877	VL-P1	NMZ1						VL-P1i
NMSO0878	VL-S1	NMZ2	NM36?	VL-1	VL-WS	VL-1	VLW-a_1, VLW-b_3, VLW-c_4	VL-S1i
NMSO0876	VL-S2	NMZ3	VL-1, VL-1_B					

*Old field names are included to give context for sample names.

B.3 Mine IDs, Database & Field Names, and Location Information from AML and Thesis Inventory*

Mine ID	Database Mine Name	Field Mine Name**	Latitude	Longitude	UTM Easting	UTM Northing	Township	Range	Section	Elevation
NMSO0811	Sophia	SH-C1	34.12785	-107.30156	287749	3778530	2S	4W	19	6992
NMSO0807	Sophia	SH-C2	34.12608	-107.30082	287813	3778331	2S	4W	19	7075
NMSO0896	Sophia	SH-C3	34.12606	-107.30090	287805	3778329	2S	4W	19	7044
NMSO0797	Ace of Spades	SH-C4	34.12912	-107.30206	287706	3778671	2S	4W	18	6906
NMSO0808	Sophia	SH-C5	34.12460	-107.30161	287737	3778169	2S	4W	19	6945
NMSO0894	Sophia	SH-P1	34.12384	-107.30280	287624	3778088	2S	4W	19	6911
NMSO0122	Sophia	SH-P2	34.12643	-107.30118	287781	3778371	2S	4W	19	7136
NMSO0901	Unknown	SH-P3	34.12009	-107.29581	288259	3777657	2S	4W	19	6656
NMSO0902	Unknown	SH-P4	34.11948	-107.29529	288306	3777588	2S	4W	19	6699
NMSO0938	Unknown	SH-P5	34.12022	-107.29600	288242	3777671	2S	4W	19	6731
NMSO0903	Unknown	SH-P6	34.12025	-107.29617	288227	3777675	2S	4W	19	6752
NMSO0904	Unknown	SH-P7	34.12032	-107.29613	288231	3777684	2S	4W	19	6752
NMSO0905	Unknown	SH-P8	34.12074	-107.29652	288196	3777731	2S	4W	19	6751
NMSO0906	Unknown	SH-P9	34.11987	-107.29689	288160	3777635	2S	4W	19	6796
NMSO0829	Unknown	SH-P10	34.12125	-107.29780	288079	3777789	2S	4W	19	6773
NMSO0821	Unknown	SH-P11	34.12134	-107.29762	288097	3777799	2S	4W	19	6775
NMSO0907	Unknown	SH-P12	34.12259	-107.29919	287954	3777941	2S	4W	19	6824
NMSO0908	Unknown	SH-P13	34.12239	-107.29888	287982	3777918	2S	4W	19	6816
NMSO0909	Unknown	SH-P14	34.11815	-107.29809	288044	3777446	2S	4W	19	6747
NMSO0830	Unknown	SH-P15	34.11816	-107.29817	288038	3777447	2S	4W	19	6742
NMSO0806	Sophia	SH-P16	34.12616	-107.3010	287796	3778341	2S	4W	19	7079
NMSO0946	Unknown	SH-P17	34.11827	-107.29417	288407	3777452	2S	4W	19	6759
NMSO0947	Unknown	SH-P18	34.11803	-107.29531	288301	3777427	2S	4W	19	6791
NMSO0799	Ace of Spades	SH-P19	34.12922	-107.30213	287700	3778683	2S	4W	18	6910
NMSO0800	Ace of Spades	SH-P20	34.12971	-107.30234	287681	3778738	2S	4W	18	6892
NMSO0801	Ace of Spades	SH-P21	34.12978	-107.30232	287684	3778745	2S	4W	18	6879
NMSO0948	Ace of Spades	SH-P22	34.12984	-107.30234	287682	3778752	2S	4W	18	6878
NMSO0949	Ace of Spades	SH-P23	34.12993	-107.30267	287652	3778763	2S	4W	18	6861
NMSO0949	Ace of Spades	SH-P24	34.12970	-107.30215	287700	3778736	2S	4W	18	6879
NMSO0950	Unknown	SH-P25	34.12318	-107.30272	287630	3778015	2S	4W	19	6883
NMSO0230	Silver Hill	SH-S1	34.12415	-107.30146	287749	3778118	2S	4W	19	6931
NMSO0898	Sophia	SH-S2	34.12440	-107.30161	287735	3778147	2S	4W	19	6917
NMSO0809	Silver Hill	SH-S3	34.12625	-107.30408	287512	3778357	2S	5W	24	6970
NMSO0122	Sophia	SH-S4	34.12653	-107.30127	287772	3778383	2S	4W	19	7118
NMSO0910	Unknown	SH-S5	34.12027	-107.29603	288240	3777678	2S	4W	19	6745
NMSO0911	Unknown	SH-S6	34.11962	-107.29668	288179	3777607	2S	4W	19	6794
NMSO0912	Unknown	SH-S7	34.11767	-107.29755	288094	3777392	2S	4W	19	6737
NMSO0802	Ace of Spades	SH-S8	34.12955	-107.30221	287694	3778719	2S	4W	18	6888
NMSO0951	Unknown	SH-S9	34.12414	-107.29921	287956	3778114	2S	4W	19	6860
NMSO0230	Silver Hill	SH-S10	34.12371	-107.30241	287660	3778169	2S	4W	19	6898
NMSO0900	Unknown	SH-T1	34.12455	-107.30328	287582	3778167	2S	4W	19	6930
NMSO0900	Unknown	SH-T1i	34.12465	-107.30331	287579	3778178	2S	4W	19	6932
NMSO0900	Unknown	SH-T1ii	34.12446	-107.30325	287585	3778157	2S	4W	19	6917
NMSO0897	Sophia	SH-T2	34.12574	-107.30046	287845	3778293	2S	4W	19	6998
NMSO0897	Sophia	SH-T2i	34.12590	-107.30063	287830	3778311	2S	4W	19	7036
NMSO0897	Sophia	SH-T2ii	34.12542	-107.30029	287860	3778258	2S	4W	19	6998
NMSO0803	Sophia	SH-T3	34.12808	-107.30016	287878	3778552	2S	4W	19	6950
NMSO0803	Sophia	SH-T3i	34.12810	-107.30019	287876	3778554	2S	4W	19	6951
NMSO0803	Sophia	SH-T3ii	34.12807	-107.30013	287881	3778551	2S	4W	19	6949
NMSO0796	Ace of Spades	SH-T4	34.12904	-107.30182	287728	3778662	2S	4W	18	6876
NMSO0796	Ace of Spades	SH-T4i	34.12909	-107.30183	287727	3778668	2S	4W	18	6880
NMSO0796	Ace of Spades	SH-T4ii	34.12903	-107.30181	287728	3778661	2S	4W	18	6872
NMSO0951	Unknown	SH-T5	34.12426	-107.29929	287949	3778127	2S	4W	19	6863
NMSO0951	Unknown	SH-T5i	34.12428	-107.29926	287953	3778129	2S	4W	19	6865
NMSO0951	Unknown	SH-T5ii	34.12426	-107.29933	287945	3778126	2S	4W	19	6866
NMSO0866	Cedar Hill	SC-D1	34.12818	-107.30843	287116	3778580	2S	5W	24	6861
NMSO0861	Cedar Hill	SC-P1	34.13147	-107.30518	287422	3778936	2S	5W	13	6910
NMSO0863	Cedar Hill	SC-P2	34.13107	-107.30584	287362	3778891	2S	5W	13	6894

Mine ID	Database Mine Name	Field Mine Name	Latitude	Longitude	UTM Easting	UTM Northing	Township	Range	Section	Elevation
NMSO0864	Cedar Hill	SC-P3	34.13150	-107.30493	287447	3778942	2S	5W	13	6920
NMSO0865	Cedar Hill	SC-P4	34.13279	-107.30457	287483	3779084	2S	5W	13	7025
NMSO0866	Cedar Hill	SC-P5	34.13502	-107.30429	287515	3778330	2S	5W	13	7016
NMSO0867	Cedar Hill	SC-P6	34.13683	-107.30402	287544	3779531	2S	5W	13	6942
NMSO0868	Cedar Hill	SC-P7	34.13724	-107.30428	287521	3779576	2S	5W	13	6912
NMSO0869	Cedar Hill	SC-P8	34.13754	-107.30386	287562	3779609	2S	5W	13	6843
NMSO0860	Unknown	SC-P9	34.13849	-107.30473	287483	3779716	2S	5W	13	6777
NMSO0870	Cedar Hill	SC-S1	34.13817	-107.30443	287510	3779680	2S	5W	13	6791
NMSO0263	Gutierrez	NMC-A1	34.13696	-107.29307	288554	3779522	2S	4W	18	6826
NMSO0872	Unknown	NMC-P1	34.13250	-107.29523	288344	3779033	2S	4W	18	6754
NMSO0952	Candelaria	NMC-P2	34.13170	-107.29275	288571	3778938	2S	4W	18	6864
NMSO0952	Candelaria	NMC-P3	34.13153	-107.29269	288576	3778919	2S	4W	18	6863
NMSO0838	Gutierrez	NMC-P4	34.13612	-107.29325	288536	3779429	2S	4W	18	6896
NMSO0263	Gutierrez	NMC-P5	34.13674	-107.29381	288486	3779500	2S	4W	18	6850
NMSO0871	Candelaria	NMC-S1	34.13229	-107.29285	288564	3779003	2S	4W	18	6879
NMSO0873	Gutierrez	NMC-S2	34.13352	-107.29307	288546	3779141	2S	4W	18	6909
NMSO0838	Gutierrez	NMC-S3	34.13644	-107.29311	288549	3779465	2S	4W	18	6900
NMSO0873	Gutierrez	NMC-T1i	34.13346	-107.29298	288553	3779135	2S	4W	18	6909
NMSO0873	Gutierrez	NMC-T1ii	34.13344	-107.29309	288544	3779132	2S	4W	18	6917
NMSO0873	Gutierrez	NMC-T2i	34.13368	-107.29311	288543	3779159	2S	4W	18	6910
NMSO0873	Gutierrez	NMC-T2ii	34.13366	-107.29319	288535	3779157	2S	4W	18	6910
NMSO0874	Unknown	NC-T1	34.14277	-107.29939	287986	3780179	2S	4W	18	6701
NMSO0874	Unknown	NC-T1i	34.14273	-107.29925	287999	3780175	2S	4W	18	6709
NMSO0874	Unknown	NC-T1ii	34.14275	-107.29950	287976	3780178	2S	4W	18	6707
NMSO0875	Unknown	WC-P1	34.14383	-107.30596	287383	3780311	2S	5W	12	6773
NMSO0875	Unknown	WC-P2	34.14358	-107.30635	287346	378284	2S	5W	12	6784
NMSO0875	Unknown	WC-P3	34.14362	-107.30770	287222	3780292	2S	5W	12	6746
NMSO0839	Unknown	Mag2-S1	34.12981	-107.28323	289445	3778709	2S	4W	17	6640
NMSO0377	Arroyo Landavaso	Mag4-S1	34.1290	-107.28461	289315	3778622	2S	4W	17	6652
NMSO0831	Unknown	Mag5-S1	34.1201079	-107.28571	289192	3777638	2S	4W	20	6679
NMSO0831	Unknown	Mag5-P1	34.12003	-107.28555	289207	3777629	2S	4W	20	6677
NMSO0831	Unknown	Mag5-P2	34.11988	-107.28542	289218	3777613	2S	4W	20	6670
NMSO0831	Unknown	Mag5-P3	34.11972	-107.28516	289241	3777594	2S	4W	20	6678
NMSO0831	Unknown	Mag5-P4	34.11966	-107.28504	289252	3777587	2S	4W	20	6679
NMSO0832	Unknown	Mag6-S1	34.11711	-107.28725	289042	3777308	2S	4W	19	6718
NMSO0832	Unknown	Mag6-S2	34.11693	-107.28745	289024	3777289	2S	4W	19	6707
NMSO0939	Unknown	Mag12-P1	34.12789	-107.29461	288390	3778520	2S	4W	19	6827
NMSO0254	Silver Hill	Mag13-P1	34.12159	-107.29182	288631	3777815	2S	4W	19	6758
NMSO0254	Silver Hill	Mag13-P2	34.12148	-107.29168	288644	3777803	2S	4W	19	6755
NMSO0254	Silver Hill	Mag13-P3	34.12146	-107.29172	288641	3777800	2S	4W	19	6755
NMSO0254	Silver Hill	Mag13-S1	34.12170	-107.29173	288639	3777828	2S	4W	19	6762
NMSO0254	Silver Hill	Mag13-S2	34.12152	-107.29183	288631	3777807	2S	4W	19	6766
NMSO0825	Unknown	Mag14-S1	34.12252	-107.29037	288767	3777915	2S	4W	19	6733
NMSO0828	Unknown	Mag15-S1	34.12155	-107.29031	288771	3777808	2S	4W	19	6730
NMSO0913	Unknown	Mag17-P1	34.12883	-107.29520	288338	3778625	2S	4W	18	6794
NMSO0914	Candelaria	Mag18-P1	34.13037	-107.29222	288616	3778790	2S	4W	18	6824
NMSO0914	Candelaria	Mag18-P2	34.13050	-107.29222	288617	3778811	2S	4W	18	6832
NMSO0914	Candelaria	Mag18-P3	34.13057	-107.29222	288617	3778804	2S	4W	18	6832
NMSO0914	Candelaria	Mag18-P4	34.13060	-107.29235	288605	3778816	2S	4W	18	6826
NMSO0915	Unknown	Mag19-S1	34.13314	-107.29063	288770	3779093	2S	4W	18	6831
NMSO0180	Arroyo Landavaso	Mag20-S1	34.13364	-107.28793	289021	3779144	2S	4W	18	6840
NMSO0916	Arroyo Landavaso	Mag20-S2	34.13358	-107.28794	289019	3779137	2S	4W	18	6832
NMSO0795	Arroyo Landavaso	Mag21-A1	34.13307	-107.28786	289026	3779080	2S	4W	18	6804
NMSO0917	Arroyo Landavaso	Mag21-C1	34.13276	-107.28780	289031	3779045	2S	4W	18	6778
NMSO0918	Arroyo Landavaso	Mag21-S1	34.13315	-107.28783	289028	3779089	2S	4W	18	6821
NMSO0918	Arroyo Landavaso	Mag21-S2	34.13309	-107.28783	289028	3779082	2S	4W	18	6809
NMSO0919	Unknown	Mag22-T1	34.13226	-107.28944	288877	3778994	2S	4W	18	6896
NMSO0919	Unknown	Mag22-T1i	34.13231	-107.28947	288875	3778999	2S	4W	18	6903
NMSO0919	Unknown	Mag22-T1ii	34.13222	-107.28944	288878	3778989	2S	4W	18	6893

Mine ID	Database Mine Name	Field Mine Name	Latitude	Longitude	UTM Easting	UTM Northing	Township	Range	Section	Elevation
NMSO0920	Unknown	Mag23-P1	34.13156	-107.28970	288852	3778926	2S	4W	18	6882
NMSO0921	Unknown	Mag23-S1	34.13158	-107.28986	288837	3778919	2S	4W	18	6878
NMSO0922	Unknown	Mag24-S1	34.13169	-107.29020	288807	3778932	2S	4W	18	6864
NMSO0923	Unknown	Mag25-S1	34.13179	-107.29062	288768	3778944	2S	4W	18	6874
NMSO0924	Unknown	Mag26-S1	34.13279	-107.29007	288821	3779054	2S	4W	18	6894
NMSO0925	Candelaria	Mag27-P1	34.13013	-107.29211	288626	3778763	2S	4W	18	6850
NMSO0926	Candelaria	Mag27-P2	34.13002	-107.29196	288640	3778751	2S	4W	18	6850
NMSO0927	Candelaria	Mag27-T1	34.12992	-107.29188	288647	3778739	2S	4W	18	6841
NMSO0927	Candelaria	Mag27-T1i	34.12996	-107.29191	288644	3778743	2S	4W	18	6847
NMSO0927	Candelaria	Mag27-T1ii	34.12984	-107.29183	288651	3778731	2S	4W	18	6838
NMSO0931	Arroyo Landavaso	Mag28-P1	34.12915	-107.29045	288777	3778650	2S	4W	18	6848
NMSO0932	Anirhoid	Mag28-P2	34.12911	-107.29018	288801	3778646	2S	4W	18	6843
NMSO0928	Candelaria	Mag29-D1	34.12889	-107.28985	288832	3778621	2S	4W	18	6849
NMSO0373	Anirhoid	Mag29-P1	34.12880	-107.28976	288839	3778610	2S	4W	18	6851
NMSO0929	Candelaria	Mag30-P1	34.12976	-107.29211	288625	3778722	2S	4W	18	6819
NMSO0929	Candelaria	Mag30-P2	34.12975	-107.29217	288620	3778720	2S	4W	18	6819
NMSO0930	Candelaria	Mag30-P3	34.12960	-107.29217	288619	3778705	2S	4W	18	6802
NMSO0818	Unknown	Mag31-P1	34.12794	-107.29327	288513	3778523	2S	4W	19	6810
NMSO0933	Unknown	Mag32-P1	34.13343	-107.28905	288917	3779123	2S	4W	18	6890
NMSO0940	Unknown	Mag33-P1	34.12854	-107.29421	288428	3778591	2S	4W	19	6865
NMSO0941	Unknown	Mag34-P1	34.12856	-107.29170	288659	3778588	2S	4W	19	6785
NMSO0942	Unknown	Mag35-P1	34.12737	-107.29137	288687	3778455	2S	4W	19	6780
NMSO0943	Anirhoid	Mag36-P1	34.12691	-107.29107	288715	3778404	2S	4W	19	6779
NMSO0820	Anirhoid	Mag37-P1	34.12826	-107.28960	288853	3778550	2S	4W	19	6830
NMSO0820	Anirhoid	Mag37-P2	34.12819	-107.28958	288855	3778542	2S	4W	19	6830
NMSO0229	Anirhoid	Mag38-S1	34.12705	-107.28947	288862	3778416	2S	4W	19	6796
NMSO0944	Emerald	Mag39-P1	34.12538	-107.28889	288911	3778230	2S	4W	19	6778
NMSO0823	Emerald	Mag40-S1	34.12452	-107.28905	288895	3778135	2S	4W	19	6758
NMSO0823	Emerald	Mag40-S2	34.12449	-107.28905	288894	3778131	2S	4W	19	6758
NMSO0822	Unknown	Mag41-C1	34.12346	-107.28717	289065	3778013	2S	4W	19	6705
NMSO0945	Unknown	Mag42-P1	34.12249	-107.29173	288642	3777915	2S	4W	19	6759
NMSO0833	Unknown	Mag43-P1	34.13008	-107.28641	289152	3778745	2S	4W	17	6718
NMSO0834	Unknown	NM169-P1	34.13118	-107.28413	289365	3778863	2S	4W	17	6697
NMSO0835	Unknown	NM169-P2	34.13129	-107.28419	289359	3778875	2S	4W	17	6693
NMSO0836	Unknown	NM169-P3	34.13167	-107.28435	289346	3778918	2S	4W	17	6887
NMSO0837	Unknown	NM169-P4	34.13179	-107.28458	289325	3778932	2S	4W	17	6695
NMSO0262	Unknown	NM169-P5	34.14003	-107.29042	288806	3779858	2S	4W	18	6643
NMSO0934	Unknown	NM169-P6	34.14181	-107.29354	288523	3780061	2S	4W	18	6672
NMSO0607	Silver Hill	NM169-P7	34.14310	-107.28773	289062	3780192	2S	4W	18	4633
NMSO0840	Unknown	NM169-S1	34.14170	-107.28745	289085	3780037	2S	4W	18	6593
NMSO0934	Unknown	NM169-S2	34.14217	-107.29333	288543	3780100	2S	4W	18	6677
NMSO0934	Unknown	NM169-T1	34.14132	-107.29324	288550	3780007	2S	4W	18	6668
NMSO0934	Unknown	NM169-T1i	34.14130	-107.29281	288590	3780003	2S	4W	18	6639
NMSO0934	Unknown	NM169-T1ii	34.14132	-107.29355	288521	3780007	2S	4W	18	6710
NMSO0879	Turquoise	NM354-A1	34.13531	-107.24086	293366	3779232	2S	4W	15	6547
NMSO0242	Turquoise/Barrett	NM354-A2	34.12960	-107.24162	293282	3778600	2S	4W	15	6642
NMSO0698	Turquoise	NM354-A3	34.13076	-107.24118	293325	3778728	2S	4W	15	6619
NMSO0608	Turquoise/Barrett	NM354-P1	34.12987	-107.24252	293199	3778632	2S	4W	15	6707
NMSO0841	Unknown	NM354-P2	34.13030	-107.24197	293252	3778679	2S	4W	15	6626
NMSO0843	Unknown	NM354-P3	34.13128	-107.24020	293417	3778784	2S	4W	15	6595
NMSO0706	Turquoise H	NM354-S1	34.13037	-107.24191	293257	3778687	2S	4W	15	6612
NMSO0877	Unknown	VL-P1	34.13967	-107.25580	291999	3779746	2S	4W	16	6469
NMSO0878	Virginia Lee	VL-S1	34.13942	-107.25218	292332	3779711	2S	4W	16	6486
NMSO0876	Lucky Dog	VL-S2	34.13943	-107.25160	292385	3779711	2S	4W	15	6475
NMSO0208	Jack Frost	NM36	34.138219	-107.252006	292345	3779578	2S	4W	16	---
NMSO0858	K7	GM-1	34.14407	-107.22424	294919	3780171	2S	4W	11	6562
NMSO0243	Turquoise/Barrett	GM-3	34.14594	-107.23442	293985	3780398	2S	4W	11	6401
NMSO0241	Turquoise/Barrett	GM-4	34.14527	-107.23425	294000	3780324	2S	4W	11	6362
NMSO0856	K5	GM-5	34.13946	-107.23806	293634	3779687	2S	4W	15	4611
NMSO0857	K6	GM-6	34.13787	-107.23872	293569	3779512	2S	4W	15	6494
NMSO0859	K	GM-7	34.13829	-107.23557	293861	3779552	2S	4W	15	6517

Mine ID	Database Mine Name	Field Mine Name	Latitude	Longitude	UTM Easting	UTM Northing	Township	Range	Section	Elevation
NMSO0850	NMB1	NM354-1	34.15578	-107.23478	293976	3781490	2S	4W	10	6226
NMSO0851	Unknown	NM354-2	34.15426	-107.23498	293954	3781322	2S	4W	10	6344
NMSO0852	NMB3	NM354-3	34.15402	-107.23495	293956	3781296	2S	4W	10	6344
NMSO0853	NMB4	NM354-4	34.16941	-107.23420	294063	3783000	2S	4W	2	6478
NMSO0842	Carnero	BM-1	34.17149	-107.23911	293615	3783242	2S	4W	3	6717
NMSO0844	Carnero	BM-2	34.17176	-107.23908	293619	3783272	2S	4W	3	6740
NMSO0845	Carnero	BM-3	34.17186	-107.23883	293642	3783281	2S	4W	3	6739
NMSO0846	Carnero	BM-4	34.17229	-107.23883	293643	3783329	1S	4W	34	6769
NMSO0847	Carnero	BM-5	34.17252	-107.23880	293646	3783355	1S	4W	34	6785
NMSO0847	Carnero	BM-6	34.17259	-107.23882	293645	3783363	1S	4W	34	6778
NMSO0848	Chloride	BM-7	34.17536	-107.23850	293680	3783670	1S	4W	34	6780
NMSO0849	Random	BM-8	34.17333	-107.23717	293799	3783442	1S	4W	34	6585

Coordinates are North American Datum 1927 with a Clarke 1866 Spheroid and may contain ± 12 ft of error.

See Tables 2 & 3 in Section 3.1.1 of thesis for list of abbreviations used to assign field mine names.

*Does not include 65 features inventoried or reclaimed during previous studies that are present in the database.

**Endpoints of trenches are indicated by lowercase Roman numerals after -T# in the field name e.g. SH-T2i, SH-T2ii. Field names for trenches without Roman numerals denote trench midpoints e.g. SH-T2.

B.4 Mine Feature Mineralogy

Mine ID	Database Mine Name	Field Mine Name	Gangue Mineralogy	Ore Mineralogy	Alteration	Lithology	Comments
NMSO0811	Sophia	SH-C1	Ba., CO ₃ -s, gt., hem., qtz.	Bb., bn., cc., cer., cpy., cv., dig., gal., spl.	Silicification	Andesite	
NMSO0807	Sophia	SH-C2	Cal., qtz.	Cu-Ox	Silicification*	Andesite	*Alteration difficult to classify
NMSO0896	Sophia	SH-C3	Cal., qtz.	<Cu-Ox	Silicification*	Andesite	*Alteration difficult to classify
NMSO0797	Ace of Spades	SH-C4	Ba., qtz.*	<<Cu-Ox	Silicification	Andesite	Platy barite coats many fractures; *drusy quartz
NMSO0808	Sophia	SH-C5	Qtz.	None	Silicification	Andesite	Non-mineralized
NMSO0894	Sophia	SH-P1	Ba., Mn-Ox, qtz.	Cu-Ox	Silicification*	Andesite	*Alteration difficult to classify
NMSO0122	Sophia	SH-P2	Cal., qtz.	<Cu-Ox	Silicification*	Andesite	*Alteration difficult to classify
NMSO0901	Unknown	SH-P3	Ba., cal., Mn-Ox, qtz.	Cu-Ox	Silicification	Andesite	Prospect on vein
NMSO0902	Unknown	SH-P4	Cal., qtz.	Cu-Ox	Silicification	Andesite	Prospect on vein
NMSO0938	Unknown	SH-P5	Ba., cal., Fe-Ox, qtz.	Cu-Ox	Silicification, argillic	Andesite	Not in database!
NMSO0903	Unknown	SH-P6	Clays	None	Argillic	Andesite	Very minor pit
NMSO0904	Unknown	SH-P7	Cal., qtz.	Cu-Ox	Argillic	Andesite	North of and adjacent to shaft along vein.
NMSO0905	Unknown	SH-P8	Ba., cal., qtz.	Cu-Ox	Argillic	Andesite/rhyolite	
NMSO0906	Unknown	SH-P9	Cal., Fe-Ox, Mn-Ox, qtz.	Cu-Ox	Silicification	Andesite	Situated on N-S dike
NMSO0829	Unknown	SH-P10	Cal., Fe-Ox, qtz.	Cu-Ox	Argillic	Andesite	
NMSO0821	Unknown	SH-P11	Ba., cal., qtz.	Cu-Ox	Argillic	Andesite	
NMSO0907	Unknown	SH-P12	Cal., qtz.	<Cu-Ox	Argillic	Andesite	Very minor pit
NMSO0908	Unknown	SH-P13	Cal., qtz.	<<Cu-Ox	Argillic*	Andesite	*Alteration difficult to classify
NMSO0909	Unknown	SH-P14	Ba., cal., qtz.	"Cc.", cv., dig., dio., for., gal., spl., tan., tmn., van., wil.	Silicification*	Andesite	
NMSO0830	Unknown	SH-P15	Ba., cal., qtz.	None	Silicification	Andesite	
NMSO0806	Sophia	SH-P16	Cal., qtz.	Cu-Ox	Silicification*	Andesite	*Alteration difficult to classify
NMSO0946	Unknown	SH-P17	Ba., CO ₃ -s, qtz.	Cu-Ox	Silicification	Andesite/Tuff	Near many other features
NMSO0947	Unknown	SH-P18	CO ₃ -s, Fe-Ox, Qtz.	Ba.	Silicification	Andesite	Prospect pit south of barite vein at SH-S6?
NMSO0799	Ace of Spades	SH-P19	Ba., CO ₃ -s, qtz.	<Cu-Ox	Silicification	Andesite	1cm euhedral qtz crystals on fractures/veins
NMSO0800	Ace of Spades	SH-P20	Ba., cal., qtz.	Cu-Ox	Silicification	Andesite	Weakly mineralized
NMSO0801	Ace of Spades	SH-P21	Ba., cal., qtz.	Cu-Ox?	Silicification	Andesite	Weakly mineralized
NMSO0948	Ace of Spades	SH-P22	Cal., qtz.	Cu-Ox?	Silicification	Andesite	Weakly mineralized
NMSO0949	Ace of Spades	SH-P23	Cal., qtz.	Cu-Ox (Mal>Chr.)	Silicification	Andesite	Veinlets of Cu-Ox.
NMSO0949	Ace of Spades	SH-P24	Ba., cal., qtz.	Cu-Ox	Silicification	Andesite	One of many features in area north of SH-C1
NMSO0950	Unknown	SH-P25	Qtz.	None	Silicification	Andesite	Non-mineralized
NMSO0230	Silver Hill	SH-S1	Ba., cal., qtz.*	Cu-Ox, for., possibly sulfides**	Silicification	Andesite/Tuff	*Drusy; **Not observed
NMSO0898	Sophia	SH-S2	Ba., cal., spe., qtz.	Cu-Ox, for., possibly sulfides*	Silicification	Andesite/Tuff	*not observed; vein trends 355°, huge pile but backfilled with trash (very dangerous!)
NMSO0809	Silver Hill	SH-S3	Qtz.	None?	Silicification	Andesite/Tuff	Unclear what commodity is. Plag phenos replaced with hem. and yellow mineral, Bromargyrite?
NMSO0122	Sophia	SH-S4	Cal., qtz.	Bb., "cc.", Cu-Ox, cv., dig., jal., mal.	Silicification	Andesite	*Calcite is banded black, white, and brown.
NMSO0910	Unknown	SH-S5	Ba., cal., Mn-Ox, qtz.*	Cu°, Cu-Ox	Silicification, argillic	Andesite/Tuff	*Amethyst; vein trends ~340°
NMSO0911	Unknown	SH-S6	Cal., Fe-Ox, Mn-Ox, qtz.	Ba.?	Silicification	Andesite	6in wide barite vein trending 340° and dipping 85°. Barite is only obvious possible commodity.
NMSO0912	Unknown	SH-S7	Cal., qtz.	Cu-Ox	Argillic	Andesite	*Alteration difficult to classify
NMSO0802	Ace of Spades	SH-S8	Ba., CO ₃ -s, qtz.	Cu-Ox	Silicification	Andesite	Waste rock less mineralized than expected
NMSO0951	Unknown	SH-S9	Ba., Mn-Ox, qtz.*	Cu-Ox	Silicification	Andesite	*Drusy
NMSO0230	Silver Hill	SH-S10	Ba., CO ₃ -s, qtz.	"Cc.", chr., cv., mal.	Silicification	Andesite	Mal.>>Chr.
NMSO0900	Unknown	SH-T1	Ba., cal., hem., qtz.	Cu-Ox	Silicification	Rhyolite	Trends 350°

Mine ID	Database Mine Name	Field Mine Name	Gangue Mineralogy	Ore Mineralogy	Alteration	Lithology	Comments
NMSO0897	Sophia	SH-T2	Ba., cal., Fe-Ox, Mn-Ox, qtz.	Cu-Ox, for., possibly sulfides*	Silicification	Andesite	*Not observed; trends 330°
NMSO0803	Sophia	SH-T3	Ba., Fe-Ox, Mn-Ox (tod.), qtz.	Cu-Ox (Chr.>Mal.)	Silicification	Andesite	NW-SE vein (330°)
NMSO0796	Ace of Spades	SH-T4	Ba., cal., qtz.	Cu-Ox ± sulfides*	Silicification	Andesite	N-S trend to feature (353°); *not observed, but likely
NMSO0951	Unknown	SH-T5	Ba., qtz.*	Cu-Ox	Silicification	Andesite	*Drusy
NMSO0866	Cedar Hill	SC-D1	Ba., cal., qtz.	Cu-Ox*, Cu-sulfides**	Silicification	Andesite	*May have cuprite here according to Vista (1977), but not observed. **Sulfides likely present, but not observed.
NMSO0861	Cedar Hill	SC-P1	Cal., qtz.	Cu-Ox*	Silicification	Andesite	*Disseminated malachite
NMSO0863	Cedar Hill	SC-P2	Ara., qtz.	None	Silicification*	Andesite	*Alteration difficult to classify
NMSO0864	Cedar Hill	SC-P3	CO3-s	None	Argillic	Andesite	
NMSO0865	Cedar Hill	SC-P4	Qtz.*	Chr., mal.	Silicification	Basalt?	*Amygdules
NMSO0866	Cedar Hill	SC-P5	Cal., qtz.	None	Silicification	Andesite	Very minor pit
NMSO0867	Cedar Hill	SC-P6	CO3-s, qtz.	None	Silicification	Andesite	
NMSO0868	Cedar Hill	SC-P7	CO3-s, qtz.	<<Chr.	Silicification	Andesite	
NMSO0869	Cedar Hill	SC-P8	Cal., sid., qtz.*	Cu-Ox	Silicification	Andesite	Massive banded siderite and quartz, secondary breccias, and slickenlines
NMSO0860	Unknown	SC-P9	Cal., qtz.	None	Silicification	Andesite	Very minor pit
NMSO0870	Cedar Hill	SC-S1	Cal., qtz.	Chr., mal.	Silicification	Andesite	
NMSO0263	Gutierrez	NMC-A1	Ba., cal., qtz.	Chr., Cu-Sulfides*, mal.	Silicification	Andesite/Rhyolite	*Not observed, but scale of feature (100ft adit connecting to shaft) suggests production from N-S vein.
NMSO0872	Unknown	NMC-P1	Qtz.*	Chr., mal.	Silicification	Andesite/Basalt?	*Amygdules
NMSO0952	Candelaria	NMC-P2	Not Recorded	Not Recorded	Not Recorded	Not Recorded	Not Recorded; Inventoried by undergraduate worker.
NMSO0952	Candelaria	NMC-P3	Not Recorded	Not Recorded	Not Recorded	Not Recorded	Not Recorded; Inventoried by undergraduate worker.
NMSO0838	Gutierrez	NMC-P4	Not Recorded	Not Recorded	Not Recorded	Not Recorded	Not Recorded; Inventoried by undergraduate worker.
NMSO0263	Gutierrez	NMC-P5	Not Recorded	Not Recorded	Not Recorded	Not Recorded	Not Recorded; Inventoried by undergraduate worker.
NMSO0871	Candelaria	NMC-S1	CO3-s*, qtz**	Cu-Ox ± sulfides***	Silicification	Andesite	*White and brown banded; **drusy and vein; ***not observed, but likely.
NMSO0873	Gutierrez	NMC-S2	Cal., Fe-Ox, qtz.	Chr.	Silicification	Andesite	Brecciated
NMSO0838	Gutierrez	NMC-S3	Ba., cal., qtz.	Chr. Cu-Sulfides*, mal.	Silicification	Andesite/Rhyolite	*Not observed, but scale of feature (100ft adit connecting to shaft) suggests production
NMSO0873	Gutierrez	NMC-T1i	Cal., qtz.	<<Cu-Ox	Silicification	Andesite	Black calcite
NMSO0873	Gutierrez	NMC-T1ii	Cal., qtz.	<<Cu-Ox	Silicification	Andesite	Black calcite
NMSO0873	Gutierrez	NMC-T2i	Cal., qtz.	<<Cu-Ox	Silicification	Andesite	Black calcite
NMSO0873	Gutierrez	NMC-T2ii	Cal., qtz.	<<Cu-Ox	Silicification	Andesite	Black calcite
NMSO0874	Unknown	NC-T1	Clays, qtz.	<Cu-Ox	Argillic	Andesite/Tuff	Shear zone with fault gouge
NMSO0875	Unknown	WC-P1	Cal.	Mal.	Argillic	Andesite	Coarse grained calcite breccia with coatings of malachite
NMSO0875	Unknown	WC-P2	Cal.	Cu-Ox	Argillic	Andesite	
NMSO0875	Unknown	WC-P3	Cal.	None	Argillic	Andesite	Brecciated
NMSO0839	Unknown	Mag2-S1	CO3-s, qtz.	Cu-Ox	Silicification	Andesite	Brecciated
NMSO0377	Arroyo Landavaso	Mag4-S1	Cal., qtz.	Chr.	Silicification	Andesite	Deep shaft with headframe.
NMSO0831	Unknown	Mag5-S1	Ba., cal., qtz.	Chr.	Silicification	Andesite/Rhyolite	
NMSO0831	Unknown	Mag5-P1	Ba., cal., qtz.	Chr.	Silicification	Andesite/Rhyolite	
NMSO0831	Unknown	Mag5-P2	Ba., cal., qtz.	Chr.	Silicification	Andesite/Rhyolite	
NMSO0831	Unknown	Mag5-P3	Ba., cal., qtz.	Chr.	Silicification	Andesite/Rhyolite	
NMSO0831	Unknown	Mag5-P4	Ba., cal., qtz.	Chr.	Silicification	Andesite/Rhyolite	
NMSO0832	Unknown	Mag6-S1	Qtz.	Chr.	Silicification	Andesite/Rhyolite	Backfilled
NMSO0832	Unknown	Mag6-S2	Qtz.	Chr.	Silicification	Andesite/Rhyolite	Backfilled
NMSO0939	Unknown	Mag12-P1	Ba., cal., Fe-Ox, Mn-Ox, qtz.	Cu-Ox.	Silicification	Andesite	Outcrop
NMSO0254	Silver Hill	Mag13-P1	Ba., CO3-s, Fe-Ox, Mn-Ox, qtz.	Cu-Ox	Silicification	Andesite	Mineralogy varies at each feature
NMSO0254	Silver Hill	Mag13-P2	Ba., CO3-s, Fe-Ox, Mn-Ox, qtz.	Cu-Ox	Silicification	Andesite	Mineralogy varies at each feature
NMSO0254	Silver Hill	Mag13-P3	Ba., CO3-s, Fe-Ox, Mn-Ox, qtz.	Cu-Ox	Silicification	Andesite	Mineralogy varies at each feature
NMSO0254	Silver Hill	Mag13-S1	Ba., CO3-s, Fe-Ox, Mn-Ox, qtz.	Cu-Ox	Silicification	Andesite	Mineralogy varies at each feature

Mine ID	Database Mine Name	Field Mine Name	Gangue Mineralogy	Ore Mineralogy	Alteration	Lithology	Comments
NMSO0254	Silver Hill	Mag13-S2	Ba., CO3-s, Fe-Ox, Mn-Ox, qtz.	Cu-Ox	Silicification	Andesite	Mineralogy varies at each feature
NMSO0825	Unknown	Mag14-S1	Ba., CO3-s, qtz.	Cu-Ox., Cu-sulfides*	Silicification	Andesite	*Not observed, but likely. See Mag15-S1.
NMSO0828	Unknown	Mag15-S1	Ba., CO3-s, qtz.	"Cc.", cpy., cv.	Silicification	Andesite	40ft shaft. No polished section.
NMSO0913	Unknown	Mag17-P1	Cal., qtz.	Mal.*	Silicification	Andesite	*Disseminated
NMSO0914	Candelaria	Mag18-P1	Ba., cal., qtz.	Cu-Ox, for.	Silicification, argillic	Andesite, rhyolite	4 pits all with same mine ID.
NMSO0914	Candelaria	Mag18-P2	Ba., cal., qtz.	Cu-Ox, for.	Silicification, argillic	Andesite, rhyolite	4 pits all with same mine ID.
NMSO0914	Candelaria	Mag18-P3	Ba., cal., qtz.	Cu-Ox, for.	Silicification, argillic	Andesite, rhyolite	4 pits all with same mine ID.
NMSO0914	Candelaria	Mag18-P4	Ba., cal., qtz.	Cu-Ox, for.	Silicification, argillic	Andesite, rhyolite	4 pits all with same mine ID.
NMSO0915	Unknown	Mag19-S1	Cal., qtz.	Cu-Ox	Silicification	Andesite	
NMSO0180	Arroyo Landavaso	Mag20-S1	Ba., cal., qtz.	"Cc.", chr., cup., cv., mal., pm., ten.	Silicification	Andesite	Vein trends 335°, dips ~90°; waste rock had 851ppm Ag, but no silver minerals observed.
NMSO0916	Arroyo Landavaso	Mag20-S2	Ba., cal., Mn-Ox, qtz.	Cu-Ox	Silicification	Andesite	Exploratory shaft south of main shaft Mag20-S1
NMSO0795	Arroyo Landavaso	Mag21-A1	Ba., cal., Fe-Ox, Mn-Ox, qtz.	Cu-Ox	Silicification	Andesite	Adit that may have connected to drift in main shaft? Trends 2° (N-S)
NMSO0917	Arroyo Landavaso	Mag21-C1	Ba., cal., qtz.	Cu-Ox	Silicification	Andesite	Exploratory cut south along strike of main shafts and adit.
NMSO0918	Arroyo Landavaso	Mag21-S1	Ba., cal., Mn-Ox, qtz.	"Cc.", Cu-Ox, Cu-sulfides*	Silicification	Andesite	*not observed, but likely. Massive waste pile and collapsed headframe suggest production from very deep workings.
NMSO0918	Arroyo Landavaso	Mag21-S2	Ba., cal., Mn-Ox, qtz.	"Cc.", Cu-Ox, Cu-sulfides*	Silicification	Andesite	*not observed, but likely. Looks like collapsed shaft that connects to drift/adit? Same mine ID as Mag21-S1.
NMSO0919	Unknown	Mag22-T1	Ba., cal., Fe-Ox, Mn-Ox, qtz.	"Cc.", cv., for., pm.	Silicification	Andesite	Trends 352°
NMSO0920	Unknown	Mag23-P1	Cal., qtz.	Cu-Ox*	Silicification	Andesite	*disseminated
NMSO0921	Unknown	Mag23-S1	Qtz.	Cu-Ox	Silicification	Andesite	*drusy; located on dike
NMSO0922	Unknown	Mag24-S1	Ba., cal., qtz.	Cu-Ox	Silicification	Andesite	Along 110° strike of dike
NMSO0923	Unknown	Mag25-S1	Fe-Ox, Mn-Ox	Cu-Ox	Silicification	Andesite	Along 110° strike of dike
NMSO0924	Unknown	Mag26-S1	Cal., qtz.	Cu-Ox	Silicification	Andesite	Vein strikes 310°
NMSO0925	Candelaria	Mag27-P1	Cal., qtz.	Cu-Ox	Silicification, argillic	Andesite	Along NW-SE vein
NMSO0926	Candelaria	Mag27-P2	Cal., qtz.	Cu-Ox	Silicification	Andesite	
NMSO0927	Candelaria	Mag27-T1	Cal., qtz.	Cu-Ox, for.	Silicification	Andesite	Vein/trench trends 325°
NMSO0931	Arroyo Landavaso	Mag28-P1	Cal., qtz.	Cu-Ox, for.	Silicification	Andesite	Exploratory pit north of vein assoc. with Mag29-D1
NMSO0932	Anirhoid	Mag28-P2	Cal., qtz.	Cu-Ox, for.	Silicification	Andesite	Exploratory pit north of vein assoc. with Mag29-D1
NMSO0928	Candelaria	Mag29-D1	Ba., cal., qtz.	Cu-Ox, for.	Silicification	Andesite	Declines at ~50°; highest Au values at 0.638ppm, but none observed.
NMSO0373	Anirhoid	Mag29-P1	Ba., CO3-s, qtz.	Cu-Ox	Silicification	Andesite	Exploratory pit south of vein assoc. with Mag29-D1
NMSO0929	Candelaria	Mag30-P1	Cal., qtz.	Cu-Ox	Silicification	Andesite	Double pits share same mine ID.
NMSO0929	Candelaria	Mag30-P2	Cal., qtz.	Cu-Ox	Silicification	Andesite	Double pits share same mine ID.
NMSO0930	Candelaria	Mag30-P3	Ba., cal., qtz.	Cu-Ox	Silicification	Andesite	Same mine ID as Mag30-P1,P2.
NMSO0818	Unknown	Mag31-P1	Cal., qtz.	Cu-Ox*	Silicification	Andesite	*disseminated malachite
NMSO0933	Unknown	Mag32-P1	Cal., qtz.	Cu-Ox	Silicification	Andesite	On hill near major shafts; coordinates est. from GPS path REAL Mag32-P1.
NMSO0940	Unknown	Mag33-P1	Ba., cal., Fe-Ox, Mn-Ox, qtz.	Cu-Ox	Silicification	Andesite	On N-S line with other features
NMSO0941	Unknown	Mag34-P1	Ba., cal., qtz.	Cu-Ox	Silicification	Andesite	Downhill from major feature. Exploratory?
NMSO0942	Unknown	Mag35-P1	Ba., CO3-s, Fe-Ox, qtz.	Cu-Ox	Silicification	Andesite	On N-S line with other features
NMSO0943	Anirhoid	Mag36-P1	Ba., CO3-s, Fe-Ox, qtz.	Cu-Ox	Silicification	Andesite	On N-S line with other features
NMSO0820	Anirhoid	Mag37-P1	Ba., Fe-Ox, Qtz.	Cu-Ox	Silicification	Andesite	On N-S line with other features
NMSO0820	Anirhoid	Mag37-P2	Ba., Fe-Ox, Qtz.	Cu-Ox	Silicification	Andesite	On N-S line with other features
NMSO0229	Anirhoid	Mag38-S1	Ba., Fe-Ox, Qtz.	Cu-Ox	Silicification	Andesite	Vein of Cu-Ox
NMSO0944	Emerald	Mag39-P1	CO3-s, qtz.	None	Silicification	Andesite	Non-mineralized
NMSO0823	Emerald	Mag40-S1	Ba., CO3-s, qtz.	Cu-Ox	Silicification	Andesite	Two shafts in N-S orientation exploring vein
NMSO0823	Emerald	Mag40-S2	Ba., CO3-s, qtz.	Cu-Ox	Silicification	Andesite	Two shafts in N-S orientation exploring vein
NMSO0822	Unknown	Mag41-C1	CO3-s, Fe-Ox, qtz.	Cu-Ox	Silicification	Andesite	Exploring small N-S vein

Mine ID	Database Mine Name	Field Mine Name	Gangue Mineralogy	Ore Mineralogy	Alteration	Lithology	Comments
NMSO0945	Unknown	Mag42-P1	Ba., CO ₃ -s, qtz.	None	Silicification	Andesite	Non-mineralized
NMSO0833	Unknown	Mag43-P1	Cal., Fe-Ox, Mn-Ox, qtz.	None	Silicification	Andesite	Non-mineralized
NMSO0834	Unknown	NM169-P1	Cal., Fe-Ox, Mn-Ox, qtz.	<<Cu-Ox	Silicification	Andesite	Very minor pit
NMSO0835	Unknown	NM169-P2	Ba., qtz.	Chr.	Silicification	Andesite	
NMSO0836	Unknown	NM169-P3	Fe-Ox, qtz.	None	Silicification	Andesite	Non-mineralized
NMSO0837	Unknown	NM169-P4	Ba., cal., qtz.	Chr.	Silicification	Andesite	Seams of chrysocolla
NMSO0262	Unknown	NM169-P5	Not Recorded	Not Recorded	Not Recorded	Not Recorded	Not Recorded; Inventoried by undergraduate worker.
NMSO0934	Unknown	NM169-P6	Not Recorded	Not Recorded	Not Recorded	Not Recorded	Not Recorded; Inventoried by undergraduate worker.
NMSO0607	Silver Hill	NM169-P7	Not Recorded	Not Recorded	Not Recorded	Not Recorded	Not Recorded; Inventoried by undergraduate worker.
NMSO0840	Unknown	NM169-S1	Ba., cal., Fe-Ox, qtz.	Chr.	Silicification	Andesite	Backfilled
NMSO0934	Unknown	NM169-S2	Cal., qtz.	Cu-Ox	Silicification	Andesite	*Black calcite
NMSO0934	Unknown	NM169-T1	Clays, qtz.	<<Cu-Ox	Argillic	Rhyolite*	*From memory, not sure.
NMSO0879	Turquoise	NM354-A1	Ba., clays, Fe-Ox, qtz.	None	Argillic	Tuff	Non-mineralized; adit driven 285°
NMSO0242	Turquoise/Barrett	NM354-A2	Not Recorded	Not Recorded	Argillic?	Rhyolite?	Needs to be revisited.
NMSO0698	Turquoise	NM354-A3	Not Recorded	Not Recorded	Argillic?	Rhyolite?	Needs to be revisited.
NMSO0608	Turquoise/Barrett	NM354-P1	Ba., chl., clays, CO ₃ -s, qtz., ver.	None	Argillic	Tuff/Rhyolite	Arlilic alteration and shear zone; *chlorite var. unknown
NMSO0841	Unknown	NM354-P2	Not Recorded	Not Recorded	Argillic?	Rhyolite?	Needs to be revisited.
NMSO0843	Unknown	NM354-P3	Not Recorded	Not Recorded	Argillic?	Rhyolite?	Needs to be revisited.
NMSO0706	Turquoise H	NM354-S1	Ba., cal., qtz.	Gal., ros.	Silicification	Andesite	Needs to be revisited.
NMSO0877	Unknown	VL-P1	Ba., cal., qtz.	"Cc.", cpy., cv., des., gal., van.	Silicification	Andesite	Pit on small hill. Less oxidized than VL-S1, S2
NMSO0878	Virginia Lee	VL-S1	Ba., cal., qtz.	Des., gal., mal., van.	Silicification	Andesite	Dugger Shaft
NMSO0876	Lucky Dog	VL-S2	Ba., cal., qtz.	Des., gal., mal., van.	Silicification	Andesite	Other shaft
NMSO0208	Jack Frost	NM36	Not Recorded	Not Recorded	Not Recorded	Not Recorded	Not Recorded; Inventoried by undergraduate worker.
NMSO0858	K7	GM-1	Not Recorded	Not Recorded	Not Recorded	Not Recorded	Not Recorded; Inventoried by undergraduate worker.
NMSO0243	Turquoise/Barrett	GM-3	Not Recorded	Not Recorded	Not Recorded	Not Recorded	Not Recorded; Inventoried by undergraduate worker.
NMSO0241	Turquoise/Barrett	GM-4	Not Recorded	Not Recorded	Not Recorded	Not Recorded	Not Recorded; Inventoried by undergraduate worker.
NMSO0856	K5	GM-5	Not Recorded	Not Recorded	Not Recorded	Not Recorded	Not Recorded; Inventoried by undergraduate worker.
NMSO0857	K6	GM-6	Not Recorded	Not Recorded	Not Recorded	Not Recorded	Not Recorded; Inventoried by undergraduate worker.
NMSO0859	K	GM-7	Not Recorded	Not Recorded	Not Recorded	Not Recorded	Not Recorded; Inventoried by undergraduate worker.
NMSO0850	NMB1	NM354-1	Not Recorded	Not Recorded	Not Recorded	Not Recorded	Not Recorded; Inventoried by undergraduate worker.
NMSO0851	Unknown	NM354-2	Not Recorded	Not Recorded	Not Recorded	Not Recorded	Not Recorded; Inventoried by undergraduate worker.
NMSO0852	NMB3	NM354-3	Not Recorded	Not Recorded	Not Recorded	Not Recorded	Not Recorded; Inventoried by undergraduate worker.
NMSO0853	NMB4	NM354-4	Not Recorded	Not Recorded	Not Recorded	Not Recorded	Not Recorded; Inventoried by undergraduate worker.
NMSO0842	Carnero	BM-1	Not Recorded	Not Recorded	Not Recorded	Not Recorded	Not Recorded; Inventoried by undergraduate worker.
NMSO0844	Carnero	BM-2	Not Recorded	Not Recorded	Not Recorded	Not Recorded	Not Recorded; Inventoried by undergraduate worker.
NMSO0845	Carnero	BM-3	Not Recorded	Not Recorded	Not Recorded	Not Recorded	Not Recorded; Inventoried by undergraduate worker.
NMSO0846	Carnero	BM-4	Not Recorded	Not Recorded	Not Recorded	Not Recorded	Not Recorded; Inventoried by undergraduate worker.
NMSO0847	Carnero	BM-5	Not Recorded	Not Recorded	Not Recorded	Not Recorded	Not Recorded; Inventoried by undergraduate worker.
NMSO0847	Carnero	BM-6	Not Recorded	Not Recorded	Not Recorded	Not Recorded	Not Recorded; Inventoried by undergraduate worker.
NMSO0848	Chloride	BM-7	Not Recorded	Not Recorded	Not Recorded	Not Recorded	Not Recorded; Inventoried by undergraduate worker.
NMSO0849	Random	BM-8	Not Recorded	Not Recorded	Not Recorded	Not Recorded	Not Recorded; Inventoried by undergraduate worker.

Mineral abbreviations can be found in beginning of main thesis text under list of minerals, abbreviations, and chemical formulae.

B.5 Mine Feature Hazard Rankings*

Mine ID	Database Mine Name	BLM Hazard	NOAMI Hazard
NMSO0180	Arroyo Landavaso	5	B
NMSO0342	Jack Frost Mine	4	B
NMSO0355	Vanadium Friend	4	B
NMSO0371	Jack Frost	4	B
NMSO0378	Heister	6	B
NMSO0608	Turquoise Claims (Barrett)	2	B
NMSO0795	Arroyo Landavaso	6	B
NMSO0858	K7	6	B
NMSO0881	Love Bug	6	B
NMSO0916	Arroyo Landavaso	1	B
NMSO0918	Arroyo Landavaso	5	B
NMSO0951	Unknown	5	B
NMSO0122	Sophia	1	C
NMSO0229	Anirhoid	5	C
NMSO0230	Silver Hill	2	C
NMSO0254	Silver Hill	5	C
NMSO0263	Gutierrez	5	C
NMSO0373	Anirhoid	1	C
NMSO0377	Arroyo Landavaso area	5	C
NMSO0706	Turquoise H	2	C
NMSO0809	Silver Hill	2	C
NMSO0810	Sophia	1	C
NMSO0818	Unknown	1	C
NMSO0819	Unknown	1	C
NMSO0823	Emerald	5	C
NMSO0825	Unknown	5	C
NMSO0828	Unknown	5	C
NMSO0831	Unknown	5	C
NMSO0838	Gutierrez	5	C
NMSO0839	Unknown	5	C
NMSO0841	Unknown	2	C
NMSO0844	Carnero	2	C
NMSO0848	Chloride	2	C
NMSO0850	NMB1	2	C
NMSO0851	Unknown	2	C
NMSO0852	NMB3	2	C
NMSO0853	NMB4	2	C
NMSO0854	NMAB1	2	C
NMSO0855	NMAB2	2	C
NMSO0862	Carnero	2	C
NMSO0870	Cedar Hill	2	C
NMSO0871	Candelaria	2	C
NMSO0873	Gutierrez	2	C
NMSO0874	Unknown	2	C
NMSO0876	Lucky Dog	2	C
NMSO0877	Unknown	2	C
NMSO0878	Virginia Lee	2	C
NMSO0879	Turquoise	3	C
NMSO0897	Sophia	2	C
NMSO0898	Sophia	2	C
NMSO0902	Unknown	5	C
NMSO0904	Unknown	1	C
NMSO0905	Unknown	1	C
NMSO0910	Unknown	5	C

Mine ID	Database Mine Name	BLM Hazard	NOAMI Hazard
NMSO0911	Unknown	1	C
NMSO0912	Unknown	3	C
NMSO0915	Unknown	2	C
NMSO0921	Unknown	3	C
NMSO0922	Unknown	3	C
NMSO0923	Unknown	3	C
NMSO0924	Unknown	3	C
NMSO0928	Candelaria	5	C
NMSO0242	Turquoise/Barrett	1	D
NMSO0243	Turquoise/Barrett	1	D
NMSO0262	Unknown	1	D
NMSO0698	Turquoise Claims	2	D
NMSO0714	Jack Frost	2	D
NMSO0208	Jack Frost	2	D
NMSO0715	Jack Frost B	2	D
NMSO0796	Ace of Spades	1	D
NMSO0797	Ace of Spades	1	D
NMSO0798	Ace of Spades	1	D
NMSO0799	Ace of Spades	1	D
NMSO0800	Ace of Spades	1	D
NMSO0801	Ace of Spades	1	D
NMSO0802	Ace of Spades	1	D
NMSO0803	Sophia	1	D
NMSO0804	Sophia	1	D
NMSO0805	Sophia	1	D
NMSO0806	Sophia	1	D
NMSO0807	Sophia	1	D
NMSO0808	Sophia	1	D
NMSO0811	Sophia	1	D
NMSO0820	Anirhoid	1	D
NMSO0821	Unknown	1	D
NMSO0822	Unknown	1	D
NMSO0824	Unknown	1	D
NMSO0826	Emerald	1	D
NMSO0827	Unknown	1	D
NMSO0829	Unknown	1	D
NMSO0830	Unknown	2	D
NMSO0832	Unknown	1	D
NMSO0833	Unknown	1	D
NMSO0834	Unknown	1	D
NMSO0835	Unknown	1	D
NMSO0836	Unknown	1	D
NMSO0837	Unknown	1	D
NMSO0842	Carnero	1	D
NMSO0843	Unknown	1	D
NMSO0845	Carnero	1	D
NMSO0846	Carnero	1	D
NMSO0847	Carnero	1	D
NMSO0849	Random	1	D
NMSO0857	K6	6	D
NMSO0859	K	2	D
NMSO0860	Unknown	1	D
NMSO0861	Cedar Hill	1	D
NMSO0863	Cedar Hill	1	D
NMSO0864	Cedar Hill	1	D

Mine ID	Database Mine Name	BLM Hazard	NOAMI Hazard
NMSO0865	Cedar Hill	1	D
NMSO0866	Cedar Hill	1	D
NMSO0867	Cedar Hill	1	D
NMSO0868	Cedar Hill	1	D
NMSO0869	Cedar Hill	1	D
NMSO0872	Unknown	1	D
NMSO0875	Unknown	1	D
NMSO0896	Sophia	1	D
NMSO0899	Unknown	1	D
NMSO0900	Unknown	1	D
NMSO0901	Unknown	1	D
NMSO0903	Unknown	1	D
NMSO0906	Unknown	1	D
NMSO0907	Unknown	1	D
NMSO0908	Unknown	1	D
NMSO0909	Unknown	1	D
NMSO0913	Unknown	1	D
NMSO0914	Candelaria	1	D
NMSO0917	Arroyo Landavaso	1	D
NMSO0919	Unknown	1	D
NMSO0920	Unknown	1	D
NMSO0925	Candelaria	1	D
NMSO0926	Candelaria	1	D
NMSO0927	Candelaria	1	D
NMSO0929	Candelaria	1	D
NMSO0930	Candelaria	1	D
NMSO0931	Arroyo Landavaso	1	D
NMSO0932	Anirhoid	1	D
NMSO0933	Unknown	1	D
NMSO0938	Unknown	1	D
NMSO0939	Unknown	1	D
NMSO0940	Unknown	1	D
NMSO0941	Unknown	1	D
NMSO0942	Unknown	1	D
NMSO0943	Anirhoid	1	D
NMSO0944	Emerald	1	D
NMSO0945	Unknown	1	D
NMSO0946	Unknown	1	D
NMSO0947	Unknown	1	D
NMSO0948	Ace of Spades	1	D
NMSO0949	Ace of Spades	1	D
NMSO0950	Unknown	1	D
NMSO0951	Unknown	1	D
NMSO0934	Unknown	1	D
NMSO0936	Pueblo Spring	1	D
NMSO0937	David	1	D
NMSO0949	Candelaria	1	D
NMSO0950	Unknown	1	D
NMSO0952	Unknown	1	D
NMSO0060	Unknown	6	O
NMSO0179	Unknown	6	O
NMSO0185	Charlie Spear	6	O
NMSO0186	Charlie Spear	6	O
NMSO0209	Jack Frost	6	O
NMSO0227	Unknown	6	O
NMSO0228	Northeast Area	6	O
NMSO0231	Silver Hill	6	O

Mine ID	Database Mine Name	BLM Hazard	NOAMI Hazard
NMSO0240	Pajaro	6	O
NMSO0241	Turquoise/Barrett	6	O
NMSO0261	Unknown	6	O
NMSO0606	Unknown	6	O
NMSO0607	Silver Hill area	6	O
NMSO0699	Turquoise/Barrett Shaft (B)	6	O
NMSO0700	Turquoise/Barrett Shaft (C)	6	O
NMSO0701	Turquoise	6	O
NMSO0703	Turquoise/Barrett Shaft (F)	6	O
NMSO0704	Turquoise/Barrett Shaft (G)	6	O
NMSO0705	Turquoise/Barrett Adit	6	O
NMSO0707	Jack Frost Area Shaft (A)	6	O
NMSO0708	Jack Frost Area Shaft (B)	6	O
NMSO0709	Jack Frost Area Shaft (C)	6	O
NMSO0710	Jack Frost Area Shaft (D)	6	O
NMSO0711	Jack Frost Area Shaft (E)	6	O
NMSO0712	Jack Frost Area Shack	6	O
NMSO0713	Jack Frost Area Mine Dump	6	O
NMSO0716	Jack Frost Area Pit and Adit	6	O
NMSO0040	Saint Vicente	0	R
NMSO0041	Saint Vicente	0	R
NMSO0042	Saint Vicente	0	R
NMSO0043	Saint Vicente	0	R
NMSO0044	Saint Vicente	0	R
NMSO0045	Saint Vicente	0	R
NMSO0046	Saint Vicente	0	R
NMSO0047	Saint Vicente	0	R
NMSO0048	Saint Vicente	0	R
NMSO0049	Saint Vicente	0	R
NMSO0050	Saint Vicente	0	R
NMSO0051	Saint Vicente	0	R
NMSO0052	Saint Vicente	0	R
NMSO0053	Saint Vicente	0	R
NMSO0054	Saint Vicente	0	R
NMSO0055	Saint Vicente	0	R
NMSO0056	Saint Vicente	0	R
NMSO0605	Saint Vicente	0	R
NMSO0702	Jack Frost	0	R
NMSO0840	Unknown	0	R
NMSO0856	K5	0	R

*Includes all mine entries from database.

Hazard Ranking Key

BLM Hazard	Name	Description
0	Remediated	Remediated
1	None	No danger level
2	Low	Sites located more than a quarter mile from areas of human activity
3	Medium	Sites near historic mining towns, historic schools, recreation areas, parks, camps, or trails
4	High	Sites near homes or school or within a quarter mile of one or more AML sites
5	Extreme	Extreme danger level
6	Unknown	Unknown danger level or not visited
7	Active Mining	Active mining: reclamation planned or underway

NOAMI Hazard	Description
A	Highest class: deep unprotected openings to surface, hazardous openings on surface, crown pillars, or waste rock piles with AMD/radioactivity
B	Deep unprotected openings to surface such as shafts, raises, and open stopes
C	Hazardous openings to surface, waste rock piles, and possible dilapidated structures associated with the mine openings; no tailings or tailings are safe
D	Minor surface features only, such as trenches, test pits, and stripping; no tailings
O	No information
R	Remediated

B.6 Mine Features with Trash

Mine ID	Database Mine Name	Field Mine Name	Types of trash	Severity	Location	Comments
NMSO0902	Unknown	SH-P4	Plastic buckets, paint cans, etc.	Moderate	In pit	Could be some toxic chemicals leaching here
NMSO0830	Unknown	SH-P15	Plastic buckets, glass, jugs, barrels, cans, nylon ropes	High	In pit	Pit is full of trash. Plastic is disintegrating, may be oil/gas contamination
NMSO0898	Sophia	SH-S2	Tires, barbed wire, refrigerator	High	Filling shaft	Very dangerous! This is a deep shaft (based on waste pile). Opening plugged with trash, but deep underneath!
NMSO0809	Silver Hill	SH-S3	Remnants of structures, glass, cans, crates	Moderate	Over large area	Explosives shed filled by woodrat nest, could be dangerous??
NMSO0910	Unknown	SH-S5	Mattress, shingles, air conditioning unit	Moderate	Filling shaft	Unclear how deep the shaft is. Trash accumulating about 15ft down where timbering begins. Could be deeper underneath!
NMSO0263	Gutierrez	NMC-A1	Beer cans and small items	Mild	In tunnel	Not too bad, but shows people are going in a potentially dangerous feature.
NMSO0832	Unknown	Mag6-S1	Tires, cans, bottles	Mild	Filling shaft	Not sure if this is a backfilled shaft (with trash) or a pit filled with trash
NMSO0879	Turquoise	NM354-A1	Beer cans and small items	Mild	Around area	Across the road is a huge amount of trash in a makeshift landfill
NMSO0608	Turquoise/Barrrett	NM354-P1	Pallet, pipes, tires, plastic bottles, cans	Moderate	In pit/shallow shaft	Unclear how deep this feature is

B.7 Patented Claims Information

Mine ID	Database Mine Name	Discovered	Mineral Survey No.	Claim Type	Patent No.	Date Patented	Record No.	STR Card	Ownership	Comments
NMSO0040	Saint Vicente	1880	522			8/5/1892	302			
NMSO0041	Saint Vicente	1880	522	Patented	21811	8/3/1892	304			Thomas J. Leeson
NMSO0042	Saint Vicente	1880	522			8/5/1892	305			
NMSO0043	Saint Vicente	1880	522			8/5/1892	306			
NMSO0044	Saint Vicente	1880	522			8/5/1892	307			
NMSO0045	Saint Vicente	1880	522			8/5/1892	308			
NMSO0046	Saint Vicente	1880	522			8/5/1892	309			
NMSO0047	Saint Vicente	1880	522			8/5/1892	310			
NMSO0048	Saint Vicente	1880	522			8/5/1892	311			
NMSO0049	Saint Vicente	1880	522			8/5/1892	312			
NMSO0050	Saint Vicente	1880	522			8/5/1892	55			
NMSO0051	Saint Vicente	1880	522			8/5/1892	56			
NMSO0052	Saint Vicente	1880	522			8/5/1892	57			
NMSO0053	Saint Vicente	1880	522	Patented	21811	8/3/1892	58			
NMSO0054	Saint Vicente	1880	522			8/5/1892	59			
NMSO0055	Saint Vicente	1880	522			8/5/1892	60			
NMSO0056	Saint Vicente	1880	522	Patented	21811	8/3/1892	303			Thomas J. Leeson
NMSO0122	Sophia		267	Patented	10743	6/30/1886	528			
NMSO0180	Arroyo Landavaso	1886	379	Patented	10603	6/11/1886	618			
NMSO0229	Anirhoid	1885	898	Patented	25504	4/13/1895	535		Bill Gallaher	
NMSO0240	Pajaro		823	Patented	19619	2/6/1892	729	160		
NMSO0263	Gutierrez		645	Patented	16978	12/26/1890	616			
NMSO0355	Vanadium Friend		1508	Patented	452077	1/6/1914	727	174	Mrs. Eula Bodenheimer leased to F.S. Phillips	
NMSO0373	Anirhoid	1885	898	Patented	25504	4/13/1895	533	118	Bill Gallaher	
NMSO0795	Arroyo Landavaso	1883	379	Patented	10603	6/11/1886	515	133		Lot 379, 20.66 acres, surveyed 4/20/1883
NMSO0796	Ace of Spades	1883	380	Patented	10604	6/11/1886	516	133	Gayle Bailey	Gayle Bailey inherited from father
NMSO0797	Ace of Spades	1883	380	Patented	10604	6/11/1886	517	133	unknown	Gayle Bailey inherited from father
NMSO0798	Ace of Spades	1883	380	Patented	10604	6/11/1886	518	133	unknown	Gayle Bailey inherited from father
NMSO0799	Ace of Spades	1883	380	Patented	10604	6/11/1886	519	133	unknown	Gayle Bailey inherited from father
NMSO0800	Ace of Spades	1883	380	Patented	10604	6/11/1886	520	133	Carnero	Gayle Bailey inherited from father
NMSO0801	Ace of Spades	1883	380	Patented	10604	6/11/1886	521	133	Carnero	Gayle Bailey inherited from father
NMSO0802	Ace of Spades	1883	380	Patented	10604	6/11/1886	522	133	Carnero	Gayle Bailey inherited from father
NMSO0803	Sophia	1887	267	Patented	10743	6/30/1886	523		Carnero	surveyed 4/18/1887
NMSO0804	Sophia		267	Patented	10743	6/30/1886	529		Cedar Hill	
NMSO0805	Sophia		267	Patented	10743	6/30/1886	531		Cedar Hill	
NMSO0806	Sophia		267	Patented	10743	6/30/1886	532		unknown	
NMSO0807	Sophia		267	Patented	10743	6/30/1886	530		Love Bug	
NMSO0810	Sophia		267	Patented	10743	6/30/1886	615		unknown	
NMSO0811	Sophia	1883	380	Patented	10604	6/11/1886	527	117	unknown	
NMSO0820	Anirhoid	1895	898	Patented	25504	4/13/1895	534		unknown	
NMSO0823	Emerald		379	Patented	10603	6/11/1886	536	133	Candelaria	
NMSO0826	Emerald		379	Patented	10603	6/11/1886	733		Candelaria	
NMSO0838	Gutierrez		645	Patented	16978	12/26/1890	617		U.S. Forest Service	
NMSO0842	Carnero		822	Patented	19618	2/6/1892	537	124		
NMSO0844	Carnero		822	Patented	19618	2/6/1892	542	124		
NMSO0845	Carnero		822	Patented	19618	2/6/1892	538	124		

Mine ID	Database Mine Name	Discovered	Mineral Survey No.	Claim Type	Patent No.	Date Patented	Record No.	STR Card	Ownership	Comments
NMSO0846	Carnero		822	Patented	19618	2/6/1892	539	124		
NMSO0847	Carnero		822	Patented	19618	2/6/1892	540	124		
NMSO0848	Chloride		549	Patented	14163	5/18/1899	543			
NMSO0862	Carnero		822	Patented	19618	2/6/1892	541	124		
NMSO0871	Candelaria	1891	899	Patented	23059	6/6/1893	544		Bill Gallaher	
NMSO0873	Gutierrez	1879	645	Patented	16978	12/26/1890	545		Tony and Ed Trujillo	
NMSO0896	Sophia		267	Permits	10743	6/30/1886	708			
NMSO0897	Sophia		267	Patented	10743	6/30/1886	709			
NMSO0898	Sophia		267	Patented	10743	6/30/1886	710			
NMSO0914	Candelaria		899	Patented	23059	6/6/1893	714			
NMSO0916	Arroyo Landavaso	1886	379	Patented	10603	6/11/1886	715			
NMSO0917	Arroyo Landavaso	1886	379	Patented	10603	6/11/1886	716			
NMSO0918	Arroyo Landavaso	1886	379	Patented	10603	6/11/1886	717			
NMSO0925	Candelaria	1891	899	Patented	23059	6/6/1893	718			
NMSO0926	Candelaria	1891	899	Patented	23059	6/6/1893	719			
NMSO0927	Candelaria	1891	899	Patented	23059	6/6/1893	720			
NMSO0928	Candelaria	1891	899	Patented	23059	6/6/1893	721			
NMSO0929	Candelaria	1891	899	Patented	23059	6/6/1893	722			
NMSO0930	Candelaria	1891	899	Patented	23059	6/6/1893	723			
NMSO0931	Arroyo Landavaso	1886	379		10603	6/11/1886	724			
NMSO0932	Anirhoid	1895	898	Patented	25504	4/13/1895	725			
NMSO0936	Pueblo Spring		208	Patented	8336	11/1/1883	728	163		Once ms195
NMSO0937	David		524	Patented	21809	8/3/1892	730			
NMSO0943	Anirhoid		898	Patented	25504	4/13/1895	731			
NMSO0944	Emerald	1886	379	Patented	10603	6/11/1886	732			
NMSO0948	Ace of Spades	1886	380	Patented	10604	6/11/1886	734			
NMSO0949	Ace of Spades	1886	380	Patented	10604	6/11/1886	735			

B.8 Mine Feature Photographs: Labeled by Field Mine Name (Mine ID)





SH-C3 (NMSO0896)



SH-C4 (NMSO0797)



SH-C5 (NMSO0808)



SH-P1 (NMSO0894)



SH-P2 (NMSO0122)



SH-P3 (NMSO0901)





SH-P6 (NMSO0903)



SH-P7 (NMSO0904)



SH-P8 (NMSO0905)



SH-P9 (NMSO0906)





SH-P12 (NMSO0907)



SH-P13 (NMSO0908)



SH-P14 (NMSO0909)



SH-P15 (NMSO0830)



SH-P16 (NMSO0806)



SH-P17 (NMSO0946)



SH-P18 (NMSO0947)



SH-P19 (NMSO0799)





SH-P22 (NMSO0948)



SH-P23 (NMSO0949)



SH-P24 (NMSO0949)



SH-P25 (NMSO0950)







SH-S3 (NMSO0809)



SH-S3 (NMSO0809)



SH-S3 (NMSO0809)



SH-S3 (NMSO0809)



SH-S4 (NMSO0122)



SH-S4 (NMSO0122)



SH-S5 (NMSO0910)



SH-S5 (NMSO0910)



SH-S6 (NMSO0911)



SH-S7 (NMSO0912)



SH-S7 (NMSO0912)



SH-S8 (NMSO0802)



SH-S9 (NMSO0951)



SH-S9 (NMSO0951)



SH-S10 (NMSO0230)



SH-S10 (NMSO0230)



SH-T1 (NMSO0900)



SH-T2 (NMSO0897)



SH-T3 (NMSO0803)



SH-T4 (NMSO0796)



SH-T5 (NMSO0951)



SC-D1 (NMSO0866)



SC-P1 (NMSO0861)



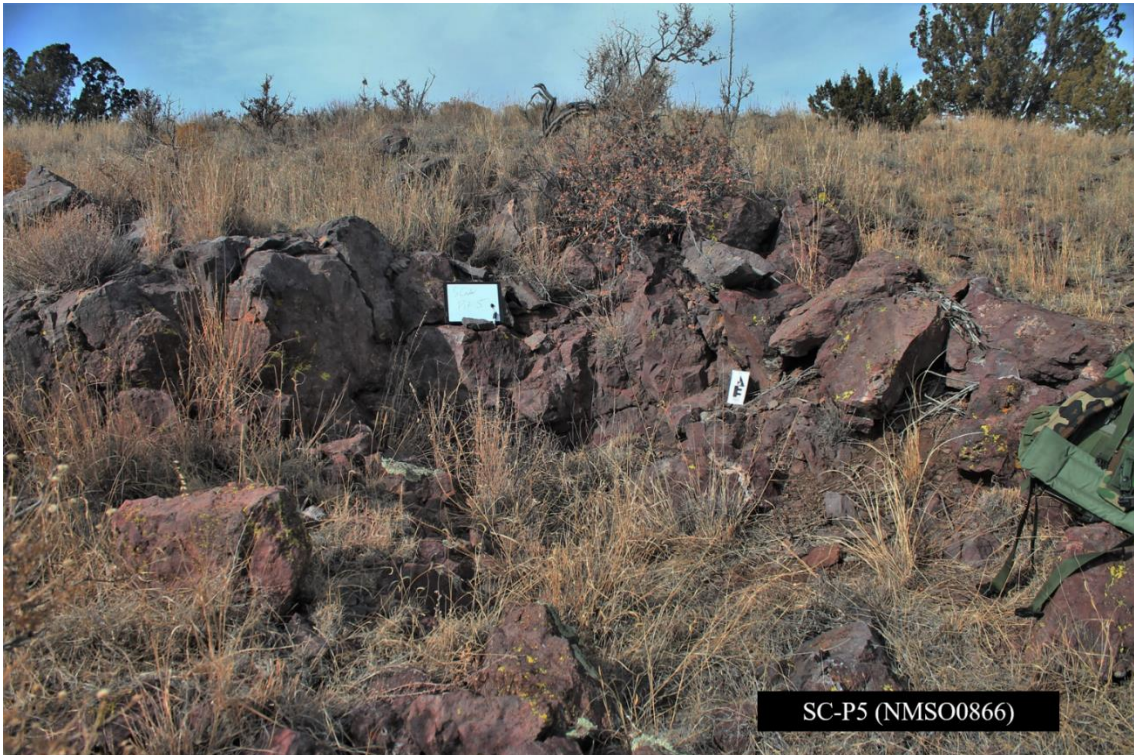
SC-P2 (NMSO0863)



SC-P3 (NMSO0864)



SC-P4 (NMSO0865)



SC-P5 (NMSO0866)



SC-P6 (NMSO0867)



SC-P7 (NMSO0868)



SC-P8 (NMSO0869)



SC-P9 (NMSO0860)



SC-S1 (NMSO0870)



NMC-P1 (NMSO0872)



NMC-P1 (NMSO0872)



NMC-S1 (NMSO0871)



NMC-S2 (NMSO0873)



NMC-T1 (NMSO0873)



NMC-T2 (NMSO0873)



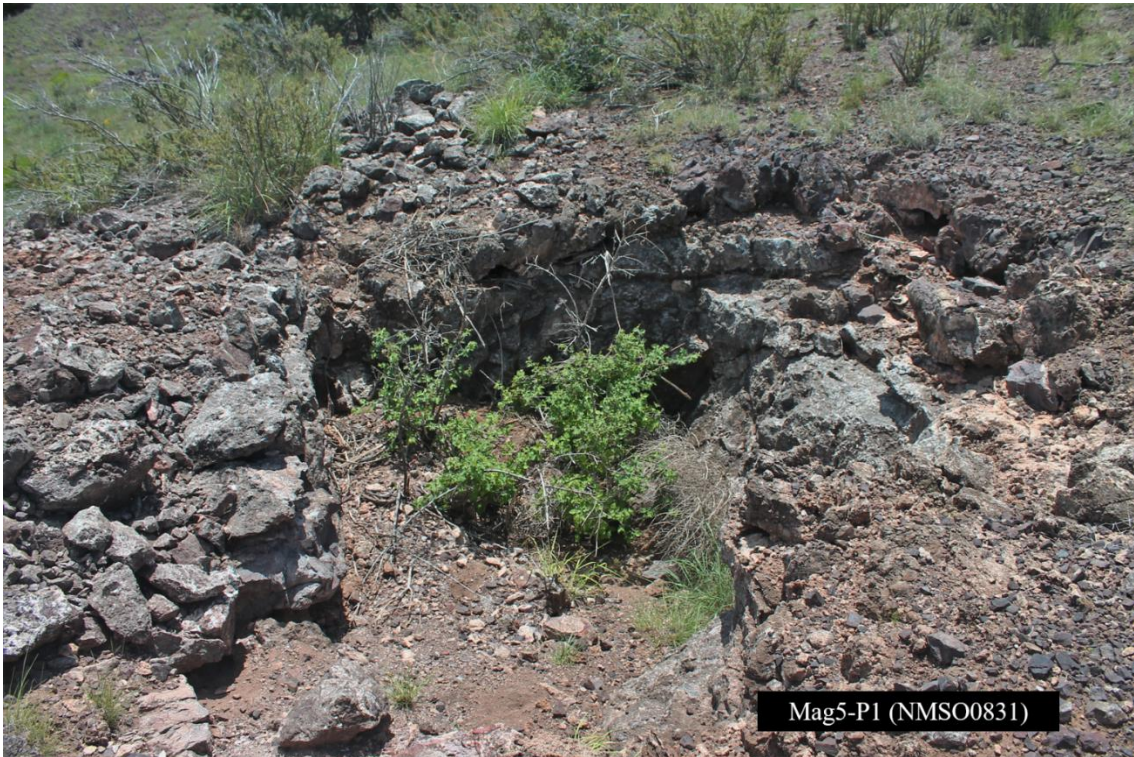
WC-P3 (NMSO0875)

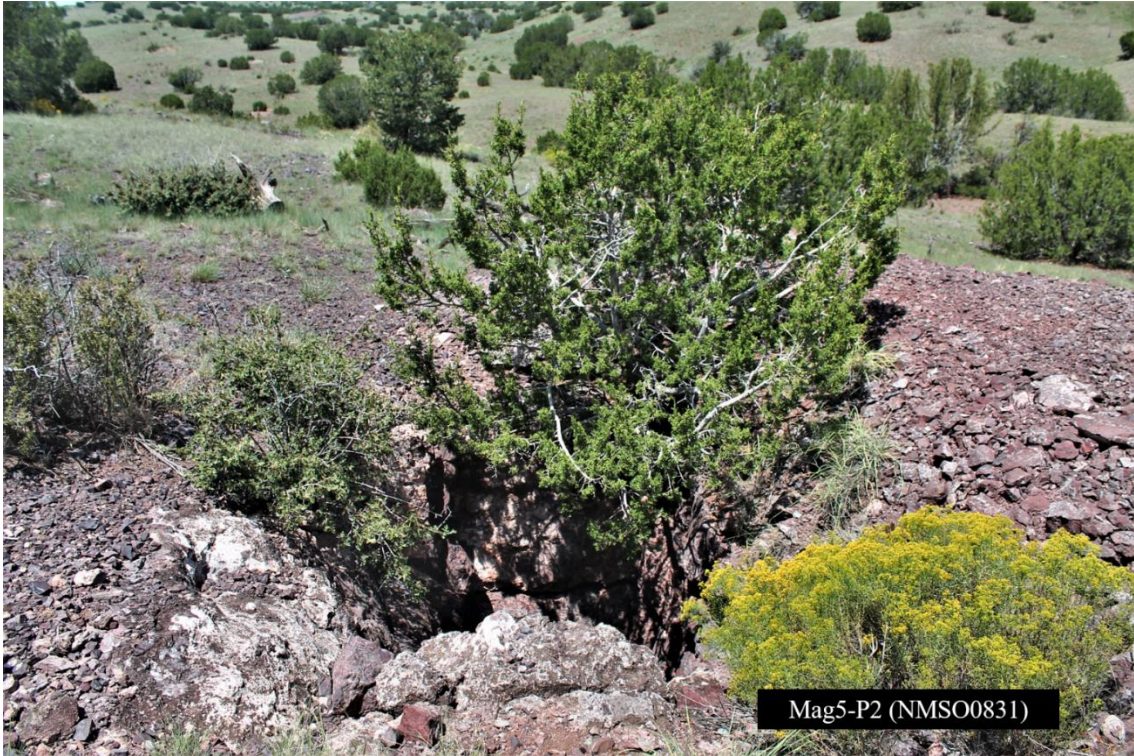


Mag2-S1 (NMSO0839)



Mag4-S1 (NMSO0377)

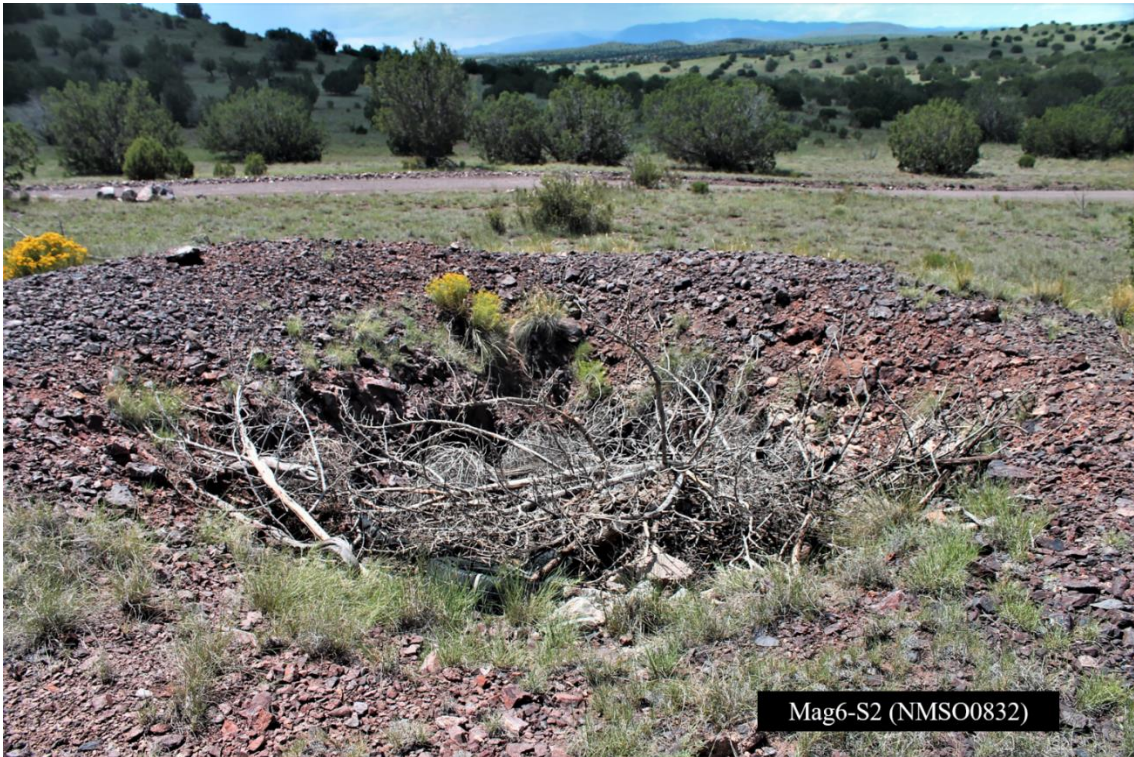








Mag6-S1 (NMSO0832)



Mag6-S2 (NMSO0832)







Mag13-P2 (NMSO0254)



Mag13-P3 (NMSO0254)



Mag13-S1 (NMSO0254)



Mag13-S2 (NMSO0254)



Mag13-S2 (NMSO0254)



Mag14-S1 (NMSO825)



Mag14-S1 (NMSO0825)



Mag15-S1 (NMSO0828)





Mag18-P1 (NMSO0914)



Mag18-P2 (NMSO0914)











Mag21-C1 (NMSO0917)



Mag21-S1 (NMSO0918)



Mag21-S1 (NMSO0918)



Mag21-S2 (NMSO0918)





Mag23-S1 (NMSO0921)



Mag24-S1 (NMSO0922)



Mag25-S1 (NMSO0923)



Mag26-S1 (NMSO0924)



Mag27-P1 (NMSO0925)



Mag27-P2 (NMSO0926)





Mag28-P2 (NMSO0932)



Mag29-D1 (NMSO0928)



Mag29-P1 (NMSO0373)



Mag30-P1 (right) & -P2 (left)
(NMSO0929)



Mag30-P3 (NMSO0930)



Mag31-P1 (NMSO0818)



Mag32-P1 (NMSO0933)



Mag33-P1 (NMSO0940)



Mag34-P1 (NMSO0941)



Mag35-P1 (NMSO0942)



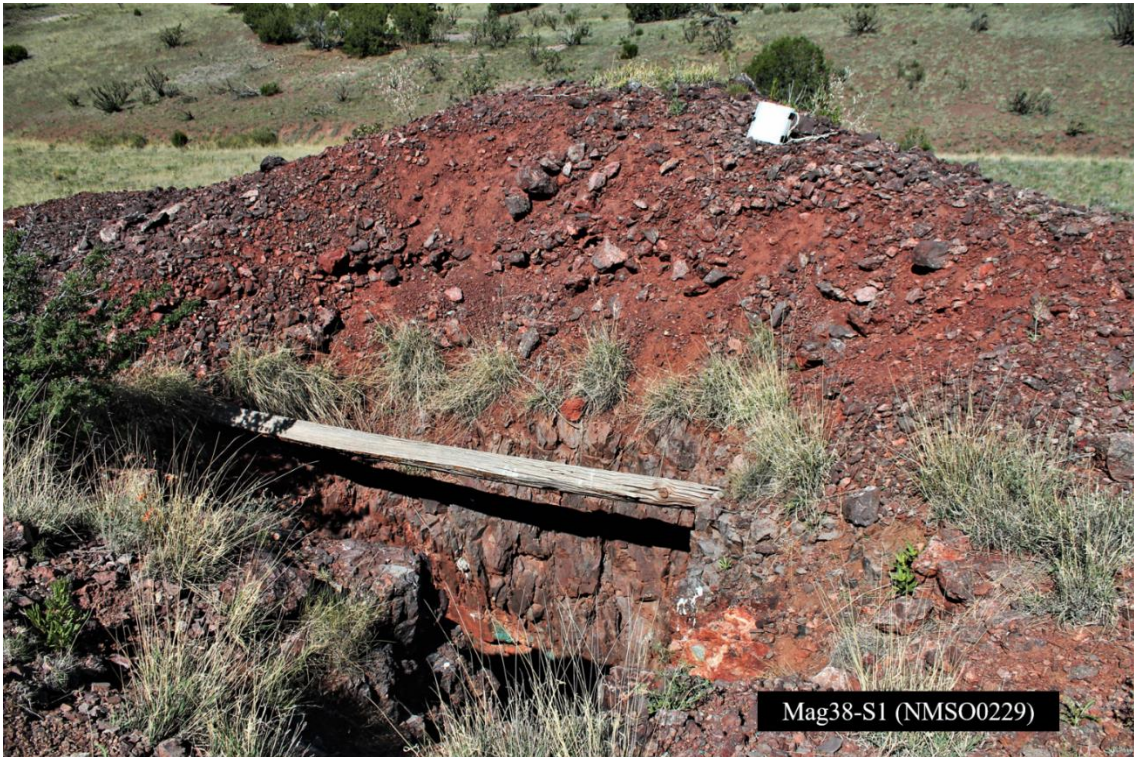
Mag36-P1 (NMSO0943)



Mag37-P1 (NMSO0820)



Mag37-P2 (NMSO0820)



Mag38-S1 (NMSO0229)



Mag38-S1 (NMSO0229)



Mag39-P1 (NMSO0944)





Mag41-C1 (NMSO0822)



Mag42-P1 (NMSO0945)





NM169-P2 (NMSO0835)

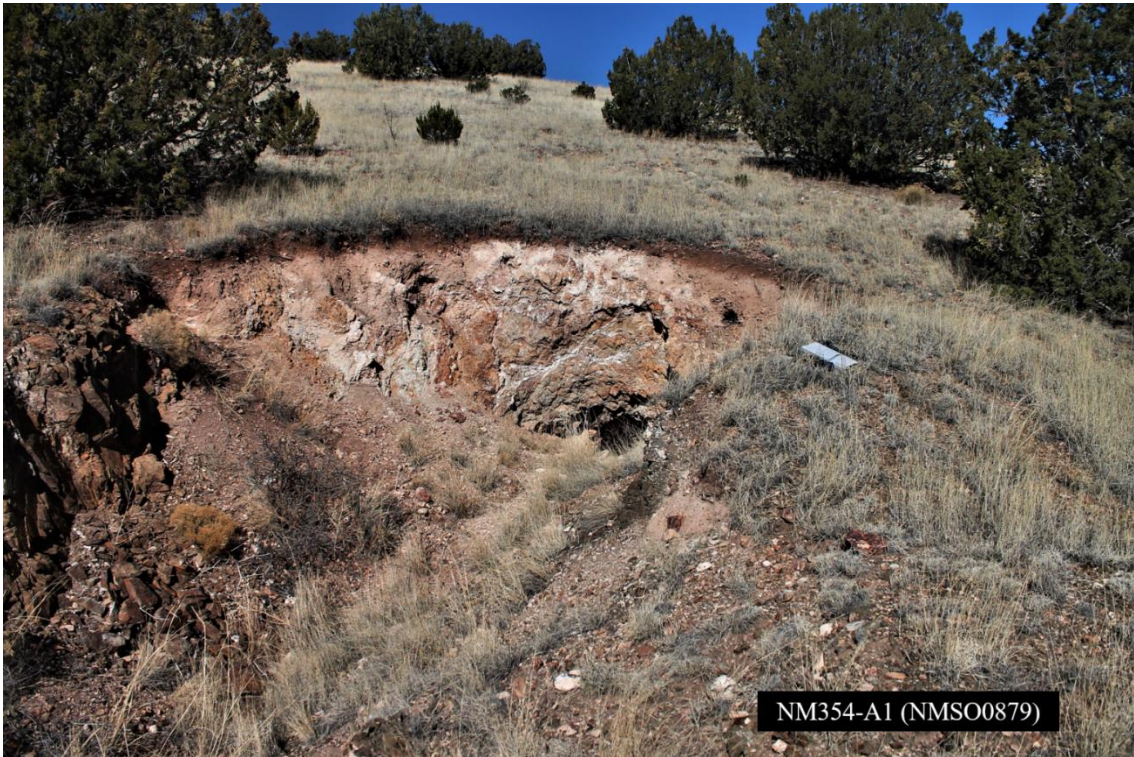


NM169-P3 (NMSO0836)





NM169-P4 (NMSO0837)



NM354-A1 (NMSO0879)



NM354-A1 (NMSO0879)



NM354-P1 (NMSO0608)

APPENDIX C

Supplementary Analytical Data

C.1 Geochemical Data

C.1.A Geochemical Data (Samples)

	ME- XRF26	ME- XRF26	ME- XRF26	ME- XRF26	ME- XRF26	ME- XRF26	ME- XRF26	ME- XRF26	ME- XRF26	ME- XRF26	OA- GRA05x	S- IR08	C- IR07	ME- XRF26
	SiO2	Al2O3	TiO2	Fe2O3	CaO	MgO	MnO	Na2O	K2O	P2O5	LOI 1000	S	C	Total
	%	%	%	%	%	%	%	%	%	%	%	%	%	%
SH-S3	49.34	14.43	1.26	9.59	9.15	8.12	0.15	3.12	1.73	0.65	1.53	0.01	0.12	99.2
SH-T2	45.68	4.57	0.42	3.73	21.1	0.43	0.34	0.42	2.77	0.16	16.67	0.24	4.59	101.12
SH-P14	31.04	0.26	0.01	0.58	0.11	0.37	0.01	0.01	0.02	0.06	1.49	6.93	0.06	40.95
Mag20-S1	57.9	8.67	0.64	10.48	0.55	0.66	0.04	0.41	5.19	0.23	4.76	1.28	0.13	90.94
Mag29-D1	65.38	4.8	0.33	2.9	1.36	0.22	0.04	0.32	2.73	0.1	4.09	2.3	0.28	84.85
Mag38-S1	58.86	8.86	0.67	6.27	3.56	0.41	0.07	0.88	4.6	0.2	5.7	1.54	0.73	92.35
NMA1A	46.54	12.12	0.99	7.99	11.1	2.97	0.22	2.47	3.38	0.48	9.61	0.13	2.51	100.51
NMA1B	50.18	5.57	0.45	14.83	2.84	0.3	0.14	0.75	3.35	0.27	5.11	1.27	0.6	85.66
NMA15	49.47	7.7	0.65	5.79	11	0.32	0.19	0.84	5.16	0.31	9.98	0.88	2.34	94.63
SC-28	58.15	13.78	1.5	8.34	0.84	0.42	0.03	0.56	9.19	0.57	2.19	0.14	0.08	95.79
SC-5A	44.74	11.64	0.99	6.91	13.6	2.34	0.14	1.61	3.67	0.37	12.56	0.04	3.06	101.67
SC-5B	44.63	11.67	1	6.99	13.75	2.36	0.14	1.66	3.59	0.38	12.48	0.04	3.04	101.73
SCP-4v	59.34	12.78	0.96	10.02	0.93	0.2	0.07	1.65	8.05	0.54	1.74	0.03	0.21	96.52
SCP-4ds	51.25	10.98	0.82	5.33	11.05	1.2	0.04	1.77	5.88	0.44	9.15	0.03	2.35	100.29
Meu-ds	53.77	16.38	1.95	10.08	1.32	3.7	0.06	4.11	4.52	0.61	2.25	<0.01	0.04	98.79
VL-1	31.96	5.6	0.49	6.68	13.3	2.44	1.24	0.52	1.44	0.21	13.79	2.57	3.42	86.3
VL-1_B	31.83	5.7	0.49	6.91	13.2	2.55	1.25	0.52	1.48	0.22	13.47	2.51	3.4	87.06
NM 24	37.98	0.23	<0.01	7.67	21.6	0.11	0.48	0.44	0.04	0.02	18.36	0.52	4.72	99.575
NM 36	77.04	2.72	0.21	2.02	1.86	0.19	0.18	0.1	0.83	0.11	2.66	1.57	0.4	89.89
NM-354B	60.75	13.44	1.4	5.49	3.33	1.09	0.48	0.35	4.69	1.01	5.27	0.14	0.82	98.26
NM-354B_2	65.29	7.62	0.93	7.87	2.52	1.14	0.11	0.11	2.84	0.69	4.79	0.81	0.46	96.455

	ME-MS42	Au-ICP21	Ag-OG62	ME-MS81	ME-MS4	ME-4ACD81	ME-4ACD81	ME-MS81	ME-MS81	ME-4ACD81	ME-MS81	ME-MS81	ME-MS81	ME-MS42	ME-4ACD81
	As	Au	Ag	Ba	Bi	Cd	Co	Cr	Cs	Cu	Ga	Ge	Hf	Hg	Li
	ppm	ppm	ppm	ppm	ppm	ppm	ppm	ppm	ppm	ppm	ppm	ppm	ppm	ppm	ppm
SH-S3	0.8	0.004	<0.5	1190	0.05	0.6	42	440	27.5	57	20.9	<5	4.7	0.011	30
SH-T2	46	0.061	37.9	>10000	0.03	9.9	15	100	2.43	9130	6.8	<5	1.5	0.079	40
SH-P14	>250	0.429	131	>10000	0.06	25.6	<1	100	0.2	1920	9.9	29	<0.2	2.06	20
Mag20-S1	>250	0.301	851	>10000	0.18	4.9	29	50	8.55	23400	14.7	<5	2.9	3.22	40
Mag29-D1	>250	0.638	481	>10000	0.1	17.8	10	40	2.6	17750	8.7	5	1.4	0.262	70
Mag38-S1	91.8	0.098	154	>10000	0.09	1.6	8	50	6.43	15050	12.4	<5	2.9	0.076	60
NMA1A	24.6	0.269	42	7500	0.09	1.6	36	340	3.9	949	15.6	<5	4.8	0.099	30
NMA1B	248	9.03	530	>10000	0.44	14.7	42	370	1.99	50400	16.4	6	1.9	2.83	40
NMA15	24.9	0.101	206	>10000	0.06	4.3	39	230	1.57	23200	8.9	<5	2.6	0.157	30
SC-28	6.9	0.459	538	1820	0.04	<0.5	11	150	12.85	29000	19	<5	5.1	0.115	20
SC-5A	7	0.01	3.7	2550	0.1	0.6	29	130	10.7	1270	17.7	<5	4.6	0.051	40
SC-5B	6.5	0.005	4.2	2660	0.1	0.6	27	130	10.6	1390	17.7	<5	4.9	0.054	40
SCP-4v	5.5	0.012	35.1	1345	0.07	<0.5	9	90	3.58	20300	18.7	<5	6.2	0.458	20
SCP-4ds	8.8	0.002	5.7	1730	0.06	<0.5	15	90	3.61	3090	17.2	<5	5.6	0.231	30
Mcu-ds	1.1	<0.001	<0.5	930	0.06	<0.5	50	110	7.09	41	20.1	<5	6.8	0.042	50
VL-1	36.9	0.111	6.4	>10000	0.33	82.4	20	130	9.19	784	12.1	<5	2.3	0.668	30
VL-1_B	37.5	0.09	8	>10000	0.3	99.8	19	130	9.45	872	12	<5	2.1	0.656	30
NM 24	>250	1.39	91.5	>10000	0.05	42.2	4	10	0.37	62400	7.2	20	<0.2	0.208	30
NM 36	5	0.16	3.5	>10000	0.14	1.4	3	80	3.72	545	5.8	<5	1.1	0.04	90
NM-354B	58	0.142	3	4530	0.24	19.9	37	480	17	326	25.2	<5	13	0.18	30
NM-354B_2	109	0.091	7	>10000	0.28	45.6	12	350	6.76	232	17.4	<5	8.1	0.379	80

	ME-4ACD81	ME-4ACD81	ME-MS81	ME-MS81	ME-4ACD81	ME-MS42	ME-4ACD81	ME-MS42	ME-MS81	ME-MS81	ME-MS81	ME-MS42	ME-MS81	ME-MS42	ME-MS8
	Mo	Ni	Nb	Rb	Pb	Sb	Sc	Se	Sn	Sr	Ta	Te	Th	Tl	U
	ppm	ppm	ppm	ppm	ppm	ppm	ppm	ppm	ppm	ppm	ppm	ppm	ppm	ppm	ppm
SH-S3	<1	210	14.4	28.5	10	2.06	22	<0.2	2	1040	0.9	<0.01	7.16	0.03	1.82
SH-T2	3	41	3.8	106	666	8.75	6	<0.2	<1	571	0.2	<0.01	2.11	0.07	3.34
SH-P14	7	6	<0.2	1.6	9790	11.15	<1	2.8	<1	9020	0.1	<0.01	0.06	<0.02	12.4
Mag20-S1	9	153	4.5	225	1720	>250	9	0.4	1	1490	0.3	0.01	2.51	0.09	7.01
Mag29-D1	1	32	2.5	110	1310	20.5	6	<0.2	<1	2130	0.2	0.02	1.4	0.05	3.22
Mag38-S1	1	32	4.9	179	378	56.5	9	<0.2	1	1440	0.3	0.01	2.77	0.09	3.27
NMA1A	<1	139	12.2	124.5	391	4.07	15	0.3	1	730	0.6	0.02	6.99	0.1	2.73
NMA1B	3	89	5.5	146.5	1705	108.5	8	0.7	1	1430	0.3	0.02	2.9	0.06	19.5
NMA15	1	96	7	192.5	323	7.81	8	0.2	1	1130	0.4	0.01	3.68	0.07	3.93
SC-28	1	45	11.1	395	25	6.58	6.7	0.2	1	1045	0.6	0.01	3.57	0.09	3.97
SC-5A	1	86	8.9	167	40	3.25	7.3	0.2	1	277	0.5	0.01	5.98	0.14	1.76
SC-5B	<1	89	9.3	163.5	39	3.13	7.2	0.2	1	277	0.5	0.02	5.62	0.13	1.68
SCP-4v	<1	162	11.4	312	35	5.48	4.4	0.3	2	153	0.6	0.01	4.89	0.1	3.3
SCP-4ds	1	54	9.7	254	17	2.68	3.4	<0.2	1	277	0.5	0.02	4.31	0.08	2.61
Mcu-ds	1	110	15.3	188	17	0.99	7.2	0.2	2	328	0.9	0.01	4.19	0.06	1.25
VL-1	6	58	5	78.1	26400	1.79	3.7	0.8	1	1960	0.3	0.02	2.21	0.14	4.36
VL-1_B	6	61	5.1	80.8	35300	2.17	3.6	0.9	1	1805	0.3	0.02	2.24	0.15	4.67
NM 24	3	16	<0.2	1.8	2270	43.9	0.9	1.6	<1	458	<0.1	0.01	<0.05	0.02	20.3
NM 36	3	12	2.3	40	7380	0.88	0.6	1.1	1	1055	0.2	0.01	1.46	0.06	1.68
NM-354B	11	92	16.4	231	1320	2.35	9.5	2.6	4	331	0.7	0.14	9.37	0.27	5
NM-354B_2	126	59	7.8	123.5	12750	16.25	5.2	2.2	2	505	0.3	0.35	4.7	0.11	3.23

	ME-MS81	ME-MS81	ME-MS81	ME-MS81	ME-4ACD81	ME-MS81	ME-MS81	ME-MS81	ME-MS81	ME-MS81	ME-MS81	ME-MS81	ME-MS81	ME-MS81	ME-MS81	ME-MS81
	V	W	Y	Zr	Zn	La	Ce	Pr	Nd	Sm	Eu	Gd	Tb	Dy	Ho	Er
	ppm	ppm	ppm	ppm	ppm	ppm	ppm	ppm	ppm	ppm	ppm	ppm	ppm	ppm	ppm	ppm
SH-S3	232	1	25.4	201	97	50.9	101	13.35	53.4	10.45	2.46	7.79	1.03	5.13	0.96	2.69
SH-T2	143	7	16.1	63	1140	15.4	31.8	3.96	16.2	3.56	0.85	3.41	0.54	2.81	0.51	1.4
SH-P14	1430	6	2.8	3	147500	2.5	1.5	0.21	0.9	1.89	<0.03	0.24	0.04	0.09	0.02	0.05
Mag20-S1	361	5	14.6	112	999	19.8	39.9	5.21	21.1	4.45	0.62	3.71	0.51	2.75	0.59	1.59
Mag29-D1	311	10	7.6	63	666	11.7	20.2	2.69	10.7	2.89	<0.03	1.93	0.27	1.37	0.28	0.84
Mag38-S1	214	21	10.8	119	428	28.3	45.2	6.57	25.6	5.03	0.2	3.39	0.44	2.15	0.42	1.25
NMA1A	273	11	23.3	184	361	41.7	88	10.7	43	8.41	2.16	6.53	0.84	4.18	0.79	2.31
NMA1B	566	40	12.3	76	4940	20.2	38.1	4.88	19.9	4.22	0.15	3.2	0.43	2.26	0.41	1.21
NMA15	132	15	19.1	105	896	28.8	58.3	7.05	27.9	5.86	1.21	4.57	0.65	3.34	0.61	1.66
SC-28	216	38	24.4	203	63	33.8	70.3	8.99	37.1	6.95	1.76	6	0.83	5.01	1.03	2.63
SC-5A	151	12	22.3	192	136	30	63.4	7.51	30.7	6.16	1.53	5.16	0.74	4.38	0.83	2.21
SC-5B	146	11	23.5	184	141	30	61.9	7.56	30.9	6.54	1.76	5.32	0.74	4.41	0.9	2.48
SCP-4v	167	25	22.6	255	69	49.2	98.5	11.75	44.6	7.9	1.94	6.22	0.92	4.54	0.83	2.43
SCP-4ds	95	5	20.2	226	70	39.6	80.3	9.77	37	6.6	1.53	5.11	0.72	4.12	0.77	2.14
Mcu-ds	224	8	33.2	277	131	36.2	77.5	10.05	40.3	8.29	2.17	7.21	1.17	6.43	1.31	3.73
VL-1	729	12	22.8	90	7270	32.7	59.4	7.48	30.4	7.4	2.18	5.48	0.85	4.39	0.71	1.69
VL-1_B	779	9	22.7	89	7570	33.3	60.3	7.37	30.3	7.26	2.01	6.3	0.84	4.49	0.72	1.7
NM 24	338	36	3.7	<2	11650	2.7	5.4	0.62	2.7	0.65	0.46	0.56	0.11	0.58	0.09	0.26
NM 36	71	2	6.1	46	220	8.9	17.8	2.22	9.8	2.39	0.59	1.7	0.23	1.16	0.21	0.49
NM-354B	231	7	43.6	486	2170	65.3	140.5	18.9	78.9	16	3.44	13.9	1.7	8.81	1.69	4.2
NM-354B_2	143	7	20.8	289	1485	37.7	77.8	9.87	37.8	6.94	1.31	4.8	0.76	4.08	0.73	2.13

	ME- MSS1	ME- MSS1	ME- MSS1	TREE
	Tm	Yb	Lu	
	ppm	ppm	ppm	ppm
SH-S3	0.34	2.36	0.31	252.17
SH-T2	0.18	1.16	0.15	81.93
SH-P14	0.02	0.28	0.1	7.84
Mag20-S1	0.22	1.59	0.21	102.25
Mag29-D1	0.13	0.92	0.15	54.07
Mag38-S1	0.17	1.22	0.17	120.11
NMA1A	0.34	1.99	0.31	211.26
NMA1B	0.15	0.99	0.17	96.27
NMA15	0.21	1.42	0.2	141.78
SC-28	0.35	1.95	0.3	177
SC-5A	0.33	2.27	0.29	155.51
SC-5B	0.34	2.07	0.38	155.3
SCP-4v	0.29	1.7	0.26	231.08
SCP-4ds	0.25	1.73	0.27	189.91
Mcu-ds	0.49	3.12	0.46	198.43
VL-1	0.25	1.48	0.19	154.6
VL-1_B	0.25	1.5	0.21	156.55
NM 24	0.11	0.14	0.04	14.42
NM 36	0.1	0.58	0.11	46.28
NM-354B	0.55	3.51	0.55	357.95
NM- 354B_2	0.27	2.04	0.26	186.49

C.1.B Geochemical Data (Standards)

	SiO2	TiO2	Al2O3	CaO	Fe2O3	MgO	MnO	Na2O	K2O	P2O5	LOI	S	C	Total	As
	%	%	%	%	%	%	%	%	%	%	%	%	%	%	ppm
MOLY 304B	75.77	0.21	12.02	0.11	2.81	0.47	0.04	0.96	4.82	0.05	2.43	0.41	0.05	100.15	5.3
CAP-MLJ_0001	75.56	0.21	12.02	0.11	2.84	0.46	0.04	0.96	4.86	0.05	2.53	0.44	0.07	100.15	6.1
MOLY 304a	75.3	0.21	12	0.11	2.85	0.45	0.04	0.95	4.85	0.05	2.28	0.44	0.05	99.58	5.7
CAP-MLS_0001a	75.39	0.2	11.94	0.1	2.82	0.44	0.04	0.95	4.82	0.05	2.37	0.47	0.06	99.65	5.4
CAP-MLJ-0001A	75.39	0.21	11.82	0.11	2.95	0.52	0.05	0.93	4.75	0.05	2.34	0.44	0.07	99.63	5.5
CAP-MLJ-0001B	75.94	0.21	11.88	0.11	2.88	0.52	0.05	0.95	4.78	0.05	2.33	0.45	0.06	100.21	5.2
CAP-MLJ-0001	75.37	0.22	11.94	0.11	2.93	0.51	0.04	0.97	4.87	0.06	2.38	0.48	0.05	99.93	5.2
CAP-MLJ-0001A	75.27	0.21	11.96	0.11	2.89	0.43	0.04	0.92	4.82	0.05	2.26	0.43	0.06	99.45	5.4
CAP-MLJ-0001B	74.75	0.21	11.84	0.11	2.88	0.43	0.04	0.91	4.79	0.05	2.15	0.45	0.05	98.66	5.3
CAP-MLJ-0001	74.28	0.2	11.83	0.11	2.93	0.45	0.04	0.91	4.75	0.06	2.29	0.49	0.06	98.4	5
CAP-MLJ-0001B	74.22	0.2	11.76	0.11	2.93	0.44	0.04	0.9	4.76	0.06	2.26	0.48	0.07	98.23	5

	Au	Ag	Ba	Bi	Cd	Co	Cr	Cs	Cu	Ga	Ge	Hf	Hg	Li	Mo	Ni
	ppm	ppm	ppm	ppm	ppm	ppm	ppm	ppm	ppm	ppm	ppm	ppm	ppm	ppm	ppm	ppm
MOLY 304B	0.006	0.8	349	2.31	<0.5	1	100	2.96	35	24.2	<5	9.6	0.01	10	24	35
CAP-MLJ_0001	0.005	0.8	378	2.42	<0.5	<1	110	2.92	35	24.7	<5	9.3	0.011	10	24	37
MOLY 304a	0.004	0.8	347	2.49	<0.5	2	100	2.74	37	22.4	<5	9.3	0.01	10	23	34
CAP-MLS_0001a	0.01	0.8	334	2.35	<0.5	1	100	2.72	35	22	<5	9.2	0.019	10	24	36
CAP-MLJ-0001A	0.001	0.7	386	2.2	<0.5	2	120	3.02	37	24.7	<5	10.1	<0.005	10	23	35
CAP-MLJ-0001B	<0.001	0.7	383	2.1	<0.5	1	120	2.89	37	24.4	<5	10	0.009	10	23	35
CAP-MLJ-0001	0.001	0.7	365	2.2	<0.5	2	110	2.94	40	23.9	<5	9.6	0.009	20	25	39
CAP-MLJ-0001A	0.003	1.1	357	2.37	<0.5	1	100	3.04	98	23.7	<5	9.3	0.007	10	24	37
CAP-MLJ-0001B	0.003	0.9	362	2.32	<0.5	2	100	2.98	101	23.8	<5	9.5	0.011	10	24	38
CAP-MLJ-0001	0.003	0.5	333	2.29	<0.5	2	100	2.75	43	23.6	<5	9.3	<0.005	10	25	37
CAP-MLJ-0001B	0.003	0.6	350	2.37	<0.5	2	110	3.02	46	23.6	<5	10.3	0.006	10	25	38

	Nb	Rb	Pb	Sb	Sc	Se	Sn	Sr	Ta	Te	Th	Tl	U	V	W	Y	Zr
	ppm	ppm	ppm	ppm	ppm	ppm	ppm	ppm	ppm	ppm	ppm	ppm	ppm	ppm	ppm	ppm	ppm
MOLY 304B	33.6	158	79	0.13	0.3	0.3	4	70.7	2.2	0.75	13.95	0.16	5.25	19	5	52.3	299
CAP-MLJ_0001	34.8	159	80	0.16	0.3	0.4	4	82.7	2.2	0.84	14.3	0.17	5.34	21	6	50.7	304
MOLY 304a	32	162.5	78	0.14	0.4	0.5	3	70.9	1.9	0.85	12.9	0.16	5.17	22	5	47.6	274
CAP-MLS_0001a	31.5	160.5	83	0.14	0.3	0.6	4	66.7	1.8	0.82	13.05	0.15	5.08	19	5	48.4	275
CAP-MLJ-0001A	35.9	172	77	0.23	2	0.4	4	77	2.2	0.88	14.4	0.21	5.48	22	5	52.7	300
CAP-MLJ-0001B	36.1	170.5	77	0.21	2	0.5	5	77.6	2.2	0.83	14.6	0.21	5.4	22	6	52.7	304
CAP-MLJ-0001	35	154	86	0.15	0.4	0.6	4	71.9	2.1	0.85	14	0.23	5.59	25	5	49.3	310
CAP-MLJ-0001A	33	156	79	0.2	0.4	0.4	4	73.6	2	0.92	13.45	0.19	5.2	20	6	48	288
CAP-MLJ-0001B	34.2	156.5	80	0.19	0.4	0.6	4	74.3	2.1	0.85	14.3	0.18	5.3	20	5	49.4	302
CAP-MLJ-0001	31	155.5	83	0.15	0.6	0.5	4	67.5	1.9	0.89	12.95	0.24	4.81	21	9	47.6	294
CAP-MLJ-0001B	33	164	86	0.15	0.6	0.6	4	71.6	2	0.99	14.1	0.26	5.67	24	5	51	324

	Zn	La	Ce	Pr	Nd	Sm	Eu	Gd	Tb	Dy	Ho	Er	Tm	Yb	Lu	TREE
	ppm	ppm	ppm	ppm	ppm	ppm	ppm	ppm	ppm	ppm	ppm	ppm	ppm	ppm	ppm	ppm
MOLY 304B	57	47.5	92.9	10.6	38.9	8.11	0.39	8.12	1.32	9.01	1.95	5.77	0.89	5.64	0.83	231.93
CAP-MLJ-0001	52	50.4	98.1	11.05	40.5	8.54	0.47	7.53	1.24	8.45	1.89	5.77	0.84	5.29	0.85	240.92
MOLY 304a	50	45.3	91.5	10.35	39.5	7.84	0.4	7.53	1.18	7.89	1.71	5.52	0.76	5.25	0.75	225.48
CAP-MLS_0001a	53	44.8	87.1	9.74	39.3	7.4	0.37	7.01	1.25	8.07	1.7	5.42	0.79	5.45	0.72	219.12
CAP-MLJ-000 1A	52	51.6	100.5	11.4	42	8.77	0.45	8.19	1.38	8.66	1.83	6.08	0.93	5.67	0.84	248.3
CAP-MLJ-000 1B	53	51.8	100.5	11.5	42	8.79	0.41	8.08	1.39	8.57	1.82	5.97	0.93	5.42	0.86	248.04
CAP-MLJ-0001	53	48	95.6	10.95	39.5	8.32	0.41	7.48	1.26	8.29	1.83	5.72	0.85	5.25	0.84	234.3
CAP-MLJ-0001A	52	48.5	96.1	10.95	39.1	7.93	0.37	7.29	1.21	8.16	1.69	5.66	0.79	5.26	0.83	233.84
CAP-MLJ-0001B	54	50.1	100	11.3	41.2	8.55	0.5	7.42	1.25	8.26	1.76	5.22	0.79	5.34	0.82	242.51
CAP-MLJ-0001	60	46.1	90.5	10.15	37.9	7.79	0.37	7.09	1.3	7.47	1.78	5.33	0.85	5.65	0.71	222.99
CAP-MLJ-0001B	62	48.6	95.8	10.8	38.4	8.2	0.38	8.29	1.19	8.14	1.77	6.03	0.75	5.39	0.83	234.57

C.2 Electron Microprobe Data

C.2.A Galena

Weight%												
DataSet/Point	Sample	S	Pb	Cu	Ag	As	Total	X	Y	Z	Comments	Date
1 / 1.	galena-01	13.69	87.25	0.00	0.00	0.00	100.94	-14317	2930	117	std	10/4/2018 14:07
2 / 1.	galena-02	13.77	86.20	0.00	0.00	0.00	99.97	-14305	2920	117	std	10/4/2018 14:15
3 / 1.	galena-03	13.62	86.72	0.00	0.00	0.01	100.34	-14297	2902	117	std	10/4/2018 14:22
4 / 1.	galena-04	13.75	86.40	0.00	0.00	0.00	100.15	-14279	2875	117	std	10/4/2018 14:29
11 / 1.	VL-WS-01	13.67	86.23	0.00	0.00	0.00	99.90	19398	23782	-12	galena	10/4/2018 15:02
17 / 1.	VL-WS-07	13.39	85.82	0.02	0.00	0.00	99.23	21068	24725	-32	galena	10/4/2018 15:25
18 / 1.	VL-WS-08	13.53	86.41	0.04	0.00	0.00	99.98	19779	25679	-19	galena	10/4/2018 15:33
25 / 1.	VL-WS-15	13.68	86.10	0.01	0.00	0.00	99.79	17484	20841	2	galena	10/4/2018 16:00
29 / 1.	NMA-1B-1-04	8.07	79.45	2.56	0.00	0.00	90.09	11523	8209	-92	Cu-bearing galena (or mixture; galena +?)	10/4/2018 16:17
30 / 1.	NMA-1B-1-05	6.26	78.33	9.06	0.00	0.02	93.68	11506	8243	-94	Cu-bearing galena (or mixture; galena +?)	10/4/2018 16:25
31 / 1.	NMA-1B-1-06	6.82	80.24	1.78	0.00	0.00	88.84	11553	8254	-92	Galena	10/4/2018 16:32
32 / 1.	NMA-1B-1-07	34.89	0.14	64.94	0.53	0.00	100.50	11420	8287	-90	CuS phase (Ag bearing)	10/4/2018 16:39
33 / 1.	NMA-1B-1-08	21.68	4.02	54.84	1.08	0.00	81.61	11509	8157	-74	CuS phase (Ag bearing)	10/4/2018 16:47
34 / 1.	NMA-1B-1-09	29.04	1.63	62.52	0.72	0.02	93.92	11608	8251	-83	CuS phase (Ag bearing)	10/4/2018 16:54
35 / 1.	NMA-1B-1-10	33.50	0.28	62.44	0.74	0.00	96.96	11408	8322	-80	CuS phase (Ag bearing)	10/4/2018 17:01
36 / 1.	NMA-1B-1-11	13.97	87.09	0.08	0.00	0.00	101.14	11782	8592	-79	galena	10/4/2018 17:09
37 / 1.	NMA-1B-1-12	23.93	0.10	71.23	1.87	0.00	97.13	11631	8394	-85	CuS phase (Ag bearing)	10/4/2018 17:16
38 / 1.	NMA-1B-1-13	22.74	0.08	70.09	1.72	0.01	94.64	11617	8466	-78	CuS phase (Ag bearing)	10/4/2018 17:24
41 / 1.	NMA-1B-1-16	0.10	63.01	0.21	0.00	0.01	63.34	11974	5683	-88	cerussite +?	10/4/2018 17:36
42 / 1.	NMA-1B-1-17	0.00	53.79	0.33	0.00	0.02	54.13	11908	5649	-88	cerussite +?	10/4/2018 17:43
43 / 1.	NMA-1B-1-18	4.42	62.94	0.82	0.00	0.02	68.20	11964	5643	-81	cerussite +?	10/4/2018 17:51
44 / 1.	NMA-1B-1-19	0.00	30.72	1.05	0.00	0.00	31.78	11862	5607	-95	cerussite +?	10/4/2018 17:58
46 / 1.	NMA-1B-1-21	13.57	86.02	0.11	0.00	0.00	99.70	10804	4608	-119	galena	10/4/2018 18:08
47 / 1.	NMA-1B-1-22	0.13	76.06	0.47	0.13	0.01	76.81	10497	4390	-124	cerussite (Ag bearing)	10/4/2018 18:15
48 / 1.	NMA-1B-1-23	0.38	72.59	0.52	6.43	0.02	79.93	10425	4416	-125	cerussite (Ag bearing)	10/4/2018 18:23
49 / 1.	NMA-1B-1-24	0.00	77.07	0.13	0.00	0.04	77.24	10389	4471	-123	cerussite (Ag bearing)	10/4/2018 18:30
50 / 1.	NMA-1B-1-25	13.67	86.65	0.04	0.00	0.00	100.35	9927	3852	-139	galena	10/4/2018 18:38
54 / 1.	NMA-1B-1-29	13.78	88.38	0.13	0.00	0.00	102.29	11118	2133	-131	galena	10/4/2018 18:55
74 / 1.	NMA-1B-2-019	15.39	0.02	19.08	15.73	0.02	50.24	13327	-2548	-101	Ag rich CuS (or sulfate)?	10/4/2018 21:14
75 / 1.	NMA-1B-2-020	15.71	0.02	20.80	24.98	0.00	61.51	13099	-2476	-92	Ag rich CuS (or sulfate)?	10/4/2018 21:21
77 / 1.	galena-05	13.68	86.39	0.03	0.00	0.00	100.10	-14274	2893	121	std	10/4/2018 21:37
78 / 1.	galena-06	13.63	86.54	0.00	0.00	0.00	100.17	-14258	2875	120	std	10/4/2018 21:44

C.2.B Chalcopyrite

Weight%																
DataSet/Point	Sample	S	Cu	Fe	Ba	Ag	Au	Sb	As	Pb	Total	Comments	X	Y	Z	Date
5 / 1.	pyr-01	53.73	0.01	47.03	0.00	0.01	0.00	0.00	0.03	0.21	101.02	std	6510	-19157	80	10/4/2018 14:37
6 / 1.	pyr-02	53.77	0.03	47.08	0.00	0.01	0.00	0.00	0.03	0.22	101.16	std	6503	-19179	80	10/4/2018 14:46
56 / 1.	NMA-1B-2-01	35.13	34.05	30.04	0.07	0.10	0.02	0.00	0.02	0.15	99.59	chalcopyrite	14004	-2693	-87	10/4/2018 19:05
57 / 1.	NMA-1B-2-02	34.07	34.09	30.57	0.09	0.10	0.00	0.00	0.03	0.15	99.10	chalcopyrite	13988	-2710	-94	10/4/2018 19:14
58 / 1.	NMA-1B-2-03	35.08	34.16	30.16	0.06	0.19	0.08	0.01	0.04	0.17	99.95	chalcopyrite	13902	-2748	-96	10/4/2018 19:23
61 / 1.	NMA-1B-2-06	34.98	34.26	30.10	0.04	0.08	0.01	0.00	0.03	0.15	99.64	chalcopyrite	11237	-2646	-140	10/4/2018 19:45
62 / 1.	NMA-1B-2-07	34.17	34.33	30.34	0.06	0.09	0.00	0.00	0.03	0.14	99.17	chalcopyrite	11333	-2647	-140	10/4/2018 19:54
63 / 1.	NMA-1B-2-08	35.22	34.30	30.62	0.09	0.12	0.00	0.00	0.02	0.13	100.51	chalcopyrite	11327	-2580	-137	10/4/2018 20:03
64 / 1.	NMA-1B-2-09	34.79	34.11	30.00	0.07	0.07	0.00	0.00	0.02	0.15	99.21	chalcopyrite	11150	-2516	-145	10/4/2018 20:11
65 / 1.	NMA-1B-2-010	34.42	34.34	30.57	0.04	0.11	0.00	0.00	0.02	0.16	99.66	chalcopyrite	11547	-2639	-136	10/4/2018 20:20
72 / 1.	NMA-1B-2-017	34.67	34.75	30.69	0.04	0.06	0.00	0.00	0.02	0.14	100.37	chalcopyrite	13129	-2383	-108	10/4/2018 20:57
73 / 1.	NMA-1B-2-018	35.27	34.89	30.85	0.03	0.05	0.00	0.00	0.03	0.15	101.27	chalcopyrite	13278	-2509	-105	10/4/2018 21:05
76 / 1.	NMA-1B-2-021	8.18	2.69	3.20	50.42	0.02	0.00	0.00	0.03	0.20	64.75	mixture; barite + cpy?	13396	-2357	-99	10/4/2018 21:29
79 / 1.	pyr-03	54.10	0.03	46.38	0.00	0.01	0.00	0.00	0.03	0.21	100.76	std	6475	-19194	83	10/4/2018 21:52
80 / 1.	pyr-04	53.81	0.00	46.79	0.00	0.01	0.00	0.00	0.03	0.22	100.86	std	6469	-19214	83	10/4/2018 22:00

C.2.C Sphalerite

Weight%										
DataSet/Point	Sample	S	Zn	Mn	Fe	Total	X	Y	Z	Date
7 / 1.	sphal-01	33.01	66.69	0.00	0.12	99.82	-21895	4214	124	10/4/2018 14:54
8 / 1.	sphal-02	33.25	67.18	0.00	0.11	100.54	-21867	4225	124	10/4/2018 14:57
39 / 1.	NMA-1B-1-14	33.86	66.28	0.00	0.16	100.30	11672	8547	-86	10/4/2018 17:31
40 / 1.	NMA-1B-1-15	34.77	66.01	0.00	0.27	101.05	11960	5673	-92	10/4/2018 17:34
45 / 1.	NMA-1B-1-20	41.13	81.38	0.00	0.32	122.83	10523	4512	-121	10/4/2018 18:05
69 / 1.	NMA-1B-2-014	33.82	67.06	0.00	0.20	101.09	16726	-10214	-81	10/4/2018 20:50
70 / 1.	NMA-1B-2-015	33.57	66.83	0.00	0.29	100.70	16765	-10019	-77	10/4/2018 20:52
71 / 1.	NMA-1B-2-016	32.27	65.69	0.00	0.24	98.20	16789	-9918	-93	10/4/2018 20:55
81 / 1.	sphal-03	33.12	66.68	0.00	0.13	99.93	-21920	4236	126	10/4/2018 22:09
82 / 1.	sphal-04	32.95	66.92	0.00	0.13	99.99	-21926	4216	127	10/4/2018 22:11

C.2.D Cerussite

Wt% Oxide																
Formula	Sample	CO2	SiO2	SO2	MgO	CaO	FeO	CuO	ZnO	PbO	Total	X	Y	Z	Date	Geo Species
12 / 1.	VL-WS-02	20.17	0.70	0.37	0.00	0.03	0.01	0.26	0.04	78.43	100	19379	23840	-12	10/4/2018 15:09	Carbonate (on the basis of 6 O)
13 / 1.	VL-WS-03	15.10	1.12	0.96	0.00	0.11	0.00	1.91	0.01	80.79	100	18291	23025	-1	10/4/2018 15:12	Carbonate (on the basis of 6 O)
14 / 1.	VL-WS-04	17.47	0.00	2.09	0.00	0.02	0.00	0.44	0.00	79.98	100	21025	24733	-27	10/4/2018 15:16	Carbonate (on the basis of 6 O)
15 / 1.	VL-WS-05	14.02	0.55	3.80	0.00	0.01	0.00	2.62	0.00	79.00	100	20945	24813	-26	10/4/2018 15:19	Carbonate (on the basis of 6 O)
16 / 1.	VL-WS-06	16.83	0.47	1.33	0.00	0.07	0.00	1.69	0.02	79.59	100	20987	24768	-24	10/4/2018 15:22	Carbonate (on the basis of 6 O)
19 / 1.	VL-WS-09	18.60	0.05	0.37	0.03	0.06	0.00	0.81	0.00	80.07	100	19772	25720	-15	10/4/2018 15:40	Carbonate (on the basis of 6 O)
20 / 1.	VL-WS-10	13.50	1.20	2.44	0.00	0.06	0.00	1.66	0.04	81.09	100	19863	25698	-12	10/4/2018 15:44	Carbonate (on the basis of 6 O)
21 / 1.	VL-WS-11	18.96	1.57	0.01	0.00	0.04	0.00	0.17	0.00	79.25	100	19819	25605	-12	10/4/2018 15:47	Carbonate (on the basis of 6 O)
22 / 1.	VL-WS-12	17.89	0.00	2.15	0.00	0.14	0.06	4.65	0.02	75.09	100	19791	25745	-22	10/4/2018 15:50	Carbonate (on the basis of 6 O)
23 / 1.	VL-WS-13	15.99	0.14	0.56	0.00	0.04	0.01	1.38	0.03	81.85	100	17406	20515	0	10/4/2018 15:53	Carbonate (on the basis of 6 O)
24 / 1.	VL-WS-14	17.01	0.27	0.46	0.03	0.12	0.00	0.96	0.13	81.02	100	17056	21243	5	10/4/2018 15:56	Carbonate (on the basis of 6 O)
26 / 1.	NMA-1B-1-01	12.29	0.07	5.80	0.00	0.37	0.00	7.73	0.10	73.63	100	11498	8232	-93	10/4/2018 16:07	Carbonate (on the basis of 6 O)
27 / 1.	NMA-1B-1-02*	4.24	0.05	9.22	0.00	0.20	0.03	2.88	0.11	83.26	100	11545	8254	-92	10/4/2018 16:11	Carbonate (on the basis of 6 O)
28 / 1.	NMA-1B-1-03*	15.49	0.06	0.60	0.00	0.37	0.00	1.59	0.13	81.75	100	11521	8218	-91	10/4/2018 16:14	Carbonate (on the basis of 6 O)
51 / 1.	NMA-1B-1-26	11.67	0.23	13.01	0.00	0.03	0.00	0.80	0.01	74.26	100	9867	3853	-135	10/4/2018 18:45	Carbonate (on the basis of 6 O)
52 / 1.	NMA-1B-1-27	10.54	0.37	14.44	0.00	0.03	0.01	1.56	0.07	72.98	100	9884	3793	-146	10/4/2018 18:48	Carbonate (on the basis of 6 O)
53 / 1.	NMA-1B-1-28	12.27	0.81	14.84	0.00	0.07	0.02	3.21	0.05	68.73	100	9987	3864	-132	10/4/2018 18:52	Carbonate (on the basis of 6 O)
55 / 1.	NMA-1B-1-30	10.45	1.08	17.45	0.00	0.12	0.36	8.26	0.03	62.24	100	11136	2167	-113	10/4/2018 19:02	Carbonate (on the basis of 6 O)
*5 um beam																

Weight%												
DataSet/Point	Sample	Mg	Si	Ca	Pb	Fe	Cu	S	Zn	C	O	Total
12 / 1.	VL-WS-02	0.00	0.33	0.02	72.80	0.01	0.21	0.18	0.03	5.50	20.91	100
13 / 1.	VL-WS-03	0.00	0.52	0.08	75.00	0.00	1.53	0.48	0.01	4.12	18.26	100
14 / 1.	VL-WS-04	0.00	0.00	0.02	74.24	0.00	0.35	1.04	0.00	4.77	19.58	100
15 / 1.	VL-WS-05	0.00	0.26	0.00	73.34	0.00	2.09	1.90	0.00	3.83	18.58	100
16 / 1.	VL-WS-06	0.00	0.22	0.05	73.88	0.00	1.35	0.67	0.01	4.59	19.22	100
19 / 1.	VL-WS-09	0.02	0.02	0.04	74.33	0.00	0.65	0.19	0.00	5.08	19.67	100
20 / 1.	VL-WS-10	0.00	0.56	0.04	75.28	0.00	1.33	1.22	0.03	3.69	17.85	100
21 / 1.	VL-WS-11	0.00	0.73	0.03	73.57	0.00	0.14	0.01	0.00	5.17	20.35	100
22 / 1.	VL-WS-12	0.00	0.00	0.10	69.71	0.04	3.71	1.08	0.02	4.88	20.46	100
23 / 1.	VL-WS-13	0.00	0.07	0.03	75.99	0.01	1.11	0.28	0.02	4.36	18.14	100
24 / 1.	VL-WS-14	0.02	0.12	0.08	75.22	0.00	0.76	0.23	0.11	4.64	18.81	100
26 / 1.	NMA-1B-1-01	0.00	0.03	0.27	68.35	0.00	6.18	2.90	0.08	3.35	18.83	100
51 / 1.	NMA-1B-1-26	0.00	0.11	0.02	68.93	0.00	0.64	6.51	0.01	3.18	20.60	100
52 / 1.	NMA-1B-1-27	0.00	0.17	0.02	67.75	0.01	1.25	7.23	0.05	2.88	20.65	100
53 / 1.	NMA-1B-1-28	0.00	0.38	0.05	63.80	0.01	2.57	7.42	0.04	3.35	22.38	100
55 / 1.	NMA-1B-1-30	0.00	0.51	0.09	57.78	0.28	6.60	8.73	0.03	2.85	23.14	100

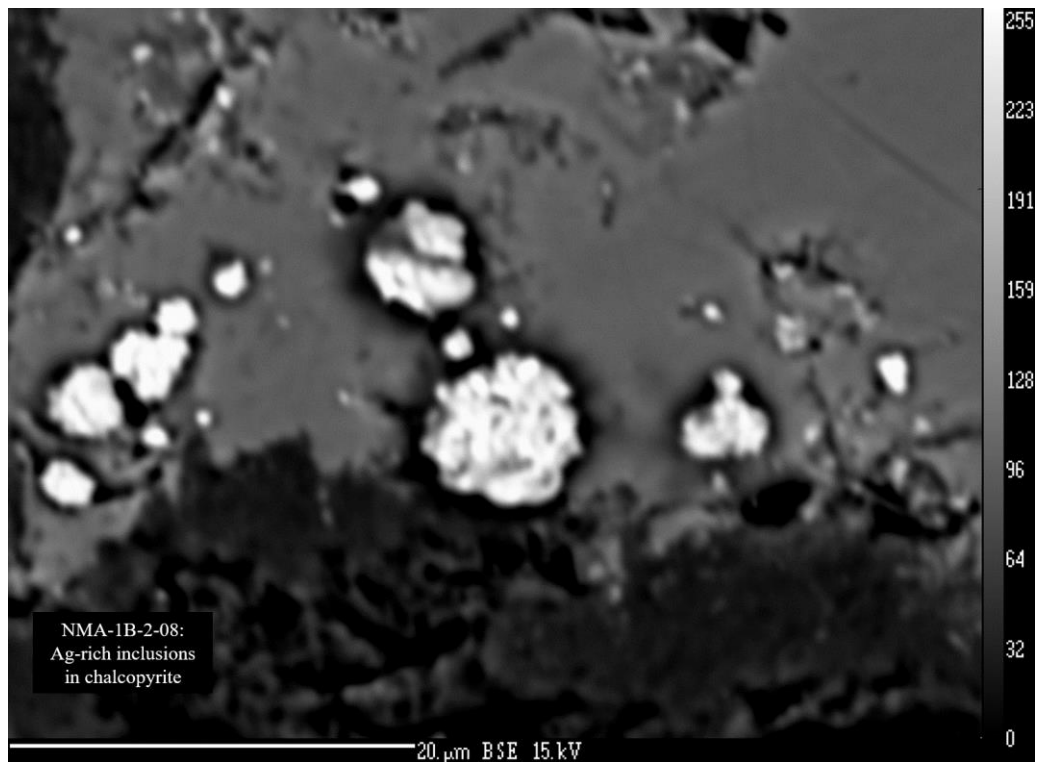
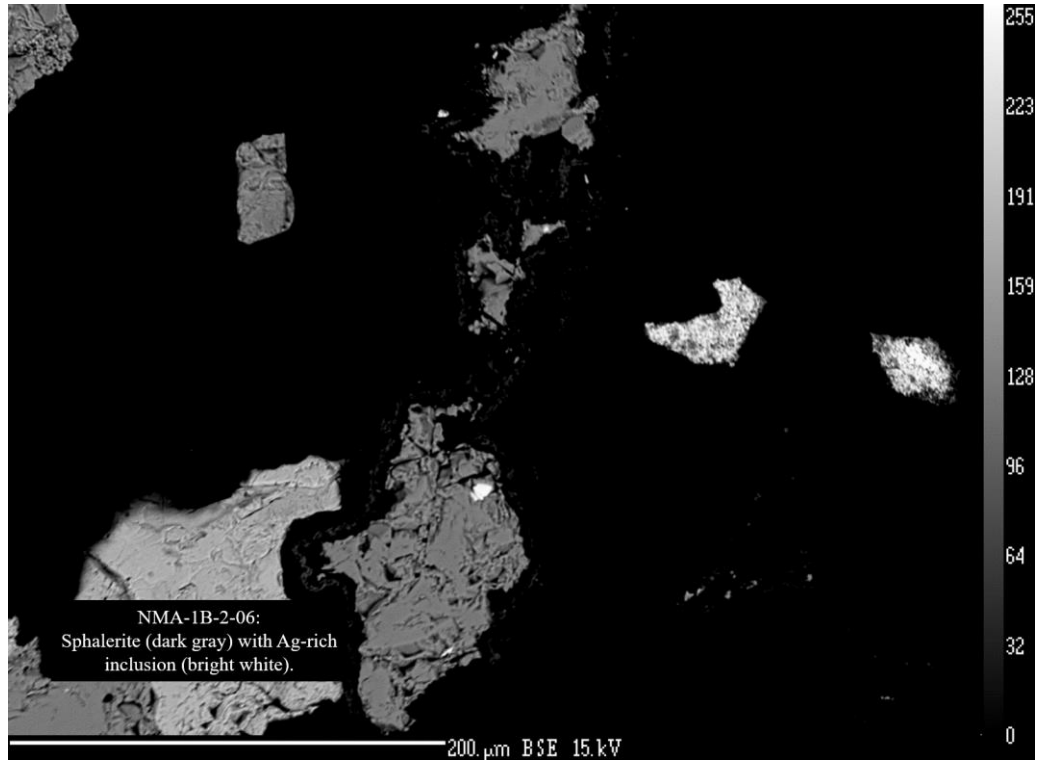
C.2.E Fe-Oxide

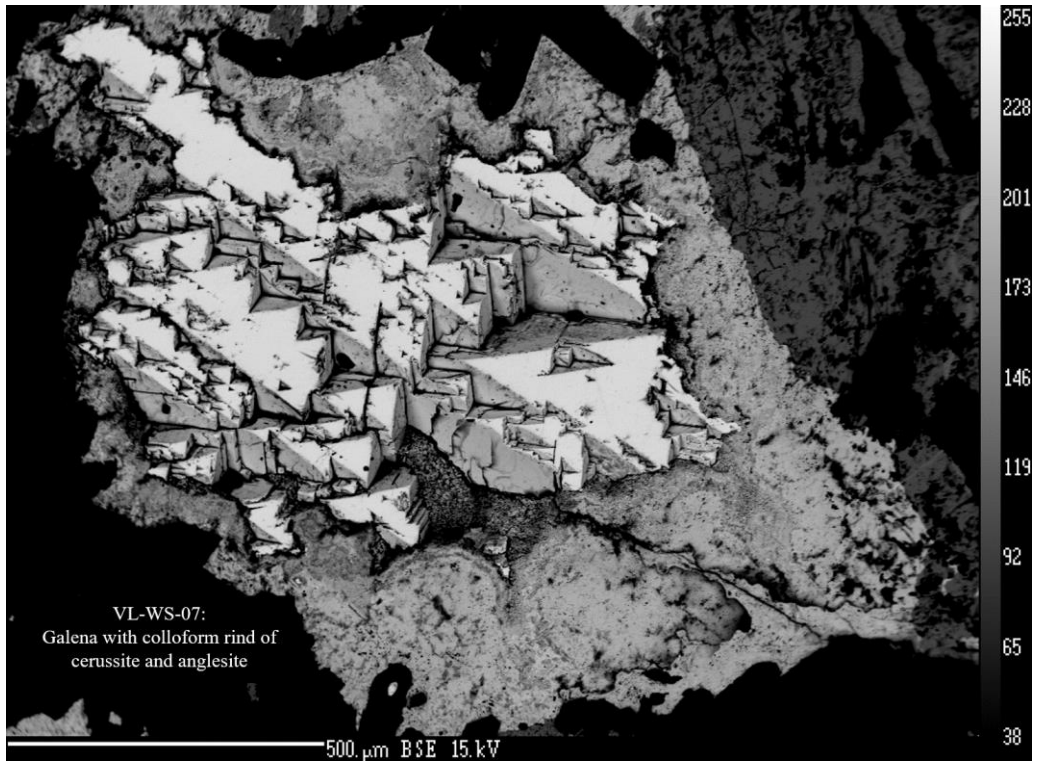
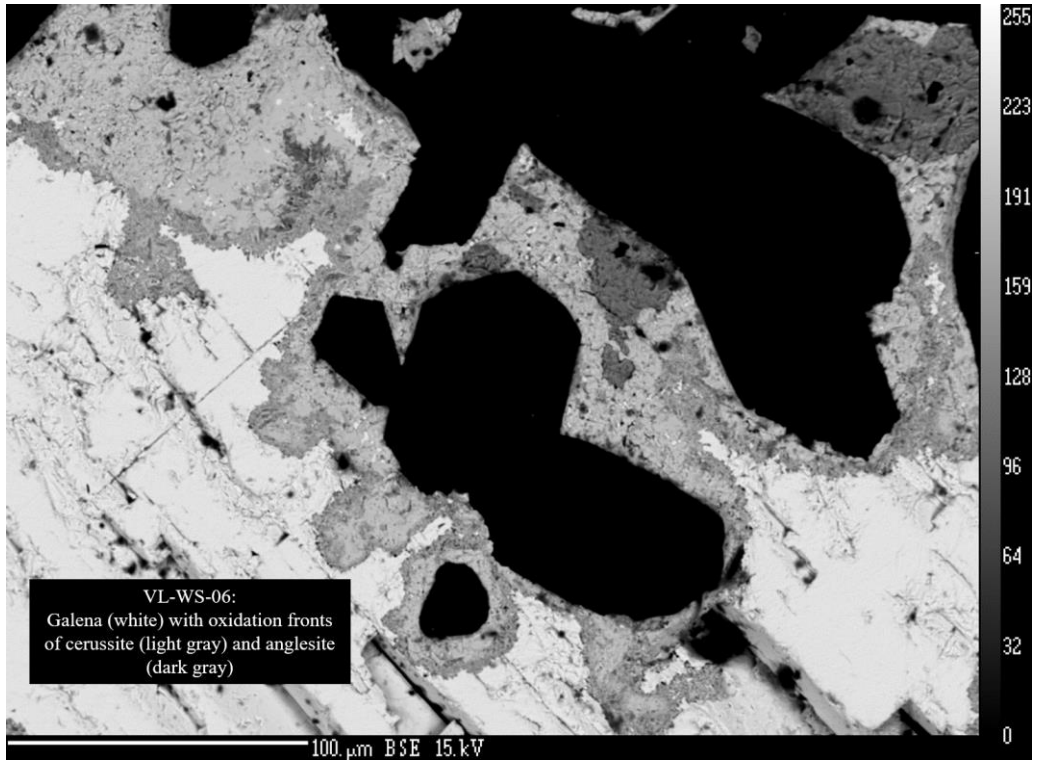
Wt% Oxide															
Formula	Sample	SiO2	SO2	Al2O3	As2O3	Au2O3	FeO	CuO	Ag2O	Total	X	Y	Z	Date	Geo Species
59 / 1.	NMA-1B-2-04	6.59	0.55	0.01	0.13	0.00	64.72	12.25	0.02	84.28	13824	-2694	-100	10/4/2018 19:31	Magnetite (on the basis of 32 O)
60 / 1.	NMA-1B-2-05	7.30	4.46	0.03	0.08	0.00	50.67	24.05	0.17	86.76	13960	-2606	-90	10/4/2018 19:38	Magnetite (on the basis of 32 O)
66 / 1.	NMA-1B-2-011	1.40	1.41	0.00	0.06	0.00	58.28	21.12	0.01	82.29	11535	-2610	-137	10/4/2018 20:29	Magnetite (on the basis of 32 O)
67 / 1.	NMA-1B-2-012	10.82	1.30	0.73	0.07	0.00	52.49	17.92	0.72	84.04	11356	-2507	-141	10/4/2018 20:36	Magnetite (on the basis of 32 O)
68 / 1.	NMA-1B-2-013	9.67	1.22	0.78	0.08	0.00	55.42	16.99	0.00	84.17	11188	-2449	-142	10/4/2018 20:43	Magnetite (on the basis of 32 O)

C.2.F Au-Ag Standards

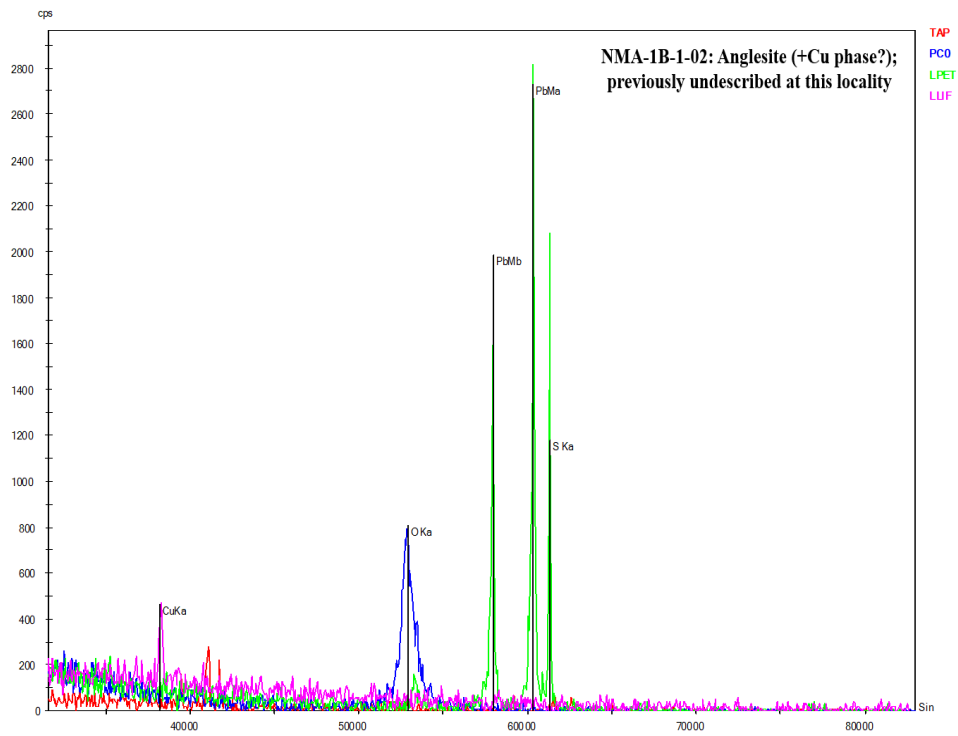
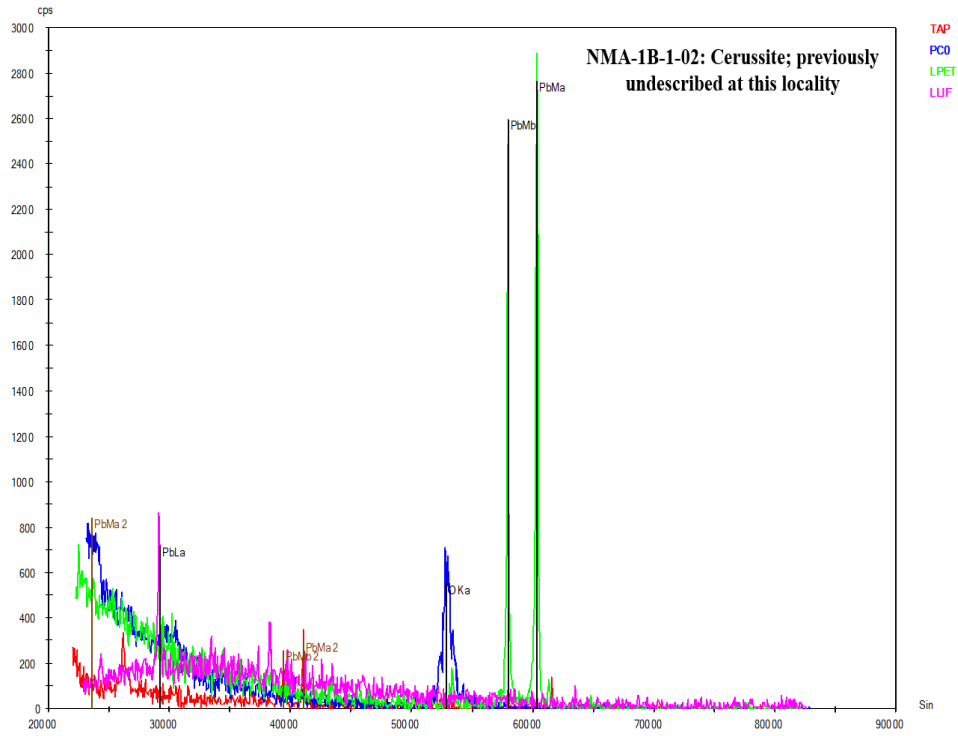
Weight%								
DataSet/Point	Sample	Au	Ag	Total	X	Y	Z	Date
9 / 1.	AuAg-01	41.03	58.01	99.05	-9982	-8158	111	10/4/2018 14:59
10 / 1.	AuAg-02	40.49	58.82	99.31	-9978	-8151	110	10/4/2018 15:01
83 / 1.	AuAg-03	39.72	59.51	99.23	-9969	-8190	113	10/4/2018 22:14
84 / 1.	AuAg-04	39.78	59.13	98.91	-9961	-8202	113	10/4/2018 22:15

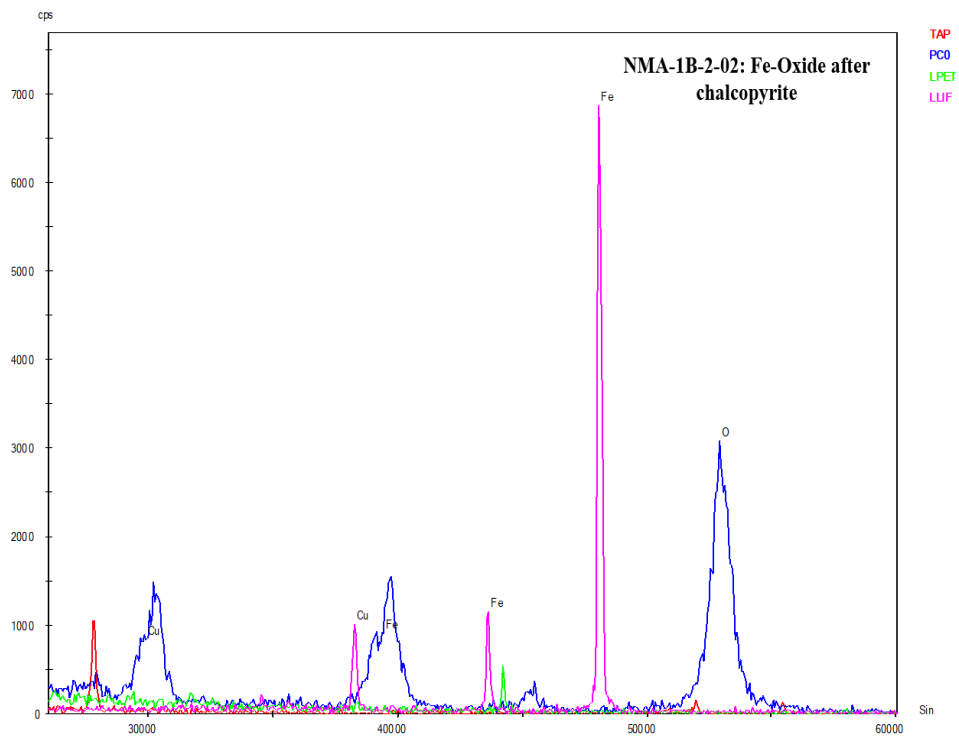
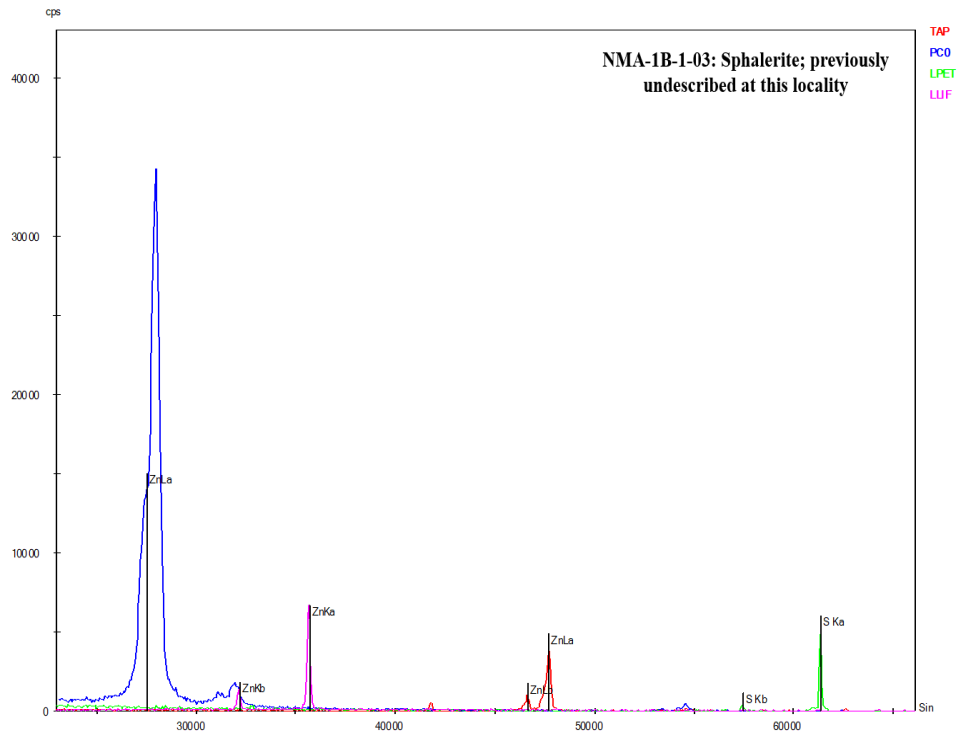
C.3 Electron Microprobe BSE Imagery



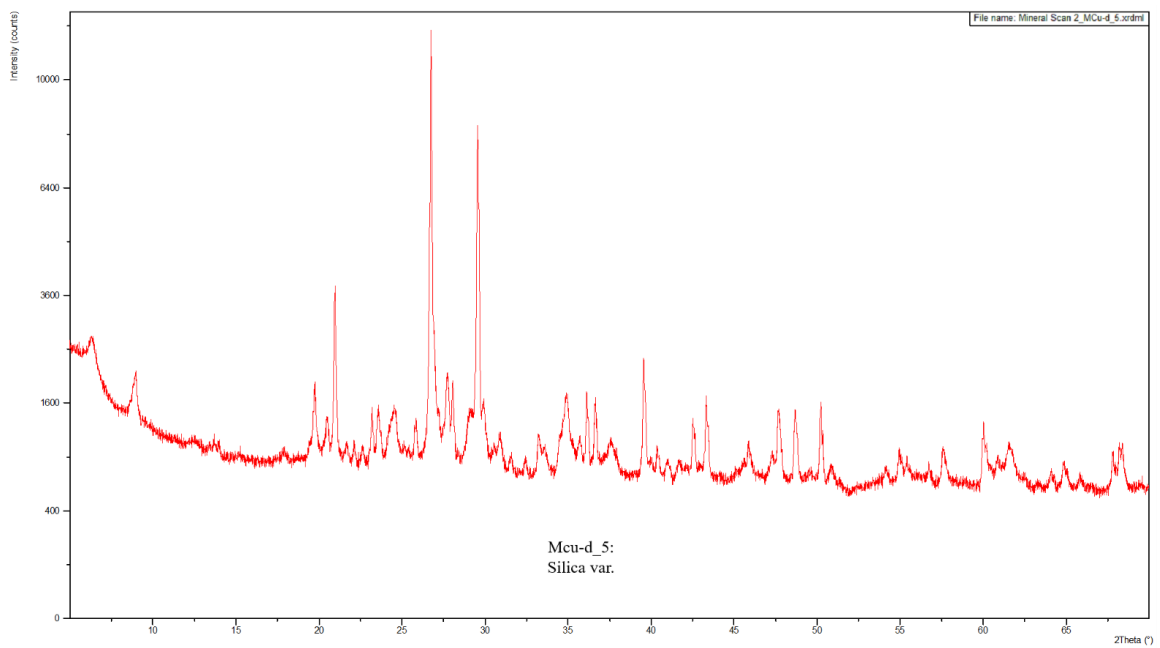
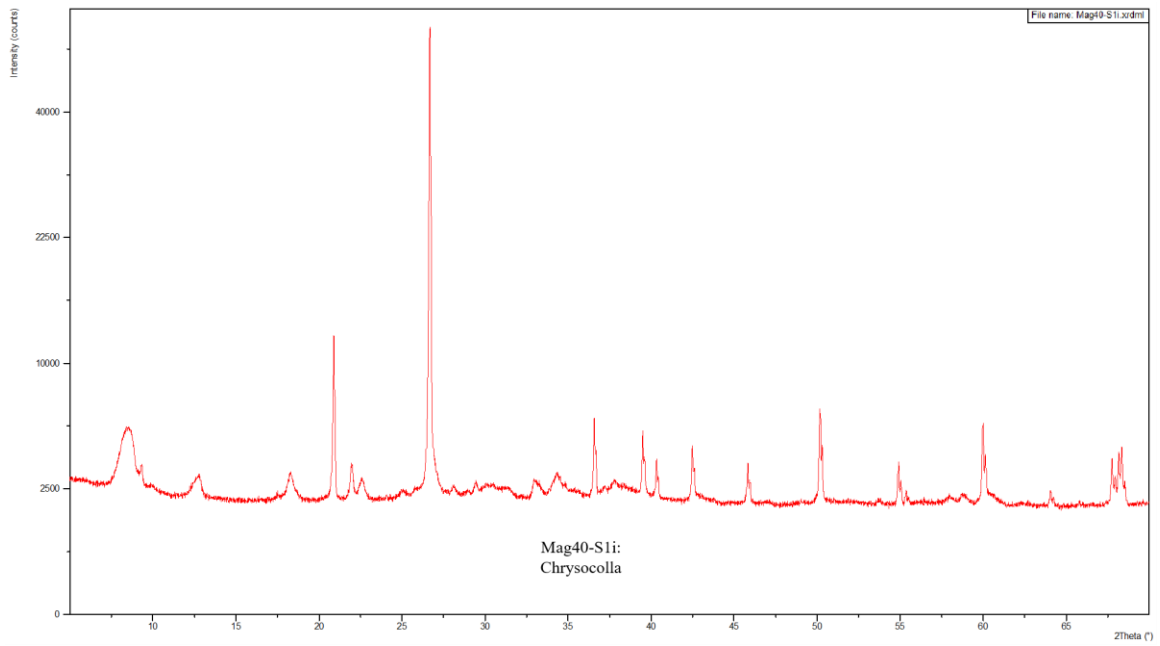


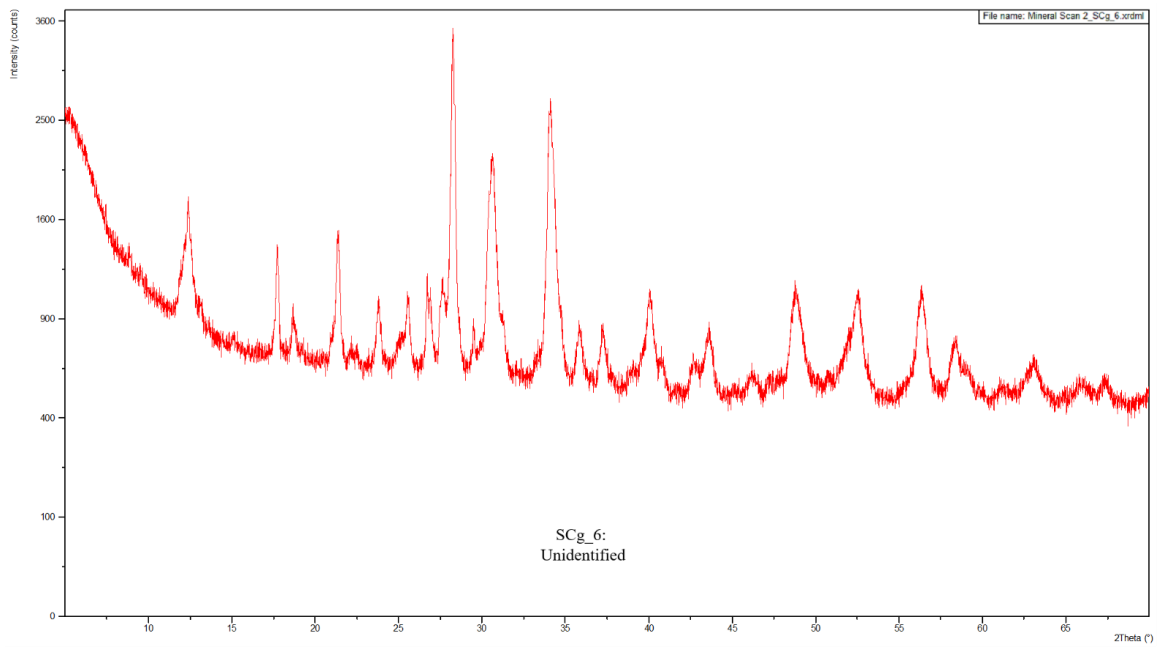
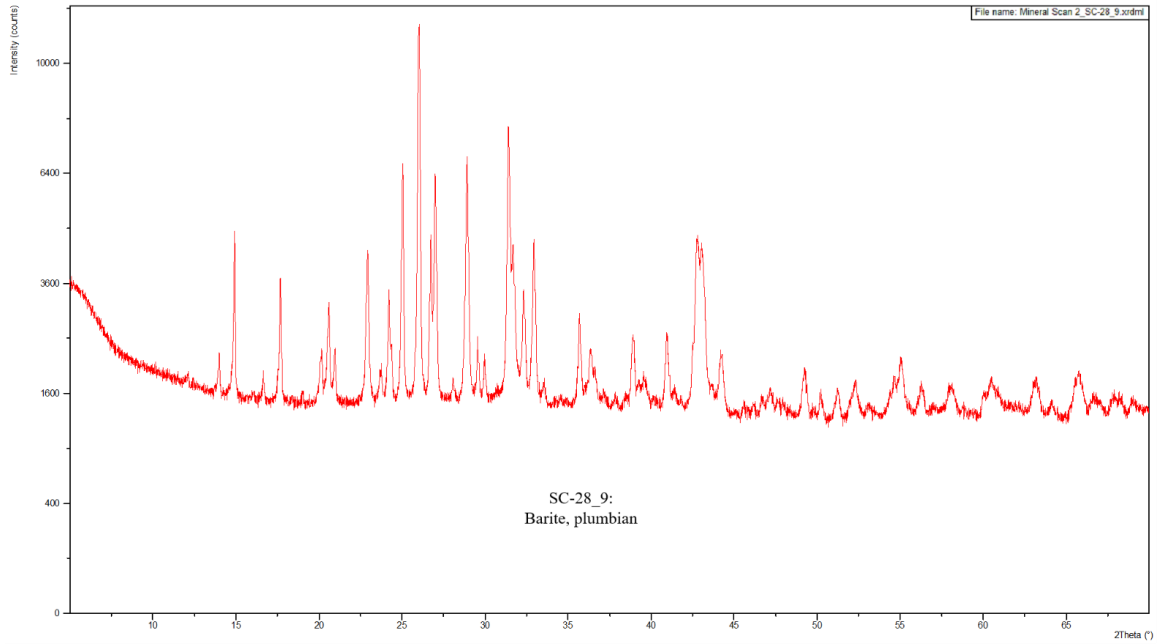
C.4 Electron Microprobe Spectra

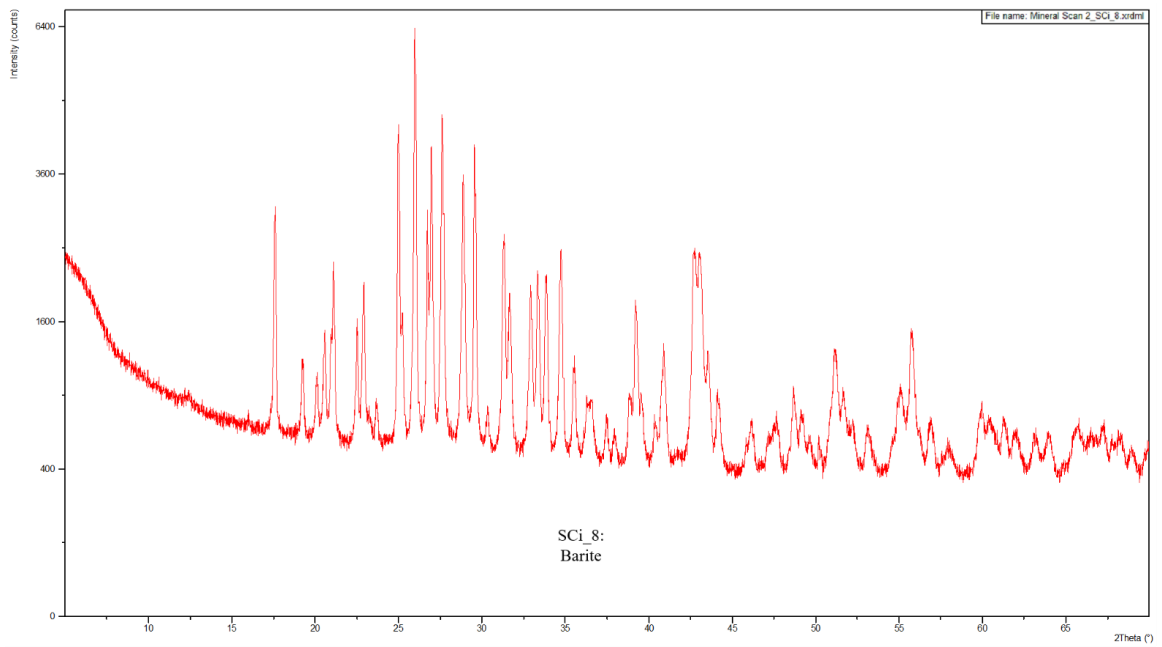
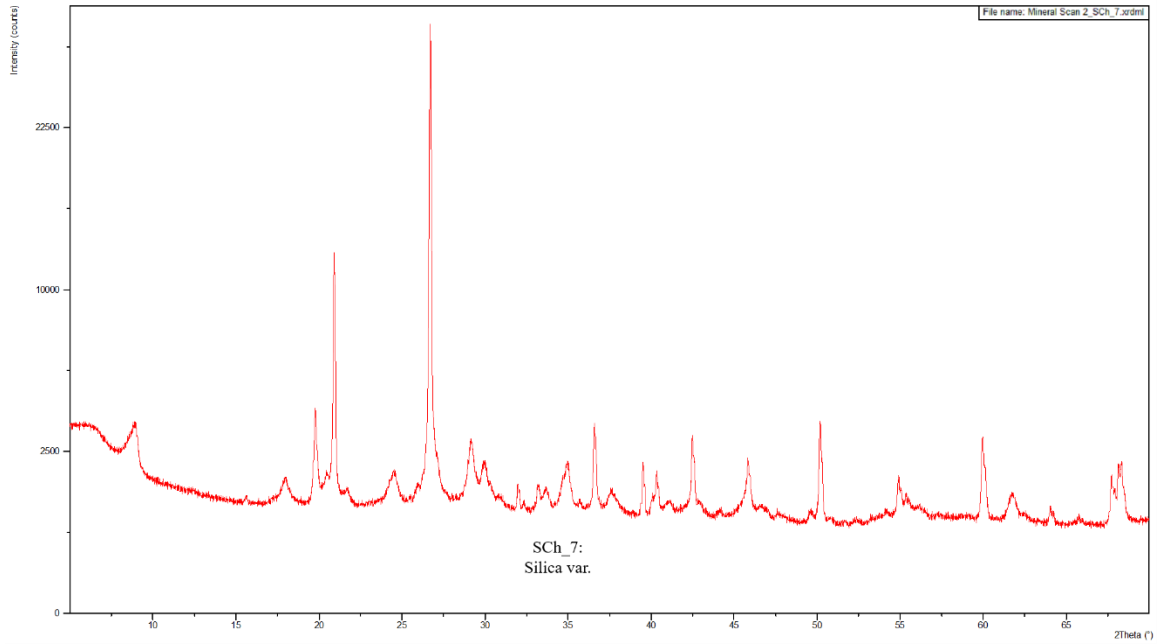


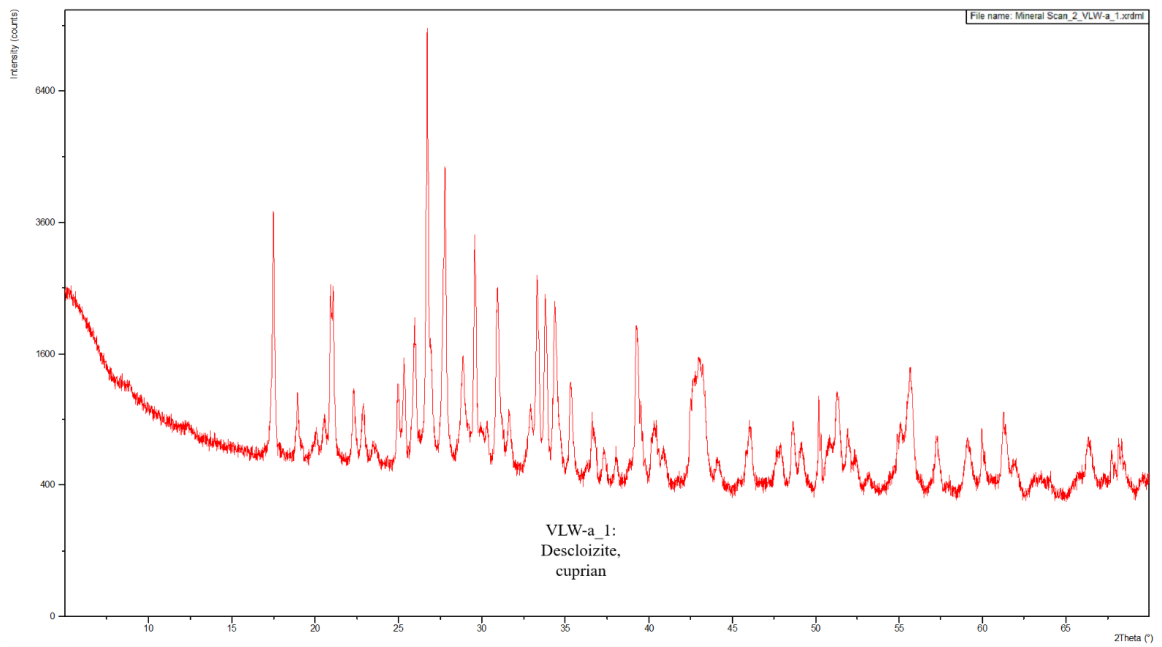
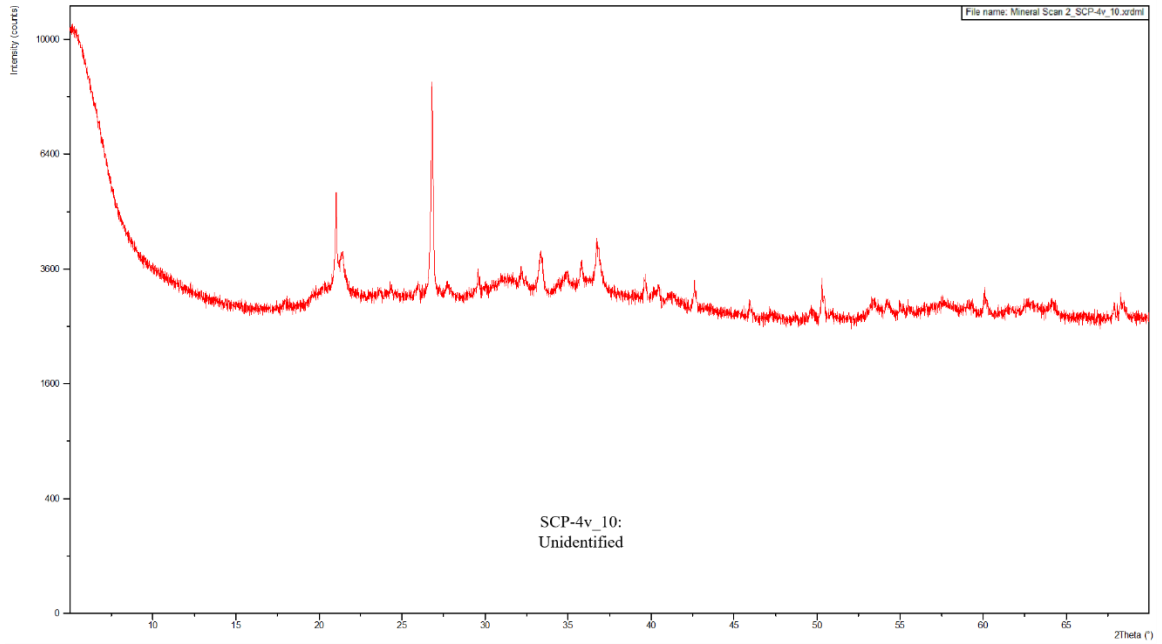


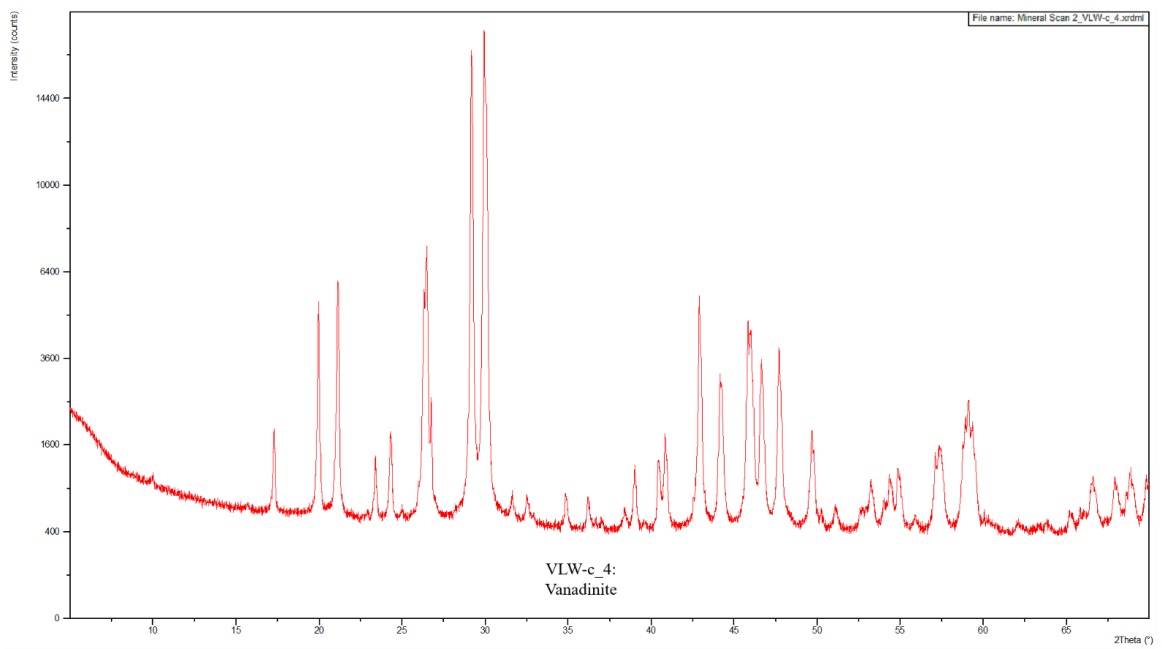
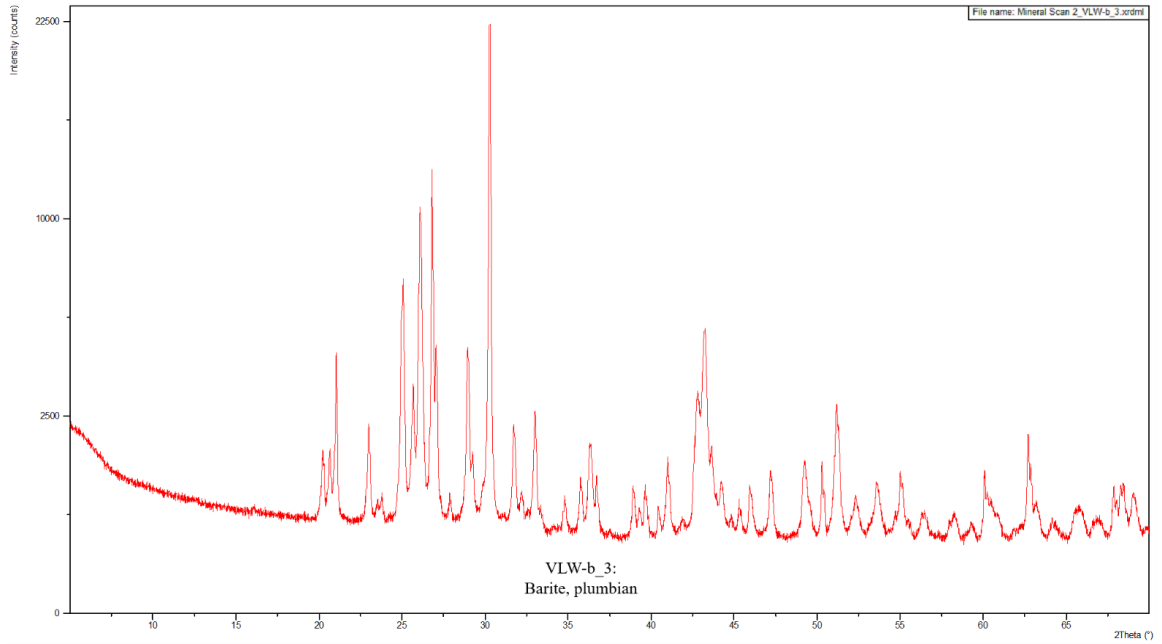
C.5 X-ray Diffractograms

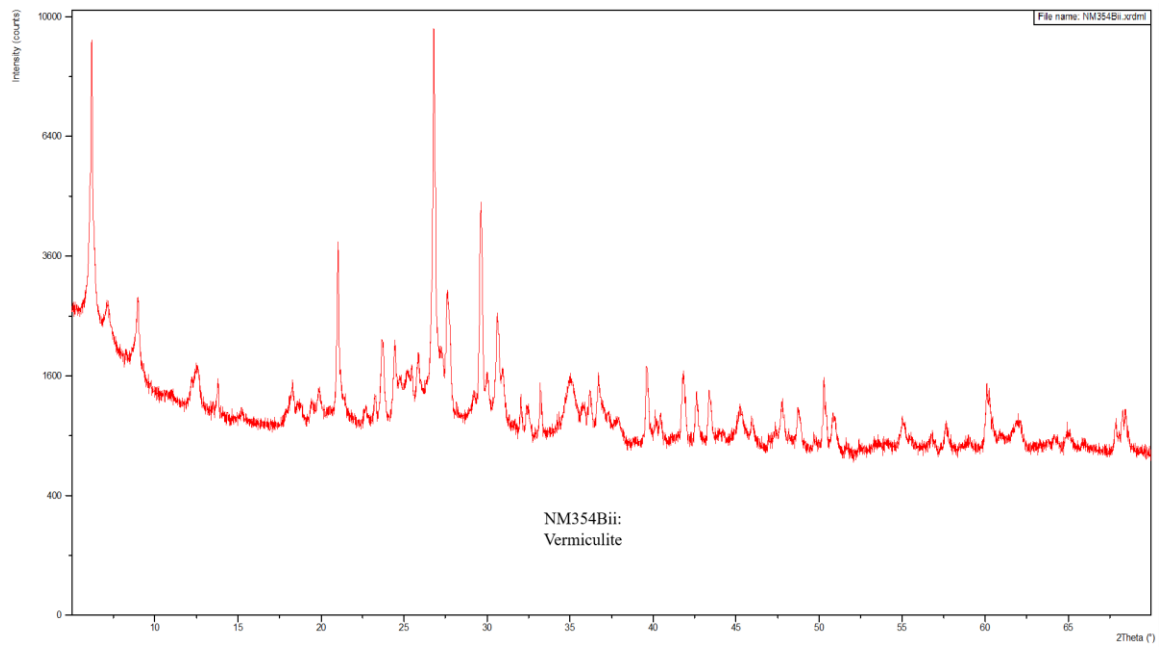
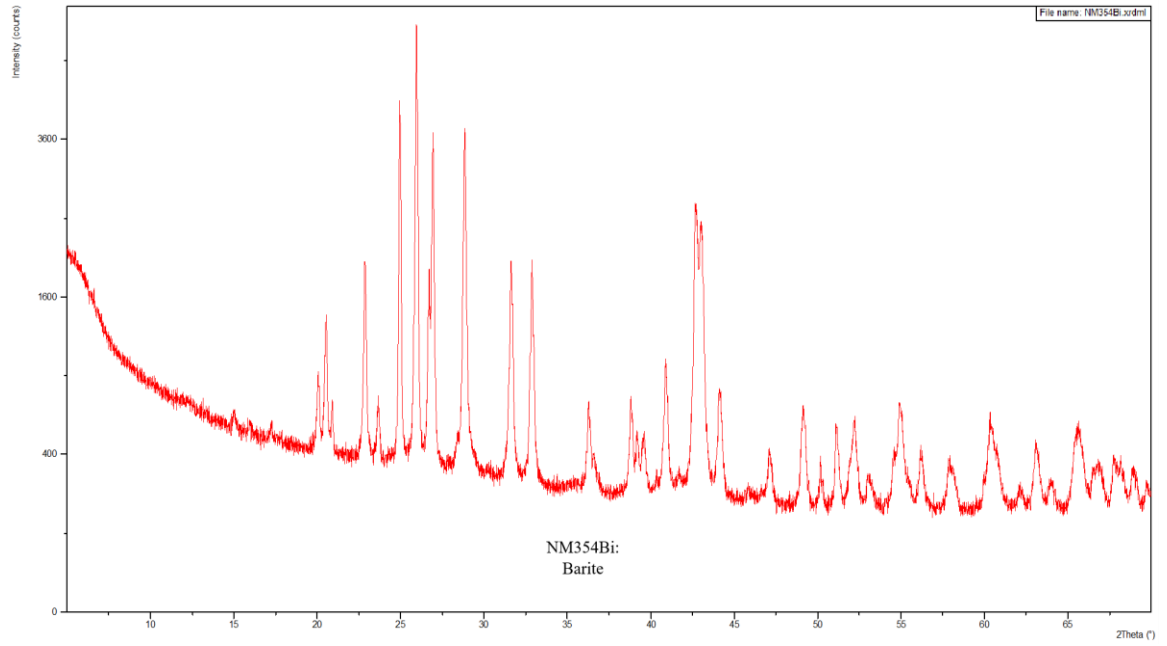


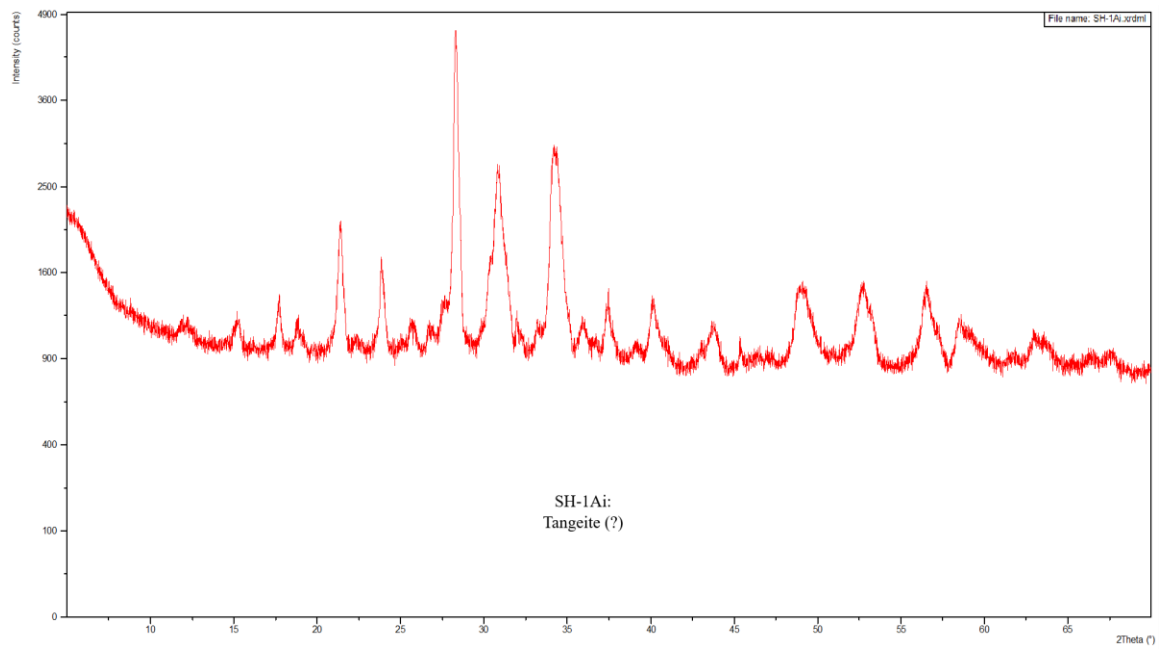
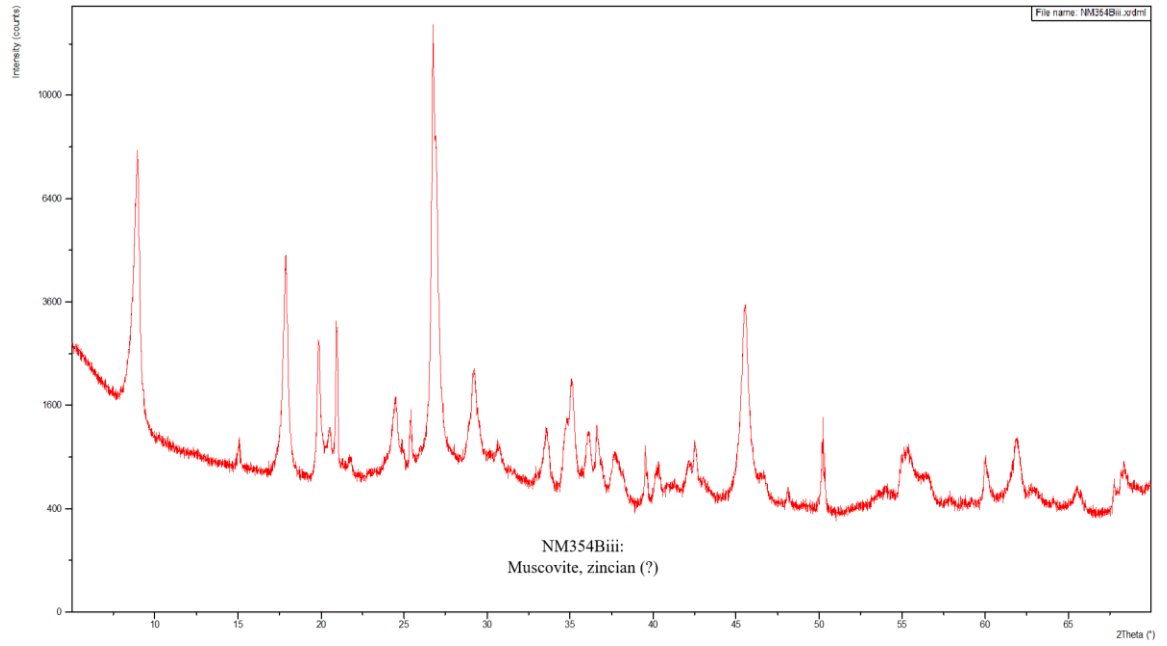


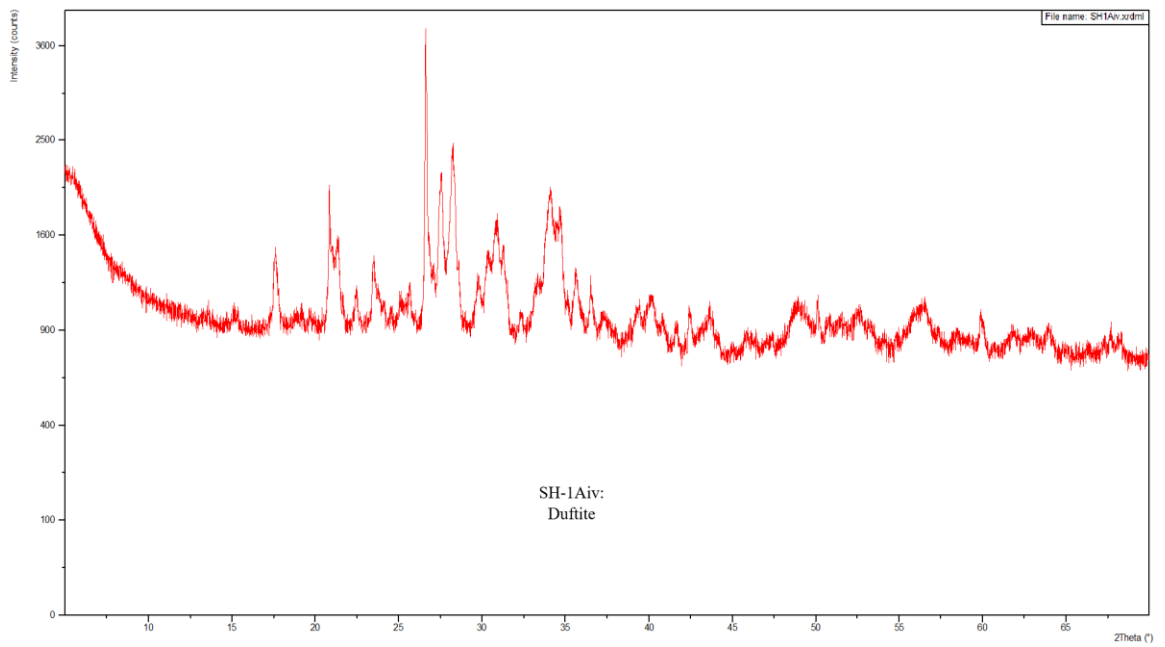
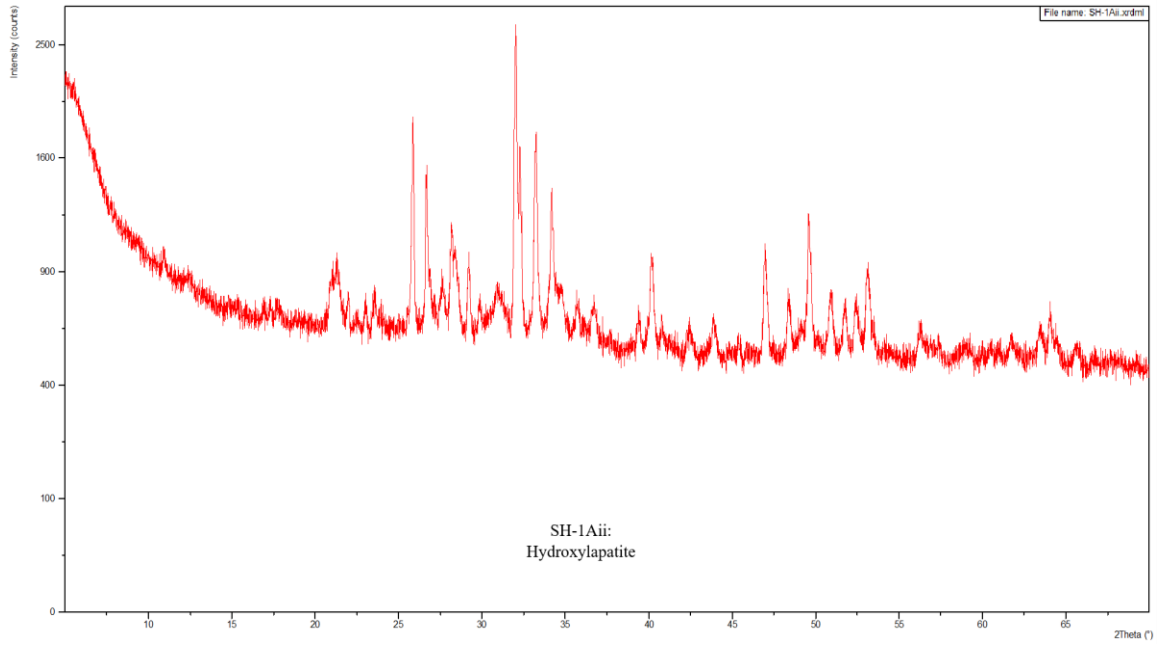


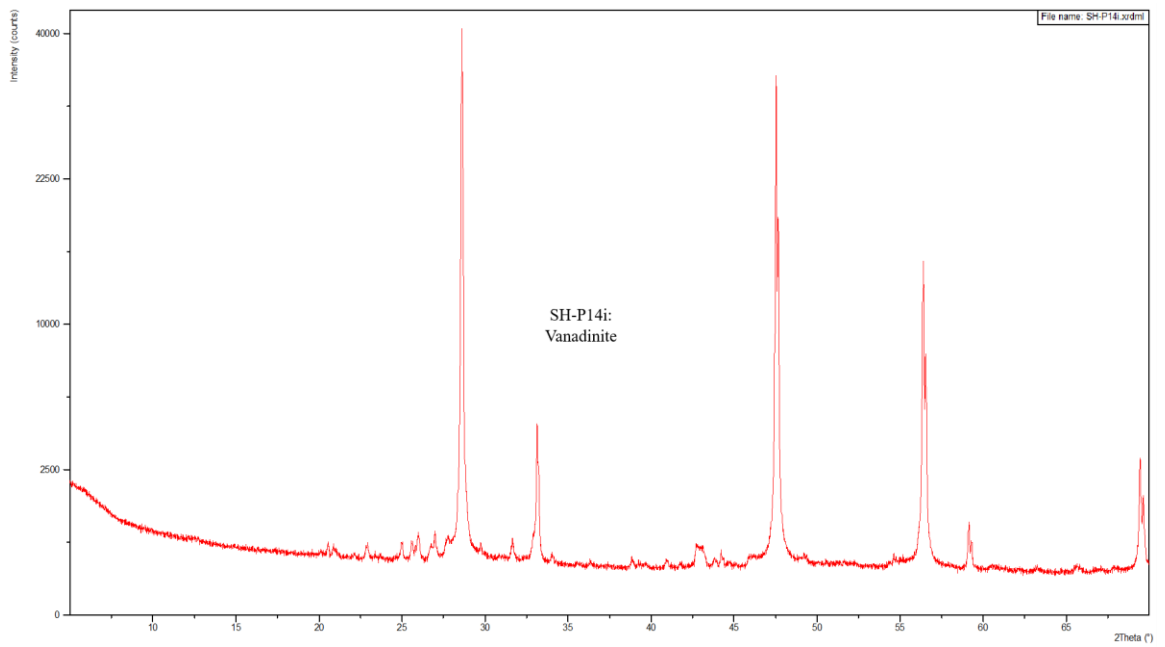
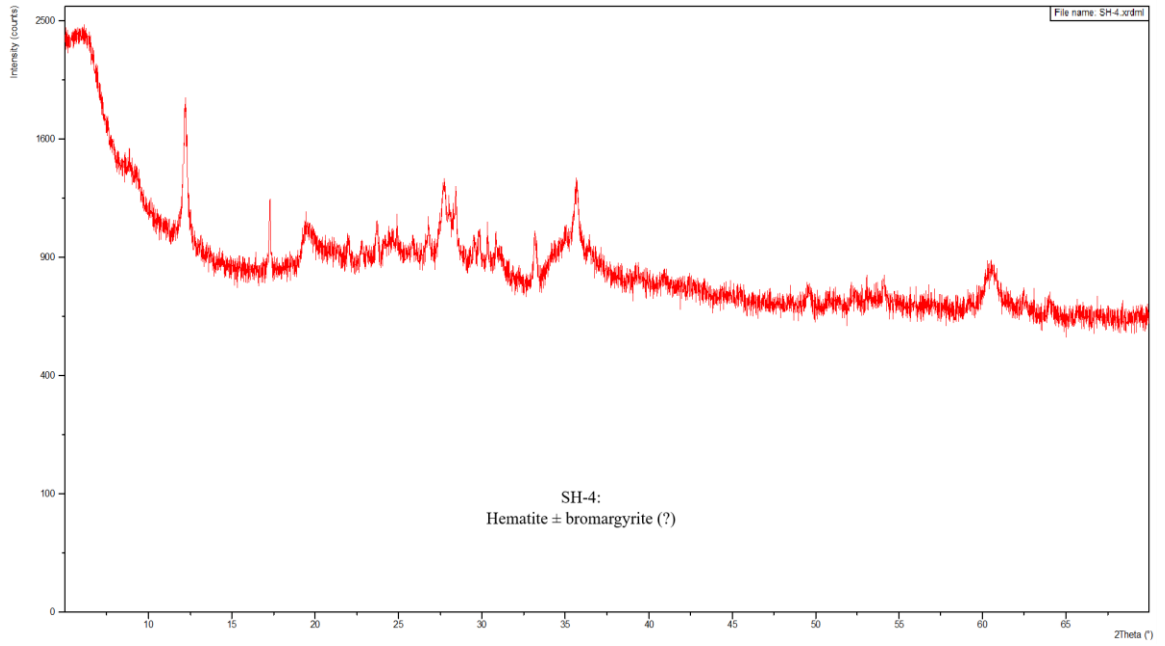


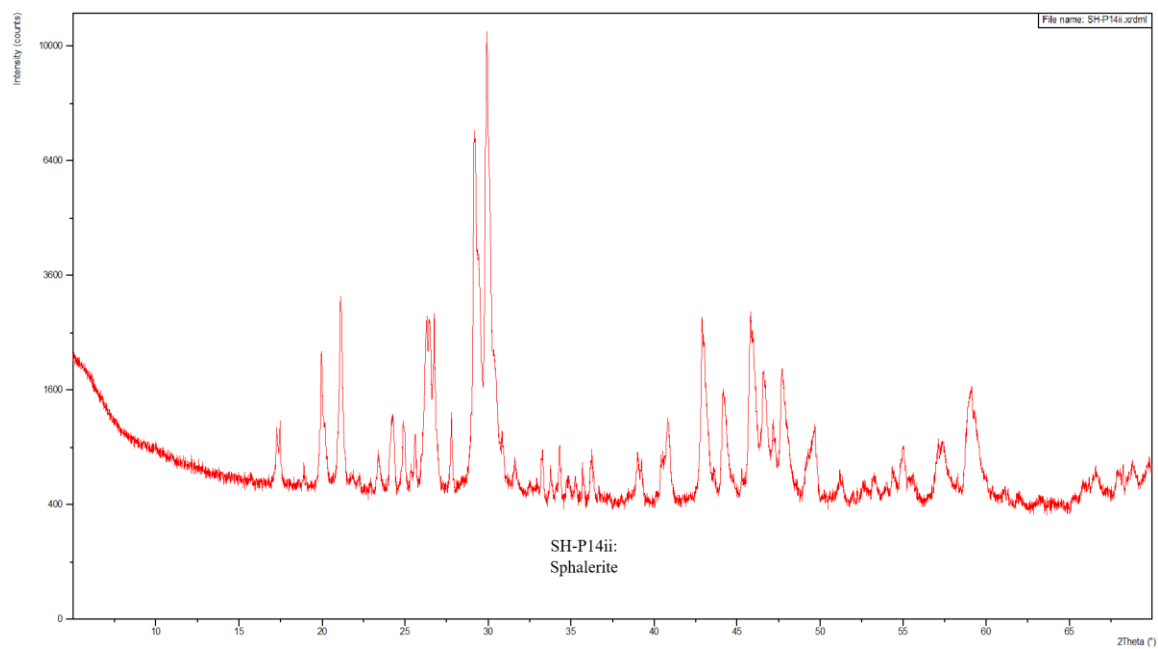




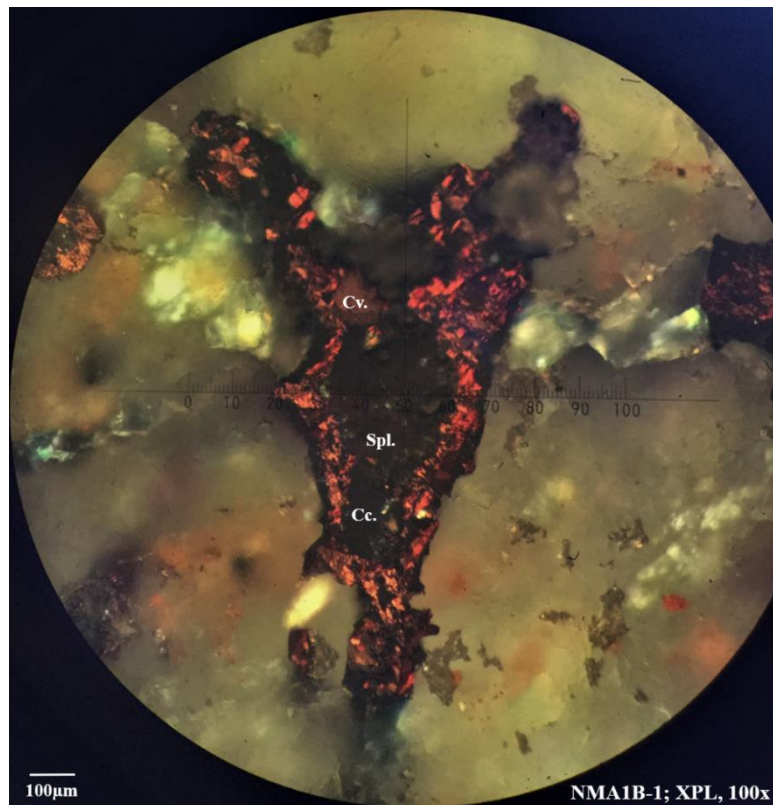
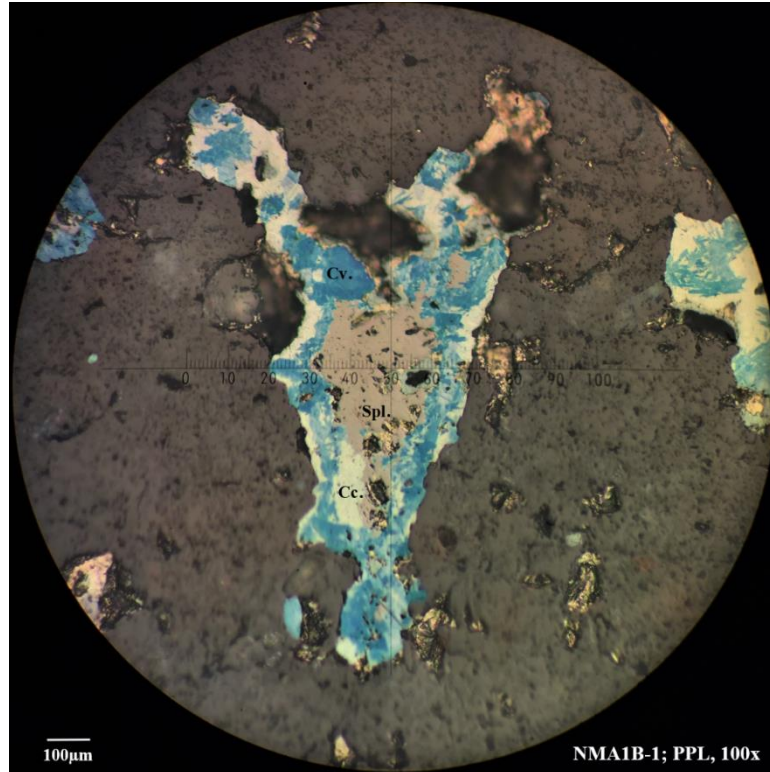


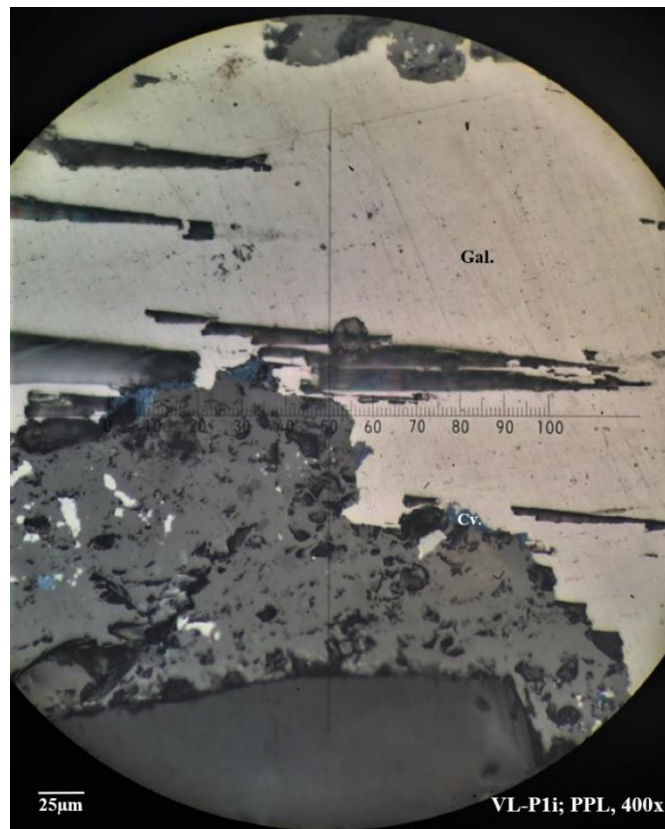
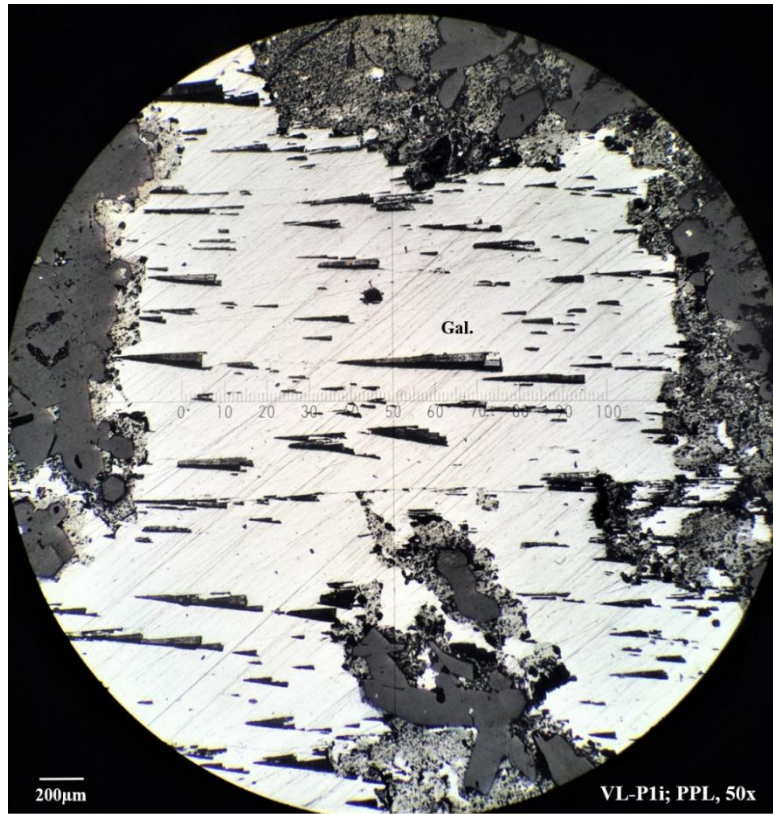


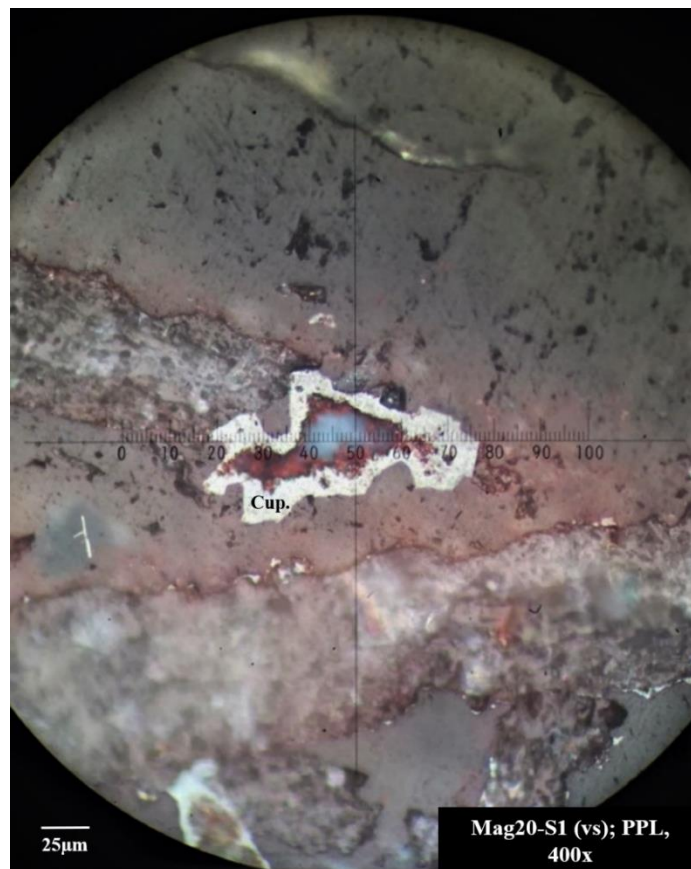
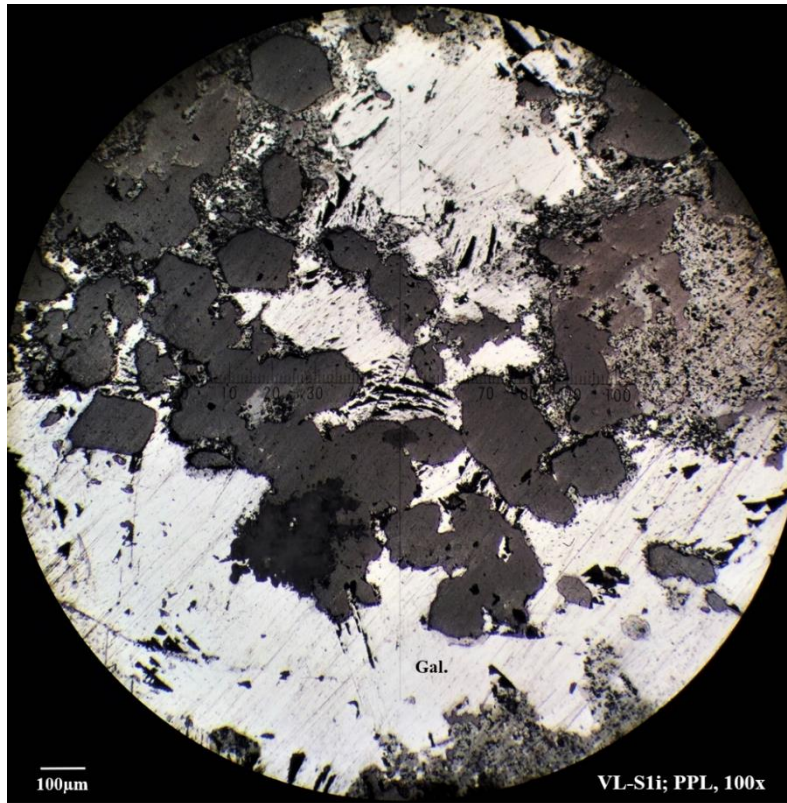


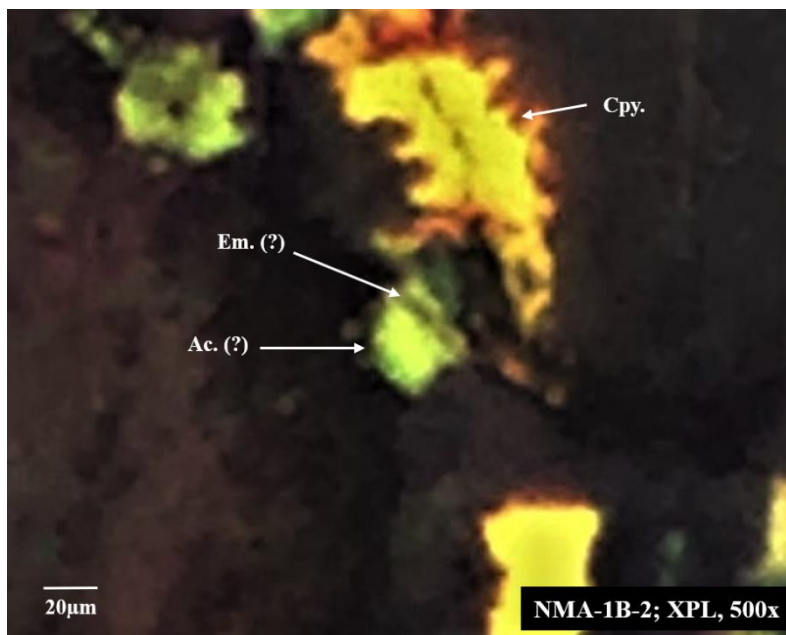
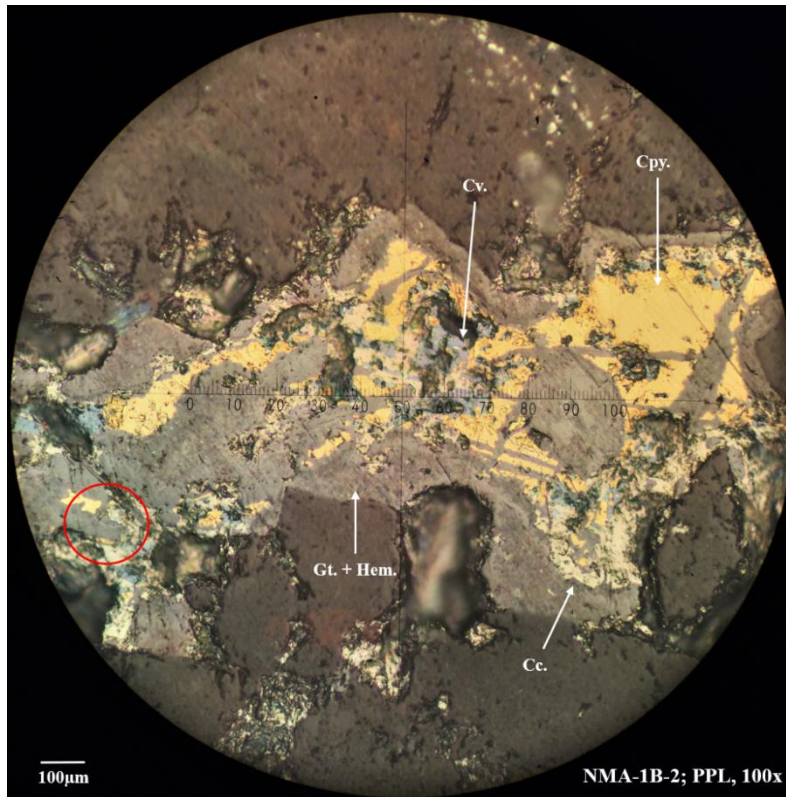


C.6 Reflected Light Photomicrographs









APPENDIX D

PERMISSIONS

This is your last appendix.

Place all of your permissions here for everything used from copyrighted material: i.e. long quotations, tables, and figures. Label each permission page with the list of figure numbers or tables or sections of your text that is from the copyrighted material.

Most journals have an online permissions process where you submit what you are using from the journal and an automatic system sends you permissions for a thesis/dissertation OR they have a blanket permission for use in a thesis/dissertation.

You must have permission for your own published work when you have signed a copyright release form; the above description for journals applies here as well.

If you are using material from an NMT thesis or dissertation, you may use the permission page at the end of the referenced thesis as your permission.

**AN INVENTORY AND MINERALOGICAL
CHARACTERIZATION OF MINES AND PROSPECTS IN THE
NORTH MAGDALENA MINING DISTRICT, SOCORRO
COUNTY, NEW MEXICO**

by

Marcus E. Silva

Permission to make digital or hard copies of all or part of this work for personal or classroom use is granted without fee provided that copies are not made or distributed for profit or commercial advantage and that copies bear this notice and the full citation on the last page. To copy otherwise, to republish, to post on servers or to redistribute to lists, requires prior specific permission and may require a fee.

